

**AN INVESTIGATION INTO THE  
MECHANISM OF ACTION OF THE  
NOVEL ANTHELMINTIC  
EMODEPSIDE**

**By**

**James Michael Willson**

**A thesis presented for the degree of  
DOCTOR OF PHILOSOPHY**

**of the  
UNIVERSITY OF SOUTHAMPTON  
in the**

**FACULTY OF MEDICINE, HEALTH AND LIFE SCIENCES  
DIVISION OF CELL SCIENCES**

**October 2003**

UNIVERSITY OF SOUTHAMPTON  
**ABSTRACT**  
FACULTY OF MEDICINE, HEALTH AND LIFE SCIENCES  
DIVISION OF CELL SCIENCES  
**Doctor of Philosophy**  
AN INVESTIGATION INTO THE MECHANISM OF ACTION OF THE NOVEL  
ANTHELMINTIC EMODEPSIDE

**James Michael Willson**

The increasing resistance of parasitic nematodes to existing anthelmintics has encouraged the search for novel compounds. Emodepside, a 24 membered cyclic depsipeptide, has been shown to act as a potent broad-spectrum anthelmintic. Emodepside causes a fast onset of paralysis of the nematodes favouring the view that it is neuropharmacologically active. The aim of this project is to define and characterise the site of action of emodepside using the pig intestinal parasite *Ascaris suum*, and the free-living nematode *Caenorhabditis elegans*.

The action of emodepside on the body wall muscle of the nematode *A. suum* was investigated. Emodepside (10 $\mu$ M) was applied for 10mins prior to ACh addition and caused a reduction in the ACh induced contraction of 39  $\pm$  4%. Emodepside was also shown to relax the dorsal muscle strip (DMS) following prolonged contraction with ACh. A slow relaxation of the DMS was then observed over a period of 10mins. Addition of 10 $\mu$ M emodepside at the point of maximum contraction, caused a faster relaxation of the DMS, 9.0%/min $^{-1}$   $\pm$  0.3 compared to the ACh control. The action of emodepside was similar to that of an inhibitory neuropeptide PF2 (SADPNFLRFamide). PF2 (1 $\mu$ M) caused a faster relaxation of the DMS (9.2%min $^{-1}$   $\pm$  0.4) compared to ACh control (7.4% min $^{-1}$   $\pm$  0.3), similar to emodepside. The ionic dependence of the response of *A. suum* muscle to emodepside was investigated using an intracellular electrophysiology recording technique. A 2 min perfusion of emodepside over muscle cells caused a slow hyperpolarisation of 5.5  $\pm$  0.1 mV, with no consistent change in input conductance after 30 min. A calcium and potassium component of emodepside action was demonstrated. In the absence of calcium, emodepside (10 $\mu$ M) caused no change in membrane potential. Re-introduction of calcium ions, resulted in a slow hyperpolarisation of 5.5  $\pm$  1.1 mV. The potassium channel blockers 4-aminopyridine and tetra-ethylammonium also blocked the emodepside induced hyperpolarisation of *A. suum* muscle cells. To elucidate whether emodepside acts pre-or post-synaptically at the neuromuscular junction, the effect of emodepside was investigated on a denervated muscle strip preparation. Application of emodepside (10 $\mu$ M) to the denervated muscle strip caused no reduction in ACh induced contraction. These studies on *A. suum* therefore suggest emodepside may inhibit nematode motility by acting pre-synaptically to trigger the release of an inhibitory neuropeptide.

To provide an insight into the molecular mechanisms and signalling pathway involved in emodepside action the model organism *C. elegans* was used. Emodepside inhibits the activity of the pharyngeal muscle (IC<sub>50</sub> 4.1nM) and was used as a bioassay to delineate the mechanism of action of this drug. To investigate whether emodepside stimulates vesicle release the rhodamine dye FM4-64, which labels active synapses, was used. Emodepside was shown to increase the rate of loss of fluorescence of this dye consistent with a stimulation of vesicle release. Emodepside resistance in *C. elegans* lacking proteins required for vesicle fusion, namely UNC-13 (206 fold less sensitive, IC<sub>50</sub>= 360nM) and synaptobrevin (29 fold less sensitive, IC<sub>50</sub>= 123nM) also suggests the action of emodepside is pre-synaptic and involves the machinery required for vesicle fusion. In the course of this study HC110R a latrophilin-like receptor was identified in *H. contortus*, as a possible target site for emodepside. In *C. elegans* two latrophilin-like genes were identified; *lat-1* and *lat-2*. RNAi to *lat-1* resulted in a 39 fold reduction in sensitivity to emodepside (IC<sub>50</sub>= 70nM) whereas only a 5.5 fold decrease in sensitivity to emodepside (IC<sub>50</sub>= 17nM) was observed for *lat-2*. The signalling pathway through which emodepside stimulates vesicle release was also investigated. *egl-30* (G $\alpha$ q) and *egl-8* (Phospholipase-C $\beta$ ) loss-of-function mutations both resulted in decreased sensitivity to emodepside, whereas *egl-30* gain-of-function mutations resulted in hypersensitivity to emodepside.

Investigation into the potential neurotransmitters that are released following emodepside stimulation, suggests a role for inhibitory neuropeptides in emodepside action. A reduced sensitivity to emodepside was observed following RNAi for the *flp-1* (IC<sub>50</sub>= 26nM) and *fip-13* (IC<sub>50</sub>= 18nM) genes. *unc-31* *C. elegans* which have mutations in the CAPS protein required for dense core vesicle exocytosis, also conferred a 5 fold resistance to emodepside (IC<sub>50</sub>= 12nM).

Taken together these data suggest a model whereby emodepside exerts its potent anthelmintic action through a latrophilin-like receptor in nematodes stimulating vesicle release through a G $\alpha$ q PLC- $\beta$ , UNC-13 pathway. A preferential release of inhibitory neuropeptides may explain the relaxation and paralysis of nematode muscle by emodepside.

## **Acknowledgements.**

I would like to thank Dr Lindy Holden-Dye and Professor Robert Walker for their time, help and guidance throughout the course of this project. A special thank you to Achim Harder for his hospitality in Germany. I would also like to thank Dr Candida Rogers, Dr Neline Kriek and Dr Neil Hopper for their technical help and advice.

Thanks also goes to every other member of wormland past and present who have put up with me and made my time so enjoyable. I would especially like to thank Kiran Amliwala with whom the RNAi experiments were run conjointly, and Fred, without whom, the *Ascaris* experiments would not have been possible! Thanks also to everyone else in the department for a fantastic working environment.

There are no words strong enough to express my appreciation to my mum (Sally), dad (Mike), sister (Sarah) and Diana who have always been there for me offering help, encouragement and support. Without this I would not have got where I am today.

I am grateful to the University of Southampton and Bayer AG, Germany for their financial support.

## Publications

**Willson, J.**, Amliwala, K., Harder, A., Holden-Dye, L., & Walker, R. J. (2003). The effect of the anthelmintic emodepside at the neuromuscular junction of the parasitic nematode *Ascaris suum*. *Parasitology* 126, 79-86.

**Willson, J.**, Harder, A., Holden-Dye, L., & Walker, R. J. (2001). A possible mechanism for the action of the novel anthelmintic emodepside, using *Ascaris suum* body wall muscle preparations. *Proceedings of the Physiology Society*, 536P

**Willson, J.**, Amliwala, K., Harder, A., Holden-Dye, L., & Walker, R. J. (2002). An investigation into the mechanism of action of the novel anthelmintic emodepside using *A. suum*. *European Worm Meeting Abstract* 121.

**Willson, J.**, Davis, A., A., Holden-Dye, L., & Walker, R. J. (2003). The  $\alpha$ -latrotoxin receptor Latrophilin, activated by the novel anthelmintic emodepside, stimulates vesicle release through a  $G\alpha_q$ , Phospholipase-C $\beta$ , UNC-13 pathway. *Neurotox 2003 Oral communication*.

**Willson, J.**, Davis, A., A., Holden-Dye, L., & Walker, R. J. (2003). The  $\alpha$ -latrotoxin receptor Latrophilin, activated by the novel anthelmintic emodepside, stimulates vesicle release through a  $G\alpha_q$ , Phospholipase-C $\beta$ , UNC-13 pathway. *Society for Neuroscience Abstracts in press*.

Trim, J. E., Holden-Dye, L., **Willson, J.**, Lockyer, M., & Walker, R. J. (2001). Characterization of 5-HT receptors in the parasitic nematode, *Ascaris suum*. *Parasitology* 122, 207-217.

Harder, A., Schmitt-Wrede, H. P., Krucken, J., Marinovski, P., Wunderlich, F., **Willson, J.**, Amliwala, K., Holden-Dye, L., & Walker, R. (2003). Cyclooctadepsipeptides-an anthelmintically active class of compounds exhibiting a novel mode of action. *Int.J Antimicrob Agents* 22, 318-331.

Amliwala, K., **Willson, J.**, Harder, A., Holden-Dye, L., & Walker, R. J. (2002). Effect of the anthelmintic emodepside on locomotion in *C. elegans*, and on the somatic muscle of *A. suum*. *Proceedings of the Physiology Society*, 543P

Amliwala, K., **Willson, J.**, Harder, A., Holden-Dye, L., & Walker, R. J. (2002). A comparison of the action of ivermectin and emodepside on *C. elegans* *European Worm Meeting Abstract* 167

## Contents

Acknowledgements.	i
Publications.	ii
Contents.	iii
Figures.	ix
Tables.	xii
Abbreviations.	xiii

<b>Chapter 1 Introduction</b>	<b>1</b>
1.1. Nematodes.	2
1.2. <i>A. suum</i> .	3
1.2.1 Life cycle of the parasitic nematode <i>A. suum</i> .	4
1.3. <i>C. elegans</i> .	5
1.3.1. <i>C. elegans</i> life cycle.	6
1.3.2. <i>C. elegans</i> as a useful biological model for study.	7
1.4. General nematode anatomy.	8
1.4.1. Body wall muscle.	10
1.4.2. Pharyngeal muscle.	10
1.5. The nervous system of the nematode.	13
1.5.1. Central nervous system.	13
1.5.2. The motor nervous system.	13
1.5.3. Neuronal control of movement.	16
1.5.4. Pharyngeal nervous system.	17
1.6. Control of pharyngeal and body wall muscle by neurotransmitters and neuromodulators.	21
1.7. Neuroactive peptides in nematodes.	21
1.7.1. Neuroactive peptides in <i>A. suum</i> .	22
1.7.2. Neuropeptides in <i>C. elegans</i> .	24
1.8. Anthelmintics and their sites of action.	26
1.8.1. Anthelmintics that act on the ACh receptor.	27
1.8.2. Anthelmintics that act on GABA-receptors.	28
1.8.3. The avermectins.	28
1.8.4. The benzimidazoles.	29
1.9. Anthelmintics and the problem of resistance.	29
1.9.1. Levamisole resistance.	29

1.9.2. Ivermectin resistance.	30
1.10. Looking for novel anthelmintics.	30
1.11. Depsipeptide anthelmintics.	31
1.11.1. Breaking of resistance by PF1022A and emodepside.	32
1.11.2. Investigating the mechanism of action of PF1022A and emodepside.	33
1.11.3. Emodepside acts through a latrophilin-like receptor.	34
1.12. $\alpha$ -LTX.	35
1.13. Multiple mechanism of action for $\alpha$ LTX.	35
1.14. Pore forming properties of $\alpha$ LTX.	37
1.15. The $\alpha$ LTX receptors.	38
1.15.1. The neurexins.	38
1.15.2. The latrophilins (CIRL).	40
1.15.2.1. Structure of latrophilin.	40
1.15.2.2. Latrophilin's role in vesicle release.	42
1.16. Project aims.	43
<b>Chapter 2. Materials and Methods <i>A. suum</i> Experiments.</b>	44
2.1. <i>A. suum</i> maintenance.	45
2.2. <i>In vitro</i> muscle strip tensions.	45
2.3. Electrophysiological studies.	46
2.4. Drugs.	47
2.5. Data analysis.	49
2.6. Statistical analysis.	49
<b>Chapter 3. Effect of emodepside on the neuromuscular system of <i>Ascaris suum</i></b>	50
3.1. Introduction.	51
3.2. The effect of varying ACh concentrations on <i>A. suum</i> dorsal muscle strip (DMS).	53
3.3. Emodepside causes a relaxation of the basal tone Of <i>A. suum</i> DMS.	54
3.4. Time dependence of emodepside action.	55
3.5. Effect of varying concentrations of emodepside on ACh-induced DMS contraction.	56

3.6. Effect of varying concentrations of emodepside on DMS pre-contracted with ACh.	57
3.7. The effect of emodepside on the excitatory and inhibitory actions of neuropeptides on <i>A. suum</i> DMS.	59
3.7.1. The Effect of Emodepside on <i>A. suum</i> DMS pre-contracted with AF2	59
3.8. A comparison of the effect of emodepside and PF2 (SADPNFLRFamide) on <i>A. suum</i> DMS.	61
3.8.1. Effect of PF2 on ACh induced DMS contraction.	61
3.8.2. Effect of addition of emodepside and subsequent addition of PF2 on DMS contraction	62
3.8.3. Effect of addition of PF2 and subsequent addition of emodepside on DMS contraction.	64
3.8.4. The Effect of the simultaneous application of PF2 and emodepside to <i>A. suum</i> DMS.	65
3.9. A comparison of the effect PF2 and emodepside on the prolonged ACh-induced contraction of <i>A. suum</i> DMS.	66
3.10. Effect of emodepside on denervated nerve preparation of <i>A. suum</i> DMS.	68
3.11. Effect of PF2 on a denervated nerve preparation of <i>A. suum</i> DMS.	69
3.12. Effect of emodepside on muscle cell membrane potential.	70
3.13. Effect of emodepside on ACh-induced depolarisation of <i>A. suum</i> muscle Cells	72
3.14. Effect of Emodepside on the AF2 induced increase in spontaneous activity of Ascaris muscle cells.	74
3.15. The ionic basis of the emodepside response in <i>A. suum</i> muscle cells.	75
3.15.1. Effect of emodepside on muscle cell membrane potential in calcium-free APF	75
3.15.2. Effect of emodepside on muscle cell membrane potential in the presence of potassium channel blockers 4AP and TEA.	77
3.15.3. Effect of emodepside on muscle cell membrane potential in potassium-free APF.	80
3.18. Discussion.	82
<b>Chapter 4. Materials and Methods <i>C. elegans</i> Experiments.</b>	86
4.1. Culturing of <i>C. elegans</i> .	87

4.2. Standard microbiological and molecular techniques.	87
4.3. Chemicals and reagents.	87
4.4. Construction of <i>C. elegans</i> complementary DNA library.	87
4.5. PCR.	88
4.5.1. PCR amplification.	88
4.5.2. Annealing temperature (Ta).	88
4.5.3 PCR cycle parameters.	88
4.5.4. Primer concentration.	89
4.5.5. PCR controls.	89
4.6. PCR amplification of B0457.1 ( <i>lat-1</i> ) gene.	89
4.6.1. Primer design.	89
4.6.2. Reaction conditions.	90
4.7. Agarose gel electrophoresis.	90
4.8. Purification of DNA.	91
4.9. Ligation of <i>lat-1</i> insert into T pCR® 2.1-TOPO® vector.	91
4.10. Transformation of competent cells.	91
4.11. Isolation of plasmid DNA from bacterial cells.	92
4.12. Isolation of <i>lat-1</i> Insert.	93
4.13. PCR amplification of <i>lat-1</i> using T7 and T3 promoter containing primers.	94
4.13.1. Reaction Conditions.	94
4.14. Synthesis double stranded RNA.	95
4.14.1. Purification of dsRNA.	95
4.14.2. Detection of dsRNA.	96
4.14.3. dsRNA Synthesis Controls.	96
4.15. Microinjection of dsRNA.	96
4.16. Synthesis of dsRNAi for the feeding method.	97
4.16..1 Reaction Conditions.	97
4.17. Ligation of <i>lat-1</i> , <i>lat-2</i> and <i>flp-13</i> fragments into L4440 feeding vector.	98
4.18. Transformation of HT115 bacteria with L4440 feeding vector.	99
4.19. Seeding of NGM plates with dsRNAi bacteria.	99
4.20. <i>C. elegans</i> growth on RNAi expressing bacteria.	100
4.21. Behavioural assays.	100
4.22. Locomotion assay.	100
4.23. Pharyngeal pumping assays.	101

4.23.1. Dissection of <i>C. elegans</i> pharynxes for pharyngeal pumping measurement.	101
4.23.2 .Counting method.	101
4.23.3. Electropharyngeogram [EPG] recordings.	101
4.24. Imaging with FM-464.	102
4.25. Statistical analysis.	103
<b>Chapter 5. Proposed Mechanism of Action of Emodepside using <i>C. elegans</i>.</b>	<b>104</b>
5.0. Introduction.	108
5.1. Effect of emodepside on <i>C. elegans</i> movement.	108
5.2. Effect of emodepside on pharyngeal pumping.	109
5.3. Effect of emodepside on wild type <i>C. elegans</i> (visual scoring method).	109
5.4. Recording electropharyngeogram (EPG) from <i>C. elegans</i> pharynxes.	111
5.5. Effect of emodepside on wild type <i>C. elegans</i> pharyngeal pumping, stimulated with 5-HT.	112
5.6. Effect of emodepside on wild type <i>C. elegans</i> pharyngeal pumping stimulated with AF1.	114
5.7. Effect of PF1022-001 (emodepside optical antipode) on pharyngeal pumping in wild type <i>C. elegans</i> .	116
5.8. Identifying the receptor through which emodepside acts.	118
5.9. Effect of emodepside on pharyngeal pumping in <i>rrf-3</i> <i>C. elegans</i> .	120
5.10. Effect of emodepside on pharyngeal pumping in <i>C. elegans</i> injected with dsRNA against the <i>lat-1</i> gene.	122
5.10.1. Effect of FLP-13 on <i>lat-1</i> dsRNA injected <i>C. elegans</i> .	124
5.11. Effect of emodepside on pharyngeal pumping in <i>C. elegans</i> fed on bacteria expressing dsRNA against the <i>lat-1</i> gene.	125
5.12. Effect of emodepside on pharyngeal pumping in <i>C. elegans</i> fed on bacteria expressing dsRNA against the <i>lat-2</i> gene.	128
5.13. Effect of emodepside on pharyngeal pumping in <i>C. elegans</i> fed on bacteria expressing dsRNA against both the <i>lat-1</i> and <i>lat-2</i> gene.	131
5.14. Does emodepside require synaptic vesicle release for its action?	133
5.15. Effect of emodepside on FM4-64 stained neurones in <i>C. elegans</i> .	134
5.16. Effect of emodepside on pharyngeal pumping in <i>snb-1</i> <i>C. elegans</i> .	136
5.17. Effect of emodepside on pharyngeal pumping in <i>unc-13</i> <i>C. elegans</i> .	138

5.18. Effect of emodepside on pharyngeal pumping in <i>unc-10</i> <i>C. elegans</i> .	140
5.19. Investigating the signalling Pathway through which emodepside acts.	142
5.19.1. Effect of emodepside on pharyngeal pumping in <i>egl-30</i> ( $G\alpha_q$ ) <i>C. elegans</i> .	142
5.19.2. Effect of emodepside on pharyngeal pumping in <i>egl-30</i> ( $G\alpha_q$ ) gain of function <i>C. elegans</i> .	144
5.19.3. Effect of emodepside on pharyngeal pumping in <i>goa-1</i> ( $G\alpha_o$ ) <i>C. elegans</i> .	146
5.19.4. Effect of emodepside on pharyngeal pumping in <i>egl-8</i> (phospholipase-C $\beta$ ) <i>C. elegans</i> .	148
5.20. Emodepside and neurotransmitter release.	151
5.20.1. Effect of emodepside on pharyngeal pumping in <i>eat-2</i> <i>C. elegans</i> .	151
5.20.2. Effect of emodepside on pharyngeal pumping in <i>avr-15</i> <i>C. elegans</i> .	153
5.20.3. The effect of emodepside on peptide release in <i>C. elegans</i> .	154
5.20.3.1. Effect of emodepside on pharyngeal pumping of <i>unc-31</i> <i>C. elegans</i> .	154
5.20.3.2. Investigating a role for <i>flp-13</i> in emodepside action.	156
5.20.3.3. Investigating a role for <i>flp-1</i> in emodepside action.	158
5.20.3.4. The effect of a simultaneous application of a SADPNFLRF amide, SDPNFLRFamide and AGSDPNFLRFamide (100nM) to <i>C. elegans</i> pharyngeal pumping.	158
5.20.3.5. Effect of emodepside on pharyngeal pumping in <i>C. elegans</i> fed on bacteria expressing dsRNA against the <i>flp-1</i> gene.	160
5.21. Discussion	162
<b>Chapter 6. Discussion.</b>	168
<b>Chapter 7 References.</b>	178
<b>Appendix 1.</b>	201

## Figures

1.1. The parasitic nematode <i>A. suum</i> .	3
1.2. The life cycle of the parasitic nematode <i>A. suum</i> .	4
1.3. The free living non parasitic nematode <i>C. elegans</i> .	5
1.4. The life cycle of the free-living non-parasitic nematode <i>C. elegans</i> .	6
1.5. General nematode anatomy.	9
1.6. The pharyngeal anatomy of <i>C. elegans</i> .	12
1.7. Organisation of motorneurones in nematodes.	15
1.8. Simplified neuronal circuit diagram controlling locomotion in <i>A. suum</i> .	17
1.9. Wiring Diagram of the <i>C. elegans</i> pharynx.	20
1.10. Chemical structure of PF1022A and emodepside.	32
1.11. The Multiple mechanisms of $\alpha$ LTX action.	36
1.12. The latrophilin receptor.	41
2.1. The denervated muscle preparation.	46
2.2. Experimental methods for <i>A. suum</i> experiments.	48
3.1. The effect of ACh on <i>A. suum</i> DMS.	53
3.2. The effect of Emodepside on the basal tone of <i>A. suum</i> DMS.	54
3.3. The time-dependent effect of emodepside on the ACh-induced contraction of DMS.	55
3.4. The effect of varying concentrations of emodepside on ACh-induced contraction of <i>A. suum</i> DMS.	56
3.5. Effects of emodepside on prolonged ACh-induced contraction of <i>A. suum</i> DMS.	58
3.6. The effect of emodepside on the response to the excitatory neuropeptide AF2 on <i>A. suum</i> DMS	60
3.7. Effect of addition of 1 $\mu$ M PF2 on ACh-induced contraction of <i>A. suum</i> DMS strip.	62

3.8. Effect of emodepside and subsequent addition of PF2 on ACh-induced contraction of <i>A. suum</i> DMS strip.	63
3.9. Effect of PF2 and subsequent addition of emodepside on ACh-induced contraction of <i>A. suum</i> DMS strip	64
3.10. Effect of PF2 and simultaneous emodepside addition on ACh-induced contraction of <i>A. suum</i> DMS strip.	65
3.11. A comparison of the effect of PF2 and emodepside on the prolonged contraction of <i>A. suum</i> DMS by ACh.	67
3.12. Effect of emodepside on <i>A. suum</i> denervated muscle strips.	68
3.13. Effect of PF2 on <i>A. suum</i> denervated muscle strips.	69
3.14. The effect of emodepside on the membrane potential of <i>A. suum</i> muscle cells.	71
3.15. The effect of emodepside on the ACh induced depolarisation of <i>A. suum</i> muscle cells.	73
3.16. The effect of emodepside on the AF2-induced increase in spontaneous activity of <i>A. suum</i> muscle cells.	74
3.17. The effect of removing extracellular calcium on <i>A. suum</i> muscle cell response to emodepside.	76
3.18. The Effect of K <sup>+</sup> channel blockers 4AP and TEA prior to emodepside-induced muscle cell hyperpolarisation.	78
3.19. The Effect of K <sup>+</sup> channel blockers 4AP and TEA following emodepside-induced muscle cell hyperpolarisation.	79
3.20. Effect of removing extracellular potassium upon <i>A. suum</i> muscle cell hyperpolarisation in response to emodepside.	81
4.1 Experimental set-up for recording EPG's from <i>C. elegans</i> pharynxes.	102
5.1. The effect of emodepside on <i>C. elegans</i> movement.	108
5.2. Effect of emodepside and PF1022A on <i>C. elegans</i> pharyngeal pumping (counting assay).	110
5.3. Example of an EPG trace, of a single pump from wild type <i>C. elegans</i> .	111
5.4. Effect of emodepside on <i>C. elegans</i> pharyngeal pumping (EPG counting assay).	113
5.5. Effect of emodepside on wild-type <i>C. elegans</i> stimulated with AF1.	115

5.6. Effect of PF1022-001 on wild-type <i>C. elegans</i> pharyngeal pumping.	117
5.7 Identifying latrophilin like receptors in <i>C. elegans</i> .	119
5.8. Effect of emodepside on <i>rrf-3</i> <i>C. elegans</i> pharyngeal pumping.	121
5.9. The effect of emodepside on RNAi induced (injected) inhibition of <i>lat-1</i> on wild type <i>C. elegans</i> pharyngeal pumping (counting assay).	123
5.10. The effect of FLP-13 on wild type and <i>lat-1</i> (injected) RNAi <i>C. elegans</i> pharyngeal pumping.	124
5.11. RNAi for <i>lat-1</i> results in behavioural abnormalities in intact <i>C. elegans</i> .	125
5.12. Effect of emodepside on RNAi uninduced (in the absence of IPTG) and induced (+ IPTG) knock-down of <i>lat-1</i> in <i>rrf-3</i> <i>C. elegans</i> pharyngeal pumping.	126
5.13. RNAi for <i>lat-2</i> results in behavioural abnormalities in intact <i>C. elegans</i> .	128
5.14. Effect of emodepside on RNAi uninduced (in the absence of IPTG) and RNAi induced (+ IPTG) inhibition <i>lat-2</i> in <i>rrf-3</i> <i>C. elegans</i> pharyngeal pumping.	129
5.15. Effect of emodepside on RNAi uninduced (in the absence of IPTG) and induced (+ IPTG) inhibition of <i>lat-1</i> and <i>lat-2</i> in <i>rrf-3</i> <i>C. elegans</i> pharyngeal pumping.	131
5.16. The effect of emodepside on exocytosis from <i>C. elegans</i> pharyngeal neurones by imaging with FM4-64.	135
5.17. Effect of emodepside on <i>snb-1</i> <i>C. elegans</i> pharyngeal pumping.	137
5.18. Effect of emodepside on <i>unc-13</i> ( <i>e1091</i> and <i>s69</i> ) <i>C. elegans</i> pharyngeal pumping.	139
5.19. Effect of emodepside on <i>unc-10</i> <i>C. elegans</i> pharyngeal pumping.	141
5.20. The effect of emodepside on <i>egl-30</i> ( $G\alpha_q$ ) <i>C. elegans</i> pharyngeal pumping (counting assay).	143
5.21. Effect of emodepside on <i>egl-30</i> ( $G\alpha_q$ ) gain of function <i>C. elegans</i> pharyngeal pumping.	145
5.22. Effect of emodepside on <i>goa-1</i> <i>C. elegans</i> pharyngeal pumping.	147
5.23. Effect of emodepside on <i>egl-8</i> ( <i>md1971</i> and <i>n488</i> ) <i>C. elegans</i> pharyngeal pumping.	149

5.24. Effect of emodepside on <i>eat-2</i> <i>C. elegans</i> pharyngeal pumping.	152
5.25. The effect of 100nM emodepside on <i>avr-15</i> <i>C. elegans</i> pharyngeal pumping (counting assay).	153
5.26. Effect of emodepside on <i>unc-31</i> <i>C. elegans</i> pharyngeal pumping.	155
5.27. Effect of emodepside on RNAi uninduced (in the absence of IPTG) and induced (+ IPTG) inhibition of <i>flp-13</i> in <i>rrf-3</i> <i>C. elegans</i> pharyngeal pumping.	157
5.28. Effect of the application of a cocktail of 3 predicted <i>flp-1</i> peptides (SADPNFLRF amide, SDPNFLRFamide and AGSDPNFLRFamide ) on wild type <i>C. elegans</i> pharyngeal pumping.	159
5.29. Effect of emodepside on RNAi uninduced (in the absence of IPTG) and induced (+ IPTG) inhibition of <i>flp-1</i> in <i>rrf-3</i> <i>C. elegans</i> pharyngeal pumping.	161
6.1. Proposed mechanism of action for the novel anthelmintic emodepside.	176

## Tables

1.1 FMRFamide peptides that affect <i>A. suum</i> muscle.	22
1.2 The <i>flp</i> genes <i>C. elegans</i> and the potential FaRPs they encode	25

## Abbreviations

Alanine	Ala	A
Arginine	Arg	R
Asparagine	Asn	N
Aspartic Acid	Asp	D
Cysteine	Cys	C
Glutamic Acid	Glu	E
Glutamine	Glu	Q
Glycine	Gly	G
Histidine	His	H
Leucine	Leu	L
Lysine	Lys	K
Methionine	Met	M
Phenylalanine	Phe	F
Proline	Pro	P
Serine	Ser	S
Threonine	Thr	T
Tryptophan	Trp	W
Tyrosine	Tyr	Y
Valine	Val	V

4-AP	4-aminopyridine
5-HT	5-Hydroxy-tryptamine
<i>A. suum</i>	<i>Ascaris suum</i>
ACh	Acetylcholine
AF1	<i>Ascaris</i> FMRFamide-like peptide one
AF2	<i>Ascaris</i> FMRFamide-like peptide two
APF	Artificial Perienteric Fluid
$\alpha$ LTX	$\alpha$ -latrotoxin
CAPS	Calcium Activated Protein for Secretion
<i>C. elegans</i>	<i>Caenorhabditis elegans</i>
cDNA	Complementary Deoxyribonucleic acid
DAG	Diacylglycerol
DMS	Dorsal muscle strip
DNA	Deoxyribonucleic acid
dsRNA	Double stranded Ribonucleic Acid
EDTA	Ethylenediamine tetra-acetic acid
EPG	Electropharyngeogram
gDNA	Genomic Deoxyribonucleic acid
Glu-Cl	Glutamate gated chloride channel
nAChR	Nicotinic acetylcholine receptor
PF1022A	cyclo(D-lactyl-L-N-methylleucyl-D-3-phenyllactyl-L-N-methylleucyl-D-lactyl-L-N-methylleucyl-D-3-phenyllactyl-L-N-methylleucyl)
GABA	$\gamma$ -amino butyric acid
PCR	Polymerase Chain Reaction
PF1	<i>Panagrellus</i> FMRFamide-like peptide one
PF2	<i>Panagrellus</i> FMRFamide-like peptide two
PLC- $\beta$	Phospholipase-C $\beta$
RNA	Ribonucleic Acid
RNA <sub>i</sub>	Ribonucleic Acid interference
TAE	Tris acetate EDTA
TBE	Tris borate EDTA
TEA	Tetraethylammonium

## CHAPTER 1

# Introduction

## 1.1 Nematodes.

Nematodes are a highly successful phylum, which have evolved to exist as either free living or parasitic. Of the free living nematodes some 12,000 species have been identified. Nematodes have been found in a diverse range of habitats such as the deep sea, fresh water and soil, where they have a significant effect on the nutrient cycle in soil. As decomposers they consume fungi, bacteria and other microflora and microfauna aiding to the health of the soil. One free-living nematode *Caenorhabditis elegans* with its fully sequenced genome is becoming a useful biological model organism for study.

In contrast, parasitic nematodes create both economic and social problems throughout the developed and developing world. Some 15,000 parasitic species have been identified. Parasitic nematodes can be divided into two main types. The first are the tissue roundworms (examples being the filarial worms). The second are the intestinal roundworms (such as *Ascaris suum* and *Ascaris lumbricoides*).

Intestinal nematodes currently infect over 3 billion people and the health of 450 million people is affected every year as a direct result of these infections. The intestinal roundworm *A. lumbricoides* alone causes 60,000 human deaths a year (World Health Organisation, 1999). Nematodes also severely affect the agricultural industry. Nematode infection of domestic livestock can be devastating for the local economy through lost productivity, death of livestock and increased use of foodstuffs. Plant parasitic nematodes have been estimated to cause 80 billion dollars worth of crop damage annually.

To tackle these problems, which result from parasitic nematode infestations in both humans and agriculture, compounds named anthelmintics were developed. These anti-parasitic drugs may act specifically at nematode receptors or ion channels, in particular at the neuromuscular junction, where their action results in a rapid therapeutic effect to the host. Alternatively other compound groups act more slowly at a range of biochemical sites.

The over use of these anthelmintic compounds has slowly led to resistance in many strains of parasitic nematodes. The requirement, therefore, for new anthelmintics acting on novel target sites within nematodes has become of both social and economic importance.

In this study, we have used both the parasitic nematode *A. suum* and the free living nematode *C. elegans* to investigate the mechanism of action of a novel type of anthelmintic drug, the cyclooctadepsipeptide emodepside.

## 1.2 *A. suum*.

The nematode *A. suum* (Fig 1.1), due to its size and relative abundance, has become a useful organism to study the mode of action of both existing and novel anthelmintics.

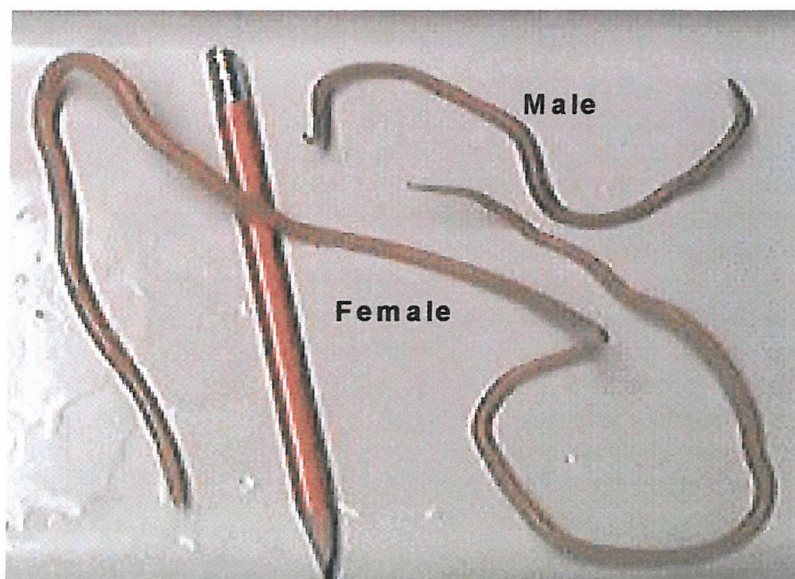


**Fig 1.1. The parasitic nematode *A. suum*.** The two separate sexes are shown. The pencil is used as an indication of size.

### 1.2.1 Life cycle of the parasitic nematode *A. suum*.

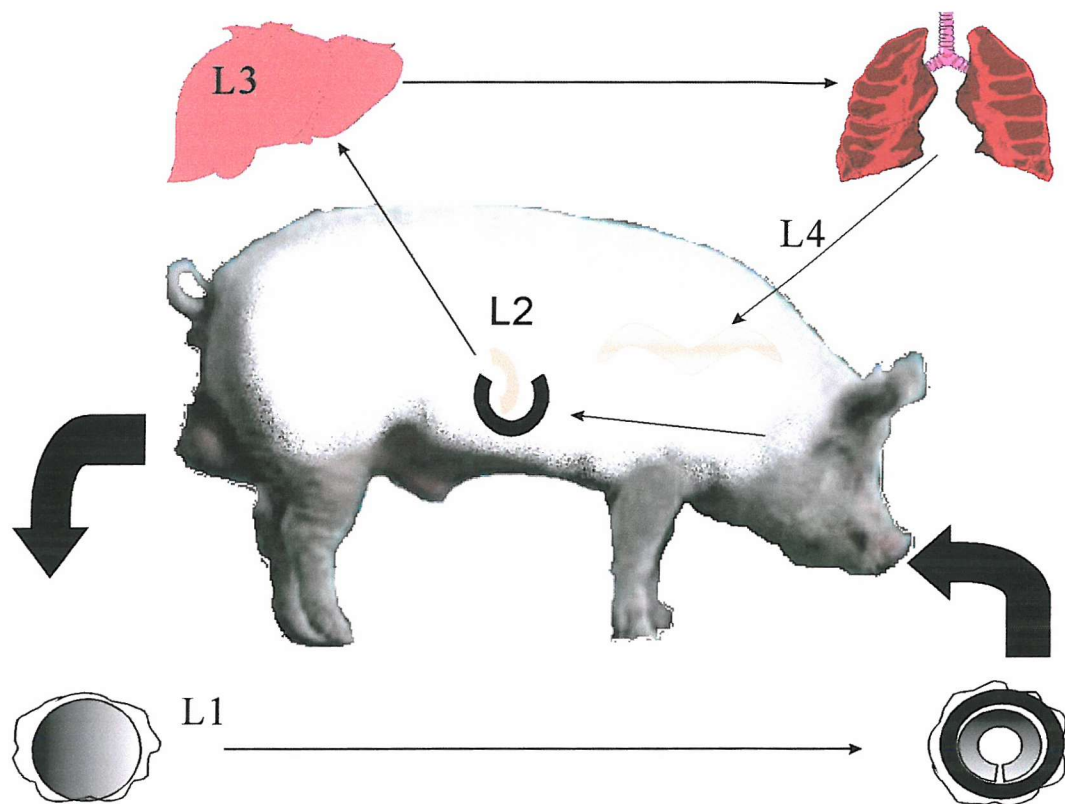


**Fig 1.2. The life cycle of the parasitic nematode *A. suum*.** The four larval stages are shown.

The female *Ascaris* produces up to 200,000 eggs a day. Within the host these eggs are passed in the faeces. The eggs' development then depends on the oxygen tension, moisture content and temperature of their environment. The eggs will then hatch when ingested by the definitive host. Hatching is stimulated by intestinal conditions, mainly of the duodenum but some hatching occurs in the stomach. The larvae which appear have either already moulted (2<sup>nd</sup> stage), or are still within the sheath of their first moult.

Upon hatching the larvae burrow into the mucosa, penetrate blood vessels and migrate to the liver where they appear as 2<sup>nd</sup> stage larvae. Here they develop over a period of two days into 3<sup>rd</sup> stage larvae. These larvae then continue to the heart where, via the pulmonary arteries, they are carried to the lung. The larvae break out of the lung capillaries into the alveoli and migrate up towards the pharynx. Here they are swallowed and return to the intestine where they begin their 3<sup>rd</sup> moult into mature adult worms (Fig 1.2).

### 1.3 *C. elegans*.

*C. elegans* is a small (1mm) free living member of the rhabditid nematode family (Fig 1.3). It is non parasitic and is found in the soil of most temperate climates, feeding primarily on bacteria. There are two sexes, a self-fertilising hermaphrodite and the male.

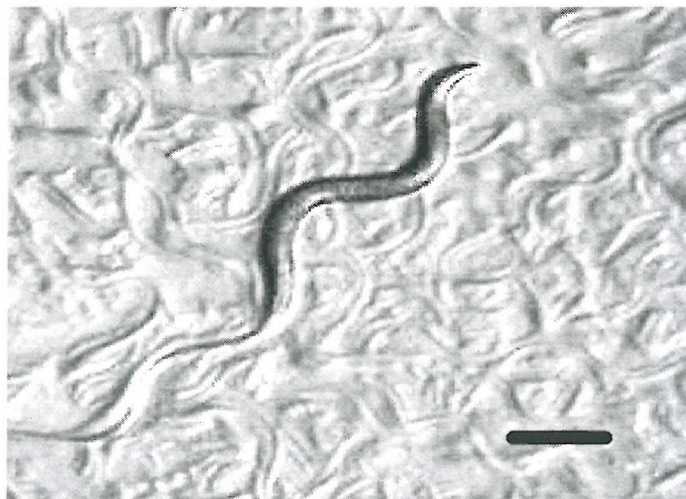


**Fig 1.3 The free living non parasitic nematode *C. elegans*.** *C. elegans* are grown on nematode growth media plates seeded with *E-coli*. *C. elegans* movement through these *E. coli* seeded plates results in characteristic 'S shaped' tracks seen in the above example. The scale bar is 200 $\mu$ m.

### 1.3.1 *C. elegans* life cycle.

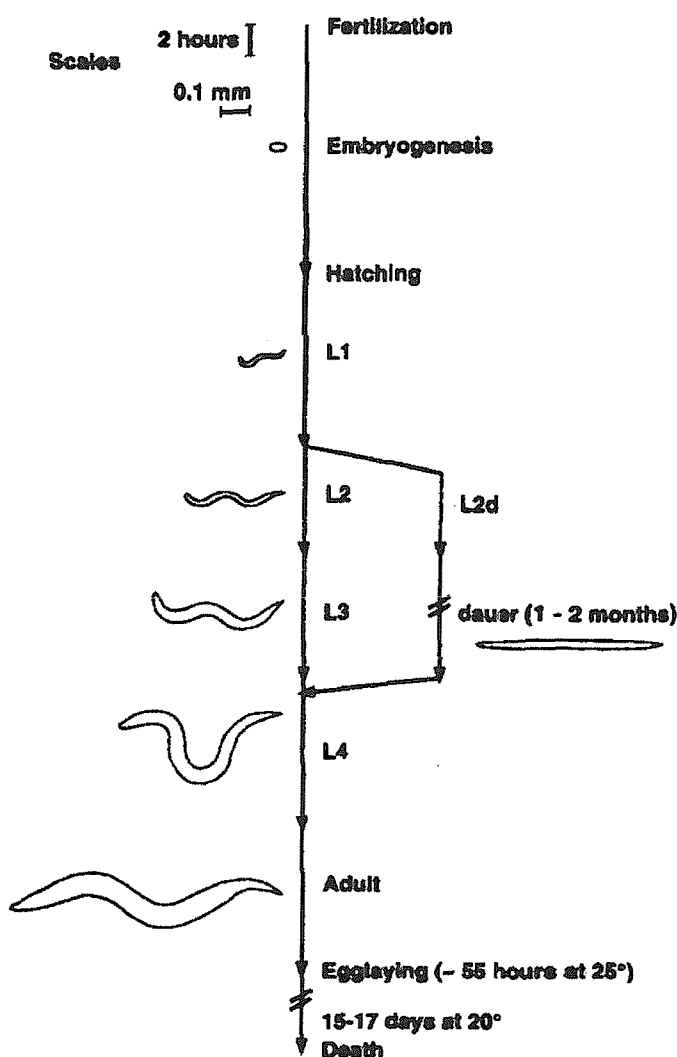


**Fig 1.4 The life cycle of the free-living nematode *C. elegans*.** The four larval stages (L1-4), the adult stage and the dauer stage are shown.

A single self-fertilising *C. elegans* hermaphrodite can produce around 280 hermaphrodite progeny, or up to 1000 hermaphrodites and males when mated with males. *C. elegans* have a rapid life cycle. Embryogenesis lasts 14 hours, post-embryonic development lasts 36 hours through which *C. elegans* develops through 4 larval stages L1 to L4 at 25 °C (Sulston & Horvitz, 1977; Sulston *et al.*, 1983) until they reach adulthood. *C. elegans* can then live for 17 days. Fertilised eggs develop in the hermaphrodite *C. elegans* for several hours. Eggs are then laid in bursts over a 7 day period. The eggs then develop over a period of 14 hours (25 °C)

to the L1 stage. The hatched larvae then rapidly grow through a series of moults, to become adults. The size and shape of *C. elegans* does not vary greatly until adulthood is reached.

If food is limited in early development, *C. elegans* take an alternative developmental pathway at the L2/L3 molt to produce the dauer larval stage. This dauer L3 stage does not feed and can survive for up to 3 months, without further development. If food later becomes available the dauer stage will develop to L4 larval stage and continue development as normal.

### **1.3.2 *C. elegans* as a useful biological model for study.**

The use of *C. elegans* as a genetic model organism developed from the ideas of Sydney Brenner (Brenner, 1974). He was interested in discovering how a simple nervous system becomes correctly connected during development. This task appeared impossible to investigate in complicated organisms like humans and mice. He believed that with *C. elegans*, due to its small size (959 cells) and transparency (developing cells can be seen and tracked) this problem could potentially be solved.

*C. elegans* also provided a way for Brenner to extend current molecular biological techniques (which at that time used bacteria and bacterial viruses) into other fields of biology. *C. elegans* were ideal for molecular studies as they were easily cultivated, could be grown in large numbers, had a short life cycle and sexual propagation was independent of population size in the self-fertilising hermaphrodite. The availability of males which can also fertilise the hermaphrodites meant stocks could be constructed by genetic crosses.

In 1998 the complete genome sequence for *C. elegans* was published, following an eight year collaborative effort between the Genome Sequencing Centre in St Louis, USA and the MRC Sanger Centre in Cambridge. The *C. elegans*' genome size is 97 megabases, contained within six chromosomes. The genome sequence predicts 19427 protein coding genes (3 times more than found in yeast and 5000 more than found in *Drosophila* and two-thirds of the number determined in humans). *C. elegans* has smaller and fewer introns than mammalian counterparts

and gene density is high (Blumenthal & Thomas, 1988). 58% of the genes appear to be nematode specific. 40% of the genes find significant matches in other organisms.

In 1998, approximately 7000 of the 19000 genes contained within the *C. elegans* genome had been assigned a function (Pennisi, 1998). Since then the use of reverse genetics has been prevalent, where it was shown that the introduction of double-stranded RNA (dsRNA) into a hermaphrodite worm resulted in a potent and specific inactivation of an endogenous gene with the corresponding sequence (Timmons & Fire, 1998). This technique, known as RNA interference (RNAi), has made it even easier to determine gene function within *C. elegans*. In a study by (Kamath *et al.*, 2003), 86% of the 19427 predicted *C. elegans* genes were investigated using RNAi, of these 10% showed a phenotype.

A number of different techniques have been developed to induce RNAi in *C. elegans*. dsRNA which matches the gene can be injected into *C. elegans* oocytes. *C. elegans* can be fed on bacteria that synthesise the dsRNA (Timmons *et al.*, 2001). *C. elegans* can also be soaked in dsRNA-containing solution (Tabara *et al.*, 1998). The specificity and potency of RNAi makes it ideal for investigating gene function beginning with only the genomic sequence. Strains that are more susceptible for RNAi, which are deficient in a RNA dependent RNA polymerase (*rrf-3* *C. elegans*), have made it easier to identify gene function in neurones (Simmer *et al.*, 2002). A recent whole genome screen using RNAi on *rrf-3* *C. elegans* identified that 23% of the predicted *C. elegans* genes showed a phenotype (Simmer *et al* 2003) compared with 10% for wild type (Kamath *et al.*, 2003).

#### **1.4 General nematode anatomy.**

Nematodes are made up of two concentric cylinders separated by a fluid-filled space, the pseudocoelom (Fig 1.5 A). The outer cylinder is coated in an extracellular collagenous cuticle and contains the nematode's musculature. This is arranged in four longitudinal strips and is attached to the cuticle via a thin strip of hypodermis. The outer cylinder also contains the nervous system (dorsal and ventral nerve cords) and an excretory / secretory system. The inner cylinder contains the pharynx and the intestine.

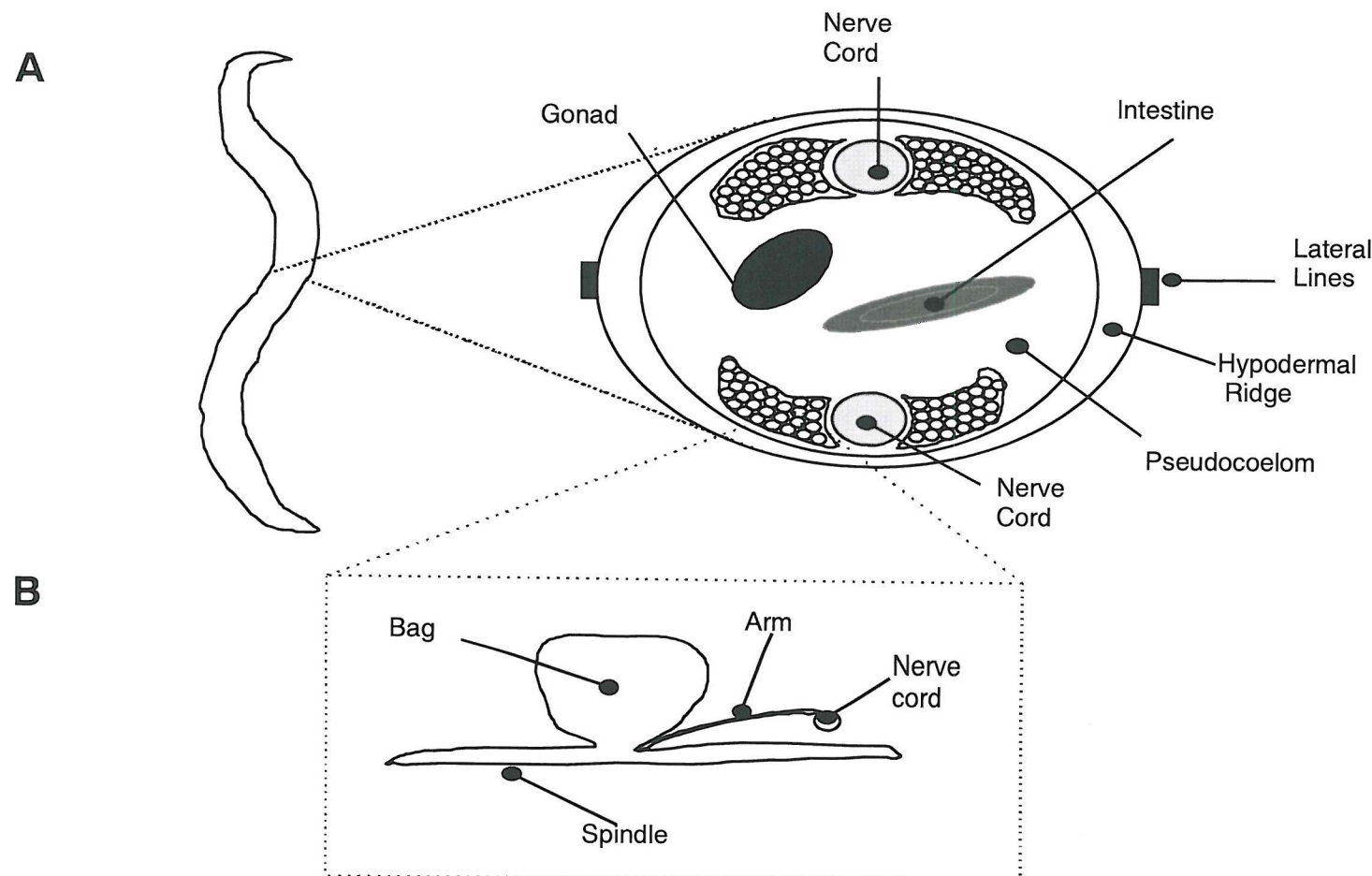


**Fig 1.5: General nematode anatomy based on *A. suum*. A. Cross section through *A. suum*. B. The neuromuscular system of *A. suum*.**

### 1.4.1 Body wall muscle.

Nematode movement requires coordinated relaxation and contraction of muscle cells. Nematode muscle cells have been extensively studied in *A. suum*. Muscle cells consist of three main functional parts, the bag (or belly) (Cappe de Baillon, 1911) the spindle, and the muscle arm (Fig1.5B). The bag, which lies in the perienteric space, is 200 $\mu$ m in diameter and contains the nucleus and particulate glycogen (Rosenbluth, 1965b). The bag structure is only present in larger nematodes as it is required to maintain its rigid structure, enabling muscle contraction and movement to occur (Harris & Crofton, 1957).

The spindle contains the actin and myosin contractile machinery. The muscle striations are arranged in an obliquely striated pattern (Rosenbluth, 1965a). They form an acute angle rather than the usual 90° angle of mammalian skeletal muscle. This obliquely striated organisation allows *A. suum* muscle to have greater extensibility (like smooth muscle) but maintain the velocity of contraction that is associated with skeletal muscle.

*A. suum* muscle cells send projections from the base of the muscle bag to make synaptic contact along the longitudinal nerve cord. Each muscle cell has on average 2.7 arms (Stretton, 1976). These arms, at the nerve cord, branch into a number of fine processes (fingers). Adjacent arms can become joined via tight junctions (Rosenbluth, 1965b) and this joining allows electrical coupling between adjacent cells (De Bell *et al.*, 1963).

### 1.4.2 Pharyngeal muscle.

In order to feed, nematodes transport food from the mouth to the intestine via a neuromuscular tube, named the pharynx. The pharynx acts as a pump to generate enough pressure to force food into the intestine. This force is required because the interior of the nematode is at a higher pressure compared to the surrounding environment (Harris & Crofton, 1957). The pharynx also acts to concentrate food particles allowing for efficient absorption and digestion.

The anatomy of the nematode pharynx has been extensively studied in *C. elegans*. The pharynx is composed of 34 muscle cells, 9 marginal cells, 9 epithelial cells, 5 gland cells and 20 neurones (Albertson & Thomson, 1976). It can be divided into three functional parts. From the anterior (mouth) to the posterior (intestine) end are the corpus, (which is further divided into the procorpus and metacorpus), the isthmus and the terminal bulb. The pharynx consists of 8 muscle types. Five are large muscle types (pm3,4,5,6, and 7). Three are small muscle types (pm1,2 and 8). Pm 1 through to 4 constitutes the anterior half of the pharynx. Pm5 constitutes the middle part of the pharynx (the isthmus). Pm6 through to 8 constitutes the posterior end of the pharynx (the terminal bulb). Muscles are arranged with triradiated symmetry, forming a Y shape around the pharyngeal lumen. When these muscles contract the pharyngeal lumen opens forming a triangular shape.

In order for normal feeding to occur two motions, pumping and isthmus peristalsis, must occur. This action allows food to enter the pharyngeal lumen, to be ground up and to then pass into the intestine (Doncaster, 1962; Seymour *et al.*, 1983). Pumping consists of a near-simultaneous contraction of the muscle of the corpus and anterior isthmus. This opens the lumen and allows liquid (containing bacteria) to flow into the corpus. The posterior isthmus however remains relaxed (closed), therefore, the bacteria remains trapped in the corpus. Relaxation of the corpus and anterior isthmus then occurs, expelling liquid back out of the mouth but retaining bacteria within the corpus (Doncaster, 1962). Isthmus peristalsis then transports bacteria from the corpus to the terminal bulb. This occurs after every fourth pump (Avery & Horvitz, 1987) The terminal bulb then acts to grind and break up bacteria which then pass into the intestine through the opened pharyngeal-intestinal valve (Doncaster, 1962) (Fig 1.6).

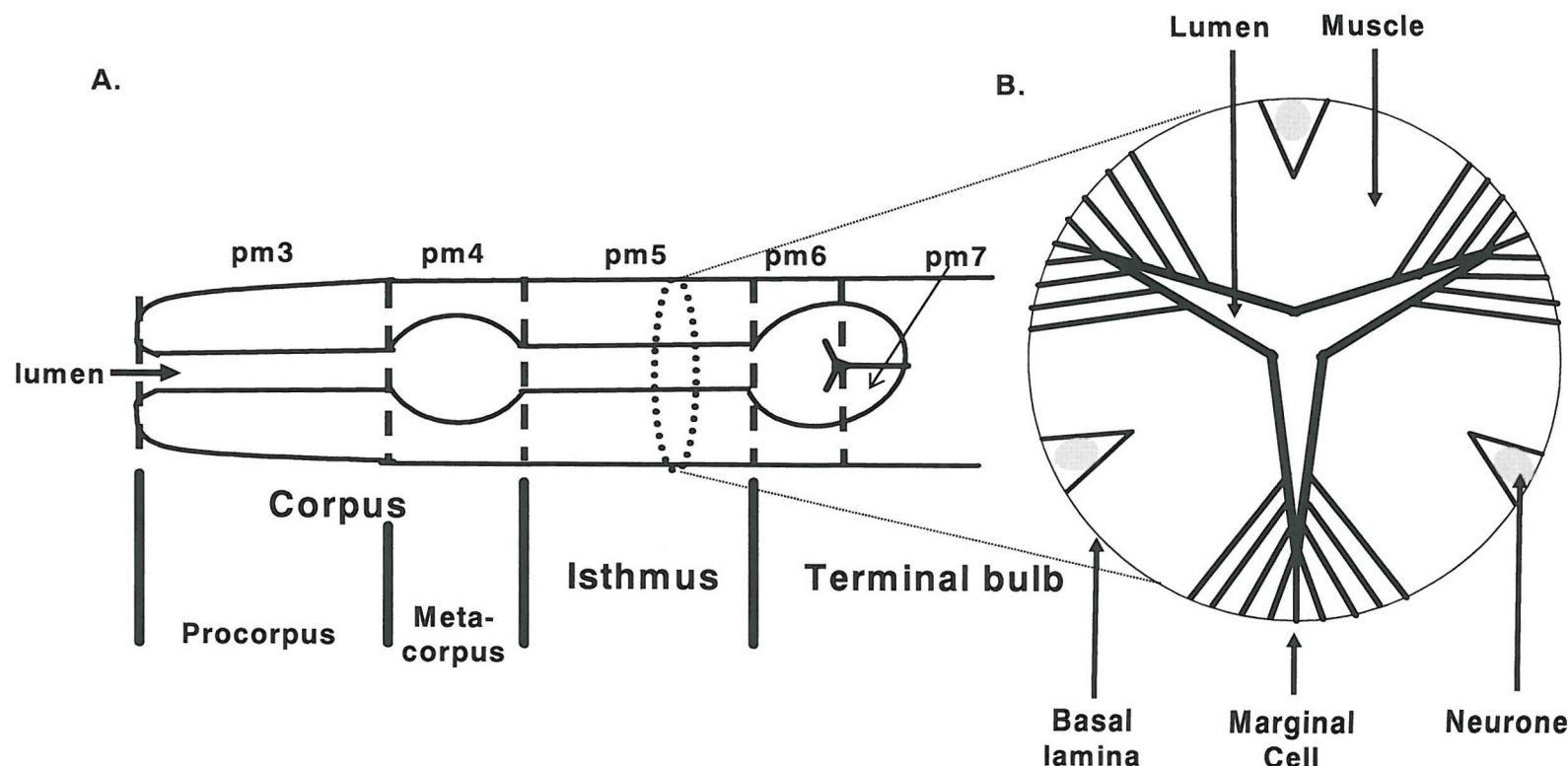


**Fig 1.6 Diagram illustrating the pharyngeal anatomy of *C. elegans*. A.** Lateral view. (Anterior to the left). The three functional parts of the pharynx are shown, the corpus (divided into the pro and metacorpus), the isthmus and the terminal bulb. The position of the large muscle types (pm3-7) are shown. **B.** Transverse section through the pharynx. Three muscle cells surround the pharyngeal lumen. When contraction occurs the lumen opens. Between the muscle cells and the apices of the lumen are three marginal cells. Embedded within the grooves of the basal membranes of the muscle cells are neurones (adapted from (Albertson & Thomson, 1976; Avery & Horvitz, 1989; Raizen & Avery, 1994))

## 1.5 The nervous system of the nematode.

Initial work on identifying the important features of the nematode nervous system used *A. suum*. There are only a small number of neurones present in *A. suum*, (298) (Goldschmidt, 1908), and they appear to have the same structure and position within each individual animal. The nervous system of *C. elegans* is nearly identical in terms of neurones, their morphology and positioning. *C. elegans* contain 302 neurones (White *et al.*, 1983), which interconnect in a reproducible manner to form a variety of neural circuits and pathways.

### 1.5.1 Central nervous system.

The arrangement and type of neurones within both *A. suum* and *C. elegans* are largely homologous. Most of the nematode nervous system is situated in the head and is organised around the circumpharyngeal ring. The head also contains sensory receptors which project their endings towards the mouth. The cell bodies for the sensory receptors, together with the interneurones and some motor neurone cell bodies, are situated between the corpus and terminal bulb of the pharynx. These cells send out processes that run circumferentially around the pharynx as a fibre bundle forming the nerve ring, which forms the major neurophile in the animal. A large number of the processes in the nerve ring enter and leave on the ventral side forming the ventral nerve cord (White *et al.*, 1976). In *C. elegans* some 5000 chemical synapses, 600 gap junctions and 2000 neuromuscular junctions have been described (White *et al.*, 1986). Indeed, genetic analysis has shown a number of basic neurobiological mechanisms such as synaptic release (Nonet *et al.*, 1993;Nonet *et al.*, 1998;Richmond *et al.*, 1999) and second messenger systems (Gross *et al.*, 1990;Mendel *et al.*, 1995), (Miller *et al.*, 1999;Nurish, 2002) conserved with the worm and more complex organisms.

### 1.5.2 The motor nervous system.

The anatomy and physiology of the *A. suum* motoneurones was described by (Stretton *et al.*, 1978). (White *et al.*, 1983) later showed that *C. elegans* also contains equivalent motoneurone classes.

The nematode motorsystem is divided into five segments each containing 11 motoneurones and 6 non-segmental interneurones which were shown to traverse the segments (Stretton *et al.*, 1978). All but two dorsal nerve fibres arise from commissures (neurones which link the dorsal and ventral nerve cords) which in turn arise from branches of cells whose processes begin within the ventral cord. The 2 dorsal fibres which do not arise from the commissures originate directly from the cranial nerve ring. The commissural neurones have their cell bodies within the ventral cord. There are no cell bodies present within the dorsal nerve cord.

From their morphology the segmental neurones can be differentiated from each other by the branching pattern of their processes. The 11 motoneurones identified in each segment form seven distinct types. Three types, namely D1 DE2 and DE3, are represented once in each segment. The remaining four types, namely VI, DE1, V-1 and V-2, occur twice in each segment. All, apart from V-1 and V-2, have commissures which project from the ventral cord to the dorsal cord. These commissures project out from the ventral cord to the right apart from DE-3 which has a left projecting commissure. (Fig 1.7)

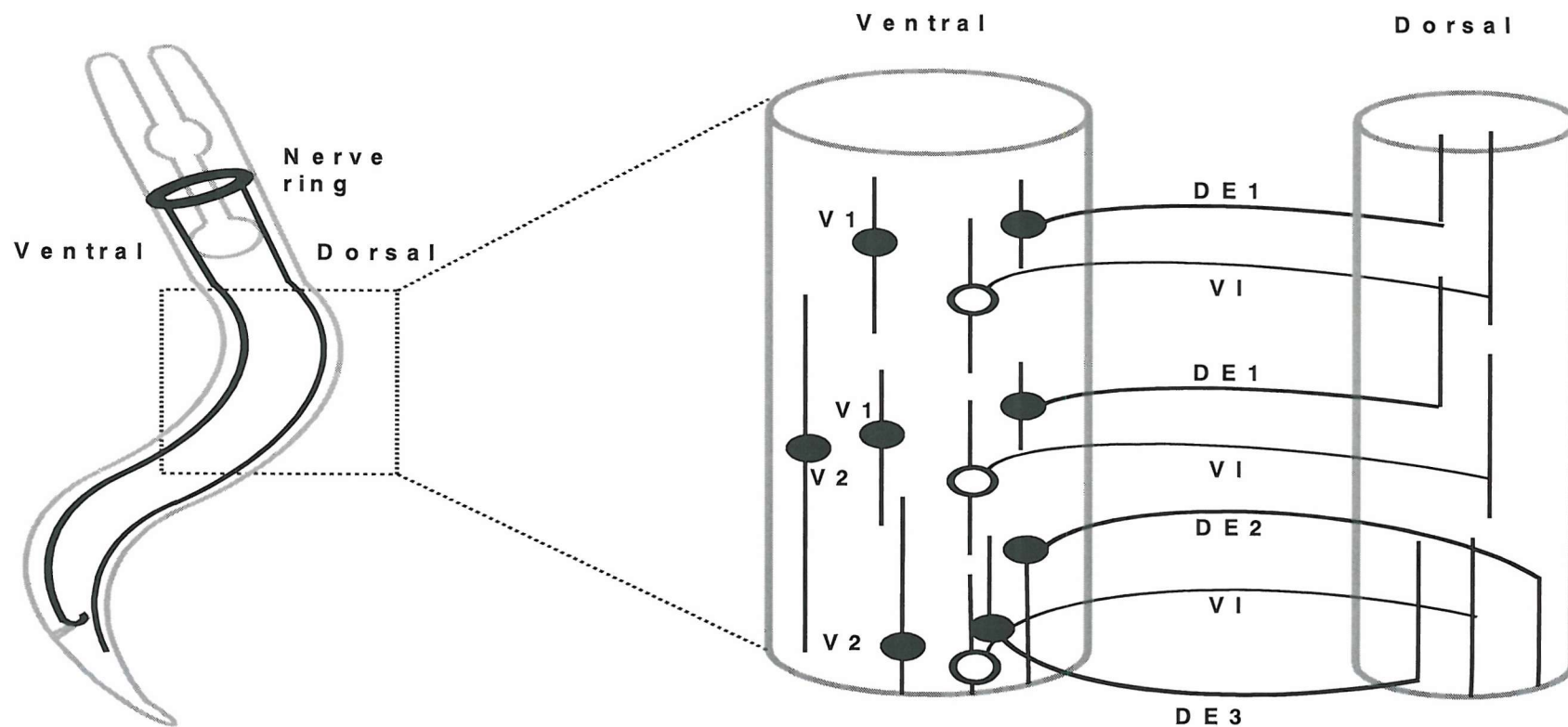


**Fig 1.7 Organisation of motorneurons (in one segment) in nematodes.** There are 3 right hand and 1 left hand commissures, which connect the ventral and dorsal nerve cord. The commissures have their cell bodies in the ventral nerve cord. Interneurones project between the segments. There are seven anatomically different types of motorneurone (which are either E, excitatory or I, inhibitory) DE1 (dorsal excitor);DE2, (dorsal excitor);DE3,(dorsal excitatory); DI (dorsal inhibitor); VI (ventral inhibitor), V1 and V2 ventral (excitatory) motorneurones. Adapted from (Martin *et al.*, 1991)

### 1.5.3 Neuronal control of movement.

Nematodes move in a characteristic sinusoidal pattern. In order for this pattern to be achieved dorsal and ventral muscle contraction must be out of phase (as dorsal muscle contracts the ventral muscle must relax). This alternating pattern of muscle contraction and relaxation is achieved by excitatory and inhibitory motoneurone interaction.

Electrical stimulation of single motoneurones and recording the response in the motoneurones muscle field in *A. suum*, showed that DI and VI were inhibitory and DE1-3, V1 and V2 were excitatory (Stretton *et al.*, 1978). Further histological and immunoreactivity studies have shown that the excitatory transmitter acetylcholine (ACh) is present in the DE1-3 and V1 and V2 neurones (Johnson & Stretton, 1985), and the inhibitory transmitter  $\gamma$ -amino butyric acid (GABA) is present in the VI and DI neurones (Johnson & Stretton, 1987).

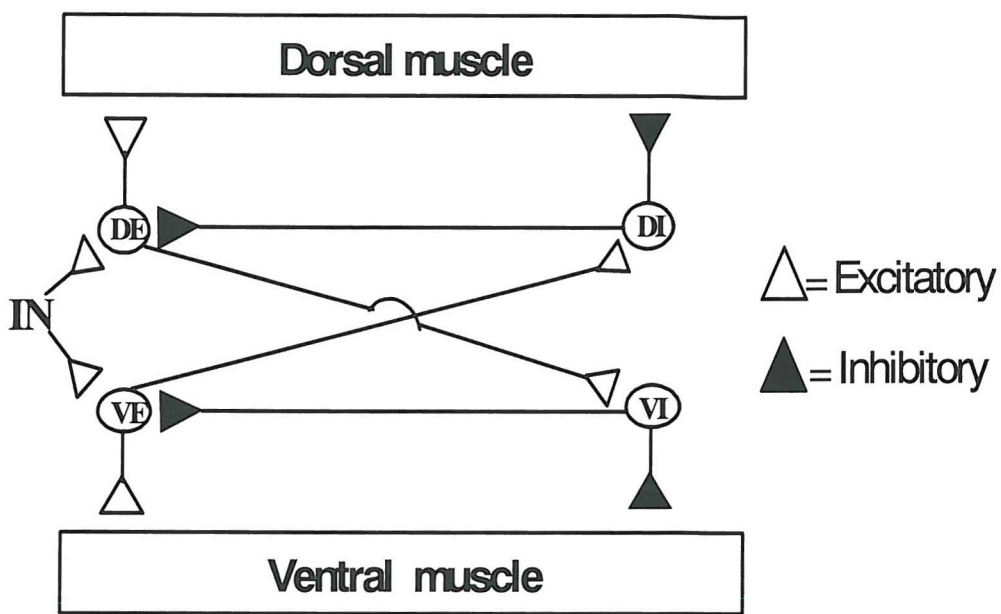


**Fig 1.7 Simplified neuronal circuit diagram controlling locomotion in *A. suum*** (Stretton *et al.*, 1978). DE denotes dorsal excitatory neurone. DI denotes dorsal inhibitory neurone. VE denotes ventral excitatory neurone. VI denotes ventral inhibitory neurone. IN denotes interneurone.

As a result of these discoveries a circuit diagram for nematode locomotion was proposed (Fig 1.7). The dorsal motorneurone DE synapses with both VI and the dorsal muscle itself. Stimulation of DE (from an excitatory large interneurone) causes excitation of the dorsal muscle directly (causing contraction), and excitation of VI. VI stimulation results in inhibition of both the ventral muscle (resulting in relaxation directly) and the excitatory motorneurone VE. The resulting relaxation of ventral muscle and contraction of dorsal muscle allows the worm to bend. VE is then stimulated by an excitatory interneurone allowing contraction of ventral muscle and relaxation of dorsal muscle in the same way. This alternating reciprocal pattern of excitation and inhibition of dorsal and ventral muscle allows the sinusoidal pattern of movement.

#### 1.5.4 Pharyngeal nervous system.

The *C. elegans* pharynx is isolated from the rest of the animal by a basement membrane. The pharyngeal nervous system contains 20 neurones which are made up of 14 anatomical types. They are divided into six bilaterally symmetrical pairs

and eight unpaired neurones. Communication between the pharyngeal nervous system and the extrapharyngeal nervous system occurs via bilateral GAP junctions between the extrapharyngeal RIP neurones and the pharyngeal I1 neurones (Avery & Horvitz, 1989). Dissection of the pharynx, and thus removing extrapharyngeal and pharyngeal nervous system interaction, has no effect on pharyngeal behaviour or electrophysiology (Avery *et al.*, 1995). The nervous system controlling pharyngeal activity is therefore a self-contained unit. A wiring diagram of the pharynx is shown in Fig 1.8

Laser ablation of all 20 neurones does not fully inhibit pharyngeal pumping, thus the pharynx is said to be myogenic (Avery & Horvitz, 1989). However, of the 20 neurones controlling pharyngeal function, 3 neurones M4, M3 and MC are required for normal pharyngeal activity. Nearly normal feeding occurs following laser ablation of all other pharyngeal neurones (Avery & Horvitz, 1989; Raizen *et al.*, 1995). Only M4 appears essential for normal development as *C. elegans* has been shown to be fertile and viable following laser ablation of all the other 19 neurones (Avery & Horvitz, 1989). M4 processes synapse onto the posterior m5 muscle of the isthmus (Albertson & Thomson, 1976). Laser ablation of M4 means that the posterior region of the isthmus remains closed resulting in bacteria being trapped in the corpus (Avery & Horvitz, 1987). The closed state of the isthmus means food does not enter the intestine and the worms starve. Positive antibody staining against choline acetyltransferase and the ACh synaptic vesicle transporter in the M4 neurone suggests ACh is released from M4 (Alfonso *et al.*, 1994).

The two M3 neurones, along with the I5 neurone are important for effective transport of bacteria within the pharyngeal lumen (Avery, 1993). The M3s are located at the corpus-isthmus boundary. They have sensory endings in the posterior corpus and motor output to the corpus and anterior isthmus. These sensory endings have processes that project to under the cuticle of the lumen and serve a mechanosensory function. They sense the contraction of the pharynx and so stimulate its relaxation (Albertson & Thomson, 1976). M3s can thus control the timing of pharyngeal relaxation (Avery, 1993). M3 was shown to form fast inhibitory glutamatergic neuromuscular synapses (Dent *et al.*, 1997).

The MC neurone is the main excitatory neurone necessary for rapid pumping as laser ablation of MC neurones in *C. elegans* grown in bacteria has been

shown to result in a reduction in pharyngeal pumping (Avery & Horvitz, 1989)). Stimulation of MC results in release of ACh (Raizen *et al.*, 1995). *C. elegans* with deficient ACh synthesis has severely reduced pumping rates (Avery & Horvitz, 1990).

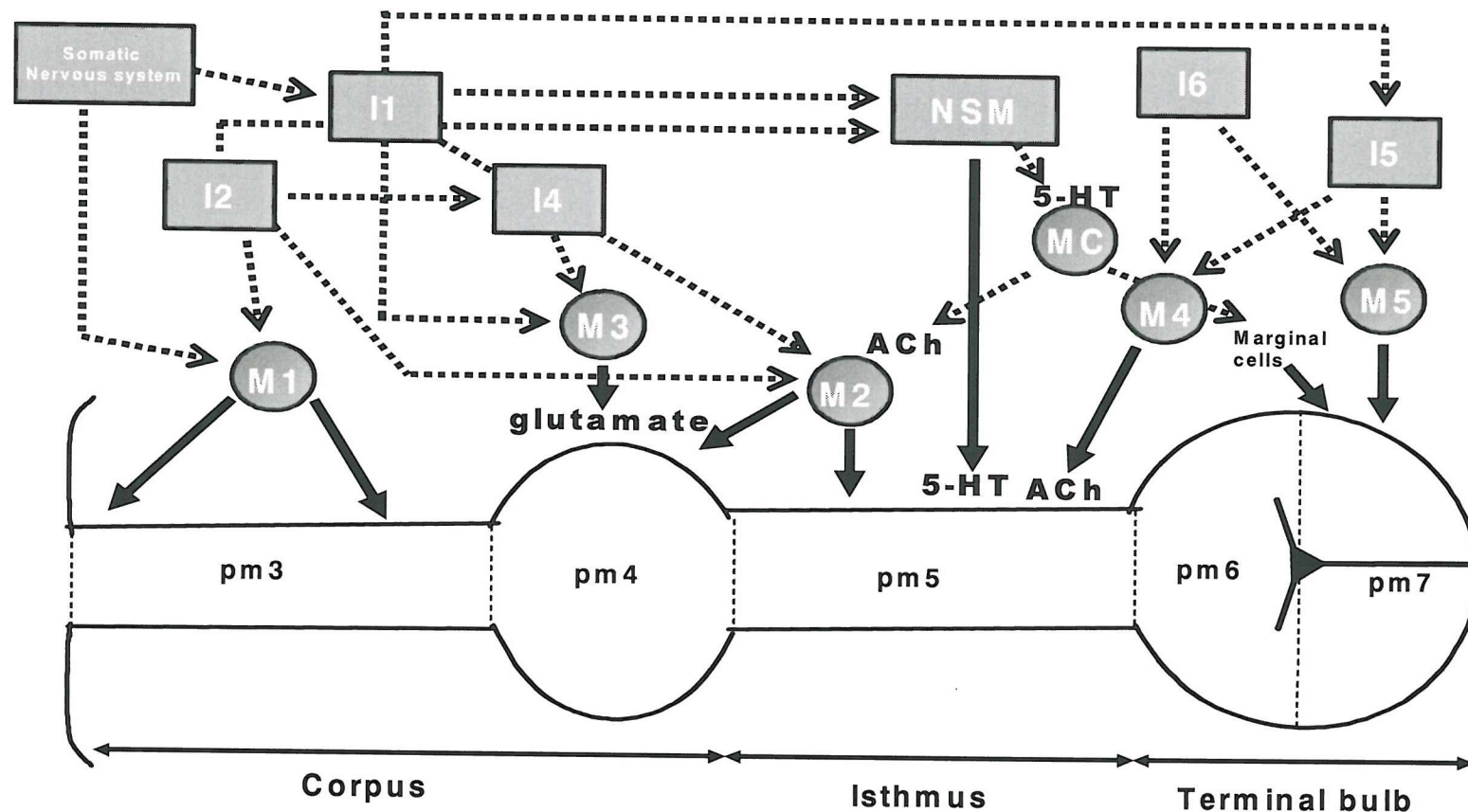


Fig 1.8 Wiring Diagram of the *C. elegans* pharynx. See text for detail (Albertson & Thomson, 1976).

## **1.6 Control of pharyngeal and body wall muscle by neurotransmitters and neuromodulators.**

The activity of body wall and pharyngeal muscle is controlled by a number of different neurotransmitters and neuromodulators (Walker *et al.*, 2000). The main excitatory transmitter effecting body wall muscle in nematodes is ACh (Johnson & Stretton, 1985; Walker *et al.*, 1992), (Richmond & Jorgensen, 1999) and the main inhibitory transmitter is GABA (Johnson & Stretton, 1987; Walker *et al.*, 1992; Richmond & Jorgensen, 1999). 5-Hydroxytryptamine (5-HT) does not affect the muscle directly but does inhibit ACh induced contraction (Trim *et al.*, 2001) in *A. suum*. In the pharynx, ACh and 5HT (Avery & Horvitz, 1990) both increase pharyngeal pumping in *C. elegans*, and GABA, glutamate (Pemberton *et al.*, 2001), octopamine and dopamine (Rogers *et al.*, 2001) inhibit pharyngeal pumping. A number of neuro-active peptides, the FaRPs (FMRFamide-Related Peptides and FLPs (FMRFamide-Like Peptides), have also been shown to cause either excitation or inhibition of body wall and pharyngeal muscle (Rogers *et al.*, 2001).

## **1.7 Neuroactive peptides in nematodes.**

Neuropeptides have been found throughout the animal kingdom, where they play diverse roles in the nervous system. FaRPs and FLPs are the most widely studied family of invertebrate regulatory peptides. These structurally-related peptide molecules most likely occur ubiquitously in invertebrate nervous systems (Walker *et al.*, 2000). Immunoreactivity to neuropeptides is widespread in nematode nervous systems, suggesting that neuropeptides are important in the neurosignalling of nematodes. The first presumptive peptidergic neurones were identified in *Acanthocheilonema viteae*, *A. suum*, *Brugia pahangi*, *Haemonchus contortus* and *Phocanema decipiens* (Davey, 1966);(Rogers, 1968). Since then extensive peptide immunoreactivity has been demonstrated in nervous tissues of *A. suum*, (Stretton *et al.*, 1991;Brownlee *et al.*, 1993) and *C. elegans* (Li & Chalfie, 1986), as well as other nematode species (Maule *et al.*, 1996;Brownlee *et al.*, 2000).

### 1.7.1 Neuroactive peptides in *A. suum*.

Peptide isolation in *A. suum* has revealed a family of about 20 *A. suum* FMRFamide-like neuropeptides. Many of these peptides have been shown to affect the contractile state of *A. suum* body wall muscle. Peptides isolated from other nematode species have also been shown to affect *A. suum* muscle. These are summarised in table 1.

Peptide	Sequence	Effects on <i>Ascaris</i> Muscle.
AF1	KNEFIRFa	Biphasic – Relaxation followed by increased muscle contractility. (Pang <i>et al.</i> , 1995)
AF2	KHEYLRFa	Biphasic – Similar to AF1 but higher potency. (Pang <i>et al.</i> , 1995)
AF3	AVPGVLRFa	Contraction. (Trim <i>et al.</i> , 1997)
AF4	GDVPGVLRFa	Contraction. (Trim <i>et al.</i> , 1997)
AF8	KSAYMRFa	Contracts ventral muscle. Relaxes dorsal muscle. (Maule <i>et al.</i> , 1994)
PF1	SDPNFLRFa	Slow relaxation. Results in a flaccid paralysis. (Franks <i>et al.</i> , 1994)
PF2	SADPNFLRFa	Similar effects to PF1 (Franks <i>et al.</i> , 1994)
PF4	KPNFIRFa	Rapid Relaxation. (Maule <i>et al.</i> , 1996)

Table 1.1 FMRFamide peptides that affect *A. suum* body wall muscle.

These compounds act either directly on the body wall muscle to change its tension, or indirectly by affecting the ACh-induced contractions or GABA-induced relaxations of *A. suum* muscle. The FaRPs can greatly affect the activity of the *A. suum* muscle. Understanding where and how these peptides act on *A. suum* muscle may be important in developing novel anthelmintics to mimic the action of these peptides.

The two peptides AF1 (KNEFIRFamide) and AF2 (KHEYLRFamide) have, when applied to *A. suum* dorsal muscle strips been shown to cause biphasic activity. They cause a relaxation followed by a slow contraction of the muscle (Pang *et al.*, 1995). There is also an increase in the frequency of rhythmic contractions and

relaxations of the muscle and the excitatory effect can last for over an hour. From these observations AF2 could be acting both pre and post-synaptically (Pang *et al.*, 1995). Post-synaptically, AF2 may be increasing the probability of generating action potentials within muscle cells. Pre-synaptically, AF2 may be acting to stimulate the excitatory motoneurones causing an increase in the release of ACh. AF2 may also be acting to inhibit the inhibitory motoneurones, thus decreasing GABA release. Although a receptor for AF2 has not been identified, a G-protein involvement in AF2-triggered receptor activation has been identified, indicating AF2 may exert its action through a G-protein coupled receptor (Kubiak *et al.*, 2003).

AF3 (AVPGVLRFamide) and AF4 (GDVPGVLRFamide) also cause a slow contraction of muscle similar to that of AF1 and AF2. Unlike AF1 and AF2, AF3 and AF4 do not stimulate any rhythmic contractions and only occasionally is the contraction preceded by an initial relaxation. AF3 and AF4 are not blocked by the nicotinic receptor antagonist mecamylamine (Trim *et al.*, 1997).

Other peptides from *Panagrellus redivivus* have also been shown to act on *A. suum* muscle. The peptides PF1 (SDPNFLRFamide) and PF2 (SADPNFLRFamide) cause a slow relaxation of *A. suum* dorsal muscle (Franks *et al.*, 1994). PF1 causes a slow chloride-independent hyperpolarisation of somatic muscle cells. PF1 may act via potassium channels as both the potassium channel blockers tetraethylammonium (TEA) and 4-aminopyridine (4AP) inhibit the action of PF1 (Franks, 1996). PF1 also has both pre and post-synaptic actions. PF1 inhibits the excitatory junction potentials (EJPs) at the neuromuscular junction, without affecting the depolarisation of muscle cells caused by exogenous additions of ACh (Holden-Dye *et al.*, 1995). This is consistent with a pre-synaptic effect. Evidence for a post-synaptic effect of PF1 comes from the fact that PF1 inhibits the contraction elicited by exogenously applied ACh (Franks *et al.*, 1994).

PF4 (KPNFIRFamide) also causes a relaxation of muscle, however, unlike PF1 and PF2, this relaxation occurs at a relatively fast rate (Maule *et al.*, 1996). PF4 was also shown to potently affect the membrane potential of muscle cells. PF4 was three orders of magnitude more potent than GABA at producing inhibition (Holden-

Dye *et al.*, 1997). The hyperpolarisation of PF4 consists of two phases, the first of which is chloride-dependent. PF4 does not act to stimulate the release of GABA since the anthelmintic ivermectin blocks the inhibitory GABA response on *A. suum* muscle but not the response to PF4 (Holden-Dye *et al.*, 1997). Therefore, there is a high possibility that a receptor for PF4 on *A. suum* muscle is allowing this fast-acting inhibitory action. The presence of an obvious endogenous PF4 -like peptide within *A. suum* has yet to be identified.

### **1.7.2 Neuropeptides in *C. elegans*.**

The completion of the genomic sequence of *C. elegans* enabled the identification of neuropeptide like genes in *C. elegans*. 22 *flp* (FMRFamide like peptides) genes were identified ( Li *et al.*, 1999a; Li *et al.*, 1999b; Nelson *et al.*, 1998a). The *flp* genes potentially encode 59 different FaRPs (summarised in Table 2). 32 neuropeptide like protein (nlp) genes have also been identified (Nathoo *et al.*, 2001). It has been predicted that these code for a further 151 putative neuropeptides in *C. elegans*.

Gene	Peptide Sequence
<i>flp-1</i>	SADPNFLRFa SQPNFLRFa ASGDPNFLRFa SDPNFLRFa AAADPNFLRFa PNFLRFa AGSDPNFLRFa
<i>flp-2</i>	SPREPIRFa LRGEPIRFa
<i>flp-3</i>	SPLGTMRFa TPLGTMRFa EAEEPLGTMRFa NPLGTMRFa ASEDALFGTMRFa EDGNAPFGTMRFa SAEPFGTMRFa SADDSAPFGTMRFa NPENDTPFGTMRFa
<i>flp-4</i>	PTFIRFa ASPSFIRFa
<i>flp-5</i>	GAKFIRFa AGAKFIRFa APKPKFIRFa
<i>flp-6</i>	KSAYMRFa (x6)
<i>flp-7</i>	SPMQRSSMVRFa (x3) TPMQRSSMVRFa (x2) SPMERSAMVRFa SPMDRSKMRFa
<i>flp-8</i>	KNEFIRFa (x3)
<i>flp-9</i>	KPSFVRFa (x2)
<i>flp-10</i>	QPKARSGYIRFa
<i>flp-11</i>	AMRNALVRFa ASGGMNRNALVRFa NGAPQPFVRFa
<i>flp-12</i>	RNKFEFIRFa
<i>flp-13</i>	SDRPTRAMDSPLIRFa AADGAPLIRFa APEASPIRFa ASPSAPLIRFa SPSAVPLIRFa ASSAPLIRFa
<i>flp-14</i>	KHEYLRFa (x4)
<i>flp-15</i>	GGPQGPLRFa RGPSGPLRFa
<i>flp-16</i>	AQTFVRFa (x2) GQTFVRFa
<i>flp-17</i>	KSAFVRFa KSQIRFa
<i>flp-18</i>	EMPGVLRFa EIPGVLRFa SEVPGVLRFa DVPGVLRFa SVPGVLRFa
<i>flp-19</i>	WANQVRFa ASWASSVRFa
<i>flp-20</i>	AMMVRFa (x 2)
<i>flp-21</i>	GLGPRPLRFG
<i>flp-22</i>	SPSAKWMRFG

**Table 1.2** The *flp* genes in *C. elegans* and the potential FaRPs they encode (taken from (Nelson *et al.*, 1998a).

Little information was known about the bioactivity of FMRFamide peptides in *C. elegans*, until advances in electrophysiological recordings from excitable cells

in *C. elegans* (Goodman *et al.*, 1998) (Francis *et al.*, 2003) presented the opportunity to directly determine their action. Initial molecular and genetic studies showed that *flp-1*-deletion phenotypes included hyperactivity and resistance to 5-HT-induced behaviours (Nelson *et al.*, 1998b; Waggoner *et al.*, 2000) indicating that *flp-1* is likely to negatively regulate locomotion. Rogers *et al.*, (2001) showed that a number of FMRFamide peptides effect pharyngeal pumping rates similar to the classical transmitters 5-HT and octopamine. AF1(KNEFIRFamide), AF2 (KHEYLRFamide), AF8 (KSAYMRFamide) and GAKFIRFamide (encoded by the *C. elegans* genes *flp-8*, *flp-14*, *flp-6* and *flp-5* respectively) increased pharyngeal pumping. SDPNFLRFamide, SADPNFLRFamide, SAEPFGTMRFamide, KPSVRFamide, APEASFIRFamide, and AQTVRFamide (encoded by the *C. elegans* genes *flp-1*; *flp-1*; *flp-3*; *flp-9*; *flp-13* and *flp-16* respectively) inhibited pharyngeal pumping.

FaRPs may provide a novel target site for the development of new anthelmintics. Many of the existing anthelmintics work on these inhibitory and excitatory motorneurones, and their synapses at the neuromuscular junction.

## **1.8 Anthelmintics and their sites of action.**

Anthelmintics work by targeting certain channels and receptors together with biochemical processes which are specific to the parasitic nematode, (review (Martin, 1997). Receptors which are targeted by existing anthelmintics include the excitatory ACh receptor and the inhibitory GABA receptor, both of which are found on nematode body wall muscle and are required for nematode movement. The following is a brief account of the four main commercially used anthelmintics.

### **1.8.1 Anthelmintics that act on the ACh receptor.**

The drugs levamisole, pyrantel and morantel all act on the nematode nicotinic ACh receptor (nACh-R). These drugs mimic the action of ACh on *A. suum* muscle cells resulting in a depolarisation and an increased input conductance of the muscle membrane to sodium and potassium ions (Harrow & Gration, 1985) Patch clamp studies have shown that these anthelmintics open non-selective cation

channels. How long this channel opens depends on the anthelmintic used (Harrow & Gration, 1985). This depolarisation of the muscle and consequent over-excitation results in a spastic paralysis of the nematode. Selective toxicity is achieved as these anthelmintics do not significantly affect the vertebrate nAChR (Martin *et al.*, 1997).

nAChR have been well described in vertebrates. The nAChR is composed of a pentameric structure built up from a combination of subunits ( $\alpha(x2)$ ,  $\beta$ ,  $\gamma$  and  $\delta$  (Unwin, 1995). 5 muscle and 12 neuronal subunit isoforms have been identified (Sargent, 1993). Subunits of nAChRs fall into two main catagories  $\alpha$ -subunits, which contribute to ACh binding, and non  $\alpha$ -subunits (Changeux & Edelstein, 1998). nAChR subunits can come together to form homomeric and hetromeric channels. Although nematode nAChRs have similar pharmacological profiles to vertebrate nAChR-s there are some differences.  $\alpha$ -Bungarotoxin does not bind to nematode nAChR-s whereas levamisole is more selective for nematode nAChRs. (Lewis *et al.*, 1980b; Richmond & Jorgensen, 1999).

Over 27 nAChR subunits have been uncovered in *C. elegans* from molecular and genetic screens of the *C. elegans* genome sequence (Mongan *et al.*, 1998; Squire *et al.*, 1995; Fleming *et al.*, 1997; Ballivet *et al.*, 1996; Baylis *et al.*, 1997; Mongan *et al.*, 2002). This is the largest number of nAChR subunits reported for any organism. The subunit composition and stoichiometry of this receptor can vary between different sub-types resulting in functional diversity of nAChRs. Although the subunit composition, and pharmacological profile, of nAChRs in *C. elegans* is not fully understood, levamisole resistant *C. elegans* have provided important information on the subunit composition of the nAChR where this anthelmintic exerts its effects. The *lev-1* and *unc-29* *C. elegans* confer strong resistance to levamisole and code for non  $\alpha$ -subunits whereas *unc-38* codes for an  $\alpha$ -subunit. (Fleming *et al.*, 1997). Ongoing studies to discover the composition and pharmacological profile of the diverse nAChR in *C. elegans* may provide new insights into developing anthelmintics that act on these nAChRs.

### **1.8.2 Anthelmintics that act on GABA-receptors.**

Piperazine is an anthelmintic which acts as a simple GABA agonist. Piperazine opens GABA receptor chloride channels on nematode body wall muscle (Martin, 1997; Holden-Dye *et al.*, 1989). Electrophysiological studies have shown that this anthelmintic causes an increase in chloride ion conductance leading to a hyperpolarisation in the muscle membrane potential and a reduction in excitability. This potentiation of the GABA receptors results in relaxation of the nematode muscle leading to a flaccid paralysis (Del Castillo *et al.*, 1963).

### **1.8.3 The avermectins.**

Avermectins, of which ivermectin, abamectin, doramectin and moxidectin are members work to increase the chloride ion permeability of nerve and muscle membranes of invertebrates. Ivermectin (22,23-dihydroavermectin B1a) paralyzes both the somatic (Kass *et al.*, 1980; Kass *et al.*, 1984) and pharyngeal (Geary *et al.*, 1993; Brownlee *et al.*, 1997) musculature of nematodes with exceptional potency.

In an attempt to identify the molecular target for ivermectin (Cully *et al.*, 1994) used *C. elegans* and the *Xenopus* oocyte expression cloning system. *C. elegans* RNA was injected into *Xenopus* oocytes. A rapidly activating reversible glutamate and an irreversible ivermectin 4"-O-phosphate (IVMPO<sub>4</sub>)-sensitive current were detected. RNA screening and expression in the *Xenopus* oocytes identified that the glutamate-gated chloride channel (GluCl)  $\alpha$  and  $\beta$  subunits were responsible for the rapidly activating reversible glutamate and irreversible IVMPO<sub>4</sub> sensitive current. The GluCl- $\alpha$  or GluCl- $\beta$  expressed individually in *Xenopus* oocytes formed homomeric channels each of which being selectively sensitive to glutamate or IVMPO<sub>4</sub>. GluCl- $\alpha$  was shown to be selectively sensitive to IVMPO<sub>4</sub> (1 $\mu$ M) and GluCl- $\beta$  was shown to be selectively responsive to glutamate (1mM). The co-expression of GluCl- $\alpha$  and  $\beta$  in the *Xenopus* system resulted in changes in the pharmacological responses to glutamate and IVMPO<sub>4</sub>. Mutations in the *avr-15* gene (which lacks a functional GluCl- $\alpha$ 2 subunit) confer strong resistance to ivermectin in the pharynx of *C. elegans* (Avery & Horvitz, 1990; Dent *et al.*, 1997; Pemberton *et al.*, 2001) indicating that the GluCl- $\alpha$ 2 is responsible for the

sensitivity of ivermectin on pharyngeal muscle. GluCl channels appear unique to invertebrate phyla thus explaining the selective toxicity of ivermectin.

#### **1.8.4 The benzimidazoles.**

Benzimidazoles (thiabendazole, mebendazole, fenbendazole) act by binding to  $\beta$ -tubulin. Under normal circumstances these polymerise with  $\alpha$ -tubulin to form microtubule structures inside the cells of nematodes and the host animal (Stryer, 1995). Benzimidazoles were shown to affect intestinal cells causing a loss of cytoplasmic tubules, a loss of transport of secretory vesicles and a failure of intestinal cells to take up glucose.

### **1.9 Anthelmintics and the problem of resistance.**

The over usage of anthelmintics has led to a problem of resistance, where existing drugs lose their efficacy against the parasite (review Sangster, 1996). Anthelmintic resistance has been seen worldwide in the sheep, pig, cattle, and horse industries. *Schistosomicides* resistance has already been seen clinically in humans.

Genetic mutations within the parasitic nematodes' DNA, for example in a gene encoding for a receptor that binds an anthelmintic, causes a reduced efficacy for that anthelmintic. As this nematode is not affected by the drug it survives and is thus able to pass on this mutation and subsequent resistance.

#### **1.9.1 Levamisole resistance.**

Levamisole mimics the action of the excitatory neurotransmitter ACh causing a spastic paralysis of the worm. Evidence from studies on levamisole resistant strains of *H. contortus* suggests that mutations in the somatic muscle nAChR may cause levamisole resistance. Resistant *H. contortus* were shown to require between a 4 to 13-fold increase in levamisole concentration to elicit the same paralysis of muscle. Known cholinergic agonists, which cause contraction in susceptible worms had little effect on resistant worms, thus suggesting that

levamisole resistant worms have changes in their ACh receptors (Sangster *et al.*, 1991).

In *C. elegans* several genes have also been identified to confer levamisole resistance. 13 loci have been identified with 7 conferring extreme resistance (Lewis *et al.*, 1980a). Some of the loci code for the structural ACh receptor genes (such as *unc-38* which encodes an  $\alpha$ -subunit and *unc-29* and *lev-1* which encode non- $\alpha$  subunits) and others may be involved in processing of the ACh receptor subunits.

### **1.9.2 Ivermectin resistance.**

Ivermectin works as an agonist and thus opens glutamate-gated chloride channels located on the muscles of the pharynx which results in inhibition of feeding. Ivermectin binds to the  $\alpha$  subunit of the GluCl channel. How ivermectin resistance occurs is still unclear. The  $\alpha$ -subunit in the GluCl receptor of *C. elegans* is encoded by a family of genes including *glc-1*, *avr-14* and *avr-15* (Cully *et al.*, 1994). Severe loss-of-function mutations however in *glc-1* or *avr-15* do not confer strong resistance to ivermectin-induced muscle paralysis (Vassilatis *et al.*, 1997) although a shift in sensitivity is observed. *C. elegans* mutations of individual GluCl genes are not resistant to ivermectin because the 3 GluCl genes, *avr-14*, *avr-15* and *glc-1* constitute a parallel genetic pathway that independently confers sensitivity to ivermectin. A triple GluCl mutant which reduces sensitivity of all three genetic pathways is required before a 4,000-fold resistance is achieved (Dent *et al.*, 2000). This ability of ivermectin to target multiple gene families may decrease the rate at which resistance evolves, although resistance to ivermectin is beginning to surface in the agricultural industry (Mejia *et al.*, 2003). Whether field based resistance results in mutations in those genes observed in *C. elegans* has yet to be determined.

## **1.10 Looking for novel anthelmintics.**

The problem of resistance of parasitic nematodes to existing anthelmintics in agriculture and also clinically, has encouraged a search for novel anthelmintics, which target sites specific to the nematode, and that differ from the existing commercially available drugs.

## 1.11 Depsipeptide anthelmintics.

Sasaki *et al.*, (1992) reported the isolation and structural determination of PF1022A, a fermentation product of *Myelia sterilia* isolated from microflora on the leaf of the plant *Camellia japonica* collected at Ibaragi Prefecture in Japan. They found PF1022A had a potent anthelmintic action towards the intestinal nematode of the chicken *Ascaridia galli*, with worms being seen to be expelled after one day.

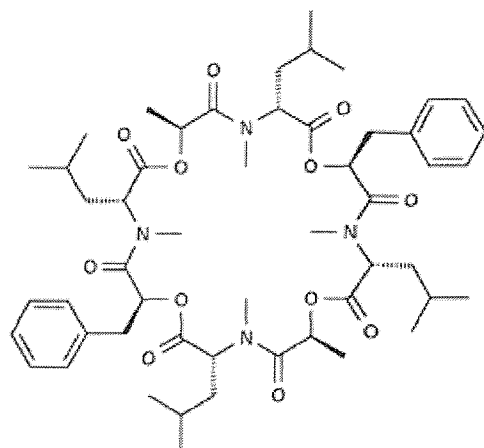
PF1022A belongs to the class of the N-methylated 24-membered cyclooctadepsipeptides (Fig 1.10A). PF1022A shares a similar structure to bassianolide, an insecticidal compound and enniatins which also have anthelmintic activity (Geßner *et al.*, 1996).

PF1022A anthelmintic activity has been shown extensively *in-vitro* and *in-vivo*. PF1022A was shown to affect motility of and at higher doses paralyse, *Angiostrongylus cantonensis* (Terada, 1992). Geßner *et al.*, (1996) showed PF1022A caused a flaccid paralysis of *A. suum* after 5 hours. PF1022A also paralyses *H. contortus* (Conder *et al.*, 1995), being 3 - 10 times more potent than ivermectin. Recent *in vivo* studies by (Samson-Himmelstjerna *et al.*, 2000) on rats infected with *Stonyloides ratti* and *Nippostrongylus brasiliensis*, dogs infected with *Ancylostoma canium*, horses infected with small strongyles (syathostomes), sheep infected with *Trichostrongylus colubriformis* and *H. contortus* and cattle infected with *Dictyocaulus viviparus* have shown that PF 1022A has very potent effects in removing these parasites with no clinical signs of animal intolerance.

In 1993 the Fujisawa Pharmaceutical Co., Ltd (Japan) patented the bis-paramorphonyl-derivative of PF1022A, named emodepside (Fig 1.10B). This semi-synthetic derivative has been shown to be highly effective against a number of nematodes in different animal species.(Nicolay *et al.*, 2000; Harder & Samson-Himmelstjerna, 2001). Emodepside has been shown to be highly effective against the adult stages of rat nematodes, *N. brasiliensis* and *S. ratti* and the mouse nematode *Heligmosomoides polygyrus* at doses of 1-10mg/Kg (Harder & Samson-Himmelstjerna, 2002).

PF1022A and its semi-synthetic derivative, emodepside appears, therefore, to have potent broad-spectrum anthelmintic activity against the major gastrointestinal nematodes of livestock and companion animals.

**A**



**B**

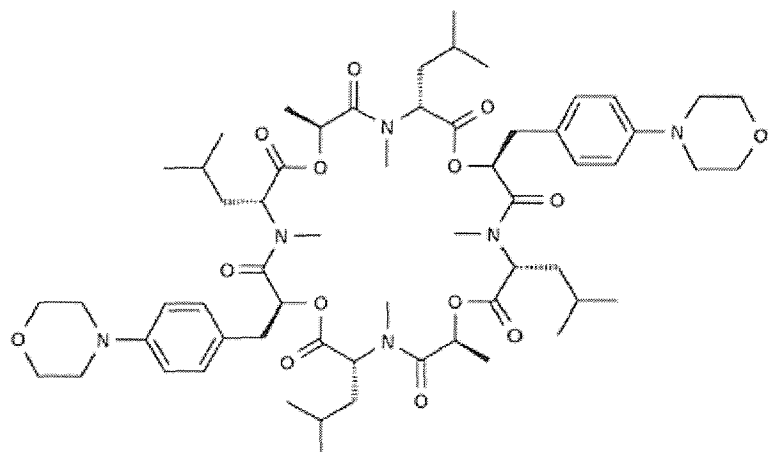


**Fig 1.10 The chemical structure of (A) PF1022A and (B) emodepside.** Taken from (Harder & Samson-Himmelstjerna, 2002)

### 1.11.1 Breaking of resistance by PF1022A and emodepside.

Both PF1022A and emodepside have been shown to possess resistance breaking properties against the usual classes of anthelmintics. PF1022A has been shown to paralyse benzimidazole and ivermectin resistant *H. contortus*. Emodepside

also paralyses benzimidazole and ivermectin resistant *H. contortus* in sheep, as well as ivermectin resistant *T. colubriformis* in sheep and *Cooperia oncophora* in cattle (Harder *et al.*, 2003). PF1022A and emodepside thus must posses a novel site of action compared to that of these known anthelmintics.

### **1.11.2 Investigating the mechanism of action of PF1022A and emodepside.**

Cyclodepsipeptides like valinomycin, enniatin A and beauvericin can form ionophores whose ion carrier properties have been studied in detail in lipid-bilayer membranes. PF1022A ionophore activity was therefore proposed as a possible mechanism of action for PF1022A. Studies by Geßner *et al.*, (1996) confirmed this theory. However, they also determined that this ionophore property does not explain anthelmintic activity. PF1022A's optical antipode PF1022-001 also has ionophore activity in a lipid-bilayer but does not cause paralysis of *A. suum*. PF1022A also has a 100-fold higher anthelmintic activity against *Heterakis spumosa*, *Nippostrongylus brasiliensis* and *Trichinella spiralis* larvae compared with this optical antipode. The possibility of pharmacokinetic differences between PF1022A and the optical antipode in explaining its poor anthelmintic activity have yet to be determined.

Initial experiments by (Terada, 1992) on an *in vitro* model of *A. cantonensis* showed that PF1022A inhibited the motility of worms. This paralysis was partially antagonised by the GABAergic antagonists picrotoxin and bicuculline, and completely reversed by the addition of N-methylcytisine, which stimulates ACh release from nematode nerve endings. Martin *et al.*, (1996) using a 2 microelectrode current clamp-technique on the pig intestinal parasite *A. suum*, showed that PF1022A does not antagonize the effects of the selective nicotinic agonist levamisole, indicating that PF1022A is not a nicotinic antagonist. Direct perfusion of PF1022A to *A. suum* muscle cells resulted in no change in membrane potential either, however a small time dependent increase in input conductance was observed. This increase in input conductance does not occur in the absence of extracellular Cl<sup>-</sup> ions, indicating a possible role for Cl<sup>-</sup> ions in PF1022A action. Further evidence for a role of GABA in PF1022A action comes from Chen *et al.*, (1996) who showed,

using a radioligand binding technique, that PF1022A displaced radiolabelled GABA and bicuculline, indicating that PF1022A may bind to GABA receptors.

It is still unclear whether PF1022A / emodepside acts through a GABAergic mechanism. Picrotoxin and bicuculline do not antagonise GABA responses on *A. suum* muscle (Wann, 1987). PF1022A appears not to be a potent GABA agonist on *A. suum* muscle cells because no marked hyperpolarisation is observed and no large change in input conductance occurs. GABA receptors appear not to be involved in emodepside action, although recent work by Beg *et al* (2003) has identified a novel excitatory GABA gated cation channel in *C. elegans*. This receptor, coded for by the *ext-1* gene, is localised to the enteric neuromuscular junction and causes muscle contraction. The channel is selective for sodium ions. PF1022A/emodepside may therefore act through this or other novel receptors.

### **1.11.3 Emodepside acts through a latrophilin-like receptor.**

During the course of this project a possible receptor for emodepside was identified (Saeger *et al.*, 2001). Using emodepside's parent compound, PF1022A, as a ligand for an immunoscreen against a cDNA expression library constructed from the parasitic worm *H. contortus*, they isolated a novel orphan heptahelical transmembrane 110kDa receptor which they termed HC110-R. HC110-R was shown to have 31% homology with G-protein coupled receptor latrophilin, in human, bovine and rat. Both HC110-R and the mammalian latrophilins share conserved sequences within specific regions of the receptor (seven transmembrane domains, the lectin binding domain, a Cys signature and a conserved 4 Cys motif before the first transmembrane region). Latrophilin was identified as one of the receptors of  $\alpha$ -Latrotoxin ( $\alpha$ LTX) (Petrenko *et al.*, 1990) a component of the black widow spider venom. These results suggest that emodepside may have an  $\alpha$ LTX - like effect in nematodes, acting through a latrophilin receptor.

## 1.12 $\alpha$ -LTX.

$\alpha$ LTX is a deadly neurotoxin found in the venom of the black widow spider. Black widows use this venom to paralyse and kill their prey.  $\alpha$ LTX causes massive exocytosis of vesicles at nerve terminals and various secretory cells. This over-release leads to the catastrophic effects of the spider bite on the neurosecretory, neuromuscular and cardiovascular system (Grishin, 1998; Saibil, 2000). The venom also contains other toxins that have similar effects on invertebrates, namely insect-specific  $\alpha$  and  $\delta$ -latroinsectotoxins (Kiyatkin *et al.*, 1993; Dulubova *et al.*, 1996), and crustacean-specific  $\alpha$ -latrocrustotoxin (Danilevich *et al.*, 1999).

$\alpha$ LTX is a large protein (over 100kDa). Its structure was resolved by Orlova *et al.*, (2000). They determined that in the presence of calcium  $\alpha$ LTX forms a tetrameric structure, with a pore running through its middle. In the absence of calcium it forms a dimer.

## 1.13 Multiple mechanism of action for $\alpha$ LTX.

$\alpha$ LTX causes a massive vesicular release from a variety of neurosecretory cells which has led to the proposal of a number of different mechanisms of action.  $\alpha$ LTX after its initial purification was shown to generate non-selective cation channels in artificial black phospholipid membranes (Finklestein *et al.*, 1976). Vesicular release also appeared to go hand in hand with an influx of calcium ions (Barnett *et al.*, 1996; Liu & Misler, 1998a; Liu & Misler, 1998b). The initial mechanism of action proposed for  $\alpha$ LTX indicated that its channel-forming property enabled extracellular calcium ions to enter these cells causing vesicular exocytosis. A problem with the mechanism arose when  $\alpha$ LTX was also shown to cause vesicular mediated release in the absence of calcium ions (Gorio *et al.*, 1978; Capogna *et al.*, 1996; Liu & Misler, 1998a). This finding led to the proposal of multiple mechanisms of action for  $\alpha$ LTX (Fig 1.11)

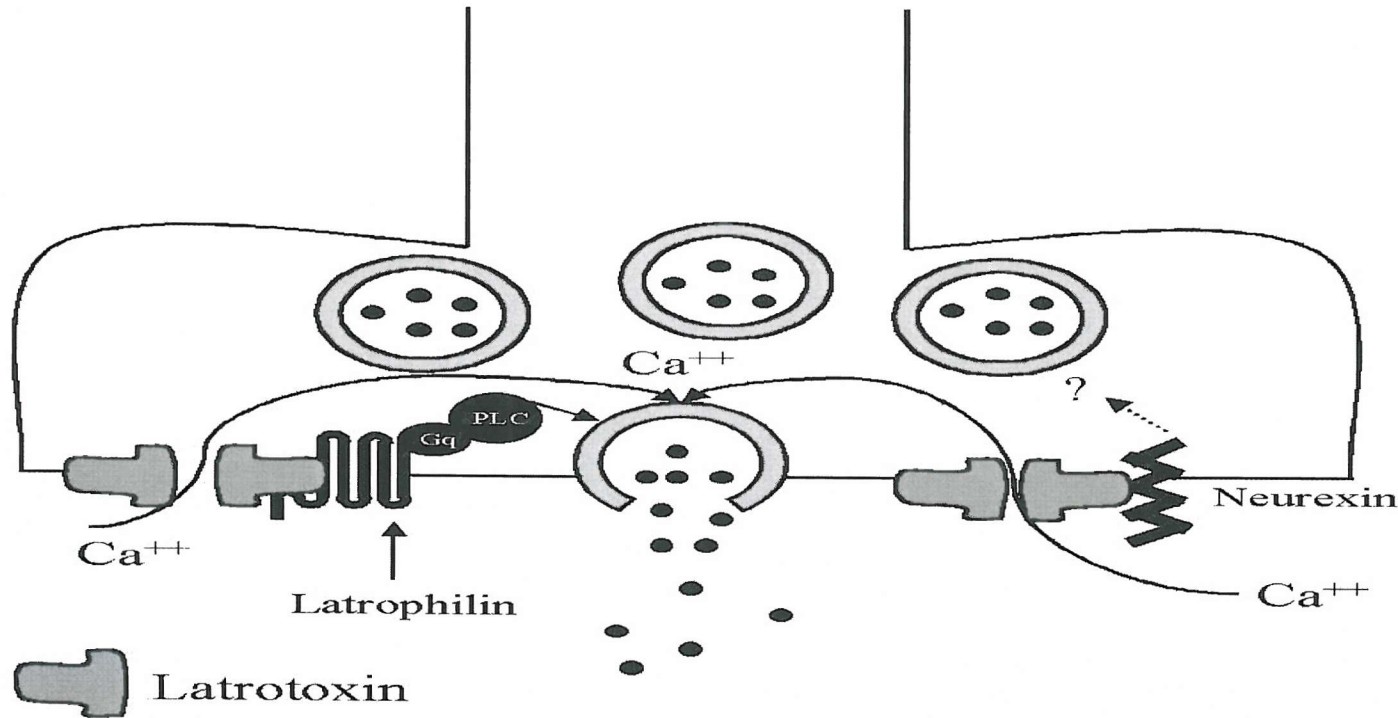


**Fig 1.11 Diagram to illustrate the multiple mechanisms of  $\alpha$ LTX action** taken from (Saibil, 2000).  $\alpha$ LTX is represented in a dimer form .  $\alpha$ LTX has three distinct mechanisms: in its tetrameric form, it forms pores in the membrane allowing influx of cations, it Binds neurexins in a calcium dependent manner, it binds latrophilin independently from calcium ions.

## 1.14 Pore forming properties of $\alpha$ LTX.

$\alpha$ LTX was shown to directly insert into the plasma membrane and form non-selective cation channels in the plasma membrane (Wanke *et al.*, 1986; Finklestein *et al.*, 1976). Using cryo-EM Orlova *et al.*, (2000) have shown direct insertion of  $\alpha$ LTX into the lipid bilayer.  $\alpha$ LTX 3D structure also looks unmistakably pore-like. The tetrameric form of  $\alpha$ LTX was shown to correlate most accurately with the  $\alpha$ LTX action causing vesicular release via pore formation. The dimeric form was unable to cause efflux of noradrenaline from isolated rat brain synaptosomes (Orlova *et al.*, 2000). The tetrameric form, however, was able to cause neurotransmitter secretion.

Based on EM images it is believed that  $\alpha$ LTX in its tetrameric form fully permeates the lipid bilayer with its base. The upper part of the tetramer remains above the membrane with its wings partially embedded within the membrane. The central channel is then able to permeabilize the membrane. These  $\alpha$ LTX channels conduct both divalent and monovalent cations such as  $\text{Ca}^{2+}$ ,  $\text{Mg}^{2+}$ ,  $\text{Na}^+$  or  $\text{K}^+$  but are blocked by  $\text{La}^{3+}$  (Hurlbut *et al.*, 1994) Channel formation is believed to occur at toxin concentrations in excess of 100pM (Liu & Misler, 1998a).

Whether  $\alpha$ LTX directly inserts into the membrane or requires receptor interaction to insert into the membrane was investigated in *Xenopus* oocytes.  $\alpha$ LTX had already been shown to spontaneously insert into a black lipid membrane and cause formation of a stable cation channel (Finklestein *et al.*, 1976). However, in *Xenopus* oocytes that do not express  $\alpha$ LTX receptors, application of  $\alpha$ LTX did not result in calcium channel opening. Only when brain proteins were expressed by injection of total brain mRNA into the oocytes (and thus synthesis of  $\alpha$ LTX receptors) were calcium channels observed (Filipov *et al.*, 1990; Umbach *et al.*, 1990). This therefore suggested that binding of  $\alpha$ LTX to receptors is necessary for the toxin to insert into biological membranes, where one of its actions is to form a non-selective cation channel (Khvotchev & Sudhof, 2000).

Investigation into the importance of a receptor-mediated action of  $\alpha$ LTX advanced when  $\alpha$ LTX<sup>N4C</sup>, a variant of the toxin, was synthesised.  $\alpha$ LTX<sup>N4C</sup> binds  $\alpha$ LTX receptors with the same affinity as wild-type LTX, but crucially fails to form pores in membranes (Ashton *et al.*, 2001; Volynski *et al.*, 2003).  $\alpha$ LTX<sup>N4C</sup> therefore provides a useful tool to investigate the receptor mediated effects of  $\alpha$ LTX.

## 1.15 The $\alpha$ LTX receptors.

$\alpha$ LTX was found to bind two main receptors in brain which differ in their calcium dependence. Both classes have been shown to be similarly abundant and bind  $\alpha$ LTX with the same nanomolar affinity. The difference between the receptors is in the calcium dependence. The neurexins are believed to be involved in the calcium-dependent pathway of  $\alpha$ LTX action (Petrenko *et al.*, 1990; Ushkaryov *et al.*, 1992) while the latrophilins (Lelianova *et al.*, 1997), (or calcium-independent receptor for latrotoxin), (Krasnoperov *et al.*, 1997) bind the toxin regardless of whether divalent cations are present or absent (Davletov *et al.*, 1998). Both pathways, however, once stimulated cause an increase in vesicular exocytosis. Intriguingly, no obvious homology can be found between these two receptors.

A third receptor implicated in  $\alpha$ LTX action has been identified. Krasnoperov *et al.*, (2002a) isolated a known receptor-like protein-tyrosine phosphatase sigma (PTP $\sigma$ ). This membrane phosphatase also is structurally unrelated to the other  $\alpha$ LTX receptors. Genetic studies in mice and *Drosophila* identified PTP $\sigma$  as a protein essential for neuronal development and axonal path finding.(Elchebly *et al.*, 1999; Krueger *et al.*, 1996)).

### 1.15.1 The neurexins.

The neurone-specific cell-surface polymorphic proteins, the neurexins, were the first receptors discovered as a potential target site for  $\alpha$ LTX (Petrenko *et al.*, 1990; Ushkaryov *et al.*, 1992). Three distinct genes, under the control of two promoters, produce neurexins in vertebrates (Missler & Sudhof, 1998). This arrangement leads to the formation of three neurexin- $\alpha$  (I $\alpha$ , II $\alpha$ , III $\alpha$ ) and three

neurexin  $\beta$  proteins (I $\beta$ , II $\beta$ , III $\beta$ ). Neurexin genes show alternative splicing patterns leading to the generation of many hundreds of isoforms (Missler & Sudhof, 1998). Neurexin  $\alpha$  and  $\beta$  have extracellular regions homologous to the extracellular matrix protein laminin, an O-linked glycosylation site, a transmembrane domain and a short C-terminal region. Neurexins are therefore classed as cell adhesion molecules. Neurexins are highly enriched at synaptic active zones (Butz *et al.*, 1998). They interact intracellularly with the PDZ domain protein CASK (a protein related to membrane guanylate cyclase) (Hata *et al.*, 1996). They also bind to synaptotagmin (Petrenko *et al.*, 1991), a protein that acts as a calcium sensor in the final stages of vesicle exocytosis. Geppert *et al.*, (1994). Neurexins also bind to the post synaptic cell adhesion molecules dystroglycan (Ichtchenko *et al.*, 1995) and neuroligins (Scheiffele *et al.*, 2000). Lethality of postnatal triple knock-out mice (to all three neurexin genes) suggests neurexins are essential for survival. These mice did not show defects in neuronal development, but do have impaired calcium triggered neurotransmitter release (Missler *et al.*, 2003). Neurexins therefore appear to play an important role in linking synaptic cell adhesion to the synaptic machinery required for vesicle fusion.

Neurexin I $\alpha$  binds to  $\alpha$ LTX in the nanomolar range making it a good candidate for the  $\alpha$ LTX receptor (Petrenko *et al.*, 1990; Ushkaryov *et al.*, 1992). Binding of  $\alpha$ LTX to neurexin was shown to be dependent absolutely on calcium (Davletov *et al.*, 1995). (Geppert *et al.*, 1998) demonstrated that  $\alpha$ LTX binding to brain membranes from neurexin I $\alpha$  knock out mice was reduced by 50% in the presence of calcium. No reduction in  $\alpha$ LTX binding was observed in the absence of calcium. Whether  $\alpha$ LTX binding to neurexins is important in stimulating vesicle release remains unclear. The mutant  $\alpha$ LTX molecule which only activates  $\alpha$ LTX receptors (as it does not form pores in the membrane) appears not to require neurexin activation. In the absence of calcium, which is essential for neurexin binding to  $\alpha$ LTX, receptor-mediated stimulation still occurs (Volynski *et al.*, 2003). This suggests that activation of the other  $\alpha$ LTX receptor latrophilin appears to be the key receptor involved in receptor-mediated stimulation of vesicle release by  $\alpha$ LTX.

## 1.15.2 The latrophilins (CIRL).

The  $\alpha$ LTX receptor latrophilin was discovered using affinity chromatography (Davletov *et al.*, 1996; Krasnoperov *et al.*, 1997). It was the only protein found to bind  $\alpha$ LTX in the absence of divalent cations. Further cloning revealed three closely related forms of latrophilin in vertebrates, (latrophilin 1, 2 and 3) (Sugita *et al.*, 1998; Ichtchenko *et al.*, 1999).

Latrophilin 1, 2 and 3 are differently expressed in a pattern that suggests a widespread function not related only to neurones. Latrophilin-1 was shown to be more brain specific (Krasnoperov *et al.*, 1997) but subsequent studies have shown low levels in all tissues (Sugita *et al.*, 1998). Latrophilin 2 is found primarily outside the brain. Both latrophilin 1 and 2 bind  $\alpha$ LTX with nanomolar affinity whereas latrophilin-3 is unable to bind (Ichtchenko *et al.*, 1999).

### 1.15.2.1 Structure of latrophilin.

The neuronally expressed cell surface receptor latrophilin is a natural chimera of a cell adhesion protein and the G-protein coupled receptor. It belongs to an unusual secretin family of ubiquitous G-protein coupled receptors (Lelianova *et al.*, 1997). It has a large extracellular domain which contains motifs found in adhesion molecules. These include lectin and olfactomedin-like sequences at the N-terminus, and a cysteine-rich domain immediately before the seven transmembrane regions. Within this region, 19 residues from the first transmembrane domain, is a sequence which represents a proteolytic cleavage signal during the maturation of the G-protein linked receptor (Krasnoperov *et al.*, 2002b). It has been termed GPS for G-protein coupled receptor proteolysis site domain. Post translational processing of the latrophilin receptor results in two non-covalently bound fragments p120 and p85. P120 represents the hydrophilic extracellularly orientated sequence and resembles that of all adhesion molecules. P85 resembles a generic G-protein coupled receptor (Fig 1.12).

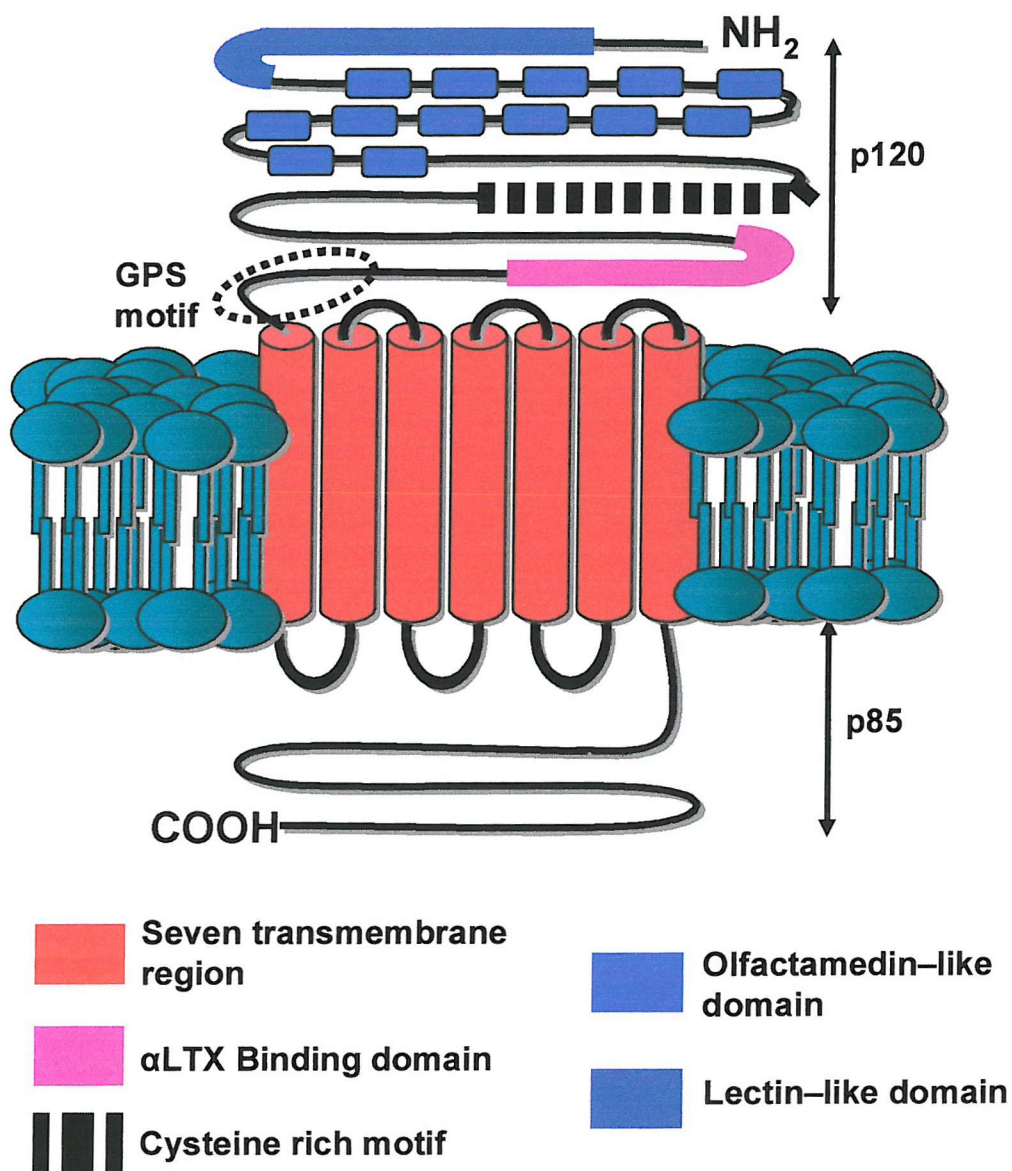


**Fig 1.12 Diagram of Latrophilin-receptor**, showing positions of the structural motifs and the G-Protein proteolysis site domain (GPS). The non-covalently bound fragments p120 (which resembles a cell adhesion molecule including an olfactomedin-like domain, an extracellular matrix protein, first identified on olfactory neuroepithelium Yokoe *et al* 1993) and p85 (which resembles a generic G-protein-coupled receptor) result from post translational processing of the latrophilin receptor. (Krasnoperov *et al.*, 2002b).

### 1.15.2.2 Latrophilin's role in vesicle release.

Many parts of latrophilin's isomers resemble those of other G-protein receptors indicating that  $\alpha$ LTX stimulated neurotransmitter release may be controlled by a receptor-mediated activation of these heterotrimeric G proteins. These types of receptors have been shown previously to bind peptide hormones and stimulate exocytosis via a second messenger mechanism (Krasnoperov *et al.*, 1997). G-protein receptors have also been shown to be highly enriched in synapses (Aronin & DiFiglia, 1992).

Vesicular release of neurotransmitter from nerve terminals requires the fusion between synaptic vesicles and the pre-synaptic membrane (Scheller, 1995; Sudhof, 1995). Vesicle fusion involves an evolutionary conserved protein cascade utilising vesicle associated and pre-synaptic membrane associated proteins. Synaptic activity is modulated by the number of vesicles termed 'the readily releasable pool' available for fusion with the pre-synaptic membrane (Rosenmund & Stevens, 1996). How latrophilin interacts with these docking / fusion processes of vesicles is unclear. Krasnoperov *et al.*, (1997) showed that latrophilin binds to syntaxin IA, a protein involved in formation of the SNARE complex, which is essential for vesicle fusion. Lelianova *et al.*, (1997) showed  $\alpha$ LTX caused an elevation in cAMP and IP<sub>3</sub> levels. They also found that latrophilin co-purifies with a 42kDa protein, which reacts with antibodies raised to G $\alpha$ <sub>o</sub>, but not against G $\alpha$ <sub>i</sub> subunits. Rahman *et al.*, (1999) have shown that G $\alpha$ <sub>q</sub>, in addition to G $\alpha$ <sub>o</sub>, is linked to latrophilin and that in cells expressing latrophilin there is an increase in inositol 1,4,5-trisphosphate (IP<sub>3</sub>) production. Receptor mediated activation by latrotoxin also results in an increase in IP<sub>3</sub> levels (Capogna *et al.*, 2003).

## 1.16 Project aims.

The increased resistance to existing anthelmintics requires the need to develop novel compounds. Emodepside is a novel drug which has a broad-spectrum and resistance breaking anthelmintic properties. The precise mechanism of action of this drug is unknown. In this study two nematode species, *A. suum* and *C. elegans*, have been used to investigate the mechanism of action of emodepside.

*A. suum* muscle has previously been used to provide insights into the mechanisms underlying the action of existing anthelmintics, so will be used in this study to establish the effects of emodepside on an *in vitro* muscle preparation and provide insight into the mechanisms underlying emodepside's potent anthelmintic action.

The model genetic organism *C. elegans* has been previously used to determine the target site of the existing anthelmintic ivermectin. *C. elegans* will therefore provide a useful organism to determine the molecular mechanisms underlying emodepside action. This investigation has been greatly aided by the availability of numerous mutants and the use of molecular techniques that interfere with gene expression.

This project, therefore, aims to use a combination of both physiological and molecular techniques on two nematode species to determine the mechanism of action of emodepside.

## CHAPTER 2

**Materials and Methods** *A. suum*

**Experiments**

## **2.1 *A. suum* maintenance.**

*A.suum* were obtained from a local abattoir and maintained for up to 5 days in artificial perienteric fluid (APF) with the following composition in mM NaCl 67, CH<sub>3</sub>COONa 67, CaCl<sub>2</sub> 3, MgCl<sub>2</sub> 15.7, KCl 3, glucose 3, Trizma® base 5, pH 7.6 with glacial acetic acid, at 37°C

## **2.2 *In vitro* muscle strip tensions.**

*A.suum* dorsal muscle strips (DMS) were prepared by dissecting a 1cm strip of the body wall muscle immediately anterior to the genital pore. This was obtained by cutting length-wise along both lateral cords and discarding the ventral portion. Any remaining intestine still attached to the somatic muscle was carefully removed. Dorsal muscle was used as it is devoid of motorneurone somata, which are only present in the ventral nerve cord. Dorsal muscle however does contain the dorsal inhibitory and dorsal excitatory motorneurone terminals, which have reciprocal synapses with each other. For denervated muscle strips, both dorsal and ventral cords were removed from the muscle strip. This was obtained by cutting along a lateral line and opening up the muscle exposing both nerve cords. The muscle strip was then cut on the inner side of the nerve cords so that only body wall muscle between the nerve cords remained (Fig 2.1). Both dorsal and denervated muscle preparations remained viable for up to two hours. Preparations that did not response to ACh were rejected.

Effects of resting tension and activity of the DMS in response to exogenous ACh were investigated by securing the muscle strips in a 15ml organ bath and connecting them by thread to a 2g isometric transducer. The preparation was subject to a 1g load and maintained at 37°C with a heated water jacket. Drugs were added in volumes of no greater than 1% of the bath volume. Drugs were rapidly mixed within the organ bath by gassing the bath with room air. Drugs were then washed out by at least 3 times the bath volume of APF. A hard copy of

the data was obtained on a flat bed chart recorder (BBC, Goerz, Metrawatt, Austria). (Fig 2.2 )

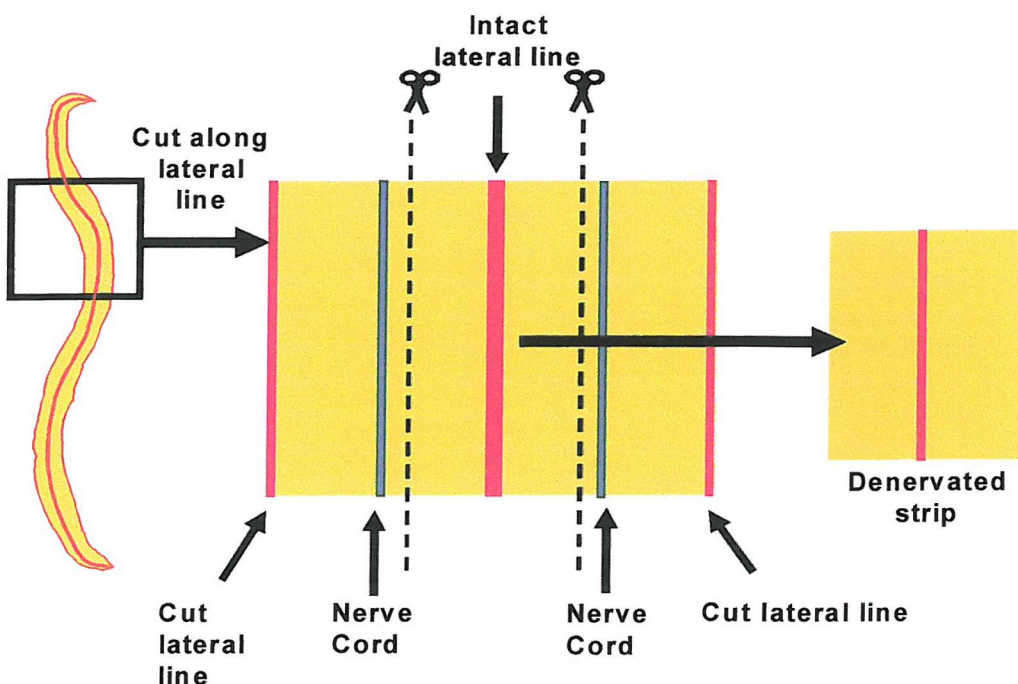


**Fig 2.1. The denervated muscle preparation.** A diagram showing the dissection procedure. *A. suum* were cut along the lateral line and opened to expose the dorsal and ventral nerve cords. The muscle was then cut on the inner side of the nerve cords. As *A. suum* muscle cells send projections to nerve cords this means that only body wall muscle is contained within the denervated preparation.

### 2.3 Electrophysiological studies.

Two-microelectrode recording was adopted for electrophysiological studies on *A. suum* somatic muscle. The DMS was pinned cuticle side down on a Sylgard® elastomer 184 (Dow Corning Wiesbaden, Germany) lined Perspex chamber and continuously perfused with APF at 32-34°C, directed at the *A. suum* muscle cell via a fine bore tube. For low potassium experiments composition of APF was in mM NaCl 67, CH<sub>3</sub>COONa 67, CaCl<sub>2</sub> 3, MgCl<sub>2</sub> 15.7, KCl 0, glucose 3, Trizma® base 5, pH 7.6 with glacial acetic acid, at 37°C. For calcium-free experiments composition of APF was in mM NaCl 67, CH<sub>3</sub>COONa 67, CaCl<sub>2</sub> 0, MgCl<sub>2</sub> 15.7, KCl 3, glucose 3, Trizma® base 5, pH 7.6 with glacial acetic acid, at 37°C.

Individual muscle bags were impaled with 2 microelectrodes containing 10mM KCl in 3 M CH<sub>3</sub>COOK (10-30 M $\Omega$ ) connected to an Axoclamp 2A amplifier. One electrode was used to record, and the second to pass current pulses (20 nA, 0.2 Hz, 500 msec), except for the AF2 experiment where only the membrane potential was recorded. The chamber was grounded using a 3 M KCl agar bridge/AgCl electrode. Input resistance could be estimated from the electronic potential resulting from current injection. Emodepside was added in the perfusate for 2 mins. Bath temperature was continuously monitored with a temperature probe placed adjacent to the muscle strip. Hard copy of data was recorded on a Gould model 35, 2-channel chart recorder (Gould instruments, Ohio, USA) (Fig 2.2).

## 2.4 Drugs.

Both ACh (Sigma Chemical Co., Poole, UK) and emodepside were prepared fresh on the day of the experiment, while AF2 and PF2 were stored at -20°C in 50 $\mu$ l aliquots of 10<sup>-3</sup> M. ACh was prepared in APF. Emodepside was initially dissolved in 100% ethanol at 10<sup>-1</sup> M and then diluted in APF so that the final concentration of ethanol in the organ bath was no greater than 0.1%.

The length of time of either ACh or emodepside addition varied depending on the experiment. For the emodepside time-dependence experiments ACh was left on for 30s. Emodepside was either left on the DMS for 2, 5, or 10 mins. In the experiment where the concentration of emodepside was varied ACh was left on for 30s and emodepside was left on for 10 mins prior to ACh re-addition. For the relaxation experiments ACh was left on for 10 mins and emodepside was left on for 10 mins. For all electrophysiology experiments 10 $\mu$ M emodepside was used and perfused with the muscle strip for 2 mins. For the AF2 experiments 1 $\mu$ M was perfused over the muscle strip for 2 minutes. The neuropeptides AF2 and PF2, were supplied by Alta Bioscience, Birmingham UK (>90% purity) and were stored at -20°C in 50 $\mu$ l aliquots of 10<sup>-3</sup> M. Emodepside was supplied by Bayer AG, Leverkusen, Germany. All other drugs were obtained from Sigma Chemical Co., Poole, UK.

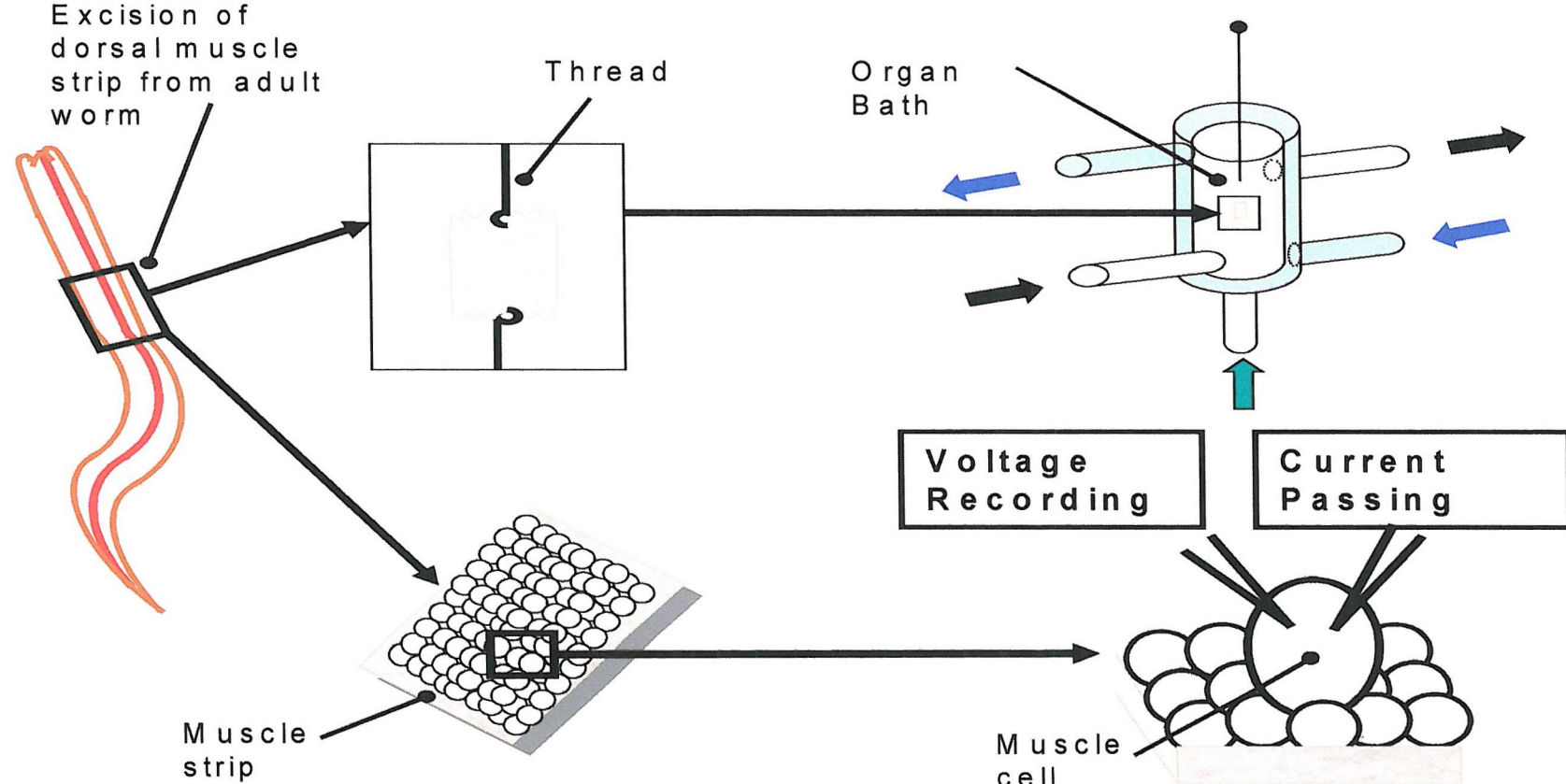


**Fig 2.2 The experimental methods for *A. suum* experiments.** **Top.** Dorsal muscle strips (1cm) were removed from *A. suum* and placed in an organ bath containing APF at 37 degrees. The muscle was tied to a 2g isometric transducer and changes in muscle tone were measured. **Bottom.** Individual muscle cells from dorsal muscle strips were impaled with 2 microelectrodes (voltage recording and current passing).

## **2.5 Data analysis.**

For each individual muscle strip tension experiment a consistent response to 30 $\mu$ M ACh was first obtained. The peak contractions of the responses were measured and deemed the maximal response. Subsequent responses were normalized with respect to the maximal response.

## **2.6 Statistical analysis.**

Data are presented as either the mean  $\pm$  S.E.Mean of 'n' independent determinations or as mean: with 95% confidence interval for 'n' experiments. Statistical significance was determined using either a paired or unpaired two tailed Students t-test with a significance level of  $P<0.05$ . The ACh excitation curve was fitted to the modified logistic equation using Graph pad prism (version 3.0 San Diego California).

## CHAPTER 3

### **Effect of Emodepside on the neuromuscular System of *Ascaris suum***

### 3.1 Introduction.

Cyclooctadepsipeptides, of which PF1022A and emodepside are members, are a new class of anthelmintic (Harder & Samson-Himmelstjerna, 2002) which inhibit nematode motility (Samson-Himmelstjerna *et al.*, 2000; Terada, 1992). The precise mechanism of PF1022A and emodepside action is unknown, although its fast onset of paralysis favours the view that it is neuropharmacologically active. Previous investigations into emodepsides mechanism of action are described in section 1.11.2. These studies focused on the inhibitory GABAergic system, however, application of PF1022A to *A. suum* muscle cells resulted in no marked hyperpolarisation, and no large change in input conductance (Martin *et al.*, 1996) which is not consistent with a GABA response (Holden-Dye *et al.*, 1989; Walker *et al.*, 1992; Parri *et al.*, 1991) PF1022A/emodepside may therefore be acting through a novel receptor causing its potent anthelmintic action.

Many of the commercially available anthelmintics act by inhibiting nematode motility. Neuronal control of nematode movement by the excitatory and inhibitory motoneurones was described in section 1.5.3. A number of classical transmitters, such as ACh and GABA, (described in section 1.6) and neuropeptides (described in section 1.7) have been shown to regulate muscle function. Many anthelmintics mimic the action of the classical neurotransmitters which control nematode movement. Such examples of these anthelmintics include levamisole that acts on the ACh receptor (Harrow & Gration, 1985) and piperazine which acts on the GABA receptor (Martin, 1982). To date no anthelmintic has been shown to mimic the action of neuropeptides.

To provide an insight into emodepsides mechanism of action an *in vitro* preparation of the dorsal muscle strip of the intestinal parasite of the pig *A. suum* will be used. The muscle preparation consists of the dorsal muscle and the dorsal nerve cord, which contains projections of the excitatory and inhibitory motoneurones. Changes in *A. suum* muscle state can therefore be measured using tension recordings. This will allow emodepside's effects on *A. suum* muscle directly or following treatment with neurotransmitters or neuromodulators to be investigated.

The use of electrophysiology techniques on *A. suum* muscle bag cells has provided an insight into the action of neurotransmitters in controlling muscle contraction and relaxation (Martin *et al.*, 1991; Walker *et al.*, 2000; Stretton *et al.*, 1978). These electrophysiology recordings have also provided insight into the mechanism of action of existing anthelmintics (Martin, 1997; Martin *et al.*, 1997). In this study 2 microelectrode recordings from *A. suum* individual muscle cells will be used to provide a further insight into emodepside action.

The resting membrane potential of *A. suum* muscle cells averages at -33mV (De Bell *et al.*, 1963). Investigations into the ionic dependence of the resting membrane potential revealed that changes in extracellular potassium had little effect on the membrane potential. Chloride ions however appeared more important in maintaining the resting membrane potential as do, but to a lesser extent, sodium ions (Del Castillo *et al.*, 1964; Brading & Caldwell, 1971). Subsequent ion flux experiments showed that the permeability ratio for each of these ions was determined as 1:4:7 for potassium, sodium and chloride ions. Later investigations into membrane properties of *A. suum* muscle cells revealed an important role of carboxylic acids. High concentrations of carboxylic acids were found in *A. suum* perienteric fluid (Hobson *et al.*, 1952). These anionic molecules accumulate within the muscle cell as a result of anaerobic respiration (Saz & Weil, 1962; Tsang & Saz, 1973). They are then secreted through a calcium-activated chloride channel (Dixon *et al.*, 1993; Valkanov *et al.*, 1994; Valkanov & Martin, 1995). This secretion of anaerobic products, therefore, has a major influence on the membrane potential of *A. suum* muscle. The ionic components that maintain the resting potential are a potential target site for emodepside.

Here, the mechanism of action of the cyclodepsipeptide emodepside, using both muscle tension recordings and recordings from individual muscle cells of *A. suum* will be investigated. Emodepside's direct effects on *A. suum* muscle will be determined, as well as any action emodepside has on the state of *A. suum* muscle following pre-treatment with excitatory and inhibitory neurotransmitters and neuromodulators. Recordings from individual *A. suum* muscle cells may provide an insight into any ionic component of emodepside action.

### 3.2 The effect of varying ACh concentrations on *A. suum* dorsal muscle strip (DMS).

The excitatory transmitter ACh caused a concentration-dependent contraction of *A. suum* DMS ( $EC_{50}=9.2\mu M$ , 95% confidence limits 8 to  $11\mu M$ , Fig 3.1) in a similar manner to that previously reported, (Baldwin & Moyle, 1949,  $EC_{50}=1-10\mu M$ ; Trim *et al.*, 1997,  $EC_{50}=13\mu M$ ), confirming that this technique is viable for investigating the mechanism of action of emodepside.

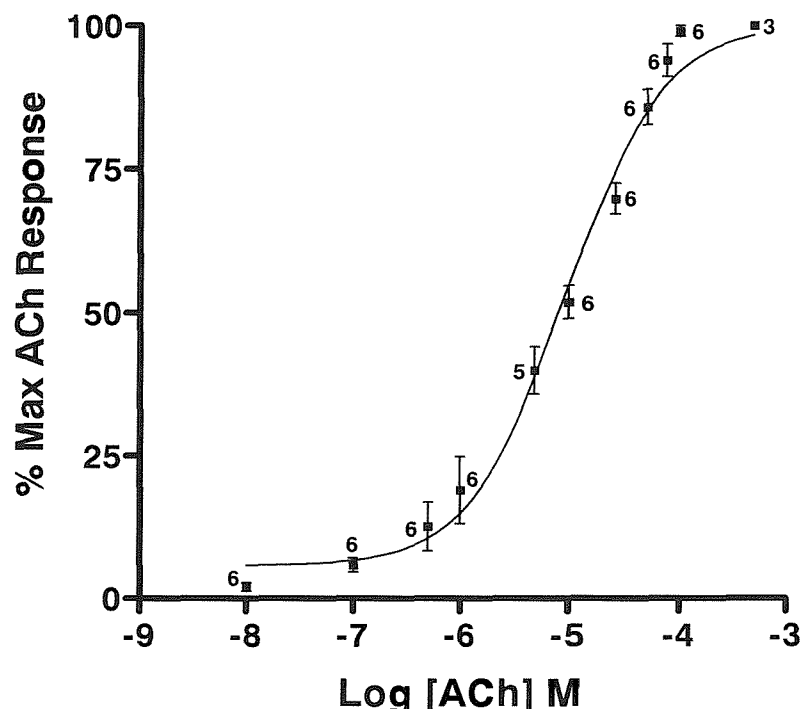


**Fig 3.1 The effect of ACh on *A. suum* DMS.** ACh causes a concentration-dependent contraction of *A. suum* muscle with an  $EC_{50}$  of  $9.2\mu M$ . Each point is the mean  $\pm$  S.E.Mean of (n) determinations.

### 3.3 Emodepside causes a relaxation of the basal tone of *A. suum* DMS.

Emodepside, at concentrations up to 10 $\mu$ M, produced a small relaxation of basal tension of the DMS ( $-0.19 \pm 0.04$  g;  $n=22$ ; Fig 3.2). This effect was irreversible within the time-course of the experiment. As the effect on basal tension was very small, the inhibitory action of emodepside against the contraction elicited by ACh was investigated.

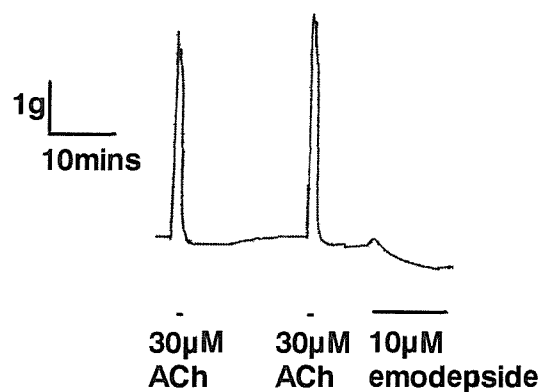


**Fig 3.2.** The effect of Emodepside on the basal tone of *A. suum* DMS. Emodepside causes a relaxation of the basal tone of *A. suum* DMS. An example trace showing relaxation of the basal tone of *A. suum* DMS following 10 $\mu$ M application of emodepside. The bars indicate duration of drug application.

### 3.4 Time dependence of emodepside action.

The time-dependent effect of emodepside on the contraction elicited by ACh was investigated. ACh (30  $\mu$ M) produced a rapid contraction of the DMS, which readily reversed on washing. Application of emodepside (10  $\mu$ M) to the muscle prior to addition of ACh (30  $\mu$ M) caused a time-dependent reduction in the amplitude of the ACh contraction (Fig. 3.3A). A 2 min application of emodepside to the *A. suum* muscle strip caused no significant reduction of ACh-induced muscle contraction ( $n=6$ ) (Fig 3.3B). Application of emodepside (10  $\mu$ M) to the muscle for 5 min prior to the addition of ACh (30  $\mu$ M) reduced the ACh contraction by  $12 \pm 6$  % ( $n=6$ ) (Fig 3.3B). 10 min emodepside application significantly reduced the contraction by  $39 \pm 6$  % ( $P<0.05$ ,  $n=6$ ) (Fig 3.3B). This effect would seem to be maximal as no further reduction in the contraction was observed when emodepside was applied for 30 min (Fig 3.3B).

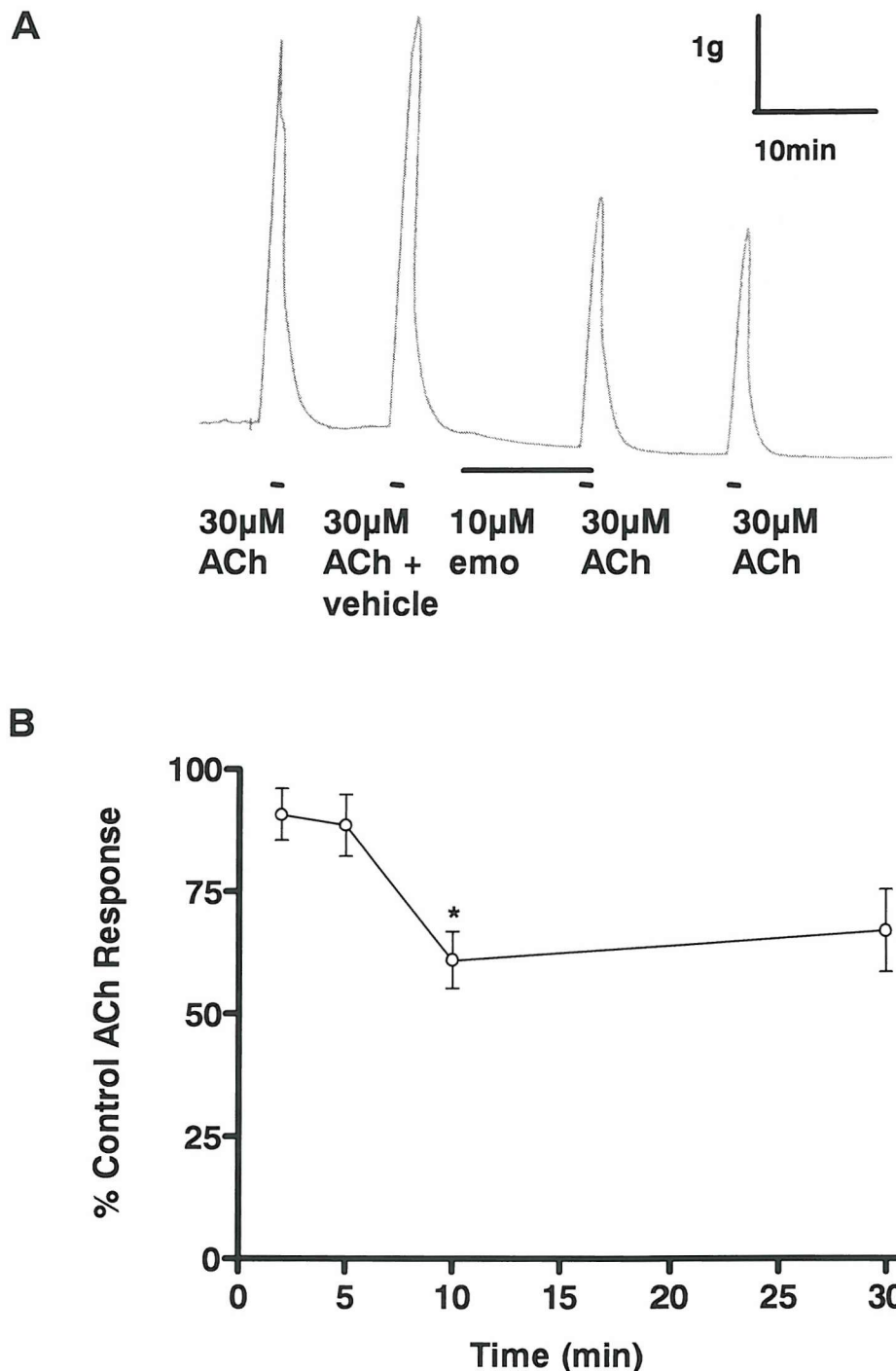


**Fig 3.3. The time-dependent effect of emodepside (10 $\mu$ M) on the response to ACh. A.** Example trace for the response to ACh after 10 min pre-incubation with emodepside. The bars indicate duration of drug application. **B.** Summary of the data from 6 experiments. The 'control' contraction is the response to 30  $\mu$ M ACh in the absence of emodepside. Emodepside was then applied to the DMS for 2,5,10 and 30mins and then the response to 30  $\mu$ M ACh was measured.

### 3.5 Effect of varying concentrations of emodepside on ACh-induced DMS contraction.

The time-dependent experiments showed that a 10 minute application of 10 $\mu$ M emodepside caused the greatest reduction in ACh-induced contraction of *A. suum* DMS, so this time-point was chosen to investigate the concentration-dependence of the inhibitory action of emodepside. Emodepside, at 0.5, 1 $\mu$ M and 5 $\mu$ M applied to the muscle strip 10 minutes prior to ACh addition, caused no significant reduction, of ACh-induced DMS contraction. 10 $\mu$ M emodepside application caused a significant reduction in the ACh-induced contraction of *A. suum* DMS ( $39 \pm 4\%$ ) ( $P<0.05, n=9$ ). The threshold concentration for inhibition of the ACh contraction was around 5 $\mu$ M (Fig 3.4). Higher concentrations of emodepside were not used due to solubility problems.

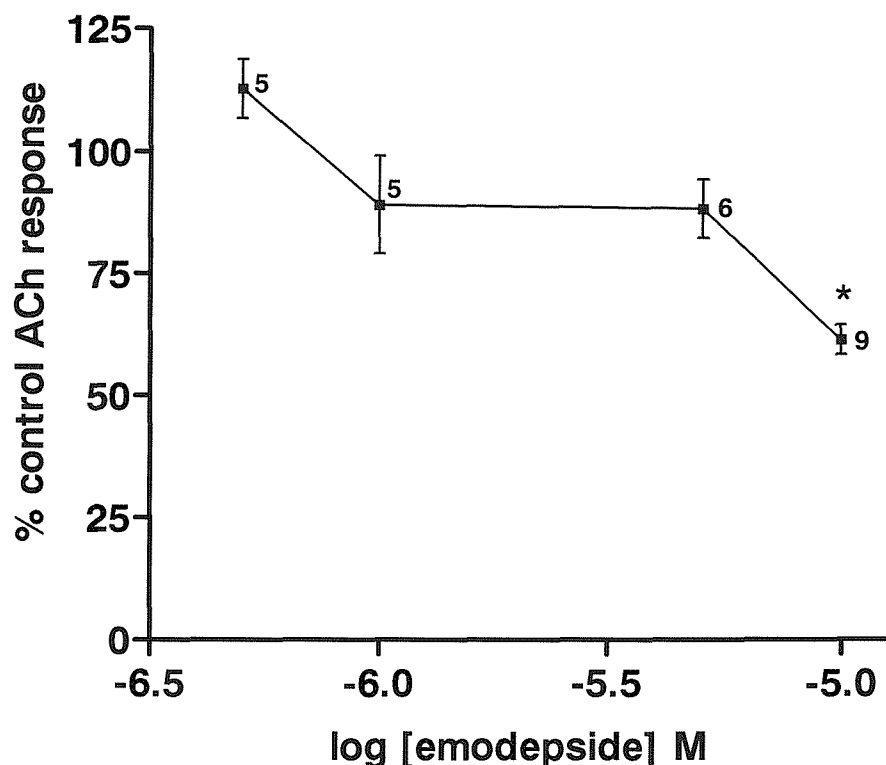


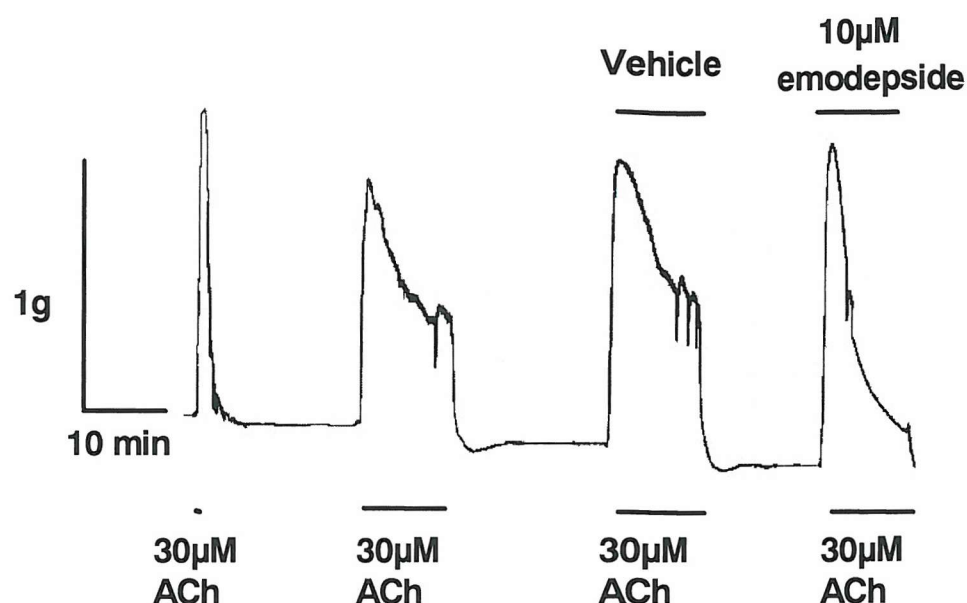
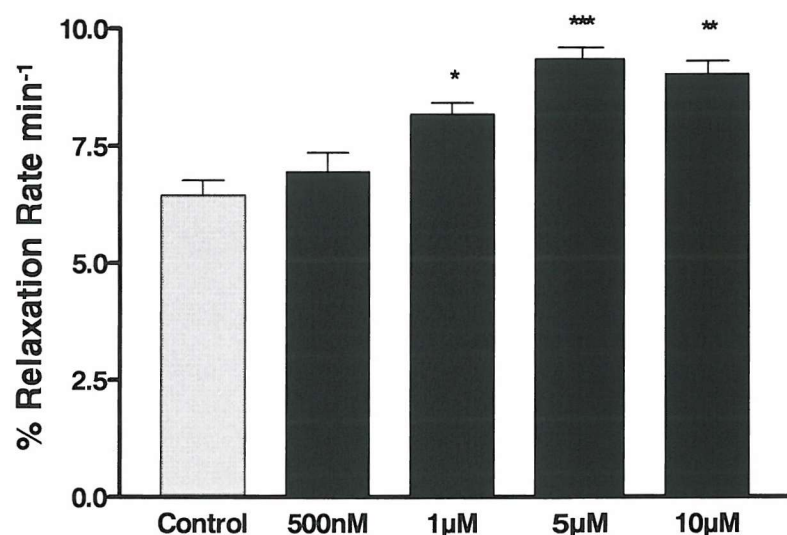
**Fig 3.4 The effect of varying concentrations of emodepside on the 30 $\mu$ M ACh induced contraction of *A. suum* DMS.** Contractions were obtained for ACh. Emodepside was then applied to the DMS at concentrations of 500nM, 1 $\mu$ M, 5 $\mu$ M and 10 $\mu$ M for 10mins before application of ACh. Each point is the mean  $\pm$  S.E.M of (n) determinations. \* $P<0.05$ , n=9.

### 3.6 Effect of varying concentrations of emodepside on DMS pre-contracted with ACh.

As reported in section 3.3, emodepside caused a slight relaxation of the basal tone of *A. suum* DMS. To investigate relaxation of the muscle by emodepside more directly, the muscle was pre-contracted with ACh (30  $\mu$ M). Emodepside was applied to the muscle at the peak of the contraction and the time-course of the subsequent relaxation followed for 10 min, at which point the preparation was washed. The relaxation rate per minute was calculated as follows;

$$\% \text{ relaxation rate min}^{-1} = \frac{P-R}{10} \times \frac{1}{100}$$

where 'P' is the muscle tension during the peak contraction and 'R' is muscle tension immediately prior to the wash. Prolonged application of ACh to the DMS caused an initial contraction followed by a slow relaxation of  $6.4 \pm 0.3 \text{ \% min}^{-1}$  ( $n=21$ ). In vehicle control experiments, addition of 0.1% EtOH at the point of maximal ACh contraction resulted in a similar relaxation rate of  $6.9 \pm 0.2 \text{ \% min}^{-1}$  ( $n=22$ ) (Fig 3.5A). Addition of 0.5 $\mu$ M emodepside at the peak of the ACh contraction had no effect on this relaxation rate ( $6.9 \pm 4.0 \text{ \% min}^{-1}$ ,  $n=6$ ). However, at higher concentrations emodepside significantly increased relaxation rate (1  $\mu$ M,  $8.2 \pm 0.2 \text{ \% min}^{-1}$ ,  $n=5$   $P<0.05$ ; 5 $\mu$ M,  $9.3 \pm 0.3 \text{ \% min}^{-1}$ ,  $n=5$ ,  $P<0.01$ ; 10  $\mu$ M,  $9.0 \pm 0.3 \text{ \% min}^{-1}$ ,  $n=5$ ,  $P<0.001$ ; (Fig 3.5B).

**A****B**

**Fig 3.5 The effect of varying concentrations of emodepside on prolonged ACh induced contraction of *A. suum* DMS.** **A.** Example of the effect of emodepside on muscle relaxation rate. The horizontal bar indicates the duration of application of ACh and the addition of either vehicle (0.1 % ethanol, indicated by arrow) or 10  $\mu$ M emodepside at the peak of the contraction. **B.** Pooled data for different concentrations of emodepside (n=5). The relaxation was measured as the difference in tension at the peak of the response and prior to the wash, expressed as a percentage of the peak contraction and divided by 10, to yield the % relaxation rate  $\text{min}^{-1}$ . ‘Control’ is the relaxation rate with ACh alone. \* P<0.05, n=5; \*\*P<0.01, n=5 \*\*\* P<0.001, n=5.

### **3.7 The effect of emodepside on the excitatory and inhibitory actions of neuropeptides on *A. suum* DMS.**

Emodepside, therefore, inhibits ACh-induced contraction of *A. suum* DMS and relaxes *A. suum* muscle directly or following pre-contraction with ACh. The neuropeptide AF2 elicits a biphasic effect on muscle tension an initial relaxation is followed by a prolonged contraction. During the contraction phase rhythmic relaxations occur muscle, (Pang *et al.*, 1995). To investigate whether emodepside has a general inhibitory action on *A. suum* DMS, the muscle was pre-contracted with AF2.

#### **3.7.1 The Effect of Emodepside on *A. suum* DMS pre-contracted with AF2.**

AF2 application to *A. suum* DMS caused an initial relaxation in only 8 out of 23 preparations. A prolonged contraction was observed in all 23 preparations. During the contraction phase, rhythmic relaxations occur. This effect persisted for more than 1 hour after just a 2 min application of AF2, consistent with the findings of (Pang *et al.*, 1995). Application of 0.5 $\mu$ M emodepside to the AF2-induced contracted DMS caused a relaxation (in 4 out of 6 preparations), but failed to completely inhibit the rhythmic AF2 activity. At higher concentrations, emodepside caused a relaxation and abolished the AF2-induced rhythmic activity (1 $\mu$ M, 6 out of 7 preps; 5 $\mu$ M, 5 out of 5 preps; and 10 $\mu$ M, 5 out 5 preps; Fig 3.6).

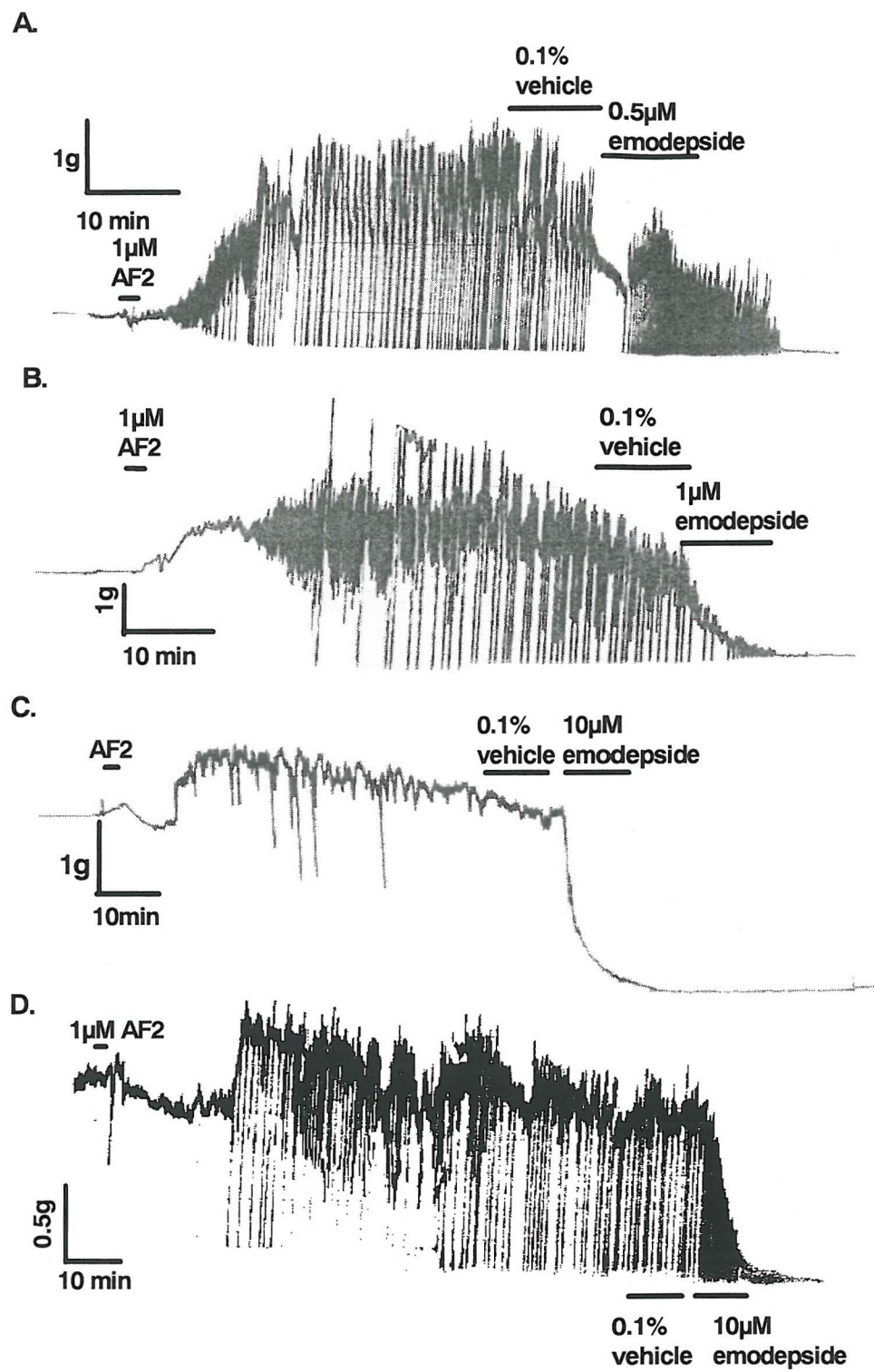


**Fig 3.6 The effect of emodepside on the response to the excitatory neuropeptide AF2.** AF2 was added to the preparation for 2 min, as indicated. A characteristic increase in rhythmic activity was observed. In control experiments this persisted for more than 1 hr. Application of either vehicle or emodepside is indicated by the bar. **A** 0.5 $\mu$ M emodepside caused a relaxation but failed to inhibit rhythmic activity. Emodepside caused a transient increase in the frequency of the rhythmic activity, followed by a complete cessation of activity at **B**, 1 $\mu$ M **C**, 5 $\mu$ M and **D** 10 $\mu$ M.

### **3.8 A comparison of the effect of emodepside and PF2 (SADPNFLRFamide) on *A. suum* DMS.**

Neuropeptides have both excitatory and inhibitory actions on *A. suum* muscle. One neuropeptide, PF2, inhibits ACh induced contraction of *A. suum* muscle, and relaxes the basal tone of *A. suum* muscle (Franks *et al.*, 1994) in a similar manner to emodepside A comparison of the effect of PF2 and emodepside on *A. suum* DMS may therefore provide an insight into emodepside mechanism of action.

#### **3.8.1 Effect of PF2 on ACh induced DMS contraction.**

A 10 minute application of 1 $\mu$ M PF2 to *A. suum* DMS caused a reduction in ACh induced contraction of  $47 \pm 6\%$  ( $P<0.05, n=6$ ) (Fig 3.7), which fully reversed after 1 hour.

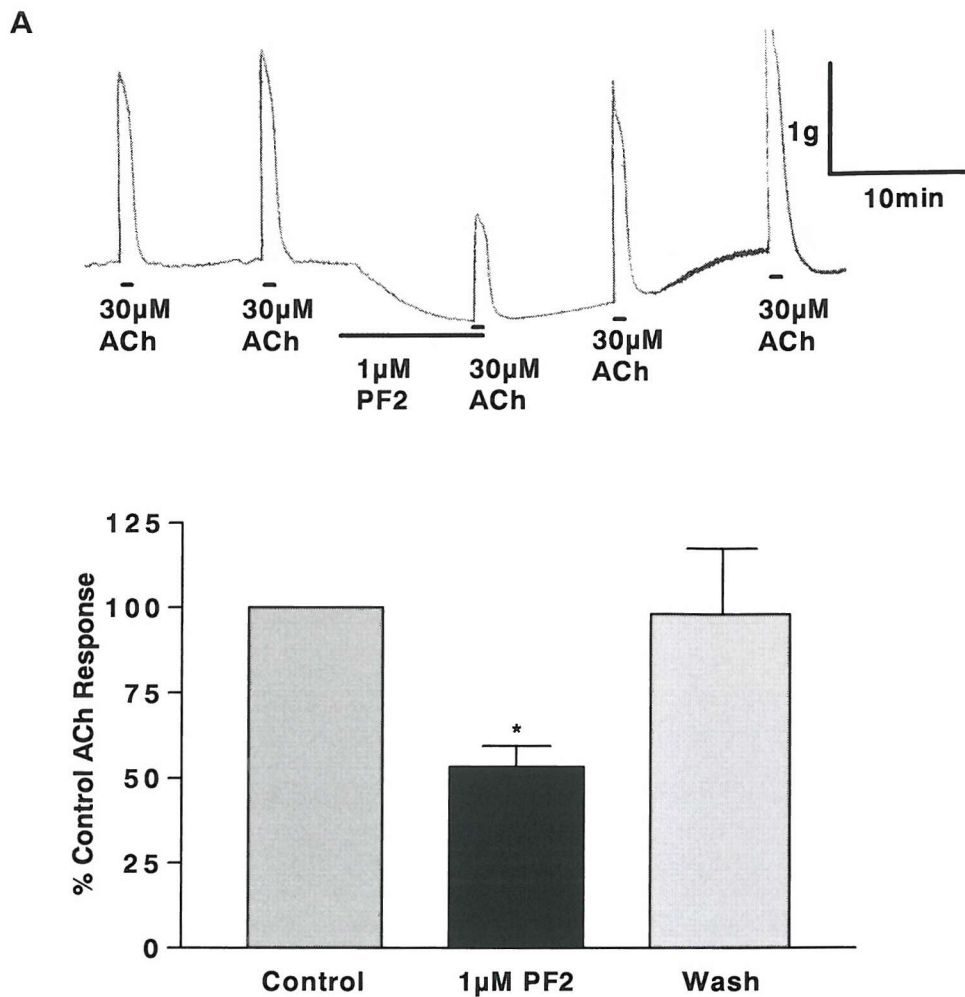


**Fig 3.7 Effect of addition of 1μM PF2 on ACh-induced contraction of *A. suum* DMS strip.** A. Representative response of a 10min application of 1μM PF2 on *A. suum* DMS. B. Pooled data for the effect of pre-incubation of the muscle with 1μM PF2, on the amplitude of the contraction to ACh. The control response is the response to 30μM ACh prior to addition of 1μM PF2. \* P<0.05, n=6.

### 3.8.2 Effect of addition of emodepside and subsequent addition of PF2 on DMS contraction.

*A. suum* muscle was investigated following pre-treatment with emodepside to determine whether emodepside inhibited the PF2 response. 10 minute application of 10μM emodepside to *A. suum* DMS strip caused a reduction of ACh-induced contraction of  $29 \pm 3\%$  (n=5). A subsequent addition of 1μM PF2 for 10mins caused a further 23% reduction of the ACh-induced contraction resulting in a  $52 \pm 9\%$  (n=5) (Fig 3.8) inhibition of the ACh-induced contraction.

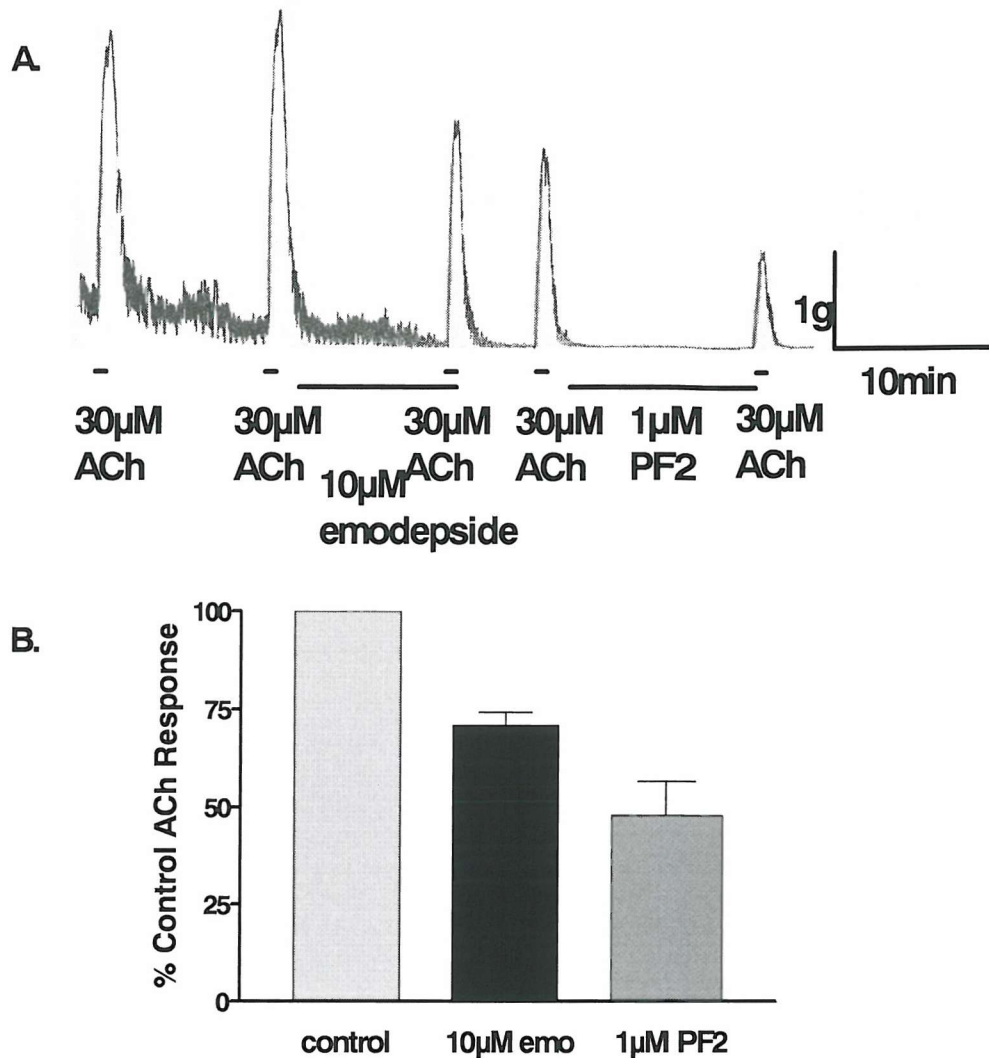


**Fig 3.8 Effect of emodepside and subsequent addition of PF2 on ACh-induced contraction of *A. suum* DMS strip. A** Representative response of a 10min application of 10 $\mu$ M emodepside followed by 10min application of 1 $\mu$ M PF2 on *A. suum* DMS. **B** Pooled data for the combined effect of pre-incubation of the muscle with PF2, followed by emodepside, on the amplitude of the contraction to ACh. The control response is the response to 30 $\mu$ M ACh prior to addition of either 1 $\mu$ M PF2 or 10 $\mu$ M emodepside.

### 3.8.3 Effect of addition of PF2 and subsequent addition of emodepside on DMS contraction.

*A. suum* DMS was then pre-treated with PF2 prior to emodepside application. A 10 minute application of 1 $\mu$ M PF2 to *A. suum* DMS strip caused a reduction of ACh-induced contraction of  $43 \pm 10\%$  ( $n=5$ ). A subsequent addition of 10 $\mu$ M emodepside for 10 mins caused no further reduction of the ACh induced contraction of the DMS (Fig 3.9).

**A**

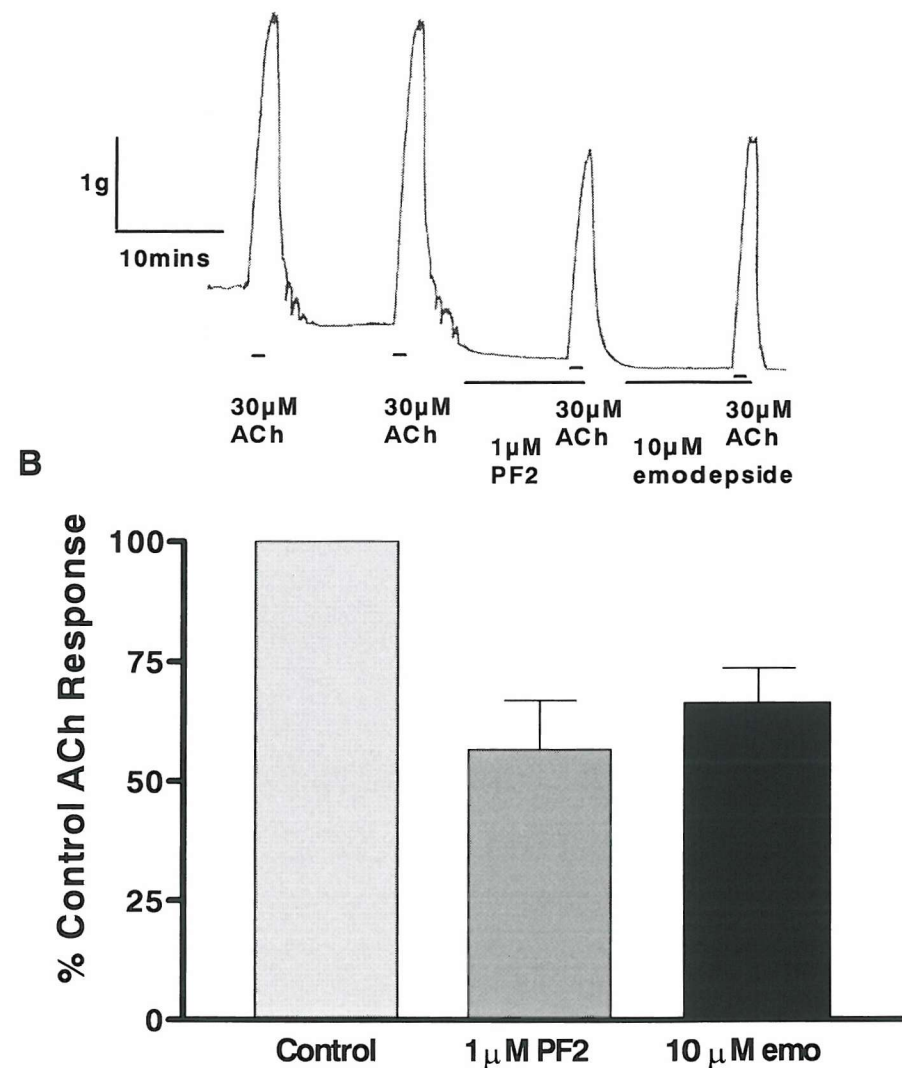


**Fig 3.9** Effect of PF2 and subsequent addition of emodepside on ACh-induced contraction of *A. suum* DMS strip. **A** Representative response of a 10min application of 1 $\mu$ M PF2 followed by 10min application of 10 $\mu$ M emodepside on *A. suum* DMS. **B** Pooled data for the combined effect of pre-incubation of the muscle with PF2, followed by emodepside, on the amplitude of the contraction to ACh. The control response is the response to 30 $\mu$ M ACh prior to addition of either 1 $\mu$ M PF2 or 10 $\mu$ M emodepside.

### 3.8.4 The Effect of the simultaneous application of PF2 and emodepside to *A. suum* DMS.

Emodepside and PF2 were then applied simultaneously to *A. suum* DMS. 1 $\mu$ M PF2 and 10 $\mu$ M emodepside applied to *A. suum* DMS prior to 30 $\mu$ M ACh application caused a reduction in the ACh-induced contraction by 56  $\pm$  3% (n=5) (Fig3.10).

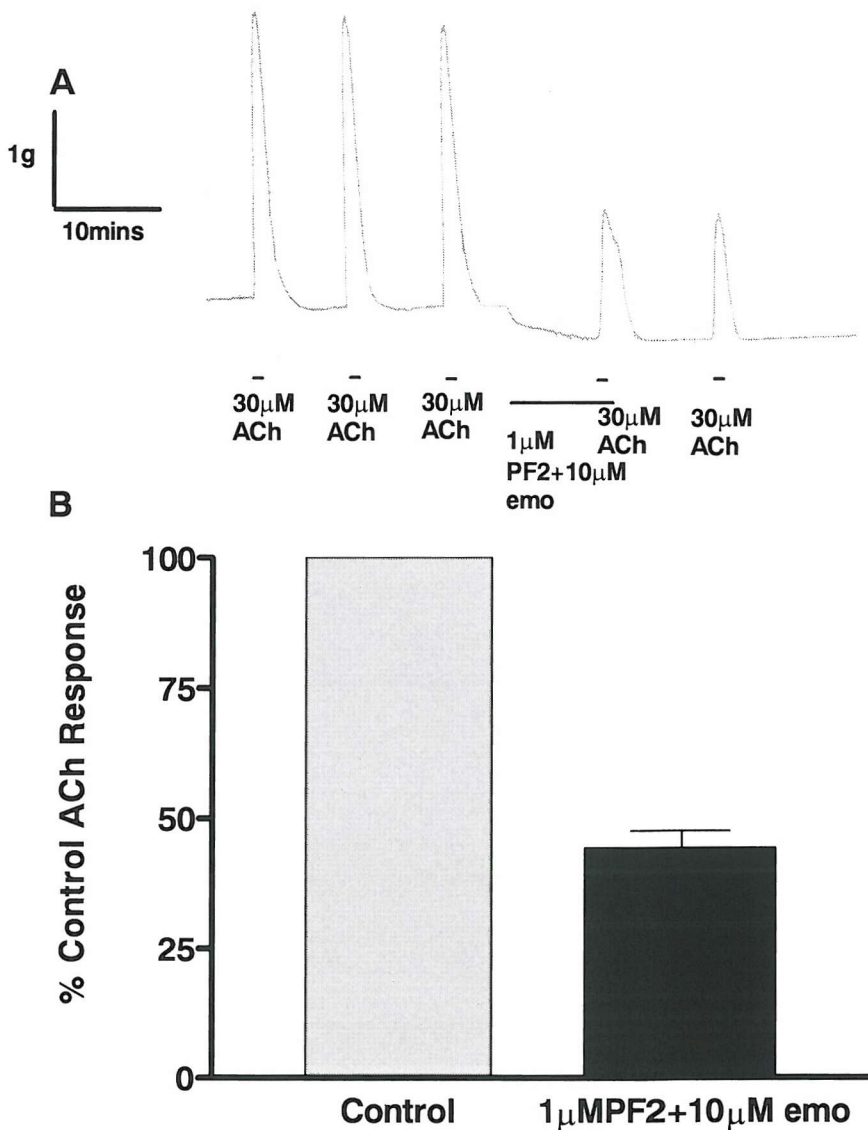


**Fig 3.10 Effect of PF2 and simultaneous emodepside addition on ACh-induced contraction of *A. suum* DMS strip.** A Representative response of a 10min application of 1 $\mu$ M PF2 and 10 $\mu$ M emodepside on *A. suum* DMS. B. Pooled data for the combined effect of pre-incubation of the muscle with PF2, and emodepside, on the amplitude of the contraction to ACh. The control response is the response to 30 $\mu$ M ACh prior to addition of 1 $\mu$ M PF2 and 10 $\mu$ M emodepside.

### **3.9 A comparison of the effect PF2 and emodepside on the prolonged ACh-induced contraction of *A. suum* DMS.**

PF2 caused a relaxation of *A. suum* DMS following prolonged ACh-induced contraction (30 $\mu$ M) similar to emodepside. ACh applied to *A. suum* DMS for 10 minutes caused an initial contraction followed by a slow relaxation of  $7.41 \pm 0.25\% \text{ min}^{-1}$  (n=6). Application of 1 $\mu$ M PF2 at the point of maximal ACh contraction caused a significant increase in the rate of relaxation of  $9.2 \pm 0.4 \% \text{ min}^{-1}$  (n=6) (P<0.01). The preparations were then left to recover (1hour). A subsequent addition of emodepside at the maximum point of ACh contraction also caused a significant increase in the rate of relaxation of  $9.0 \pm 0.4 \% \text{ min}^{-1}$  (n=6), (P<0.05), similar to PF2 (Fig 3.11).

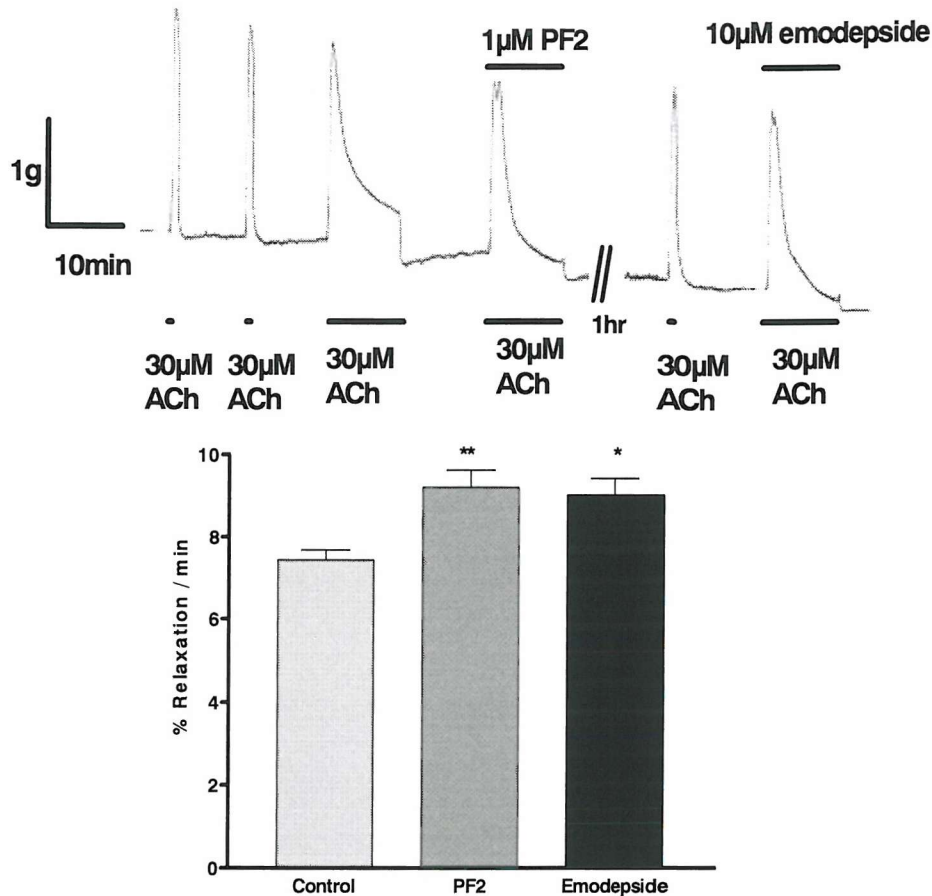
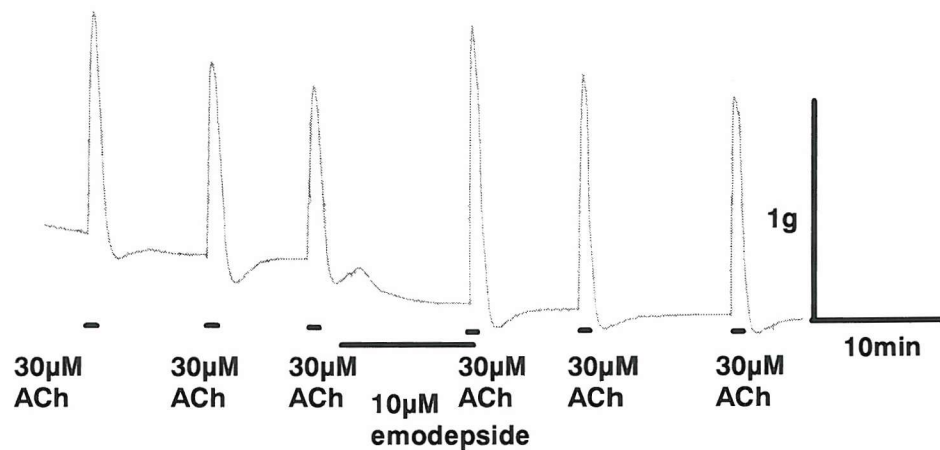


**Fig 3.11 A comparison of the effect of PF2 and emodepside on the prolonged contraction of *A. suum* DMS by ACh. A.** Example of the effect of PF2 on muscle relaxation rate. The horizontal bar indicates the duration of application of ACh. The bar indicates either the addition of 1 $\mu$ M PF2, or 10 $\mu$ M emodepside at the peak of contraction. **B** Pooled data showing comparison of PF2 and emodepside relaxation rates. The relaxation was measured as the difference in tension at the peak of the response prior to wash, expressed as a percentage of the peak concentration and divided by 10, to yield the % relaxation rate  $\text{min}^{-1}$ . 'Control' is the relaxation rate with ACh alone \* $P<0.05$ , n=6 \*\* $P<0.01$  n=6. Prolonged ACh application resulted in an initial contraction followed by a slow relaxation which did not return to baseline prior to wash. PF2 and emodepside application resulted in a faster relaxation which returned to baseline before wash.

### 3.10 Effect of emodepside on denervated nerve preparation of *A. suum* DMS.

To determine whether the inhibitory action of emodepside may involve neurotransmitter release from the nerve cord onto the muscle, the action of emodepside on muscle strips from which the nerve cord had been removed was tested. This was obtained by cutting along a lateral line and opening up the muscle exposing both nerve cords. The muscle strip was then cut on the inner side of the nerve cords so that only body wall muscle between the nerve cords remained (diagram section ). All 6 preparations responded to ACh with a contraction, however 10  $\mu$ M emodepside applied for 10 min failed to inhibit this contraction (Fig 3.12).

A.



B.

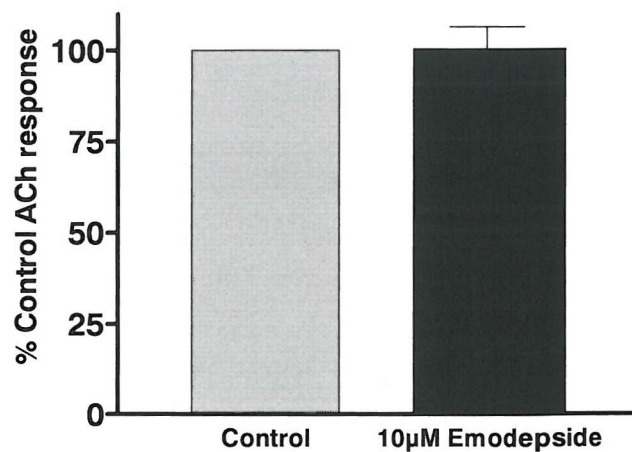


**Fig 3.12 Effect of 10min application of 10 $\mu$ M emodepside on *A. suum* denervated muscle strips.** A. Representative response of 10 $\mu$ M emodepside on denervated muscle strip. B. Pooled data for the effect of 10 $\mu$ M emodepside on the amplitude of the contraction to ACh. The control response is the response to 30 $\mu$ M ACh prior to addition of 10 $\mu$ M emodepside.

### 3.11 Effect of PF2 on a denervated nerve preparation of *A. suum* DMS.

As PF2 and emodepside action on *A. suum* muscle are similar, PF2 action was also investigated on the denervated muscle preparation. PF2 caused an inhibition of  $55 \pm 12\%$  ( $n=2$ ) of ACh ( $30\mu\text{M}$ ) induced contraction of an *A. suum* denervated muscle preparation (Fig 3.13).

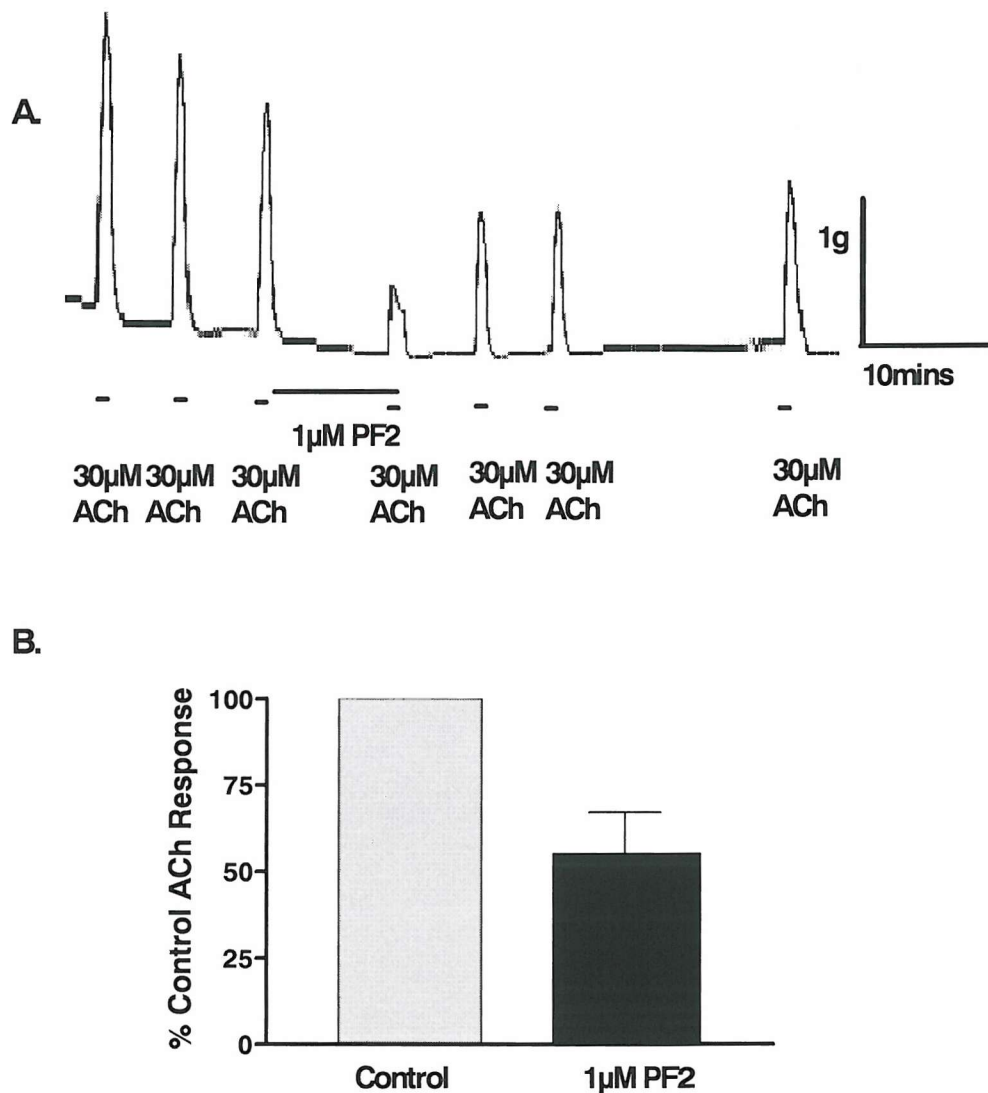


**Fig 3.13 Effect of a 10min application of  $1\mu\text{M}$  PF2 to *A. suum* denervated muscle strips. A.** Representative response of  $10\mu\text{M}$  PF2 on denervated muscle strip. **B.** Pooled data for the effect of  $1\mu\text{M}$  PF2 on the amplitude of the contraction to ACh. The control response is the response to  $30\mu\text{M}$  ACh prior to addition of  $1\mu\text{M}$  PF2.

### **3.12 Effect of emodepside on muscle cell membrane potential.**

10 $\mu$ M and 1 $\mu$ M emodepside application for 2 minutes to *A. suum* muscle cells caused a significant slow hyperpolarisation of *A. suum* muscle cells with no change in input conductance. After 30 minutes the average membrane potential change was  $-2.4 \pm 0.6$  mV,  $P < 0.001$  (paired t-test),  $n=6$  for 1 $\mu$ M emodepside and  $-5.4 \pm 0.96$  mV ( $P < 0.001$  paired t-test),  $n=8$ , (Fig 3.14) for 10 $\mu$ M emodepside. 100nM emodepside ( $-0.7 \pm 0.1$  mV,  $n=2$ ) failed to cause a significant hyperpolarisation of *A. suum* membrane potential.

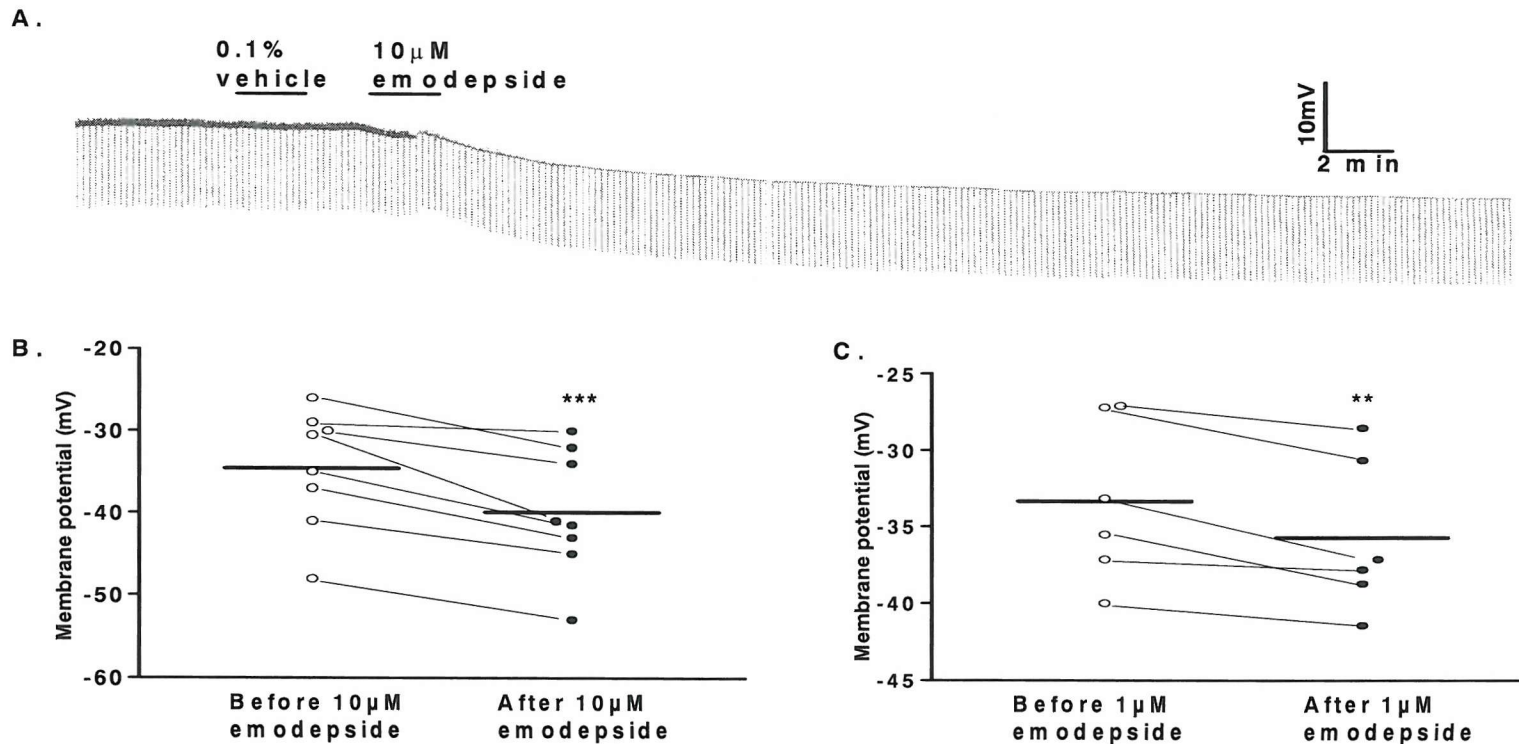


**Fig 3.14. The effect of emodepside on the membrane potential of *A. suum* muscle cells.** A Representative response to 10 $\mu$ M emodepside. The horizontal bar indicates the duration of application. (Vehicle was without effect). Scale bars are 10 mV and 2 min. The downward deflections are caused by injection of hyperpolarizing current pulses (0.1 Hz, 20 nA, 500 ms) and provide a measure of cell input resistance. Note the decrease in 'noise' in the presence of emodepside. This is consistent with the abolition of spontaneous activity by emodepside. B. Graph summarizing the data from 8 similar experiments following 10 $\mu$ M emodepside application. (○) Resting membrane potential (●) 30mins after a 2 min perfusion of emodepside. Each point indicates an individual muscle cell recording. The bars indicate the average value. \*\*\* P<0.001, n=8, \*\* P<0.01 n=6.

### **3.13 Effect of emodepside on ACh-induced depolarisation of *A. suum* muscle Cells.**

10 $\mu$ M ACh application for 30secs caused a depolarisation of *A. suum* muscle cells of  $6.8 \pm 1.8$  mV. A subsequent application of emodepside (10 $\mu$ M) for 30mins caused a hyperpolarisation of the muscle cells of  $3.2 \pm 0.7$ mV. A further application of 10 $\mu$ M ACh following emodepside addition caused a depolarisation of  $6.7 \pm 2.2$ mV (Fig 3.15).

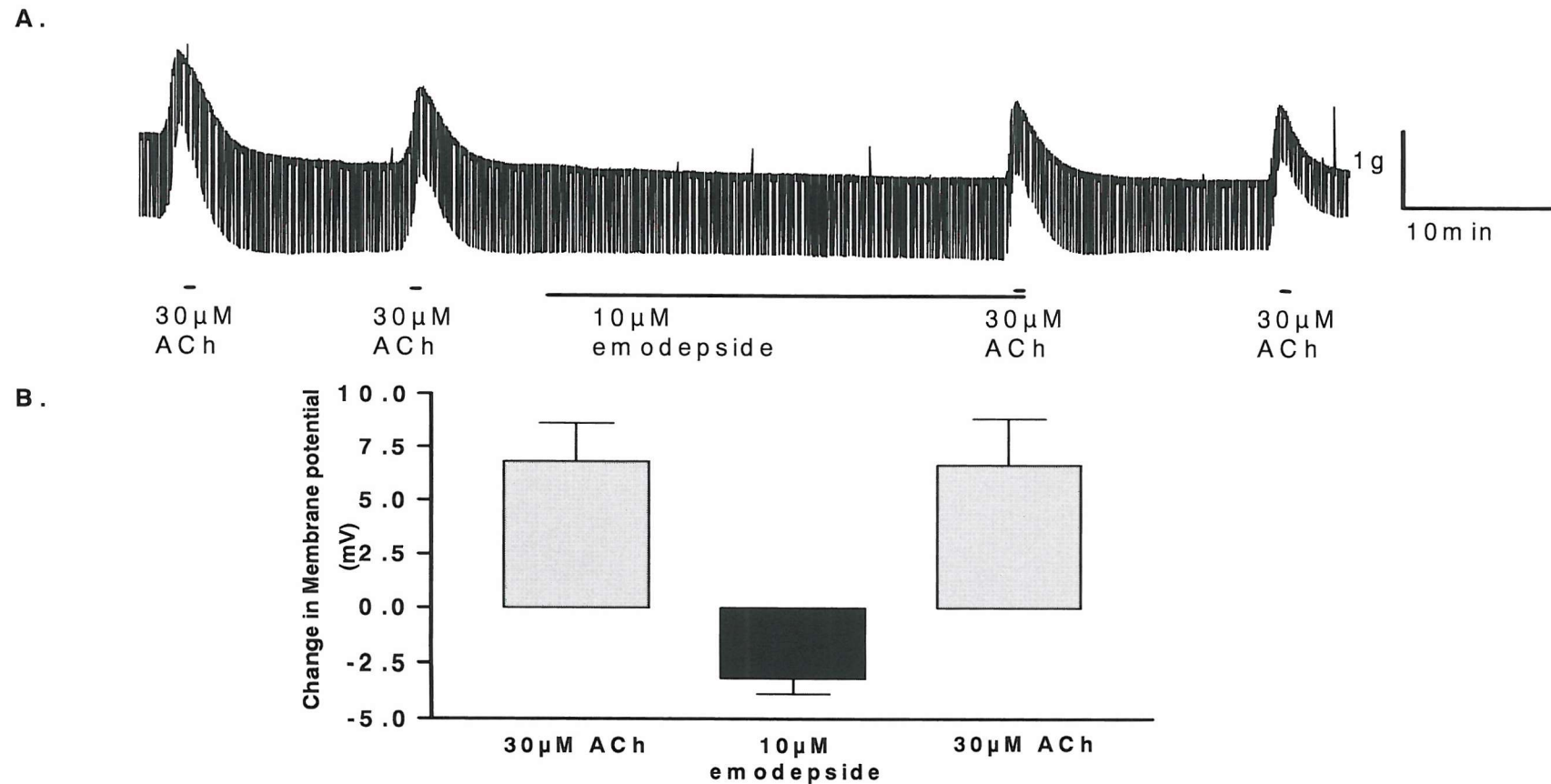


**Fig 3.15. The effect of emodepside on the ACh induced depolarisation of *A. suum* muscle cells.** A. Representative response to 30 $\mu$ M ACh and 10 $\mu$ M emodepside. The horizontal bar indicates the duration of application. Scale bars are 10 mV and 10 min. The downward deflections are caused by injection of hyperpolarizing current pulses (0.1 Hz, 20 nA, 500 ms) and provide a measure of cell input resistance. B. The graph summarizes the data from 4 similar experiments.

### 3.14 Effect of Emodepside on the AF2 induced increase in spontaneous activity of *A. suum* muscle cells.

AF2 (1 $\mu$ M for 2 min) caused a depolarisation and a sustained increase in the size of muscle cell spontaneous, depolarising spikes (from  $0.7 \pm 0.01$  mV to  $4.7 \pm 1.1$  mV; n=6). Subsequent addition of emodepside (10 $\mu$ M for 2 min) reduced the amplitude of the spikes to  $1.4 \pm 0.4$  mV after 30mins. Further addition of AF2 (1  $\mu$ M for 2 min) resulted in no further change in spike amplitude ( $1.4 \pm 0.5$  mV after 30 minutes) (Fig 3.16).

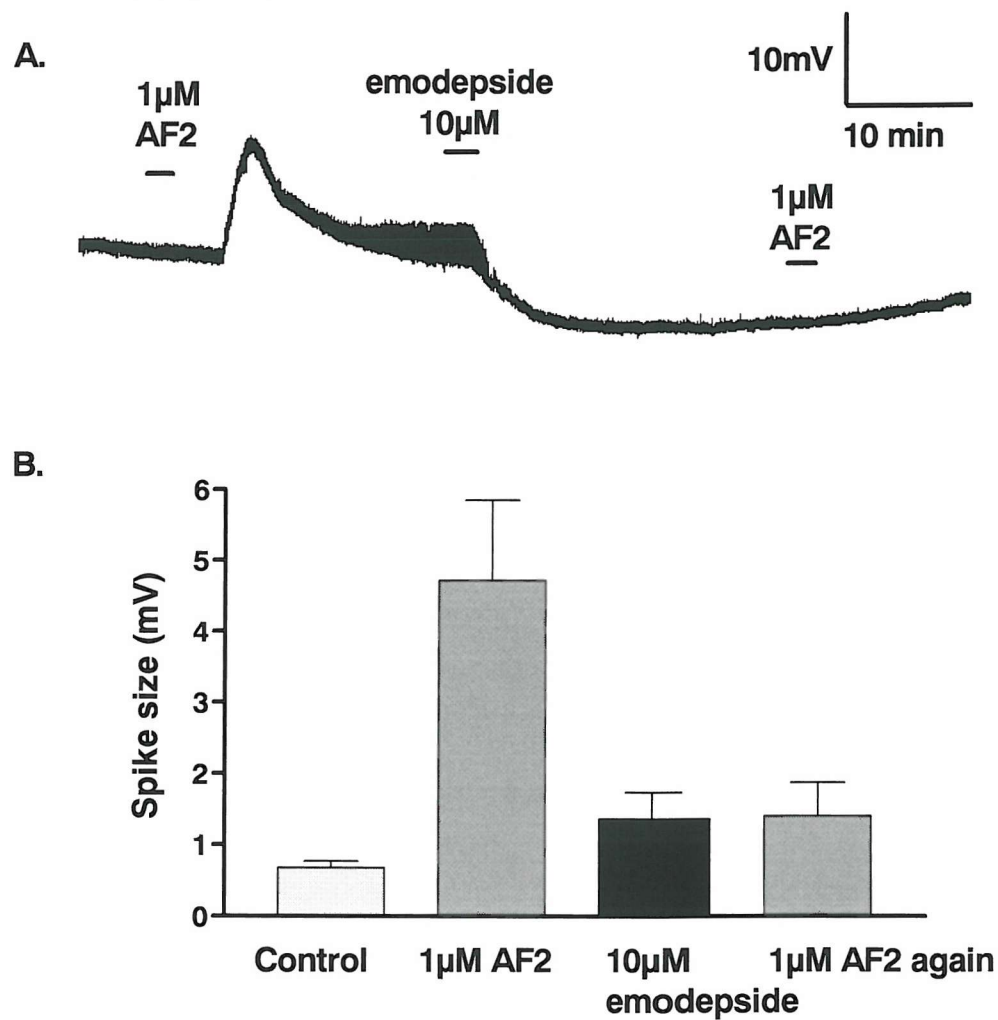


**Fig 3.16 The Effect of emodepside on the AF2-induced increase in spontaneous activity of *A. suum* muscle cells. A.** Representative recording of AF2 causing an increase in spontaneous activity, and inhibition by emodepside. The bars indicate duration of drug application. **B.** Pooled data showing the effect of emodepside on AF2-induced increase in spontaneous spike potentials. Control is the spontaneous activity before AF2 addition.

### **3.15 The ionic basis of the emodepside response in *A. suum* muscle cells.**

#### **3.15.1 Effect of emodepside on muscle cell membrane potential in calcium-free APF.**

10 $\mu$ M Emodepside applied to *A. suum* muscle cells for 2 minutes in calcium-free APF resulted in a hyperpolarisation of only  $2.19 \pm 1.1$ mV after 30minutes (n=8). 30 minutes after calcium ions were re-introduced into the APF, the muscle cells had significantly hyperpolarized by  $5.5$ mV  $\pm 1.1$ mV ( $P<0.002$ ), indicating a full recovery of the emodepside response (Fig 3.17).

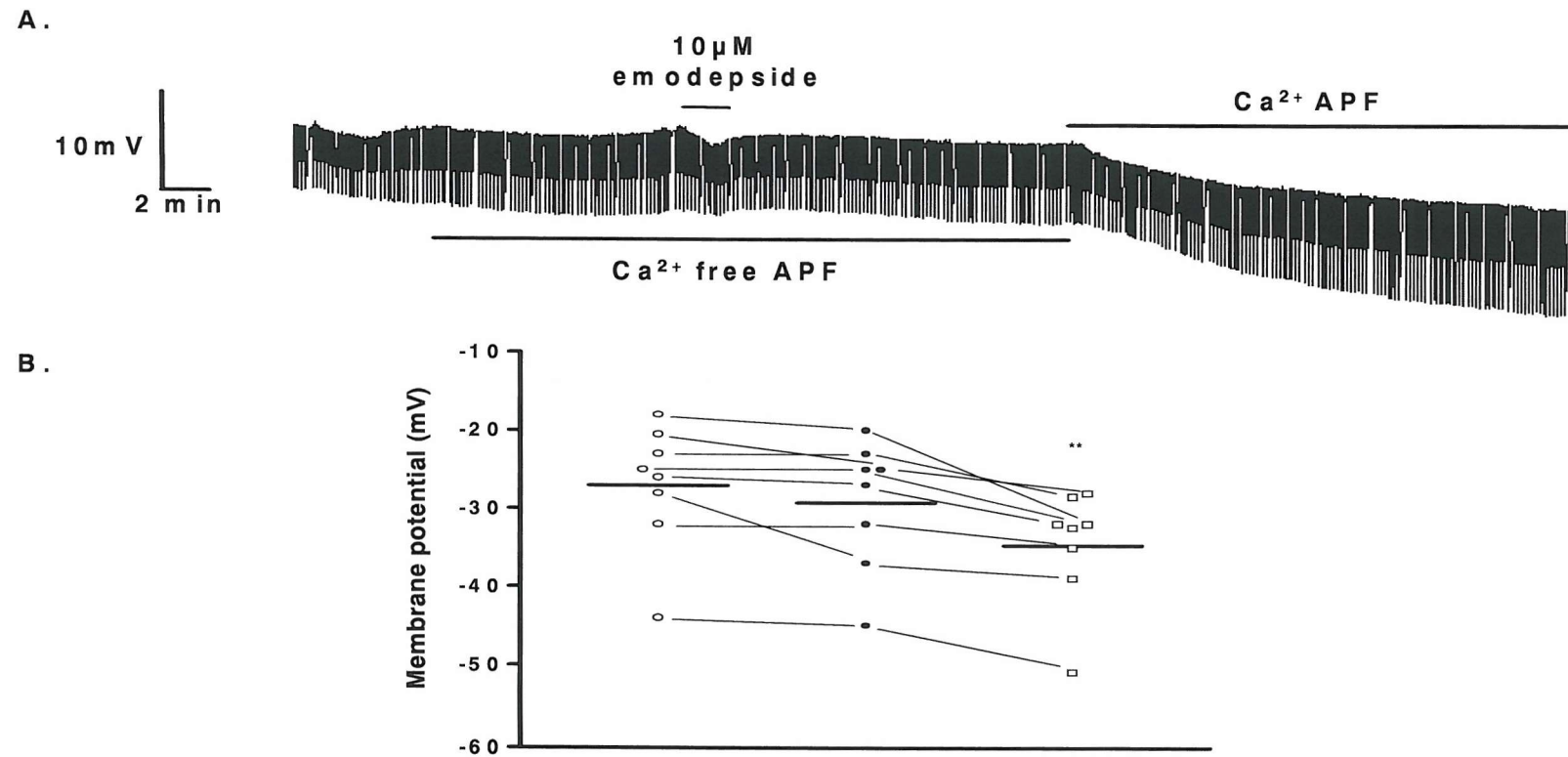


**Fig 3.17. The effect of removing extracellular calcium on *A. suum* muscle cell response to emodepside.** A. Representative recording of the effect of removal of calcium ions on emodepside action. The horizontal bar indicates the duration of application. (Vehicle was without effect). Scale bars are 10 mV and 2 min. The downward deflections are caused by injection of hyperpolarizing current pulses (0.1 Hz, 20 nA, 500 ms) and provide a measure of cell input resistance. The bar indicates the removal and subsequent re-introduction of calcium ions. B. The graph shows data from 8 similar experiments; (○) membrane potential in normal APF; (●) membrane potential 30mins after 2 min emodepside perfusion in the absence of calcium; (□) membrane potential 30 mins after re-introduction of calcium ions. \*\*P<0.002, n=8.

### **3.15.2 Effect of emodepside on muscle cell membrane potential in the presence of potassium channel blockers 4AP and TEA.**

Perfusion of the potassium channel blockers 4AP (250 $\mu$ M) and TEA (5mM) onto *A. suum* muscle cells caused a depolarisation of  $2.8 \pm 0.52$ mV (n=5). A 2 minute, 10 $\mu$ M application of emodepside in the presence of TEA and 4AP caused no change in muscle cell membrane potential after 10 minutes. Following wash of the TEA and 4AP the muscle cells hyperpolarized by  $5.18 \pm 1.96$ mV after 30 minutes. However, compared to the original membrane potential, emodepside caused a  $2.4 \pm 2.12$ mV hyperpolarisation of the muscle cells, indicating only a slight recovery of the emodepside response (Fig 3.18). This recovery was not statistically significant.

10 $\mu$ M of emodepside applied to individual muscle cells prior to TEA (250 $\mu$ M) and 4AP (5mM) application caused a hyperpolarisation of  $4.2 \pm 0.86$ mV after 10 minutes (n=4). Application of TEA and 4AP blocked this hyperpolarisation, and a slight depolarisation of  $2.15 \pm 0.9$ mV occurred. Following wash of the K<sup>+</sup> channel blockers no subsequent hyperpolarisation was observed but note this only occurred in two experiments (Fig 3.19).

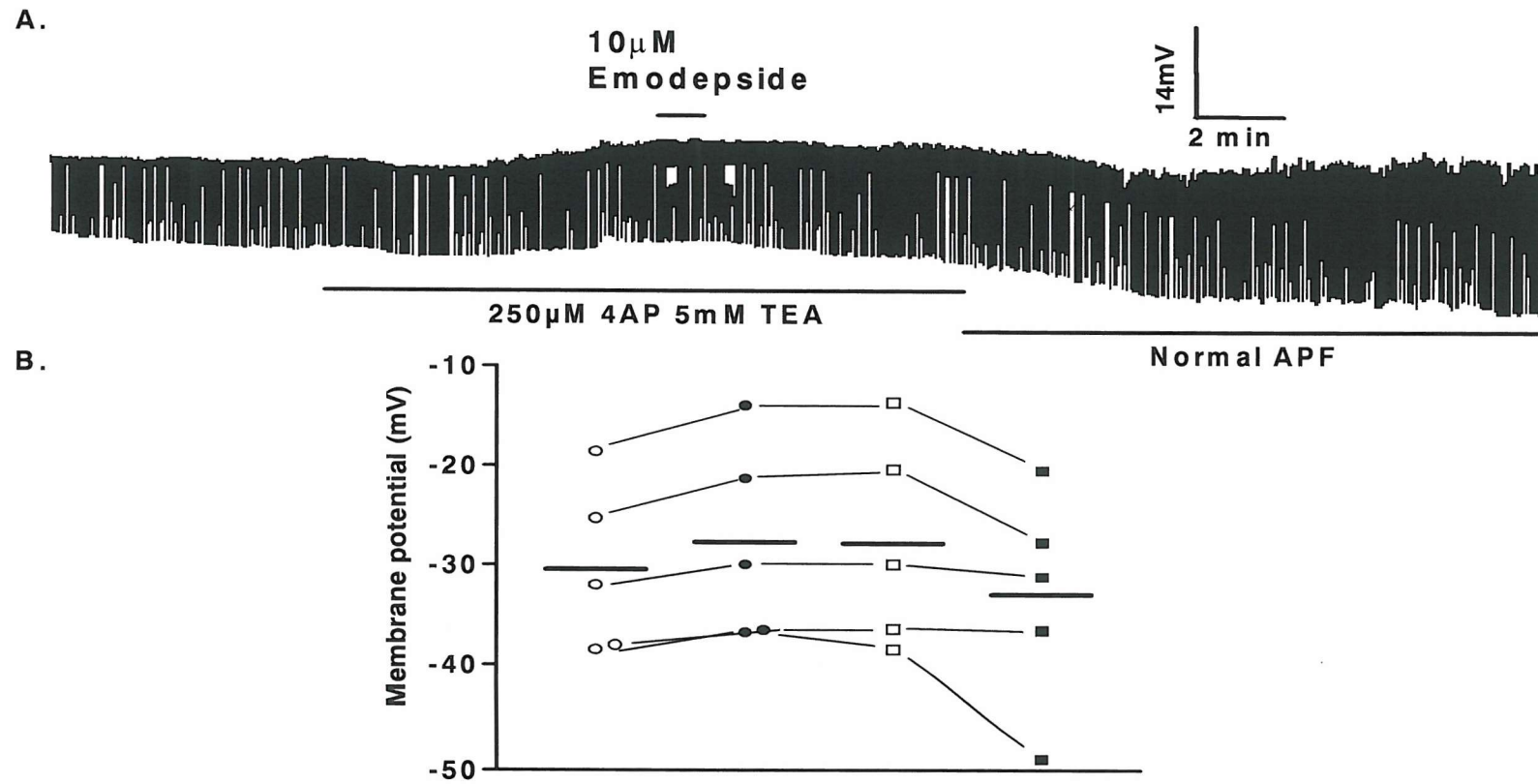


**Fig 3.18 Effect of K<sup>+</sup> channel blockers 4AP and TEA prior to emodepside-induced muscle cell hyperpolarisation.** A. Representative recording of the effect of TEA and 4AP prior to emodepside-induced hyperpolarisation. The bars indicate duration of drug application. The bar indicates either the removal or re-introduction of TEA and 4AP. B. Effect of emodepside on membrane potential in 4AP and TEA (○) Resting membrane potential. (●) Membrane potential in 4AP and TEA. (□) Membrane potential 30mins after a 2 min emodepside perfusion. (■) Membrane potential 30mins after removal of TEA and 4AP

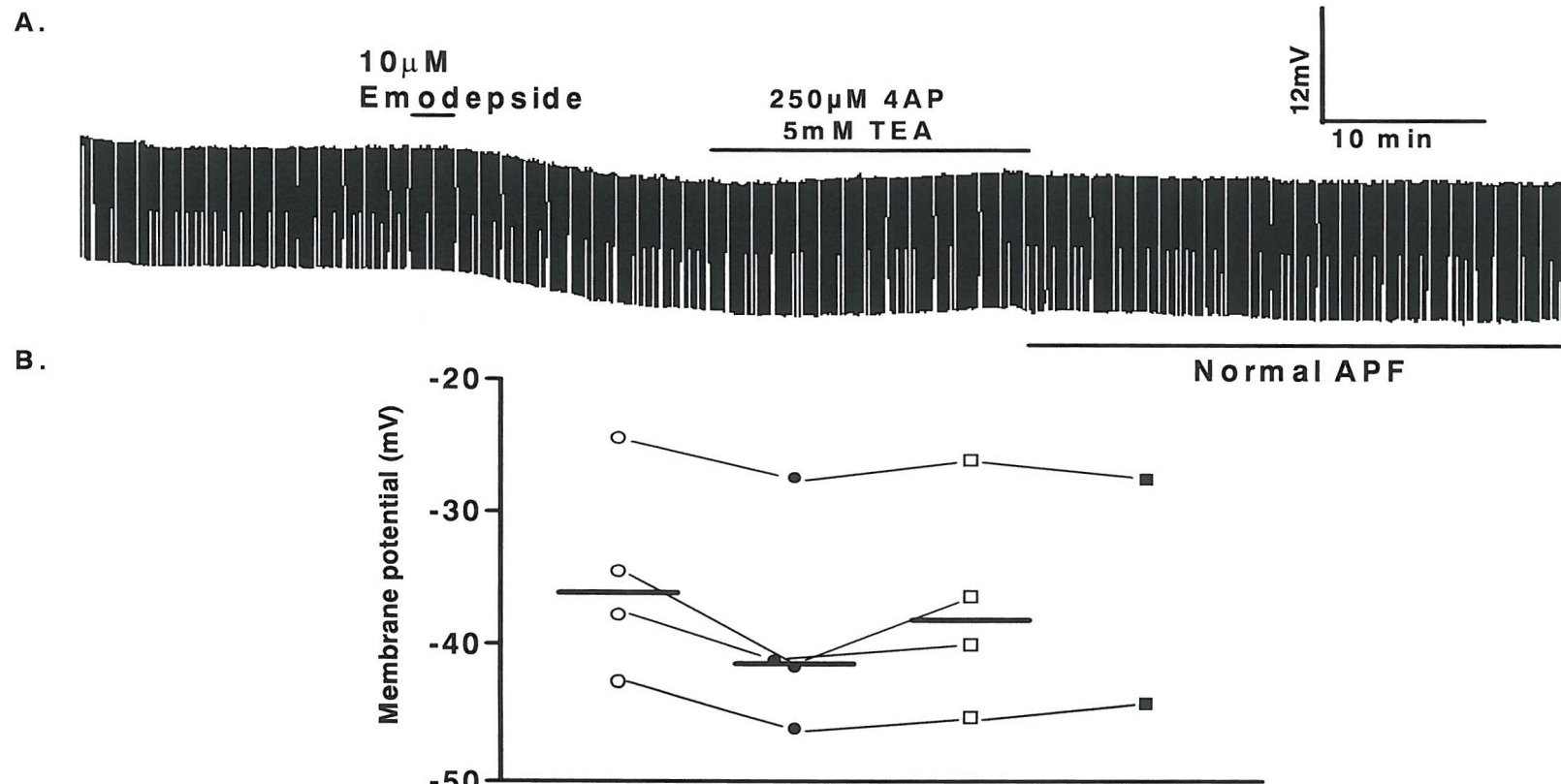
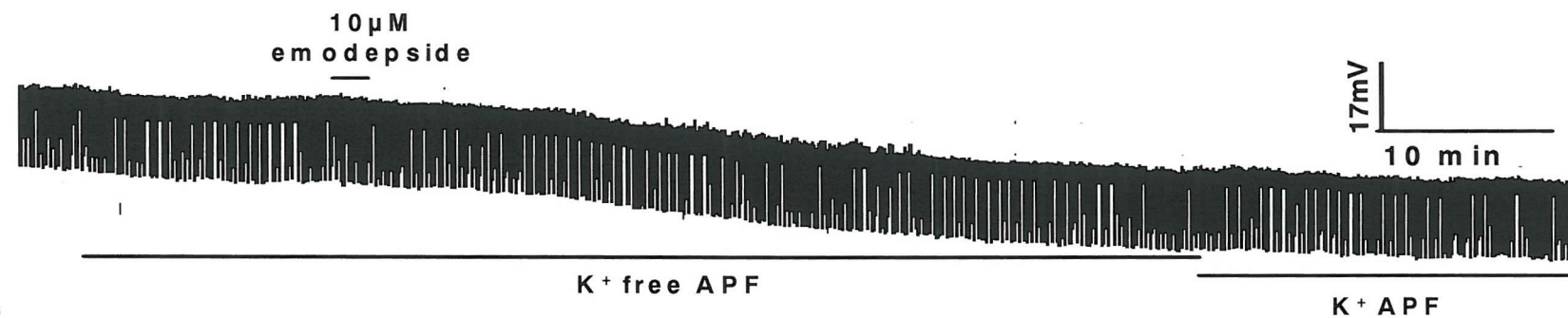


**Fig 3.19 Effect of  $K^+$  channel blockers 4AP and TEA following emodepside-induced muscle cell hyperpolarisation.** A. Representative recording of the effect of TEA and 4AP following emodepside induced hyperpolarisation. The bars indicate duration of drug application. The bar indicates either the removal or re-introduction of TEA and 4AP. B. Effect of emodepside on membrane potential in 4AP and TEA. (○) Resting membrane potential. (●) Membrane potential 10mins after a 2 min emodepside perfusion. (□) Membrane potential 10mins after introduction of TEA and 4AP. (■) Membrane potential 30mins after removal of TEA and 4AP

### **3.15.3 Effect of emodepside on muscle cell membrane potential in potassium-free APF.**

Perfusion of potassium free APF onto *A. suum* muscle cells resulted in a membrane hyperpolarisation of  $2.5 \pm 0.95$ mV after 10 minutes.  $10\mu\text{M}$  emodepside applied to *A. suum* muscle cells for 2 minutes in potassium-free APF resulted in a significant hyperpolarisation of  $12 \pm 3.7$  mV after 30minutes ( $P<0.05$ ,  $n=5$ ). This change in membrane potential was also significantly different when compared to the change in membrane potential following emodepside application in normal APF (section 3.12,  $P<0.05$ ). 10 minutes after potassium ions were re-introduced into the APF the muscle cells hyperpolarized by  $4.1 \pm 1.4$ mV (Fig 3.20).

A.



B.

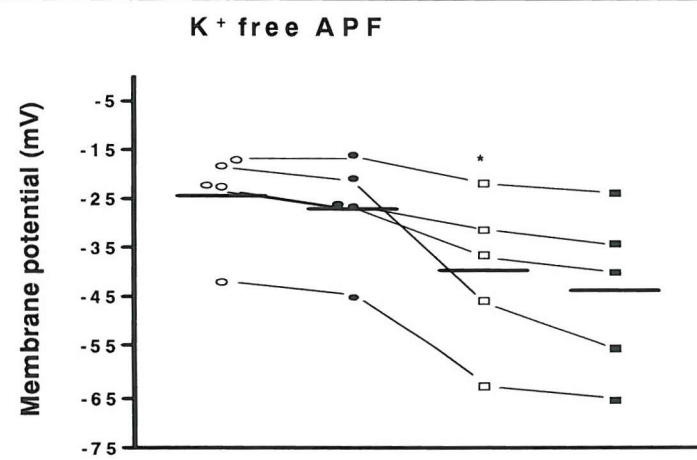


**Fig 3.20 Effect of removing extracellular potassium upon *A. suum* muscle cell hyperpolarisation in response to emodepside. A.** Representative recording of the effect of zero potassium on emodepside-induced hyperpolarisation. The bars indicate duration of drug application. The bar indicates either the removal or re-introduction of K<sup>+</sup> ions. **B.** Effect of emodepside on membrane potential in zero K<sup>+</sup> (○) Resting membrane potential. (●) Membrane potential in zero K<sup>+</sup>. (□) Membrane potential 30mins after a 2 min emodepside perfusion. (■) Membrane potential 10mins after re-introduction of K<sup>+</sup> ions

### 3.18 Discussion.

Emodepside relaxed an isolated dorsal muscle strip of *A. suum*, reflecting the ability of this anthelmintic to paralyse parasitic nematodes. The cellular basis for this was therefore investigated. As the effect of emodepside on basal muscle tension was very slight, the inhibitory action of the compound on the contraction elicited by ACh was determined. ACh has previously been shown to elicit contraction by activation of a nicotinic receptor on the somatic muscle (Colquhoun *et al.*, 1991). ACh caused a concentration-dependent excitation of *A. suum* muscle with an EC<sub>50</sub> of 9±2µM. It would be expected that an inhibitory compound would exert a physiological antagonism of this response. Consistent with this, pre-incubation of the muscle with emodepside caused a concentration- and time-dependent reduction in the amplitude of the ACh contraction. This effect was significant at 10µM emodepside and maximal at 10 min incubation. The effect was irreversible and it is likely that this reflects the highly lipophilic nature of emodepside. The ACh contraction was not decreased by more than 40%, even at the highest concentration (10 µM) of emodepside tested, and higher concentrations were not tested due to limitations of solubility of the compound. This range of concentration although relatively high is consistent with the findings of (Geßner *et al.*, 1996) who demonstrated that PF1022A at concentrations of 10µM caused paralysis of *A. suum* over a 24hour period. The inhibitory action of emodepside was also observed on muscle strips pre-contracted with ACh. In the continued presence of ACh the initial, peak contraction is followed by a slow reduction in muscle tension, or 'fade' in the response, prior to the wash. This fade may be due to desensitisation of the muscle. Addition of emodepside at the peak of the contraction increased the relaxation rate of the muscle with a threshold for the effect at less than 1 µM. This was relatively slow in onset, and the tension did not fully relax back to baseline before the wash. The inhibitory action of emodepside was not specific for ACh-mediated contraction as it also inhibited the action of the excitatory neuropeptide, AF2. Emodepside also did not inhibit ACh induced depolarisation of *A. suum* muscle cells or alter the change in conductance following ACh application, suggesting emodepside does not directly inhibit the ACh induced contraction of *A. suum* muscle, but indirectly through a different mechanism.

There are a number of possible cellular mechanisms that may underlie this inhibitory action of emodepside. For example, emodepside may exert its action by stimulating the release of an inhibitory neurotransmitter or modulator from pre-synaptic terminals to relax the muscle. Therefore, emodepside action on muscle from which the major nerve cords had been removed was tested. The 'denervated' muscle may have been compromised by the dissection procedure as the base-line tension was not stable and the response to ACh was reduced compared to an intact preparation. In these denervated preparations, emodepside did not inhibit the response to ACh, although a slight relaxation of the basal tension of the denervated muscle strip was observed. Therefore, it would seem that removing the nerve cord reduced the major inhibitory action of emodepside. This implies that emodepside exerts its effect indirectly by stimulating the release of an inhibitory neurotransmitter or neuromodulator. However, a slight post-synaptic action of emodepside on the *A. suum* muscle strip could not be ruled out, as a slight relaxation of the denervated muscle strip was still observed following emodepside application.

Further evidence that the action of emodepside is mediated *via* an action at pre-synaptic nerve terminals was also provided from electrophysiological experiments. Intracellular recordings demonstrated that emodepside elicited a slow hyperpolarisation of muscle cells. The threshold concentration for the action of emodepside on muscle membrane potential was of the same order as that observed for muscle relaxation, indicating that this hyperpolarisation is likely to be directly involved in the inhibitory action of emodepside. As with the inhibitory action of emodepside on muscle tension, this hyperpolarisation did not reverse on washing. Removal of calcium ions from the perfusate abolished the hyperpolarisation to emodepside. This is consistent with a role for calcium-dependent neurotransmitter release in the mechanism of action of emodepside.

If emodepside is acting to release an inhibitory transmitter or modulator onto the muscle then the question arises, what is it? Previous studies have suggested that emodepside may act by mimicking the action of the endogenous inhibitory neuromuscular junction transmitter GABA (Martin *et al.*, 1996; Chen *et al.*, 1996). GABA acts to hyperpolarize and relax the muscle *via* a GABA-gated chloride

channel (Parri *et al.*, 1991; Holden-Dye *et al.*, 1989). The action of emodepside on the electrophysiological properties of the muscle are not like the actions of GABA. GABA has been shown to elicit a fast hyperpolarisation associated with an increased input conductance, consistent with the opening of ligand-gated chloride channels (Martin, 1982). In contrast, no consistent change in input conductance was observed in the presence of emodepside. Taken together, the data do not support a role for GABA, or its receptor, in the action of emodepside.

A family of FMRF-amide like peptides are also known to have potent effects on nematode muscle (Geary *et al.*, 1992). Two of these peptides, PF1 (SDPNFLRFamide) and PF2 (SADPNFLRFamide) are structurally very similar, and both of these have a potent inhibitory action on *A. suum* somatic muscle (Holden-Dye *et al.*, 1995; Franks, 1996). To determine whether a PF1/2-like peptide may be involved in the response to emodepside, the action of emodepside with that of PF2 was compared. As for emodepside, a maximally effective concentration of PF2, 1  $\mu$ M (Franks *et al.*, 1994) elicited a slow but incomplete relaxation of dorsal muscle tonically contracted with ACh. Pre-incubation of the muscle with PF2 also reduced the amplitude of subsequent contractions to ACh, in a similar manner to emodepside.

Electrophysiologically the response to PF2 is similar to the response to emodepside. PF2 causes a slow hyperpolarisation with no consistent change in input conductance (Holden-Dye *et al.*, 1995). The hyperpolarisation caused by PF2 is blocked by potassium channel blockers (Walker *et al.*, 2000; Franks, 1996). Similarly, the hyperpolarisation caused by emodepside was also blocked by potassium channel blockers, and enhanced in conditions of low external potassium. Therefore it would seem that the ionic mechanism for the response to PF2 and to emodepside is similar.

So, could emodepside be acting on the same receptor as PF2? The receptors for PF2 are likely to be located post-synaptically on the muscle as the inhibitory effect of PF2 on the ACh contraction was also observed in a denervated muscle strip. Emodepside, though, failed to elicit its effect on a denervated preparation, suggesting emodepside is not acting on the PF2 like receptor directly although a

change in the basal tone of the denervated *A. suum* muscle strip following emodepside addition can not completely rule out a direct emodepside effect.

So could emodepside be acting indirectly to stimulate release of a PF2-like neuropeptide?. A supermaximal application of PF2 prior to emodepside addition blocked the inhibition of the ACh-induced contraction of *A. suum* DMS by emodepside. A supermaximal application of exogenous PF2 may lead to PF2 receptor saturation and thus would block emodepside action, if emodepside stimulates release of PF2-like inhibitory peptides. However emodepside appears not to stimulate release of a maximal concentration of PF2-like peptides, as following pre-incubation of the *A. suum* DMS with emodepside, exogenously applied PF2 still results in a reduction in the ACh-induced contraction. This leads to the possibility that emodepside may stimulate the release of a number of different inhibitory neuropeptides which act on different receptors on nematode muscle.

Overall, these data are consistent with the hypothesis that the major target site for emodepside is pre-synaptic, triggering the release of inhibitory neuropeptides from inhibitory nerve terminals, and that these peptides then elicit muscle relaxation. Due to limits in *A. suum* experimental procedures, in particular genetic and molecular analysis, the potential pre-synaptic target site and mechanism of emodepside action is unable to be investigated further in *A. suum*. However, a nematode species ideal for molecular and genetic analysis, the free-living nematode *C.elegans* can be used to clarify emodepsides pre-synaptic mechanism of action.

## CHAPTER 4

### Materials and Methods *C. elegans* Experiments

#### **4.1 Culturing of *C. elegans*.**

*C. elegans* was cultured under standard conditions (Brenner, 1974), Nematode growth medium (NGM) for *C. elegans* was made and pre-autoclave, with the following composition per 500ml; NaCl 1.5g, Agar 10g, Peptone 1.25g, Distilled water 487.5ml. Post-autoclave the medium was supplemented with the following 1M sterile solutions; CaCl<sub>2</sub> 0.5ml, MgSO<sub>4</sub> 0.5ml, KH<sub>2</sub>PO<sub>4</sub> 12.5ml, cholesterol 0.5ml of 5mg/ml stock.

Hermaphrodite animals were fed and grown on a bacterial lawn (OP50) and picked for experiments from 3-5 day -old plates. *C. elegans* strains used and details of mutations are listed in Appendix 1.

#### **4.2 Standard microbiological and molecular techniques.**

Basic microbiological and molecular biological methods were performed according to (Sambrook *et al.*, 1989).

#### **4.3 Chemicals and reagents**

DNA and RNA modifying enzymes were purchased from Promega (UK), New England Biolabs (NEB) or Boehringer Mannheim (Germany) and were used as recommended by the manufacturers. cDNAs were transcribed *in vitro* using the Promega Ribomax T7 and T3 Transcription Systems. All other reagents were analytical grade or better and purchased from Sigma (UK).

#### **4.4 Construction of *C. elegans* complementary DNA library.**

Complementary DNA (cDNA) was synthesised from *C. elegans* mRNA using Superscript™ Choice system for cDNA synthesis (GibcoBRL, USA).

## **4.5 PCR.**

### **4.5.1 PCR amplification.**

New primer pairs were used for all PCR reactions, therefore, each underwent a complete optimisation using the positive control DNA. This included varying primer concentrations, annealing temperature and PCR cycle parameters. MgCl<sub>2</sub> concentration is also important for PCR conditions but, the MgCl<sub>2</sub> concentration was already optimised within the supplied enzyme buffer.

### **4.5.2 Annealing temperature (Ta).**

This is the temperature at which the primers anneal to their complimentary sequences on the target DNA. This depends on, and varies with, the melting temperature (T<sub>m</sub>) and the base sequence of the primers used:

$$Ta = Tm - 5^{\circ}C = 2(A\&T) + 4(G\&C) - 5^{\circ}C$$

Therefore, to assess the effect of changing annealing temperature on the specificity and efficiency of the PCR amplification, annealing temperatures ranging from 55°C to 65°C were analysed for each primer pair.

### **4.5.3 PCR cycle parameters.**

The number of PCR cycles plays a critical role and is dependent on the efficient optimisation of the other parameters. One PCR cycle consists of the initial heat denaturation of the double stranded DNA template into 2 single strands. This is followed by cooling the reaction mixture to a temperature, which will allow the primer to anneal to its target sequence. Finally, the temperature is increased to allow the optimal extension of the primer by the DNA polymerase. These 3 steps are repeated leading to an exponential increase in the number of copies of DNA generated. Therefore, for optimal PCR it is essential that DNA be

examined in the exponential phase of amplification. For this, PCR was performed using a range of PCR cycles (28-40).

#### **4.5.4 Primer concentration.**

The efficiency of amplification can be compromised if the concentration of primer is too low. Therefore, PCR was optimised with primer concentrations from 1-2pM.

#### **4.5.5 PCR controls.**

To ensure accuracy and efficiency of PCR, the following controls were used:

- PCR amplification in the absence of cDNA,
- PCR amplification in the absence of Taq polymerase.

### **4.6 PCR amplification of B0457.1 (*lat-1*) gene.**

#### **4.6.1 Primer design.**

A fragment of the latrophilin-like gene B0457.1 (*lat-1*) was amplified from *C. elegans* genomic DNA using two 21 base oligonucleotide produced by OSWEL Laboratories at Southampton University:

PRIMER 1 - 5'CGTTCCATCCAACATCAACTG3' (sense).

PRIMER 2 - 5'CCATTCCATAAAGCGGCTGAC3' (antisense).

#### 4.6.2 Reaction conditions.

Reagent	Volume (50µl total mix)
Water	39.5
Primer 1	2
Primer 2	2
DNTPs	2
Buffer	2
Template DNA	2
TAQ	0.5

Cycling conditions were optimised to denaturation of template at 94°C for 30secs, annealing of primer pair at 55°C for 1min and elongation at 72°C for 1min. PCR was performed on a PE Applied Biosystems Geneamp 2400.

The quality and integrity of isolated DNA was verified by 1% agarose gel electrophoresis with ethidium bromide staining.

#### 4.7 Agarose gel electrophoresis.

Agarose was dissolved by heating in 25ml 1xTBE buffer (89mM Tris, 89mM Boric Acid, 1.8mM EDTA), to achieve a 1% agarose solution. Upon cooling, 1.3µl of 1x working solution of ethidium bromide was added to the gel solution. The gel solution was poured in a H2 Horizontal Electrophoresis unit (Anachem) and allowed to polymerize at room temperature for 20 min.

5µl of the PCR reaction was added to 1µl of 6x tracking dye (invitrogen). Agarose gels were run at 80 volts for ~ 30min in 1xTBE running buffer. The integrity and size of DNA samples was verified by co-migration of 1Kb DNA ladder (Promega). Records of gels were kept by transillumination of the gel using a UV light box and photographed with a digital camera.

#### **4.8 Purification of DNA.**

The total amount of PCR amplified cDNA was loaded onto 0.8% TAE (40mM Tris, 40mM acetic acid, 1mM EDTA, pH 8.0) agarose gel following addition of 1 $\mu$ l 6x loading dye (invitrogen). Agarose gels were run at 80 volts for ~ 30min in 1xTAE buffer. Gels were then illuminated using UV light box and sections of gel containing DNA were removed and then purified using QIAQuick Gel extraction kit (Qiagen).

#### **4.9 Ligation of *lat-1* insert into T pCR® 2.1-TOPO® vector.**

Purified *lat-1* insert was ligated with pCR® 2.1-TOPO® vector under the following conditions:

Reagent	PCR Product
PCR insert	3 $\mu$ l
Salt Solution	1 $\mu$ l
Water	1 $\mu$ l
Vector (pCR® 2.1-TOPO®)	1 $\mu$ l
Final Volume	6 $\mu$ l

The reaction was left for 5 minutes at room temperature (22-23°C) and immediately transferred to ice.

#### **4.10 Transformation of competent cells.**

2 $\mu$ l of the TOPO-ligation reaction was added to One Shot Chemically competent *Escherichia coli* and incubated at 4°C for 30mins. Cells were heat shocked for 30 seconds at 42°C, followed by incubation on ice for 2min. 250 $\mu$ l of SOC medium was added to the competent cells and mixed for 1hr at 37°C. 25 $\mu$ l, 50 $\mu$ l and 125 $\mu$ l aliquots of the competent cell mix were spread onto LB Ampicillin Agar Plates. These plates were prepared by the addition of 15g bacto-

agar per litre of standard LB (Luria-Bertani) medium (g/l 10 Bactotryptone, 10 Bacto-yeast extract: 10 sodium chloride, pH7.0 with 5M NaOH), and sterilized. Following cooling to below 50°C to prevent loss of antibiotic function, ampicillin was added at a concentration of 50µg/ml, to allow only bacterial cells expressing the pCR® 2.1-TOPO®vector (which contains an ampicillin resistant gene) to culture. 40µl of 50ng/ml X-gal was added to the plates to allow selection of blue/white colonies. The pCR® 2.1-TOPO®vector contains the gene LacZα which is disrupted if an insert is correctly ligated into the vector. X-gal is then unable to be broken down by *E. coli* containing the vector with the correct insert and so grow as white colonies. Any *E. coli* with the vector containing an intact LacZα gene (so no insert) will appear as blue colonies.

Plates were then cultured overnight at 37°C and individual white colonies then picked and transferred to 10ml LB medium containing ampicillin. These colonies were then incubated overnight at 37°C whilst shaking to optimise colony growth.

#### **4.11 Isolation of plasmid DNA from bacterial cells.**

DNA was isolated from bacterial cells using the QIAprep Miniprep Kit (QIAGEN), according to the manufacturer's instructions.

9ml of bacterial culture was centrifuged at 13K rpm to isolate the bacterial cells. The supernatant was then decanted off and the bacterial cells resuspended. Cells were then lysed using NaOH/SDS buffer and this buffer was then neutralised in high salt buffer to precipitate any denatured proteins, chromosomal DNA, cellular debris and SDS. Resulting lysate was centrifuged at 13K rpm for 10min, leaving DNA in the supernatant which was pipetted onto a 1ml spin column. Supernatant was spun through the column silica gel membrane for 1min at 13K rpm into a collecting tube, leaving the DNA bound to the column membrane. This membrane was then treated with alkali buffer to wash through any salts and ensure that only DNA was bound to the membrane and DNA was

eluted from the column using RNase-free H<sub>2</sub>O and centrifugation at 13Krpm for 1min. This method produced 1-2 $\mu$ g of DNA.

The quality and integrity of isolated DNA was verified by 1% agarose gel electrophoresis with ethidium bromide staining. 5 $\mu$ l of the DNA obtained from the plasmid mini-prep was added to 1 $\mu$ l of 6x tracking dye and loaded into the wells. Agarose gels were run at 80 volts for ~30min in 1xTBE running buffer. Size of DNA samples was verified by co-migration of 1Kb DNA ladder. Records of gels were kept by transillumination of the gel using a UV light box and photographed with a digital camera.

#### **4.12 Isolation of *lat-1* Insert.**

Plasmid DNA containing the LAT-1 insert was isolated using a specific restriction enzyme reaction. DNA was incubated in the presence of EcoR1 enzyme for 90min at 37°C under the following reaction conditions:

Reagent	
Water	49.5 $\mu$ l
Buffer	6 $\mu$ l
Plasmid	3 $\mu$ l
Enzyme	1.5 $\mu$ l
Final Volume	60 $\mu$ l

The total amount of restriction digest was loaded onto 0.8% TAE agarose gel following addition of 1 $\mu$ l 6x loading dye. Agarose gel were run at 80 volts for ~30min in 1xTAE buffer. Gels were then illuminated using UV light box and sections of gel containing insert DNA were removed and then purified using QIAQuick Gel extraction kit (Qiagen).

#### **4.13 PCR amplification of *lat-1* using T7 and T3 promoter containing primers.**

LAT-1 fragment containing T7 and T3 promoters was amplified from the purified LAT-1 insert using a 30 base oligonucleotide for primer 1 (T7), and 30 base oligonucleotide for primer 2 (T3), produced by OSWEL Laboratories at Southampton University:

PRIMER1 (T7) - 5'TAATATACGACTCACTATA**GGGCCATAAAGCG3'**

---

T7 PROMOTER

PRIMER 2 (T3) - 5'AATTAACCCTCACTAAAGGGCCATAAAGCG3'

---

T3 PROMOTER

##### **4.13.1 Reaction Conditions.**

Reagent	Volume (50µl total mix)
Water	36.5
Primer 1	2
Primer 2	2
dNTPs	2
Buffer	2
Purified insert DNA	5
TAQ	0.5

Cycling conditions were optimised to denaturation of template at 94°C for 30secs, annealing of primer pair at 55°C for 1min and elongation at 72°C for 1min. PCR was performed on a PE Applied Biosystems Geneamp 2400.

## 4.14 Synthesis double stranded RNA.

The PCR product containing the latrophilin fragment with T7 and T3 promoters was used to make double stranded RNA. dsRNA was synthesised using Ribomax™ Large scale RNA production Systems Kit, from DNA (Promega) containing both T7 and T3 promoters for 4hr at 37°C, under the following conditions:

Reagent	
Water	4µl
rNTPs	10µl
Buffer	2µl
DNA	2µl
T7 enzyme	1µl
T3 enzyme	1µl
Final Volume	20µl

After 4hr 1µl of DNase was added for 15min to remove DNA.

### 4.14.1 Purification of dsRNA.

dsRNA was purified from reaction buffers using ice cold phenol: chloroform: isopropanol.

To inhibit further dsRNA synthesis 115µl of water and 15µl of ammonium acetate were added to the dsRNA synthesis reaction. An equal volume of H<sub>2</sub>O saturated phenol and chloroform (75µl and 75µl) was added to the 150µl dsRNA reaction mix. The mix was then vortexed for 1min to ensure thorough mixing and centrifuged at 13K rpm for 10min at room temperature. The upper phase was removed into a fresh Eppendorf to which was added 150µl of chloroform. The sample was vortexed and centrifuged for 5mins at 13K rpm at room temperature. Again the upper phase was removed into a fresh Eppendorf to which was added

150 $\mu$ l of isopropanol. The samples were incubated at -20°C for 30mins and then centrifuged at 13Kpm for 15mins at 4°C. The clear supernatant was removed and the samples left to air dry for 10mins. 50 $\mu$ l of nuclease free water was added to dissolve the dsRNA

#### **4.14.2 Detection of dsRNA.**

5 $\mu$ l of the dsRNA was loaded onto 0.8% TAE agarose gel following addition of 1 $\mu$ l 6x loading dye. Agarose gels were run at 80 volts for ~ 30min in 1xTAE buffer. Gels were then illuminated using UV light box and photographed with a digital camera

#### **4.14.3 dsRNA Synthesis Controls**

To ensure correct synthesis of dsRNA from the DNA template the following controls were used:

- single stranded RNA was synthesised in the presence of either the T7 or T3 enzyme;
- dsRNA synthesis in the absence of both T7 and T3 enzymes.

### **4.15 Microinjection of dsRNA.**

Microinjection needles were pulled on a Sutter Flamin-Brown P2080 from aluminosilicate glass capillaries with an outer diameter of 1.0mm and filled with dsRNA. The tip of the microinjection needle was broken against a coverslip to allow dsRNA to flow out. The loaded needle was placed into the collar of an instrument holder to which was attached, via plastic tubing, a controllable pressure source. The needle assembly was mounted onto a micromanipulator. 3-5 day old wild type (Bristol N-2 strain) were picked and stuck to a slide containing a thin layer of dried 2% agarose and several drops of Halocarbon oil, and transferred to an inverted microscope. The injecting needle was positioned next to the worm's external body cavity, and pushed against the worm until an

indentation in the worm's cuticle was observed. A gentle tap was then applied to the micromanipulator causing the needle to penetrate the worm. Pressure was then applied causing the dsRNA solution to infiltrate the inner body of the worm. The needle was removed and the injected worm placed on a seeded agar plate. After two days worms were picked for experimentation.

#### **4.16 Synthesis of dsRNAi for the feeding method.**

Fragments of the *lat-1*, *lat-2* and FLP-13 genes were amplified from *C. elegans* genomic DNA using oligonucleotides produced by Invitrogen Ltd. The primers designed for *lat-1*, *lat-2* and FLP-13 are summarised in the table below. For the *flp-1* gene the L4440 feeding vector containing the *flp-1* gene fragment was obtained from Chris Keating, University of Sussex, Brighton.

Oligonucleotide Primer Description	Sequence 5'---3'
B0457.1 ( <i>lat-1</i> ) Forward	CGTTCCATCCAACATCAACTG
B0457.1 ( <i>lat-1</i> ) Reverse	CCATTCCATAAAGCGGCTGAC
B0286.2 ( <i>lat-2</i> ) Forward	ATTCCAGGCATGGACAGAAC
B0286.2 ( <i>lat-2</i> ) Reverse	CTCGATTTCGTTGTTGCTCA
FLP-13 Forward	CTCTGCTCTACCAAGTAGGGT
FLP-13 Reverse	AAATGAAGTACAGATATCACG

##### **4.16.1 Reaction Conditions.**

The following reaction conditions were used for PCR amplification of fragments of the *lat-1*, *lat-2* and *flp-13* gene

Reagent	Volume (50 $\mu$ l total mix)
Water	36.5
Primer 1	2
Primer 2	2
dNTPs	2
Buffer	2
Purified insert DNA	5
TAQ	0.5

Cycling conditions were optimised to denaturation of template at 95°C for 2 min, followed by 30 cycles of 94°C for 30 sec, annealing of primer pair at 55°C for 1 min, elongation at 72°C for 1 min, and ending with a final extension at 72°C for 5 min. PCR was performed on a MJ Research inc., Peltier Thermal Cycler (200). The quality and integrity of isolated DNA was verified by 1% gel electrophoresis with ethidium bromide staining (explained in section 4.7)

#### **4.17 Ligation of *lat-1*, *lat-2* and *flp-13* fragments into L4440 feeding vector.**

The DNA fragments of *lat-1*, *lat-2* and *flp-13* designated for RNAi obtained by polymerase chain reaction (PCR) from *C. elegans* cDNA or genomic DNA and were cloned into the L4440 feeding vector under the following conditions

Reagent	PCR Product
PCR insert	3 $\mu$ l
Buffer	1 $\mu$ l
Water	1 $\mu$ l
Feeding Vector	5 $\mu$ l
Final Volume	10 $\mu$ l

The reaction was left at 15°C for at least 12 hours.

#### **4.18 Transformation of HT115 bacteria with L4440 feeding vector.**

1 $\mu$ l of the ligation reaction was added to 100 $\mu$ l of HT<sub>115</sub> (DE3) RNase III-deficient *E. coli* strain, preferential for RNAi feeding (Timmons *et al* 1998), and incubated at 4°C for 30mins. Cells were heat shocked for 1 minute at 37°C, followed by incubation on ice for 2min. 1ml of SOC medium was added to the competent cells and mixed for 1hr at 37°C. 10 $\mu$ l, 100 $\mu$ l and 250 $\mu$ l aliquots of the competent cell mix were spread onto LB tetracycline and Ampicillin agar plates. These plates were prepared by the addition of 15g bacto-agar per litre of standard LB (Luria-Bertani) medium (g/l 10 Bactotryptone, 10, Bacto-yeast extract, 10 sodium chloride: pH7.0 with 5M NaOH), and sterilized. Following cooling to below 50°C to prevent loss of antibiotic function, 100 $\mu$ g/ml ampicillin and 12.5 $\mu$ g/ml tetracycline was added, to allow only bacterial cells expressing the L4440 feeding vector (which contains an ampicillin and tetracycline resistant gene) to culture.

Plates were then cultured overnight at 37°C and individual white colonies then picked and transferred to 10ml LB medium containing tetracycline and ampicillin. These colonies were then incubated between 8 and 18 hours at 37°C whilst shaking to optimise colony growth.

#### **4.19 Seeding of NGM plates with dsRNAi bacteria.**

Bacteria grown for 8hrs were then seeded directly onto NGM plates containing 1mM IPTG and 50 $\mu$ g/ml Amp, (induced) or 50 $\mu$ g/ml Amp only (un-induced control). Seeded plates were allowed to dry at room temperature and induction was continued at room temperature overnight.

#### **4.20 *C. elegans* growth on RNAi-expressing bacteria.**

Single L4-stage hermaphrodite worms (RNAi sensitive *rrf-3* (NL2099) strain) were placed onto NGM plates (either Amp only or Amp + IPTG) containing seeded bacteria expressing dsRNA for each gene and were incubated for 40-60 hrs at 15°C. Then, three F2 worms were independently replica plated onto plates seeded with the same bacteria and were allowed to populate the plate. The adult progeny from these F2 worms were assayed for emodepside sensitivity. As a control *rrf-3* *C. elegans* grown on IPTG NGM plates containing untransformed HT115 bacteria were assayed for emodepside sensitivity and were found to respond to emodepside similar to normal *rrf-3* *C. elegans*.

#### **4.21 Behavioural assays.**

Two behavioural assays were used to test emodepside action on *C. elegans*, a locomotion assay and a pharyngeal pumping assay.

#### **4.22 Locomotion assay.**

Several whole *C. elegans* were placed into a 3 cm Petri dish containing modified Dent's saline. *C. elegans* body bends were counted for 30 seconds. Drugs were applied to the Petri dish and body bends were measured at 1, 5, 15 and 20 minutes, and 24 hours.

## **4.23 Pharyngeal pumping assay.**

Two assays were used to measures *C. elegans* pumping rates, a counting method and an electropharyngeogram recording.

### **4.23.1 Dissection of *C. elegans* pharynxes for pharyngeal pumping measurement.**

Individual worms were placed in a Petri dish containing modified Dent's saline (mM: 144 NaCl, 10 MgCl<sub>2</sub>, 1 CaCl<sub>2</sub> 6 KCl, and 5 Hepes, pH 7.4). A razor blade was used to cut the worm just posterior to the pharynx, which caused the cuticle to retract, exposing the isthmus and terminal bulb. This semi-intact worm preparation consisted of the pharynx, the nerve ring, and the enteric nervous system.

### **4.23.2 Visual scoring method.**

Dissected *C. elegans* pharynxes were placed into a 3 cm Petri dish containing Dent's saline and 500nM 5-HT. Pharyngeal pumps were counted over 30 seconds for two minutes. Drugs were applied to the Petri dish and after 10 minutes pharyngeal pumping was recorded.

### **4.23.3 Electropharyngeogram [EPG] recordings.**

Dissected *C. elegans* heads were transferred to a custom built chamber (volume 500 $\mu$ l) on a glass clover slip. Suction pipettes were pulled from borosilicate glass (Harvard instruments, diameter 1mm). Tip diameter ranged from 20 to 40 $\mu$ m depending on the size of the worm. The suction pipette was filled with Dent's saline and mounted in a holder with a tubing port through which suction can be applied. The pipette was lowered into the chamber and placed close to the nose of the worm. Suction was applied to capture the worm.

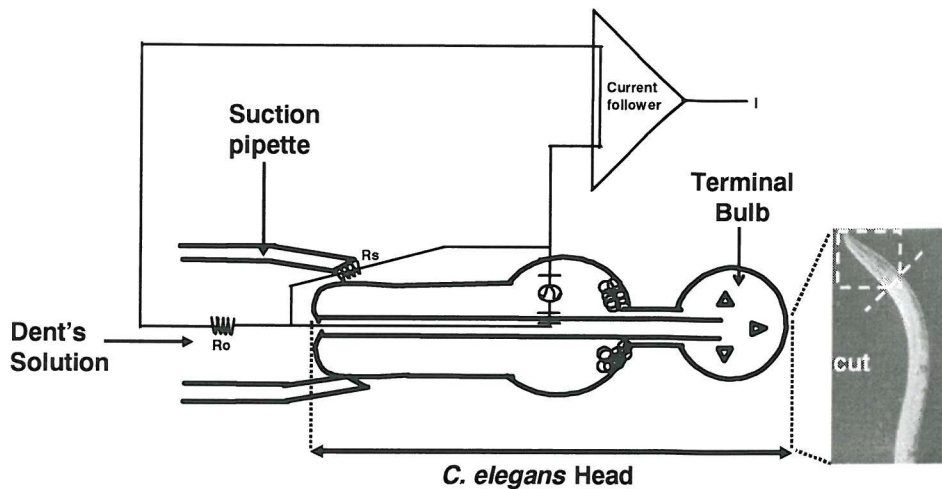


**Fig 4.1 Experimental set-up for recording EPG's from *C. elegans* Pharynxes.** The pharynx is exposed by cutting just above the pharyngo-intestinal valve. A suction pipette is then placed close to the nose of the worm. Suction is then applied to capture the worm.

The suction pipette was connected to a silver electrode, which was connected to a HS2 head stage (Axon Instruments), which in turn was connected to an Axoclamp 2B-recording amplifier. Data were acquired using axoscope 8.0 (Axon Instruments), and a hard copy was displayed on a Gould RS 3200 chart recorder. Dissected pharynxes were recorded in normal Dent's for 2mins. Normal Dent's was when replaced with Dent's containing 500nM, or 1 $\mu$ M 5-HT for 2mins, where stated. Dent's containing no 5-HT and various concentrations of emodepside was then applied for 10 minutes. Dent's containing 5-HT was then re-applied. The rate of pumping in 5-HT following emodepside application was then expressed as a percentage of the initial pumping rate in 5-HT before any drug addition. *unc-13* *C. elegans* pump poorly in the presence of 500nM 5-HT. To obtain comparable pumping rates 1 $\mu$ M 5-HT was used. *unc-31* *C. elegans* have a higher resting pharyngeal pumping rate. For comparable pumping rates no 5-HT was used.

#### 4.24 Imaging with FM4-64.

Loading of FM4-64 was performed similar to (Kay *et al* 1999). *C. elegans* were transferred to a Petri dish containing modified Dent's saline. The tip of the *C. elegans* head was 'nicked' with a razor blade to remove the cuticle and expose

the pharyngeal muscle. *C. elegans* exposed pharynxes were loaded with 5 $\mu$ M FM4-64 in the presence of normal Dent's or high potassium Dent's (mM: 144 NaCl, 10 MgCl<sub>2</sub>, 1 CaCl<sub>2</sub> 25 KCl, and 5 Hepes, pH 7.4) for 5 mins. The wash procedure was as follows: wash for 1 min in 0 Ca<sup>2+</sup> Dent's, followed by a 2 min wash with 1mM  $\beta$ -Cyclodextrin sulfobutyl ether, 7 Sodium Salt in 0 Ca<sup>2+</sup> Dent's. The exposed pharynxes were then washed in normal Dent's, and placed on a slide. Confocal images were collected on a Zeiss Axioskop 2 LSM 510 meta laser scanning microscope. 100nM emodepside was added to the slide. Confocal images were then re-taken 10 minutes after application of drug.

#### **4.25 Statistical analysis.**

Data are presented as either the mean  $\pm$  S.E.Mean of 'n' independent determinations or as mean: with 95% confidence interval for 'n' experiments. Statistical significance was determined using unpaired two tailed Student's t-test with a significance level of P<0.05. Inhibition curves were fitted to the modified logistic equation using Graph pad prism (version 3.0 San Diego California).

## CHAPTER 5

### **Proposed Mechanism of Action of Emodepside using *C. elegans***

## 5.0 Introduction.

With the completion of the *C. elegans* genome project in 1998, *C. elegans* has become a useful model organism for studying signalling pathways. The relative ease of genetic manipulation techniques such as RNA interference, and the availability of numerous mutant strains, has enabled the discovery of drug target sites. It was the use of *C. elegans* that enabled the target site for the anthelmintic ivermectin to be identified (Cully *et al.*, 1994).

In order to determine the mechanism of action of the 24 membered cyclic depsipeptide, emodepside, its effect was investigated on *C. elegans*. In chapter 3, it was shown that emodepside causes a relaxation of *A. suum* muscle and the major target site for emodepside appears to be pre-synaptic. Emodepside was also shown to mimic the effects of the inhibitory peptide PF2, favouring the view that emodepside causes vesicle release of an inhibitory peptide, leading to muscle relaxation and worm paralysis.

Saeger *et al.*, (2001) proposed a possible protein target site for emodepside. A  $\lambda$ ZAPII expression cDNA library from the parasite *H. contortus* was constructed and screened with an emodepside-KLH conjugate and anti-emodepside-KLH antiserum. Screening of  $1.5 \times 10^6$  non amplified recombinant clones resulted in isolation of the receptor, HC110-R. This receptor was shown to have similar homology to a latrophilin receptor found in mammals. Latrophilin was identified as a possible target site for the black widow toxin  $\alpha$ LTX.  $\alpha$ LTX causes a massive vesicular release at the synapse. In mammals, latrophilin appears to be the important receptor in  $\alpha$ LTX's induced stimulation of vesicular release (Capogna *et al.*, 2003). Latrophilin is a 7 trans-membrane G-protein coupled receptor. The mechanism by which latrophilin causes vesicular release is unclear, but involves the  $G_q$ , G-protein and phospholipase (PLC $\beta$ ) pathway (Rahman *et al.*, 1999; Capogna *et al* 2003).

Synaptic transmission depends on the efficient coordination of multiple events, including synaptic vesicle fusion, retrieval, and docking prior to a second round of fusion (for review see Fon & Edwards, 2001; Li & Chin, 2003). At the

synapse, vesicles are localised to the nerve terminal, specifically to an active zone. This area is close to the synaptic cleft and the post-synaptic density. Here synaptic vesicles are either directly in contact with the membrane (the readily releasable pool (Rosenmund & Stevens, 1996), or clustered over the synaptic cleft, (the reserve pool). The reserve vesicle pool is recruited to resupply the readily releasable vesicle pool following conditions of high-frequency stimulation. The resupply of the readily releasable pool vesicles occurs by the 'priming' of additional docked vesicles.

Vesicle fusion involves an interaction of a number of different synaptic proteins. Of importance are the proteins involved in the SNARE complex. The complex consists of vesicle-associated SNARE (v-SNARE), synaptobrevin (VAMP), and two target or plasma membrane SNAREs (tSNARE), SNAP-25 and syntaxin. The SNARE proteins, synaptobrevin (located on the synaptic vesicle), syntaxin and SNAP-25 (located on the pre-synaptic membrane) form *trans* complexes that bring vesicle and pre-synaptic membrane into close apposition to drive membrane fusion (Weber *et al.*, 1998).

Calcium influx and its use by downstream sensors provide the major point of regulation in this process. In addition, a number of second messengers that accumulate following nerve terminal receptor activation have been shown to regulate recruitment of vesicles to the readily releasable pool (Stevens & Sullivan, 1998). Recent interest has focussed on UNC-13 as a key priming molecule for this releasable pool and an essential mediator of these second messenger regulated events (Brose *et al.*, 1995; Martin, 2002).

UNC-13 is an active zone specific plasma membrane associated protein essential for synaptic vesicle release in *Drosophila*, mammals and *C. elegans* (Aravamudan *et al.*, 1999; Augustin *et al.*, 1999; Richmond *et al.*, 1999). Consistent with this important function, *C. elegans unc-13* loss of function mutants exhibit uncoordinated movement and varying degrees of paralysis (Brenner, 1974; Kohn *et al.*, 2000; Maruyama & Brenner, 1991) and are deficient in release of most neurotransmitters (Miller *et al.*, 1996). Conversely, over expression of the mammalian homologue, MUNC-13, in cultured *Xenopus* neuromuscular systems

increases synaptic transmission (Betz *et al.*, 1996).

Insight into the molecular determinants of the priming action of UNC-13 was provided by cloning of *unc-13* and the identification of C1 and C2 binding domains (Kohn *et al.*, 2000; Maruyama & Brenner, 1991). The C1 domains bind diacylglycerol (DAG) and phorbol esters (Burns & Bell, 1991), whereas C2 domains bind calcium and phospholipids (Kaibuchi *et al.*, 1989). The function of this protein appears to be conserved between *C. elegans*, *Drosophila* and mice as PLC $\beta$  and DAG are also major determinants of DUNC-13 synaptic levels in *Drosophila* (Aravamudan & Broadie, 2003) and MUNC-13s were also shown to be the main pre-synaptic DAG/ $\beta$  phorbol ester receptors in hippocampal neurones (Rhee *et al.*, 2002). Upstream regulators of UNC-13 have also been identified in *C. elegans*. Activation of G $\alpha$ q, phospholipase-C $\beta$  (PLC $\beta$ ) and the DAG binding protein UNC-13 led to increased acetylcholine release at neuromuscular junctions (Lackner, *et al* 1999), whilst G $\alpha$ <sub>o</sub> activation inhibits acetylcholine release at the synapse by reducing levels of UNC-13 at release sites through a DAG kinase pathway (Nurrish *et al* 1999).

In this chapter a possible mechanism of action for emodepside is investigated using a combined approach of RNAi and available *C. elegans* mutants. The question whether emodepside is causing vesicular release via interaction with a latrophilin-like receptor and the subsequent activation of any signalling pathway is investigated.

## 5.1 Effect of emodepside on *C. elegans* movement.

First there was a need to establish that emodepside would paralyse *C. elegans*. Prior to application of 10 $\mu$ M emodepside *C. elegans* moved at a rate of  $87 \pm 6$  body bends/min (n=6) in solution. 20 minutes after the application of 10 $\mu$ M emodepside the number of body bends/min significantly decreased to  $46 \pm 7$  body bends/min (n=5, P<0.05), compared to control worms (in the absence of emodepside),  $73 \pm 5$  body bends/min (n=5). After 24hrs *C. elegans* body bends/min in 10 $\mu$ M emodepside had significantly decreased further, to  $12 \pm 7$  body bends/min (n=9, P<0.01), compared to the control *C. elegans* in no emodepside ( $56 \pm 8$  body bends/min, n= 11). The fall in body bends after 24 hours in control experiments was a result of no movement (due to death), observed in 1 out of 9 *C. elegans*, compared with 5 out of 9 *C. elegans* in the presence of drug, (Fig 5.1).

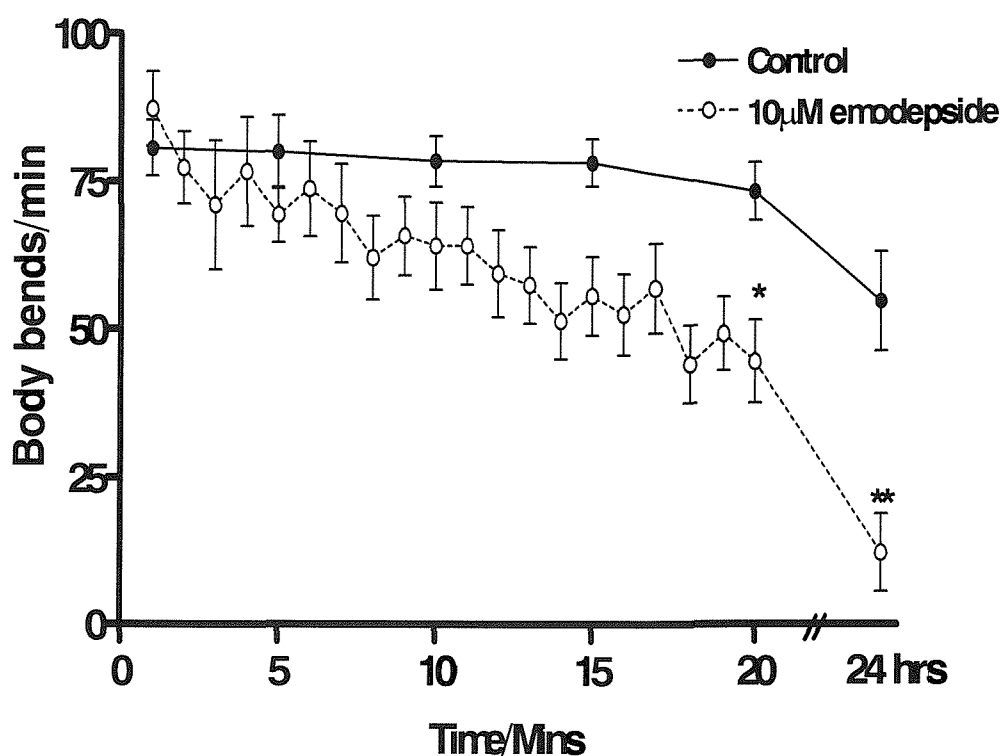


**Fig 5.1 The effect of emodepside on *C. elegans* movement.** The solid line are *C. elegans* in no emodepside. The dotted line are *C. elegans* in 10 $\mu$ M emodepside. \*P<0.05 (n=9) \*\*P<0.01 (n=11). The fall in body bends after 24 hours in control experiments was a result of no movement (due to death) observed in 3 *C. elegans*.

## 5.2 Effect of emodepside on pharyngeal pumping.

The pharyngeal muscle of *C. elegans* is an accessible preparation which enables a more definitive experimental technique to be used to investigate the mechanism of action of emodepside. The pharynx of *C. elegans* is a rhythmically active myogenic muscle that pumps food into the intestine of the animal (Avery & Horvitz, 1989). For these experiments, the pharyngeal muscle was exposed to the external medium by transecting the anterior of the worm from the body at the level of the pharyngeo-intestinal valve. The preparation therefore included the pharynx, the intact enteric nervous system, the anterior nerve ring and the anterior sensory neurones. In the absence of any stimulation the pharynx pumps at a rate of around 0.1Hz. Therefore, in order to determine the effects of emodepside the pharyngeal neuronal circuits were activated by two different stimuli, 5-HT and AF1 (Rogers *et al.*, 2001).

To measure pharyngeal pumping rates in *C. elegans* two assays were used. The first was a counting assay. The second was an electropharyngeogram (EPG) set-up, which records the extracellular changes that occur during pharyngeal pumping by placing an electrode on the buccal cavity of the animal.

## 5.3 Effect of emodepside on pharyngeal pumping (Visual scoring method).

In adult hermaphrodites, emodepside caused a potent concentration-dependent inhibition of pharyngeal pumping (Fig 5.2) with an  $IC_{50}$  of 4.6nM (95% confidence limits, 0.98 to 22nM). This was compared to emodepside's parent compound PF1022A which caused an inhibition of pharyngeal pumping with an  $IC_{50}$  of 25nM (95% confidence limits, 10 to 61nM, Fig 5.2).

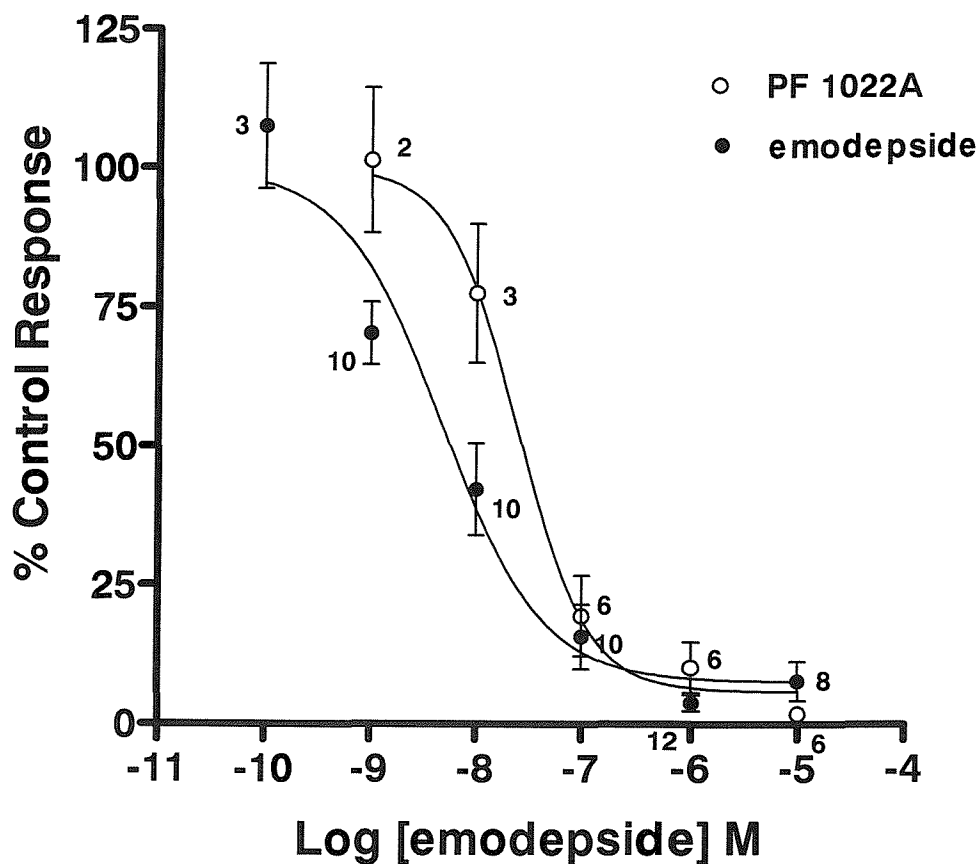


**Fig 5.2.** The effect of emodepside PF1022A on *C. elegans* pharyngeal pumping (counting assay). The protocol involved counting pharyngeal pumping in the presence of 500nM 5-HT every 30secs for 2 minutes prior to emodepside addition. Emodepside and PF1022A were applied for 10minutes after which pharyngeal pumping was measured for 30 seconds. Emodepside cause a concentration-dependent inhibition of pharyngeal pumping with an  $IC_{50}$  of 4.6nM compared to an  $IC_{50}$  of 25nM for PF1022A.

## 5.4 Recording electropharyngeogram (EPG) from *C. elegans* pharynxes.

A typical example of a wild type *C. elegans* pharyngeal pump is shown in Fig 5.3. The first upward spike (E) marks the depolarisation of the muscle membrane that initiates muscle contraction. The large downward spike (R) marks the repolarisation of the corpus muscle that precedes corpus muscle relaxation. During the period of depolarisation, inhibitory postsynaptic potentials (IPSPs) from the M3 motoneurone are evident. Wild type *C. elegans* pump duration in the presence of 500nM 5-HT lasted  $152 \pm 10$  msec, (n=31). IPSPs were observed in 37 out of 45 of wild type *C. elegans*.

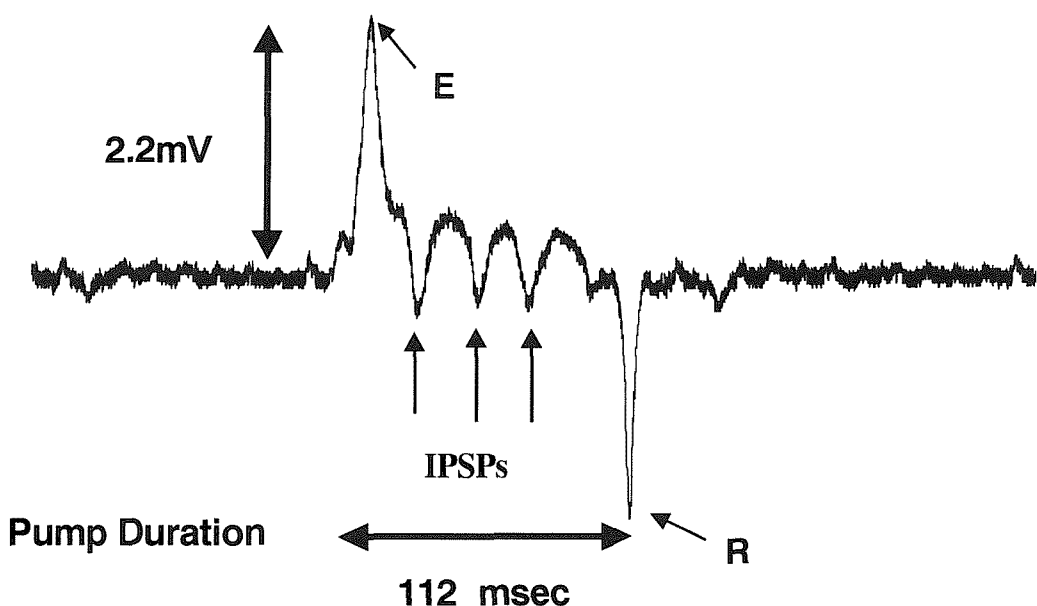


**Fig 5.3. Example of an EPG trace, of a single pump from wild type *C. elegans*.** E and R correspond to excitation and relaxation phases of the pharyngeal muscle contraction. IPSPs are thought to arise from synaptic transmission generated from the M3 inhibitory motoneurone.



## **5.5 Effect of emodepside on wild type *C. elegans* pharyngeal pumping, stimulated with 5-HT.**

5-HT was applied to the pharynx to activate neuronal and muscle activity, allowing a consistent level of pharyngeal pumping prior to emodepside application. Emodepside caused a concentration-dependent inhibition of pharyngeal pumping, similar to the counting assay shown in section 5.3. The  $IC_{50}$ s were comparable;  $IC_{50}$  of 4.1nM (95% confidence limits 0.79 to 21nM, Fig 5.4), EPG assay compared to 4.6nM (95% confidence limits 0.98 to 22nM) counting assay. No change was observed in pump duration following emodepside application.

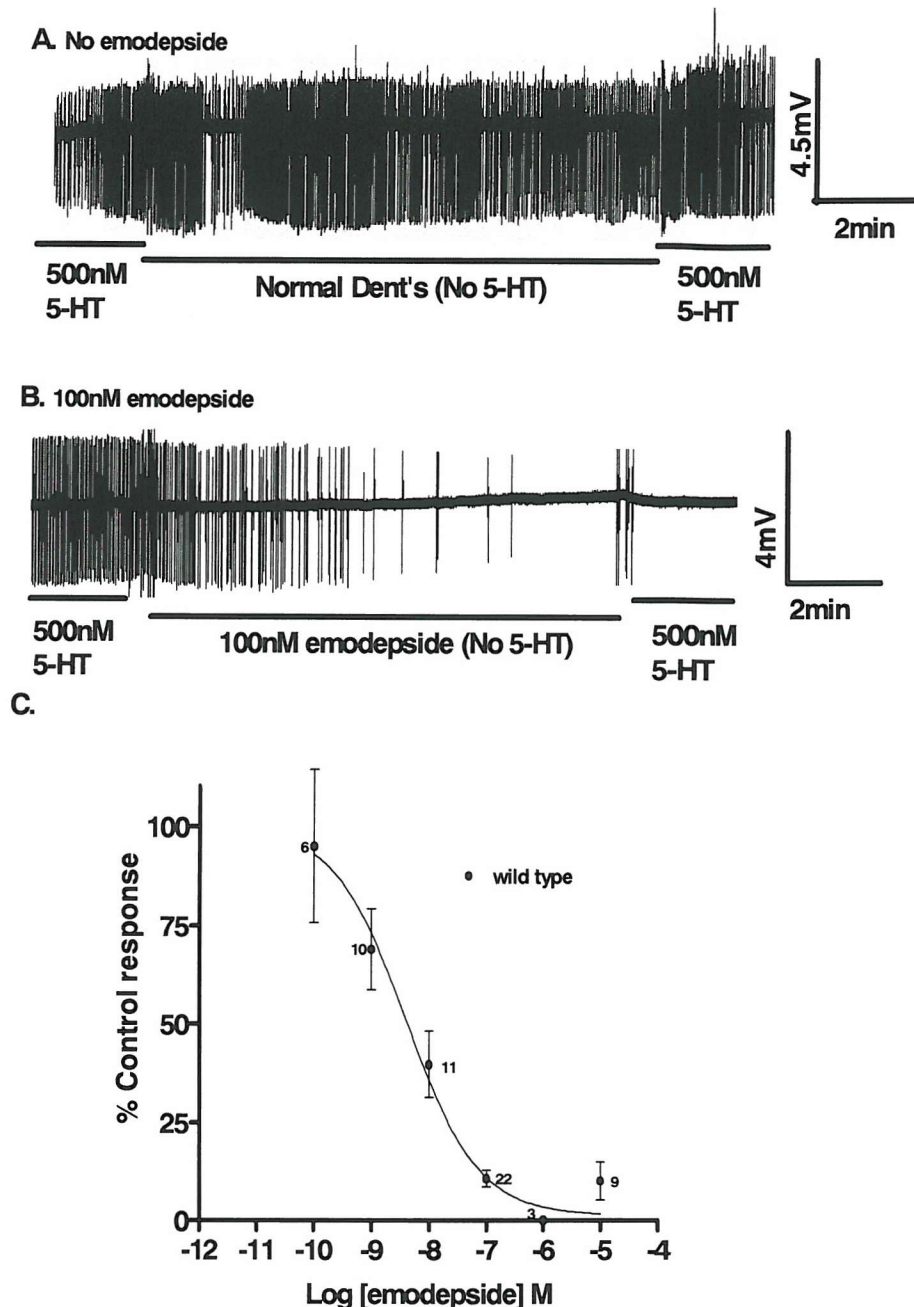


**Fig 5.4 Effect of emodepside on *C. elegans* pharyngeal pumping (EPG counting assay).**

**A.** An extracellular recording of the pharyngeal muscle (EPG). Each vertical line represents the electrical activity associated with a single muscle pump; therefore this provides a readout of the activity of the muscle. 5-HT, 500nM, is applied to stimulate pumping. The protocol involved applying 5-HT for 2 min time periods separated by a 10min application of either vehicle control (0.1% ethanol), or emodepside. **A** typical result from a control experiment in which the pharynx continues to pump throughout the entire time-course of the experiment.. **B.** The effect of 100nM emodepside on pharyngeal pumping. Note the disappearance of the pumps during the period of emodepside application and the failure of the muscle to respond to the second application of 5-HT. **C.** Concentration-response curve for the effect of varying concentrations of emodepside on pharyngeal pumping rates in wild type *C. elegans*. % control response is the rate of pumping in 5-HT following emodepside application compared to the initial pumping rate in 5-HT. Each point is the mean  $\pm$  S.E.M of (n) determinations

## **5.6 Effect of emodepside on wild type *C. elegans* pharyngeal pumping stimulated with AF1.**

The effect of emodepside was also investigated on pharyngeal neuronal and muscle activity stimulated by AF1. Emodepside (100nM) caused a similar inhibition of pharyngeal pumping following stimulation of the pharynx by AF1 (100nM). (97%  $\pm$  3, (n=5), following stimulation by AF1, compared to a 90%  $\pm$  2, n=22, following stimulation by 500nM 5-HT, P<0.05, Fig 5.5).

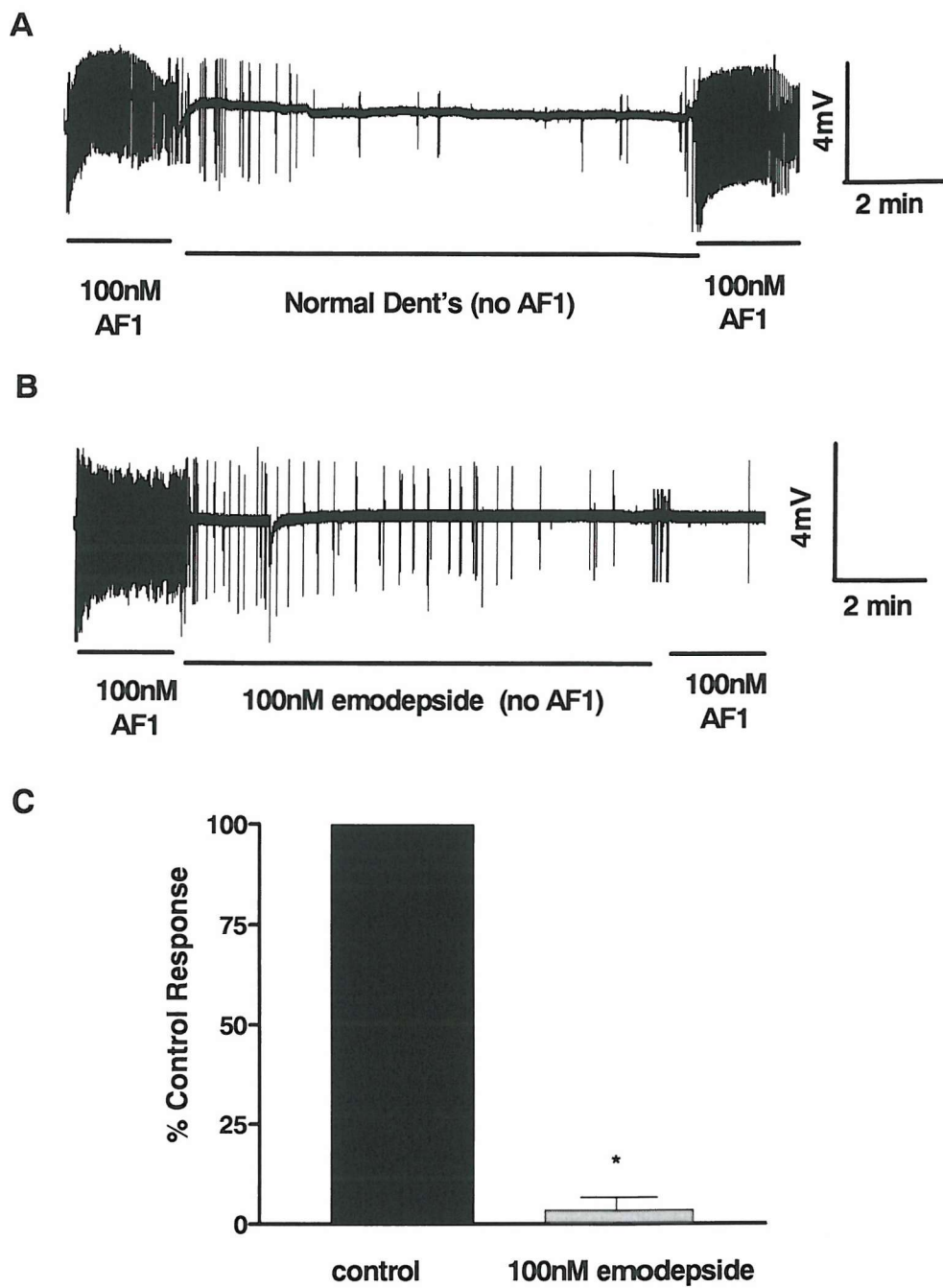
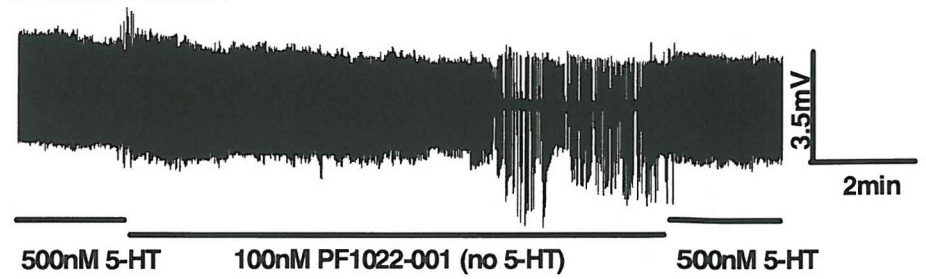


**Fig 5.5. Effect of emodepside on wild-type *C. elegans* stimulated with AF1 (100nM).** Protocol was as described in Fig 5.4.A a typical result from a control experiment in which the pharynx pumps at similar rates throughout the entire time-course of the experiment B. The effect of 100nM emodepside on AF1 stimulated pharyngeal pumping in wild type *C. elegans*. Note the disappearance of the pumps during the period of emodepside application and the failure of the muscle to respond to the second application of AF1.C. Graph showing the effect of 100nM emodepside on pharyngeal pumping rates in wild type *C. elegans* stimulated with AF1. % control response is the rate of pumping in AF1 following emodepside application compared to the initial pumping rate in AF1. Each point is the mean  $\pm$  S.E.M. of 6 determinations.\*P<0.05 n=5.

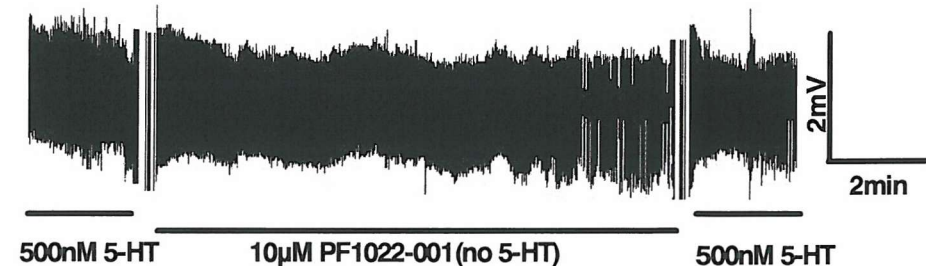
## **5.7 Effect of PF1022-001 (emodepside optical antipode) on pharyngeal pumping in wild type *C. elegans*.**

PF1022-001 is a structural isomer of emodepside. It has no anthelmintic activity (Geßner *et al.*, 1996). The effect of PF1022-001 was investigated on pharyngeal pumping rates of wild type *C. elegans*. PF1022-001 (100nM, and 10 $\mu$ M failed to inhibit *C. elegans* pharyngeal pumping rates, compared to control, Fig 5.6).

**A. 100nM PF1022-001**



**B. 10 $\mu$ M PF1022-001**



**C.**

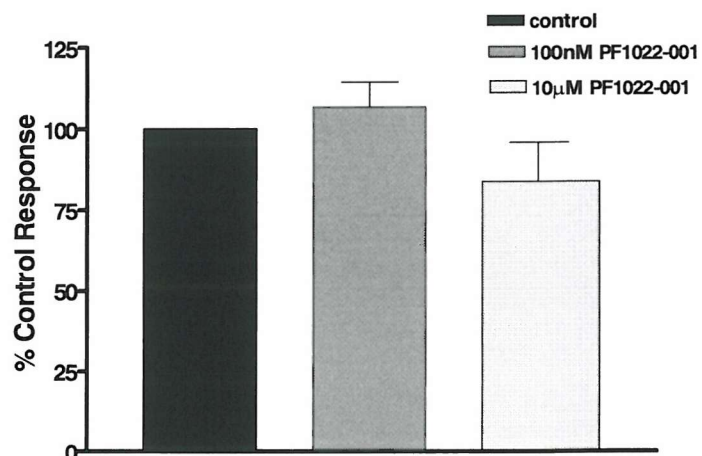


**Fig 5.6 Effect of PF1022-001 on wild-type *C. elegans* pharyngeal pumping.** Protocol was as described in Fig 5.4 A The effect of 100nM PF1022-001 on pharyngeal pumping of wild type *C. elegans*. Note the pharynx continues to pump throughout the entire time-course of the experiment. B. The effect of 10 $\mu$ M PF1022-001 on pharyngeal pumping in wild type *C. elegans*. C. Graph showing the effect of 100nM and 10 $\mu$ M PF1022-001 on pharyngeal pumping rates in wild type *C. elegans*. % control response is the rate of pumping in 5-HT following emodepside application compared to the initial pumping rate in 5-HT. Each point is the mean  $\pm$  S.E.M of 6 determinations.

## 5.8 Identifying the receptor through which emodepside acts.

(Saeger *et al.*, 2001) showed emodepside binds to a latrophilin-like receptor in *H. contortus* named HC110R. A BLASTA search of the *C. elegans* genome data base with HC110R identified two candidate latrophilin-like receptors; *lat-1* (B0457.1) and *lat-2* (B0286.2) (Fig 5.7). *lat-1* has 46% identity and *lat-2* has 20% identity to HC110R. Here, RNA interference was used to reduce expression of both *lat-1* and *lat-2* genes. Two methods of RNAi were used, an injection method and a feeding method. For the feeding method the *rrf-3* *C. elegans* strain was used. *rrf-3* *C. elegans* have been shown to be more sensitive to RNAi (Simmer *et al.*, 2002).

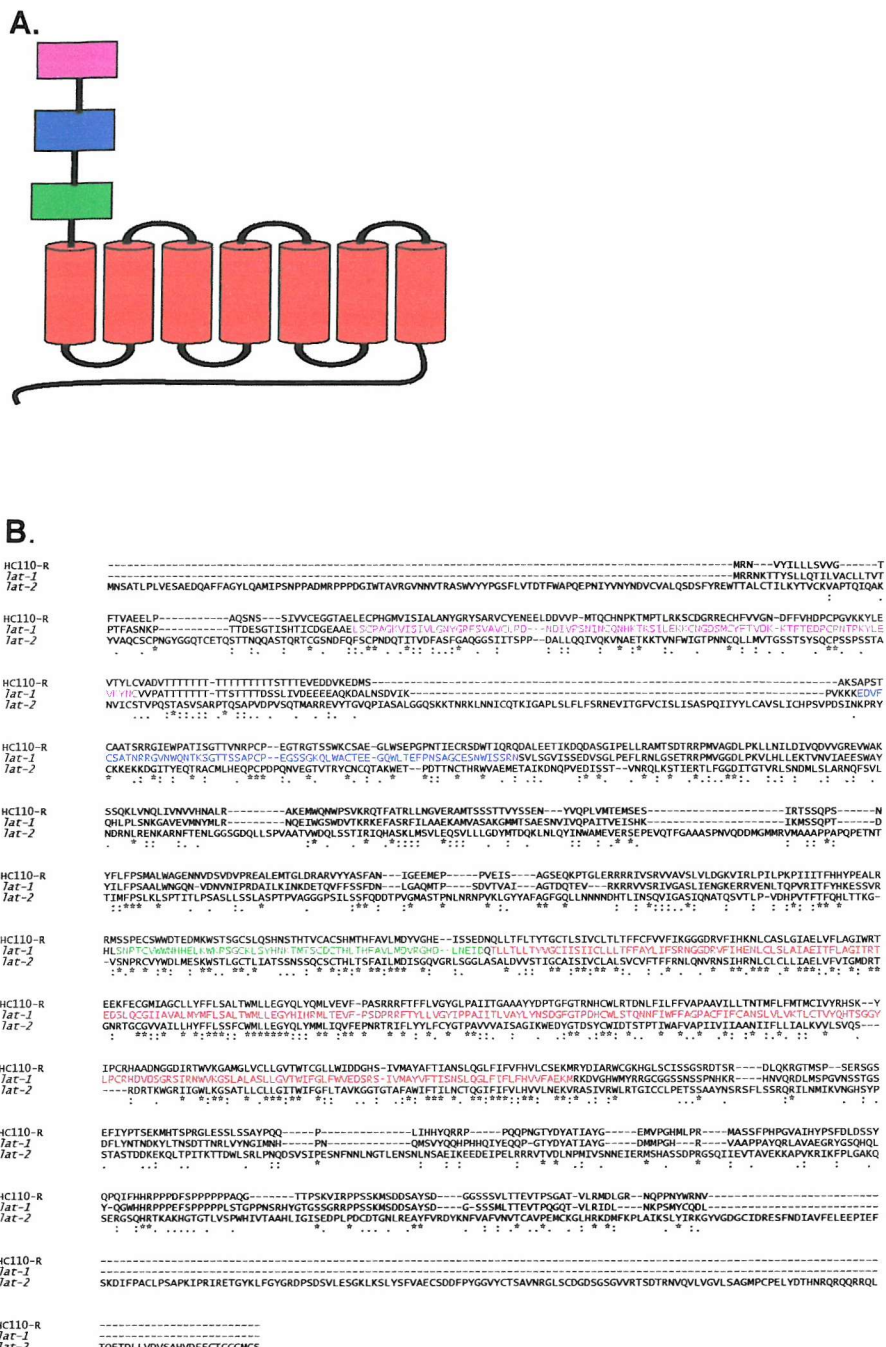
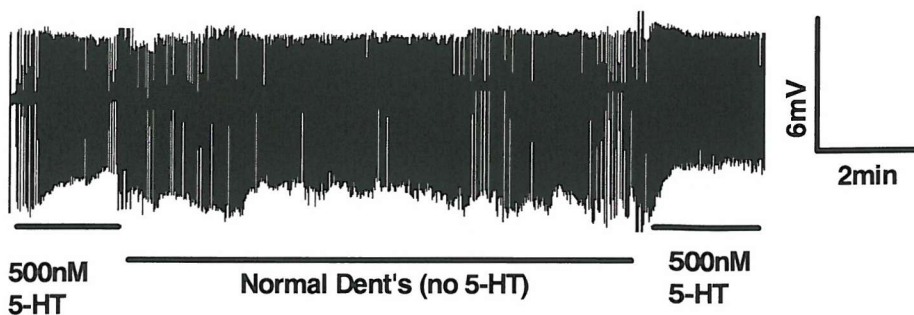


**Fig 5.7 Identifying latrophilin-like receptors in *C. elegans*.** **A.** Diagram showing the conserved domains within the *C. elegans lat-1* receptor. Galactose binding lectin domain (purple) Hormone receptor domain (blue), Latrophilin/CL-1-like GPS domain (green) and 7 transmembrane receptor, secretin family (red). **B.** Alignment of HC110R receptor in *Haemonchus contortus* against two Latrophilin-like receptors in *C. elegans*, B0457.1(*lat-1*) and B0286.2 (*lat-2*). For *C. elegans* B0457.1 (*lat-1*) galactose binding lectin domain (purple) hormone receptor domain (blue), latrophilin/CL-1-like GPS domain (green) and 7 transmembrane receptor, secretin family (red). *lat-1* has 46% identity and *lat-2* has 20% identity to HC110R.

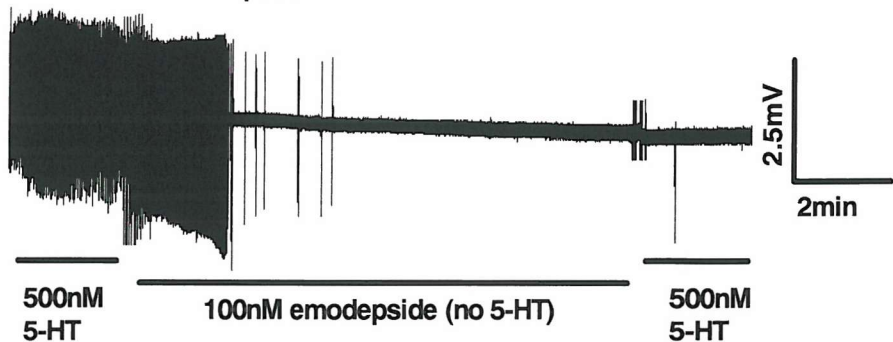
## 5.9 Effect of emodepside on pharyngeal pumping in *rrf-3* *C. elegans*.

Emodepside caused a concentration-dependent inhibition of pharyngeal pumping on *rrf-3* *C. elegans*, similar to wild type *C. elegans*. The IC<sub>50</sub>s were comparable 2.9nM (95% confidence limits, 1.8 to 4.5nM, Fig 5.8) compared with 4.1nM (95% confidence limits, 0.79 to 21nM, Fig 5.4) for wild type.

**A. *rrf-3* no emodepside**



**B. *rrf-3* 100nM emodepside**



**C.**

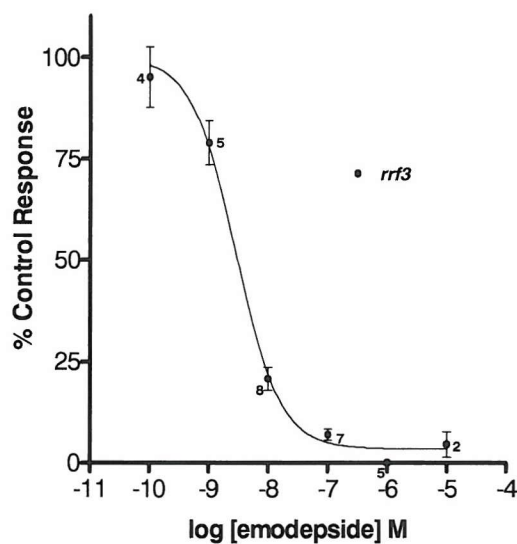


**Fig 5.8 Effect of emodepside on *rrf-3* *C. elegans* pharyngeal pumping.** Protocol was as described in Fig 5.4. **A.** a typical result from a control experiment in which the pharynx continues to pump throughout the entire time-course of the experiment. **B.** The effect of 100nM emodepside on pharyngeal pumping. Note the disappearance of the pumps during the period of emodepside application and the failure of the muscle to respond to the second application of 5-HT. **C.** Concentration response curve for the effect of varying concentrations of emodepside on pharyngeal pumping rates in *rrf-3* *C. elegans*. % control response is the rate of pumping in 5-HT following emodepside application compared to the initial pumping rate in 5-HT. Each point is the mean  $\pm$  S.E. Mean of (n) determinations

## **5.10 Effect of emodepside on pharyngeal pumping in *C. elegans* injected with dsRNA against the *lat-1* gene.**

The effect of emodepside on pharyngeal pumping rates in *lat-1* injected dsRNAi *C. elegans* was investigated. Application of 100nM emodepside to wild type *C. elegans* caused a decrease in pharyngeal pumping of  $84 \pm 6\%$  (n=10) similar to water injected *C. elegans* ( $84 \pm 7$ , n=5). Emodepside (100nM) application to *lat-1* RNAi *C. elegans* caused only a  $35 \pm 7\%$ , (n=21) reduction in pharyngeal pumping rates ( $P<0.05$ ). 1 $\mu$ M emodepside application to wild type and water injected *C. elegans* caused a similar reduction in pharyngeal pumping rates of  $96 \pm 1\%$  (n=12) and ( $91 \pm 5\%$  n=5) respectively. 1 $\mu$ M application of emodepside to *lat-1* RNAi *C. elegans* reduced pharyngeal pumping rates by  $53 \pm 7\%$  (n=5), ( $P<0.01$ ). 10 $\mu$ M emodepside application to wild type *C. elegans* caused a  $92 \pm 4\%$  (n=8) reduction in pharyngeal pumping similar to water injected *C. elegans*  $98 \pm 1\%$  (n=5). 10 $\mu$ M application of emodepside to *lat-1* RNAi *C. elegans* caused a  $61 \pm 7\%$  (n=10) ( $P<0.01$ ) reduction in pharyngeal pumping rates (Fig 5.11)

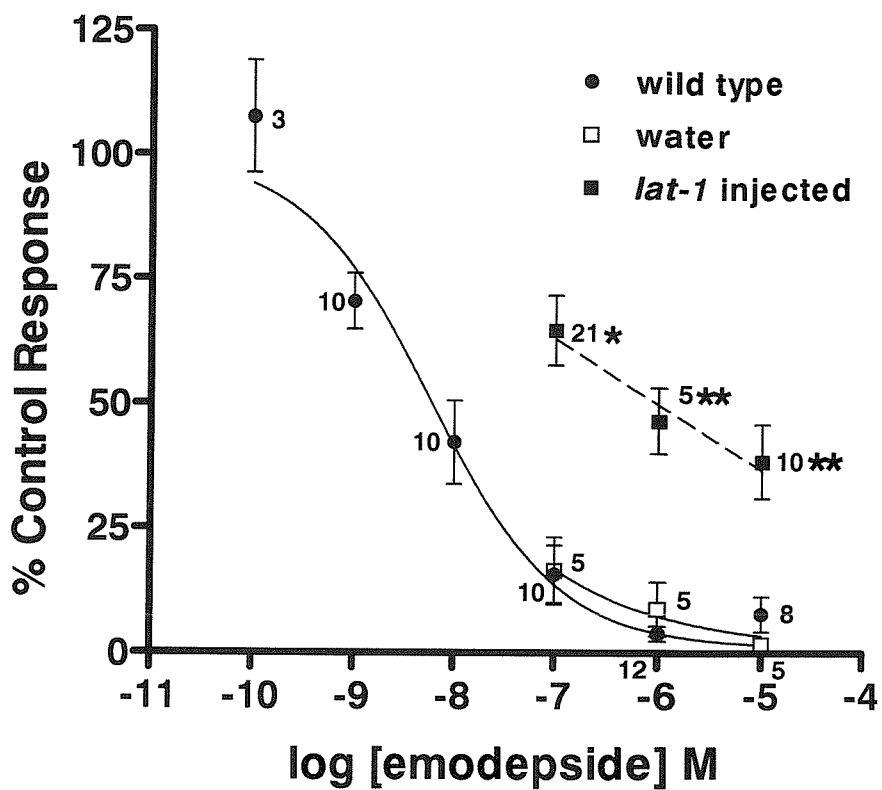


**Fig 5.9. The effect of emodepside on RNAi (injected) induced inhibition of *lat-1* on wild type *C. elegans* pharyngeal pumping (counting assay).** Protocol was as described in Fig 5.2. Concentration response curve for the effect of varying concentrations of emodepside on pharyngeal pumping rates on RNAi *lat-1* wild type *C. elegans*. % control response is the rate of pumping in 5-HT following emodepside application compared to the initial pumping rate in 5-HT. Each point is the mean  $\pm$  S.E.M. of (n) determinations., \*  $P<0.05$ , 100nM emodepside, n=21., \*\*  $P<0.01$ , 1 $\mu$ M emodepside, n=5 and \*\*\*  $P<0.001$ , 10 $\mu$ M emodepside, n=10.

### 5.10.1 Effect of FLP-13 on *lat-1* dsRNA injected *C. elegans*.

To determine whether *lat-1* knock down *C. elegans* still responded to an inhibitory signal, the effect of a known inhibitory peptide was tested on *lat-1* RNAi *C. elegans*. Application of 1 $\mu$ M FLP-13 to wild type *C. elegans* caused a significant reduction in pharyngeal pumping to  $90 \pm 24$  pumps/min, ( $P<0.01, n=5$ ). 1 $\mu$ M FLP-13 application to *lat-1* RNAi *C. elegans* caused a similar significant reduction in pharyngeal pumping rates  $74 \pm 18$  pumps/min, ( $P<0.001, n=5$ ) (Fig 5.12).

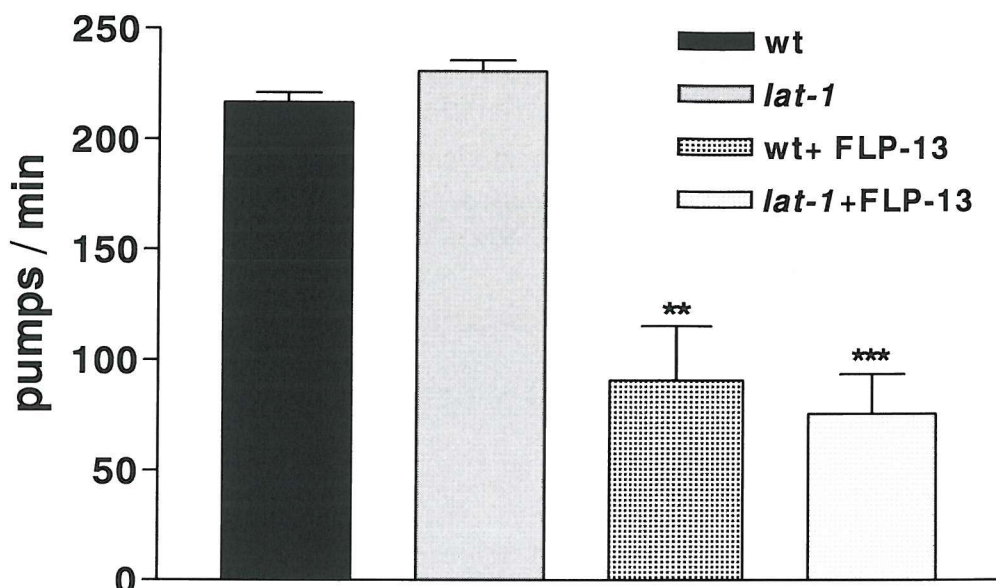


**Fig 5.10. The effect of FLP-13 (1 $\mu$ M) on wild type(wt) and *lat-1* (injected) RNAi *C. elegans* pharyngeal pumping.** The protocol was as for Fig 5.2. FLP-13 inhibited pharyngeal pumping in *lat-1* RNAi *C. elegans* similar to wild type. The black bars are wild type *C. elegans*. The grey bars are *lat-1* knock-down *C. elegans*. Each point is the mean  $\pm$  S.E.M of 5 determinations\*\*  $P<0.01$ , \*\*\*  $P<0.001$

## 5.11 Effect of emodepside on pharyngeal pumping in *C. elegans* fed on bacteria expressing dsRNA against the *lat-1* gene.

The effect of emodepside on pharyngeal pumping rates in *C. elegans*-fed bacteria expressing dsRNA against *lat-1* was investigated. In order to express the dsRNA, HT115 (DE3) bacteria require IPTG. *C. elegans* (*rrf-3*) were therefore grown on plates in the presence (induced) or absence (uninduced control) of IPTG.

RNAi for *lat-1* resulted in an uncoordinated (*unc*) phenotype characterized by loopy exaggerated body bends. In addition these animals had prolonged pharyngeal pump duration ( $225 \pm 23$  msec, compared to  $180 \pm 13$  msec, in uninduced control n=15 Fig 5.9) in the absence of 500nM 5-HT.

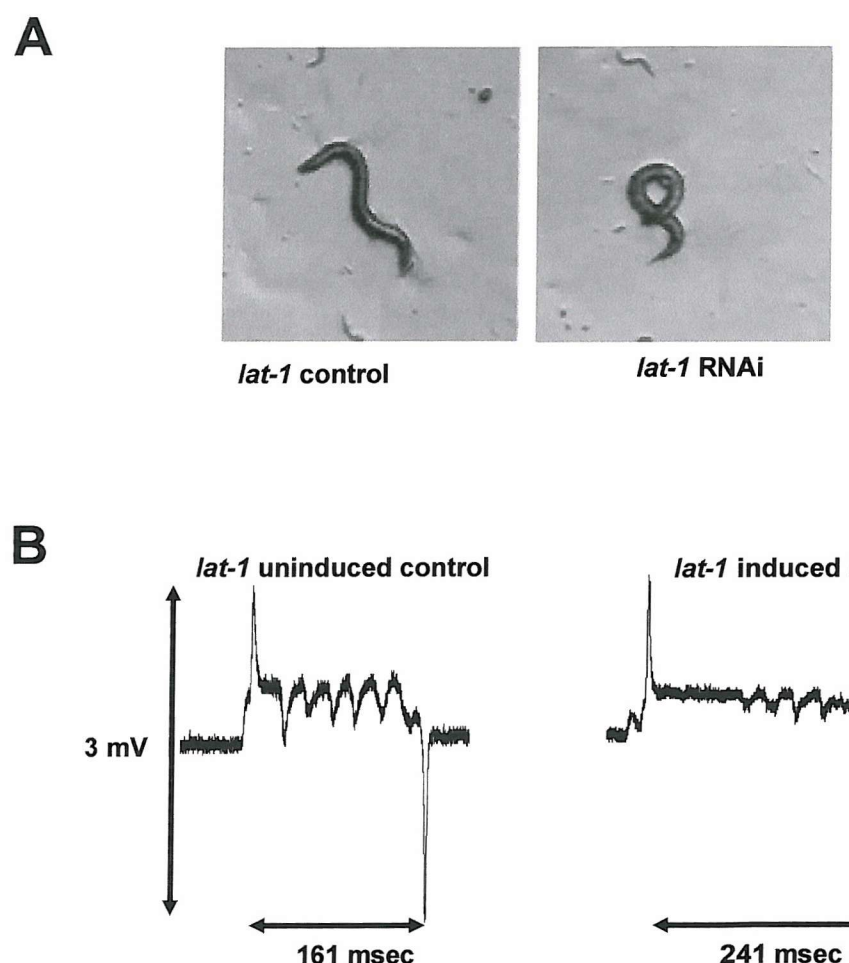


**Fig 5.11. RNAi for *lat-1* results in behavioural abnormalities in intact *C. elegans*. A.** Animals treated with RNAi for *lat-1* exhibit loopy body bends compared to uninduced control. **B.** RNAi for *lat-1* increased the duration of pharyngeal pumps. The traces show an EPG from an RNAi treated animal compared to control

RNAi of *lat-1* (induced) *C. elegans* (*rrf-3*) were 39 fold less sensitive to emodepside ( $IC_{50}=70\text{nM}$ , 95% confidence limits, 22 to 219nM, Fig 5.12, compared to uninduced control  $IC_{50}=1.8\text{nM}$ , 95% confidence limits 0.3 to 10nM, Fig 5.12, and non-RNAi *rrf-3*  $IC_{50}=2.9\text{nM}$ , 95% confidence limits 1.8 to 4.5nM). Significance was observed for 100 and 10nM ( $P<0.05$ ,  $n=5$ ) emodepside addition.

A.

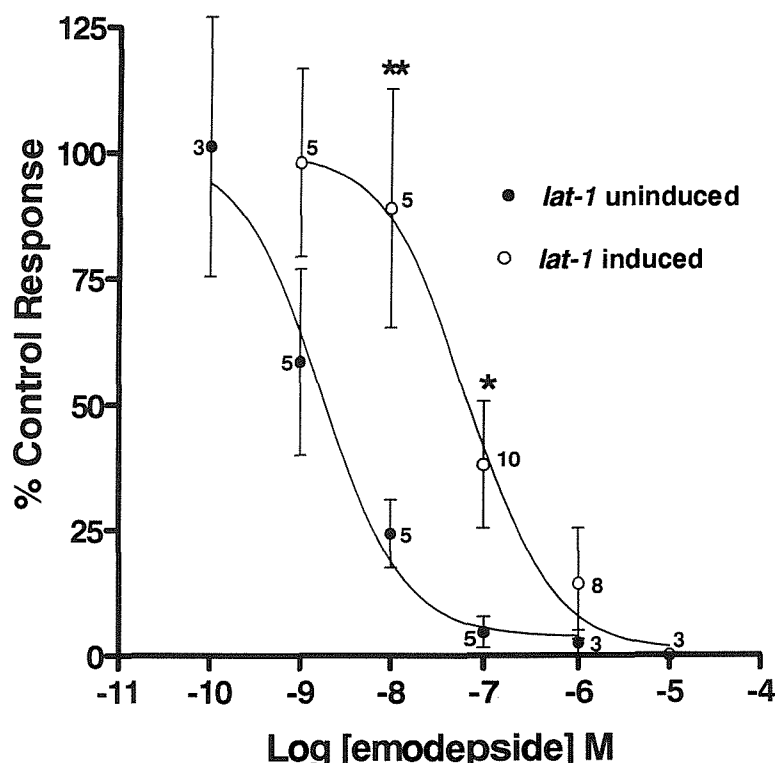
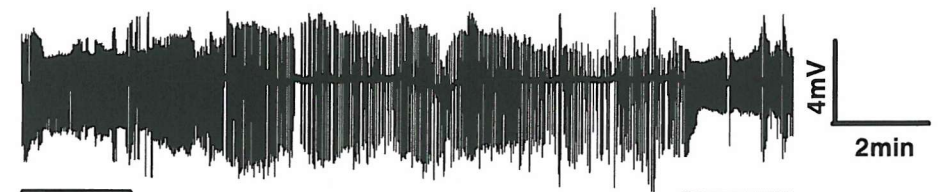
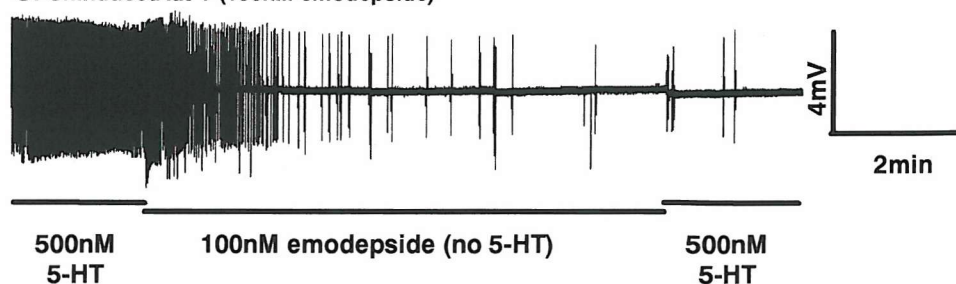


**Fig 5.12. Effect of emodepside on RNAi uninduced (in the absence of IPTG) and induced (+ IPTG) knock-down of *lat-1* in *rrf-3* *C. elegans* pharyngeal pumping.** Protocol was as described in Fig 5.4. A. Concentration response curve for the effect of varying concentrations of emodepside on pharyngeal pumping rates on RNAi knock down *lat-1* *rrf-3* *C. elegans*. % control response is the rate of pumping in 5-HT following emodepside application compared to the initial pumping rate in 5-HT. Each point is the mean  $\pm$  S.E.Mean of (n) determinations. \*\*  $P<0.01$ ,  $n=5$  \*  $P<0.05$ ,  $n=10$ .

**B. Uninduced *lat-1* (no emodepside)**



**C. Uninduced *lat-1* (100nM emodepside)**



**D. Induced *lat-1* (no emodepside)**



**E. Induced *lat-1* (100nM emodepside)**

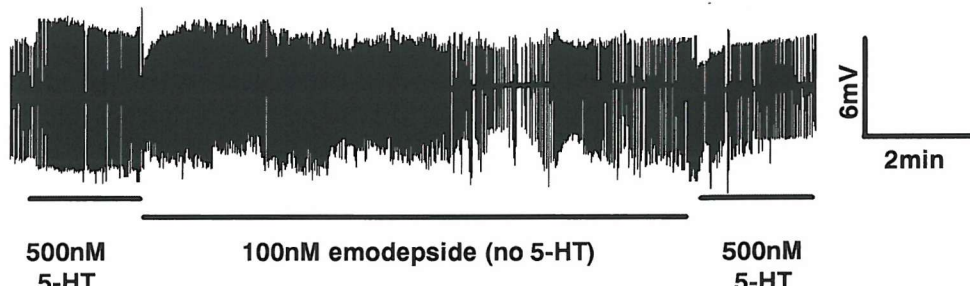


**Fig 5.12 (cont)** **B** a typical result from an uninduced *lat-1* control experiment in which the pharynx continues to pump throughout the entire time-course of the experiment. **C.** The effect of 100nM emodepside on pharyngeal pumping in uninduced *lat-1 rrf-3* *C. elegans*. Note the disappearance of the pumps during the period of emodepside application and the failure of the muscle to respond to the second application of 5-HT. **D.** a typical result from an induced *lat-1* control experiment in which the pharynx continues to pump throughout the entire time-course of the experiment. **E.** The effect of 100nM emodepside on pharyngeal pumping in induced *lat-1 rrf-3* *C. elegans*. Note the ability of the muscle to respond to 5-HT following emodepside application compared with C.

### 5.12 Effect of emodepside on pharyngeal pumping in *C. elegans* fed on bacteria expressing dsRNA against the *lat-2* gene.

The effect of emodepside on pharyngeal pumping rates in *C. elegans*-fed bacteria expressing dsRNA against *lat-2* was investigated. RNAi for *lat-2* resulted in a behavioural abnormality which was restricted to an effect on the frequency of pharyngeal pumps in the absence of 5-HT,  $5 \pm 2$  pumps/min,  $n=21$ , compared to control,  $27 \pm 9$  pumps/min  $n=22$ , Fig 5.13).

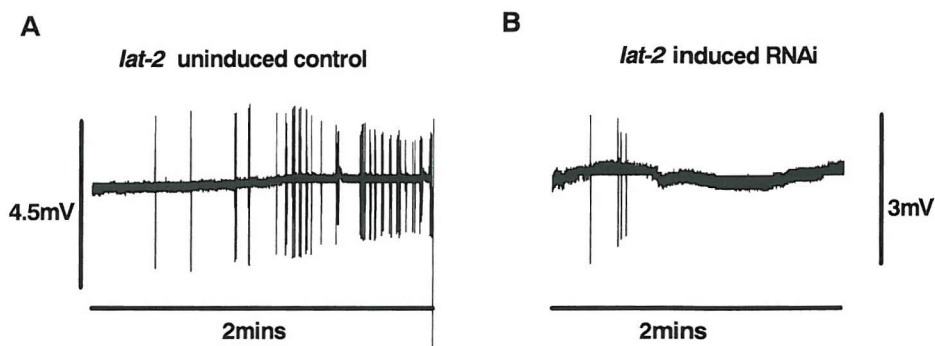


**Fig 5.13 RNAi for *lat-2* results in behavioural abnormalities in intact *C. elegans*. A. *lat-2* uninduced control. B. RNAi for *lat-2* decreases the frequency of pharyngeal pumping.**

*Lat-2* RNAi were 5.5 fold less sensitive to emodepside ( $IC_{50}=17\text{nM}$ , 95% confidence limits 5.9 to 45nM, Fig 5.14), compared to uninduced ( $IC_{50}=2.9\text{nM}$ , 95% confidence limits 0.9 to 8.8nM, Fig 5.14) and non-RNAi *rrf-3* ( $IC_{50}=2.9\text{nM}$ , 95% confidence limits 1.8 to 4.5nM). No significant differences were observed for any emodepside concentrations.

**A.**

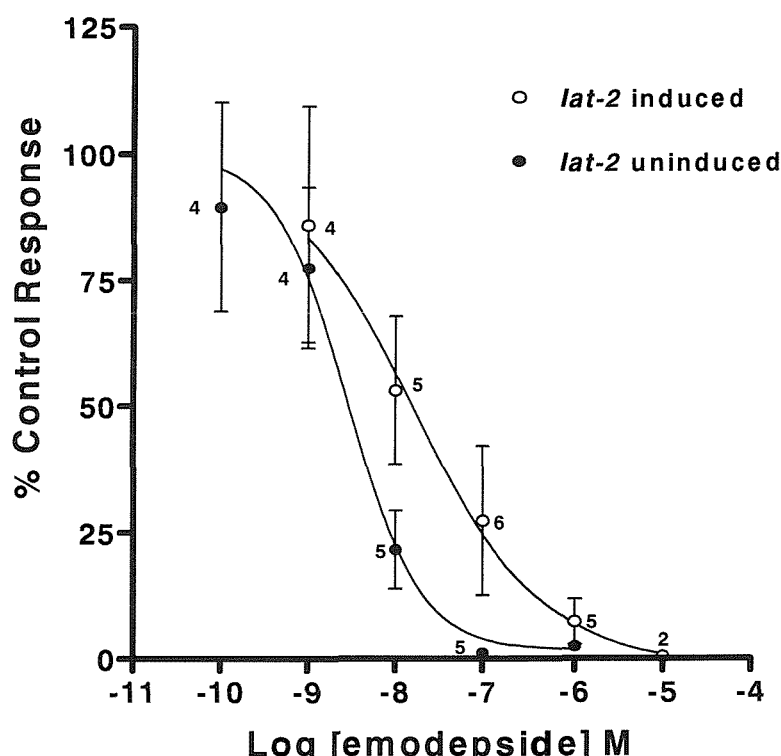
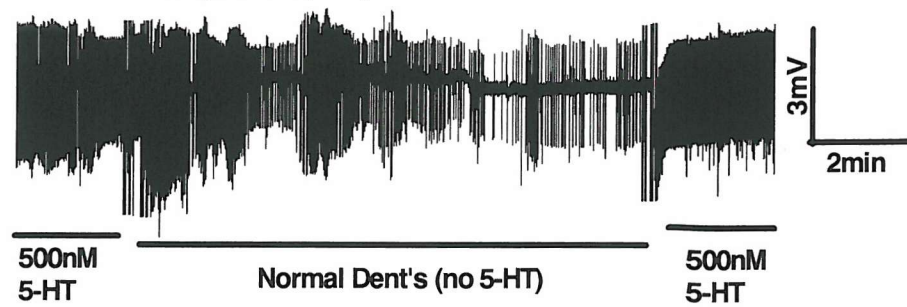
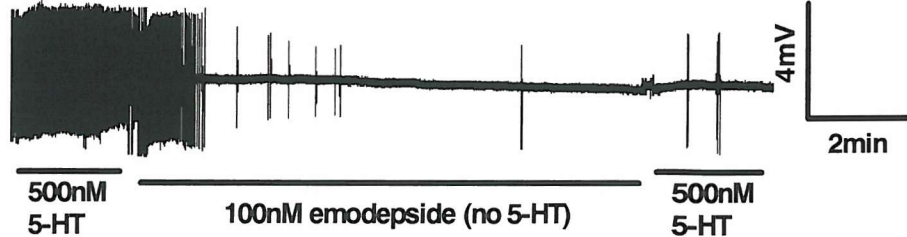


**Fig 5.14 Effect of emodepside on RNAi uninduced (in the absence of IPTG) and RNAi induced (+ IPTG) inhibition *lat-2* in *rrf-3* *C. elegans* pharyngeal pumping.** Protocol was as described in Fig 5.4 A. Concentration response curve for the effect of varying concentrations of emodepside on pharyngeal pumping rates on RNAi knock down *lat-2 rrf-3* *C. elegans*. % control response is the rate of pumping in 5-HT following emodepside application compared to the initial pumping rate in 5-HT. Each point is the mean  $\pm$  S.E.Mean of (n) determinations.

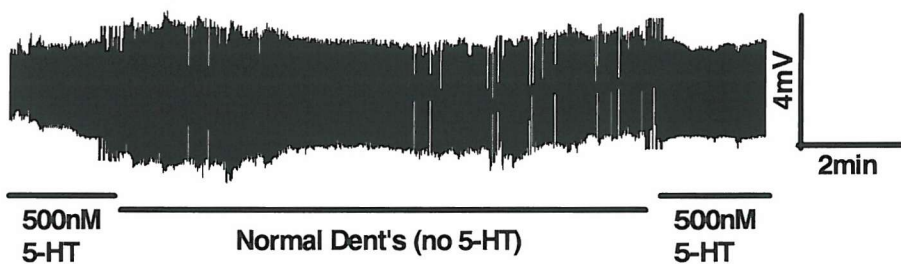
B. Uninduced *lat-2* (no emodepside)



C. Uninduced *lat-2* (100nM emodepside)



D. Induced *lat-2* (no emodepside)



E. Induced *lat-2* (100nM emodepside)

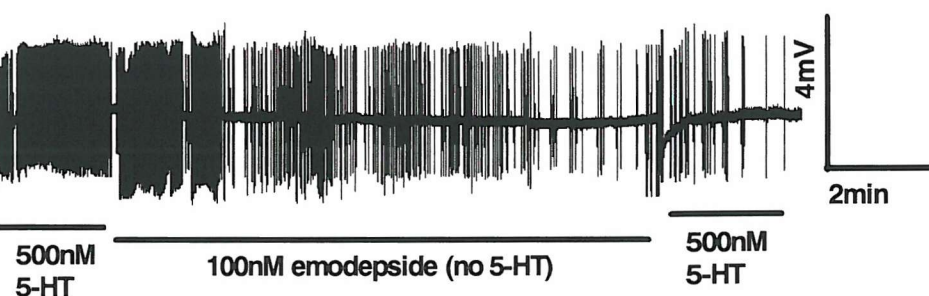


**Fig 5.14 (cont) B** a typical result from an uninduced *lat-2* control experiment in which the pharynx continues to pump throughout the entire time-course of the experiment. **C.** The effect of 100nM emodepside on pharyngeal pumping in uninduced *lat-2 rrf-3* *C. elegans*. Note the disappearance of the pumps during the period of emodepside application and the failure of the muscle to respond to the second application of 5-HT. **D.** a typical result from an induced *lat-2* control experiment in which the pharynx continues to pump throughout the entire time-course of the experiment. **E.** The effect of 100nM emodepside on pharyngeal pumping in induced *lat-2 rrf-3* *C. elegans*. Note a slight response of the muscle to 5-HT following emodepside application.

### 5.13 Effect of emodepside on pharyngeal pumping in *C. elegans* fed on bacteria expressing dsRNA against both the *lat-1* and *lat-2* gene.

The effect of emodepside on pharyngeal pumping rates in *C. elegans* fed bacteria expressing dsRNA against *lat-1* and *lat-2* was investigated. *lat-1* and *lat-2* RNAi *C. elegans* were 8 fold less sensitive to emodepside ( $IC_{50}=17\text{nM}$ , 95% confidence limits 9.3 to 31nM, Fig 5.15), compared to uninduced ( $IC_{50}=2.1\text{nM}$ , 95% confidence limits 0.7 to 6nM, Fig 5.15) and non-RNAi *rrf-3* ( $IC_{50}=2.9\text{nM}$ , 95% confidence limits 1.8 to 4.5nM). Significance was observed for 10nM emodepside concentration ( $P<0.05$ ).

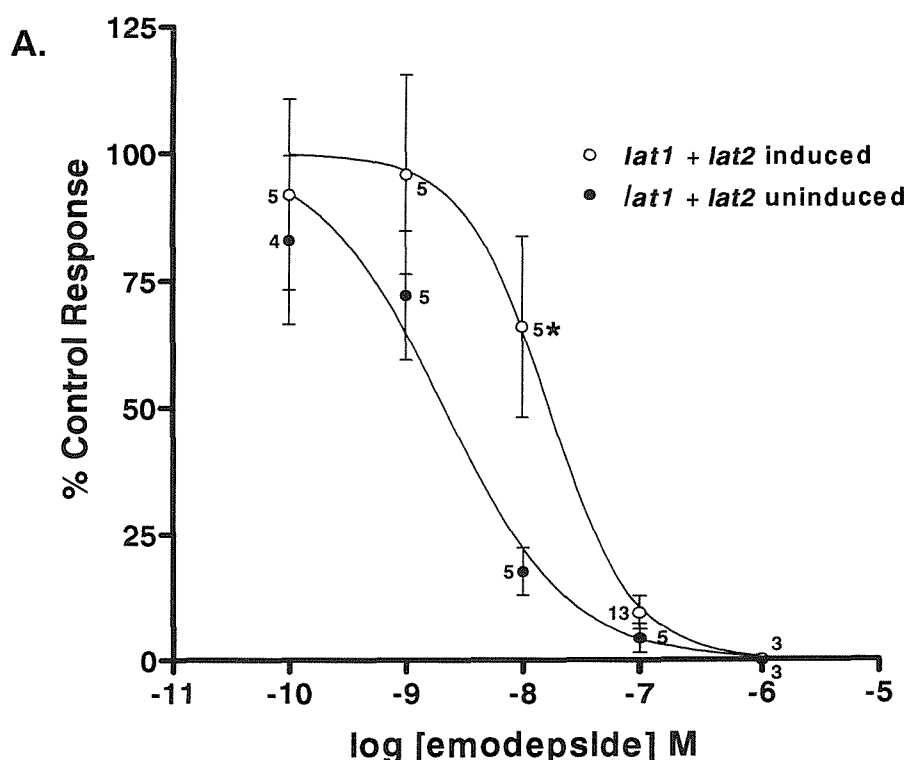
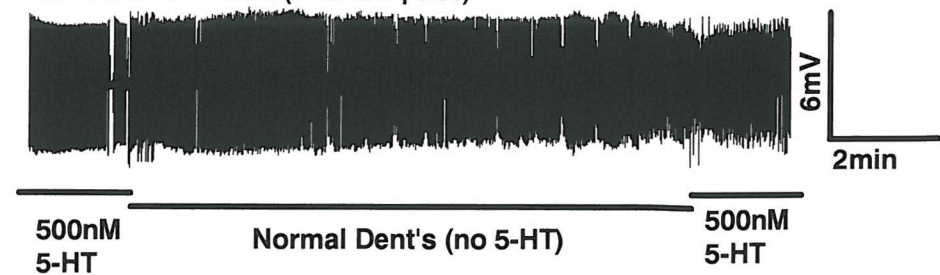
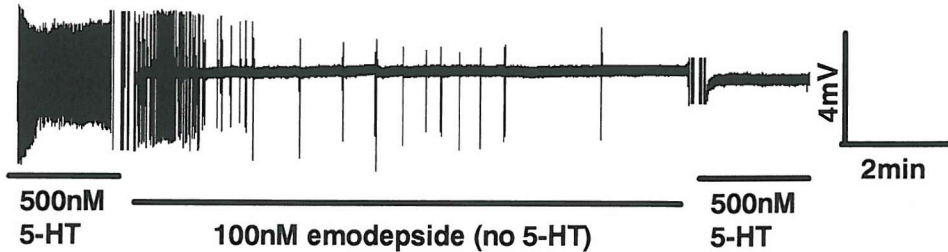


**Fig 5.15. Effect of emodepside on RNAi uninduced (in the absence of IPTG) and induced (+ IPTG) inhibition of *lat-1* and *lat-2* in *rrf-3* *C. elegans* pharyngeal pumping.** Protocol was as described in Fig 5.4 A. Concentration response curve for the effect of varying concentrations of emodepside on pharyngeal pumping rates on RNAi inhibition of *lat-1* and *lat-2* *rrf-3* *C. elegans*. % control response is the rate of pumping in 5-HT following emodepside application compared to the initial pumping rate in 5-HT. Each point is the mean  $\pm$  S.E. Mean of (n) determinations.\*  $P<0.05$ , n=5.

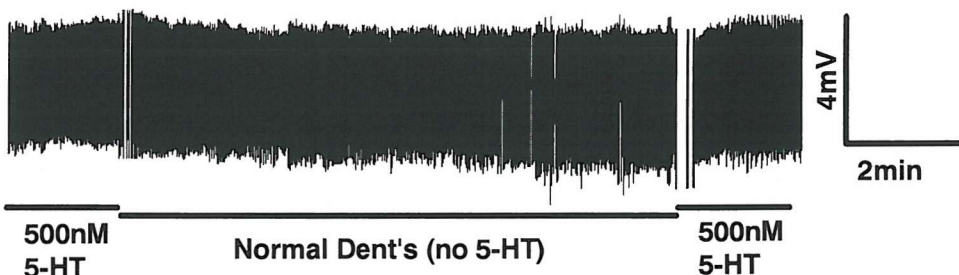
**B. Uninduced *lat-1+lat-2* (no emodepside)**



**C. Uninduced *lat-1+lat-2* (100nM emodepside)**



**D. Induced *lat-1+lat-2* (no emodepside)**



**E. Induced *lat-1+lat-2* (100nM emodepside)**

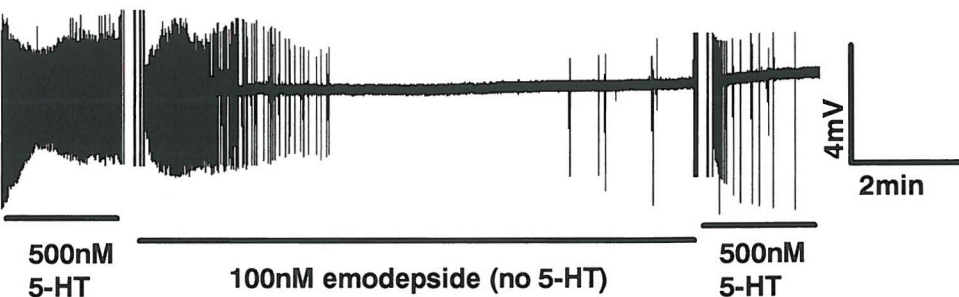


**Fig 5.15 (cont)** **B** a typical result from an uninduced *lat-1* and *lat-2* control experiment in which the pharynx continues to pump throughout the entire time-course of the experiment. **C.** The effect of 100nM emodepside on pharyngeal pumping in uninduced *lat-1* and *lat-2* *rrf-3* *C. elegans*. Note the disappearance of the pumps during the period of emodepside application and the failure of the muscle to respond to the second application of 5-HT. **D.** a typical result from an induced *lat-1* and *lat-2* control experiment in which the pharynx continues to pump throughout the entire time-course of the experiment. **E.** The effect of 100nM emodepside on pharyngeal pumping in induced *lat-1* and *lat2 rrf-3* *C. elegans*. Note a slight response of the muscle to 5-HT following emodepside application.

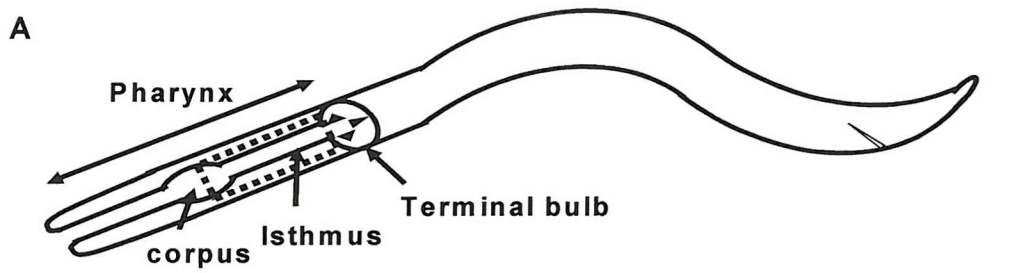
## 5.14 Does emodepside require synaptic vesicle release for its action?

Latrophilin is a candidate receptor for  $\alpha$ LTX, (Davletov *et al.*, 1996;Krasnoperov *et al.*, 1996) through which stimulation of vesicle release occurs (Davletov *et al.*, 1998). In chapter 3, it was shown that emodepsides main site of action appears pre-synaptic. Vesicular release of neurotransmitter from nerve terminals requires the fusion of synaptic vesicles to pre-synaptic membranes (Scheller, 1995;Sudhof, 1995). Vesicle fusion involves the interaction of a plethora of vesicle associated and pre-synaptic membrane associated proteins. In order to investigate whether emodepside causes vesicle release two methods were used. To test whether emodepside would trigger loss of fluorescence from putative synaptic regions in *C. elegans* pharynx, activity-dependent uptake of the rhodamine fluorescent marker FM4-64 was used. This dye labels active synapses (Betz *et al.*, 1992;Cochilla *et al.*, 1999). The second method involved use of *C. elegans* mutants deficient in proteins associated with vesicle release.

## 5.15 Effect of emodepside on FM4-64 stained neurones in *C. elegans*.

To confirm that FM4-64 co-localises to active synapses, FM4-64 loading was performed in normal and high potassium Dent's. In normal potassium a pattern of non-specific staining was observed around the metacorpus and intestine of the worm. The staining was not punctate. In high potassium (25mM), FM4-64 was localised to puncta especially in the isthmus region (Fig 5.16A) of the pharynx (Fig 5.16 B). Loading of FM4-64 was therefore performed in high potassium Dent's.

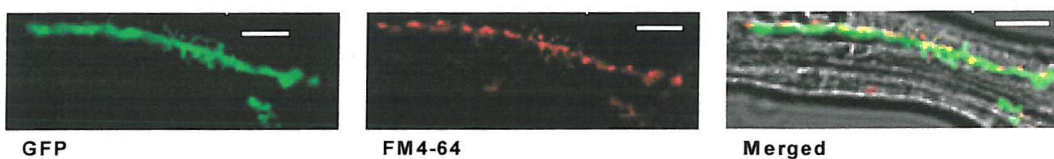
To confirm that FM4-64 uptake was localized to synaptic regions *dpy-20(e1362) IV; evIs111 (NW1229);gfp C. elegans* were used. This strain exhibits a pan-neuronal GFP fluorescence (Altun-Gultekin *et al.*, 2001). FM4-64 labelling was localised to puncta and co-localised with the pan-neuronal GFP expression (Fig 5.16 C). Application of 100nM emodepside to these labelled neurons caused a loss of FM4-64 fluorescence from these synaptic regions (10 out of 12 preparations) compared to vehicle fluorescence which was stable for up to 30mins (n=4, Fig 5.16 D). Co-localisation of FM4-64 and GFP is shown in Fig 5.16E.



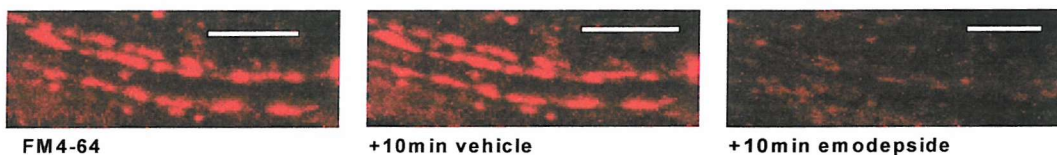
**B** Effect of low and high potassium Dent's on FM4-64 labelling



**C** Co-localisation of GFP labelled neurones with FM4-64



**D** Staining with FM4-64 following 100nM emodepside



**E** Merged GFP, FM4-64 images.

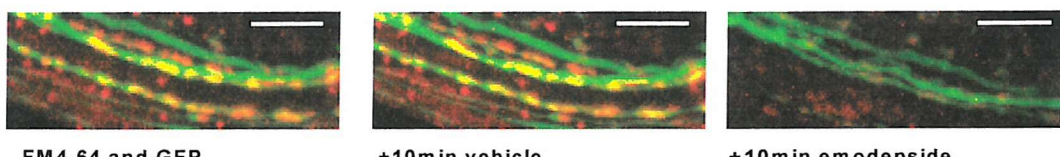


**Fig 5.16. The effect of emodepside on exocytosis from *C. elegans* pharyngeal neurones by imaging with FM4-64.** *C. elegans* pharynxes were dissected with their embedded enteric neurones. Wild type or a pan neuronal GFP expressing strain (NW1229):(Altun-Gultekin *et al.*, 2001) were used in these experiments. A Diagram showing the position of the isthmus within the *C. elegans* (dotted rectangle) where FM4-64 labelling was imaged.. B. FM4-64 loading in normal potassium (left) and 25mM potassium (right) respectively. C. Co-localization of FM4-64 staining with GFP labelled neurons (left), FM4-64 staining (middle) and merged image (right). Yellow indicates co-localization of FM4-64 and GFP. D. FM4-64 staining following loading in high potassium (which marks regions with high vesicle recycling prior to drug addition (left). FM4-64 staining following 10 minute addition 0.1% ethanol vehicle (middle). FM4-64 staining following 10 minute 100nM emodepside addition (right) E. The same preparation as in D showing the overlay of red and green fluorescence

## **5.16 Effect of emodepside on pharyngeal pumping in *snb-1* *C. elegans*.**

Synaptobrevin (VAMP), a vesicle localized protein (Trimble 1988) facilitates vesicle mediated release by forming a complex with syntaxin and SNAP-25 (Sollner *et al.*, 1993). Synaptobrevin hypomorphic *C. elegans* mutants exhibit a variety of behavioural abnormalities consistent with a general defect in efficacy of synaptic transmission (Nonet *et al.*, 1998). *snb-1* *C. elegans* were 29 fold less sensitive to emodepside than wild type controls ( $IC_{50} = 123\text{nM}$ , 95% confidence limits 33 to 460nM, compared to 4.2nM, 95% confidence limits 1.5 to 11nM, Fig 5.17 ). Significance was observed for 100nM ( $P < 0.01$ ,  $n=12$ ) and 10nM ( $P < 0.01$ ,  $n=5$ ) emodepside.

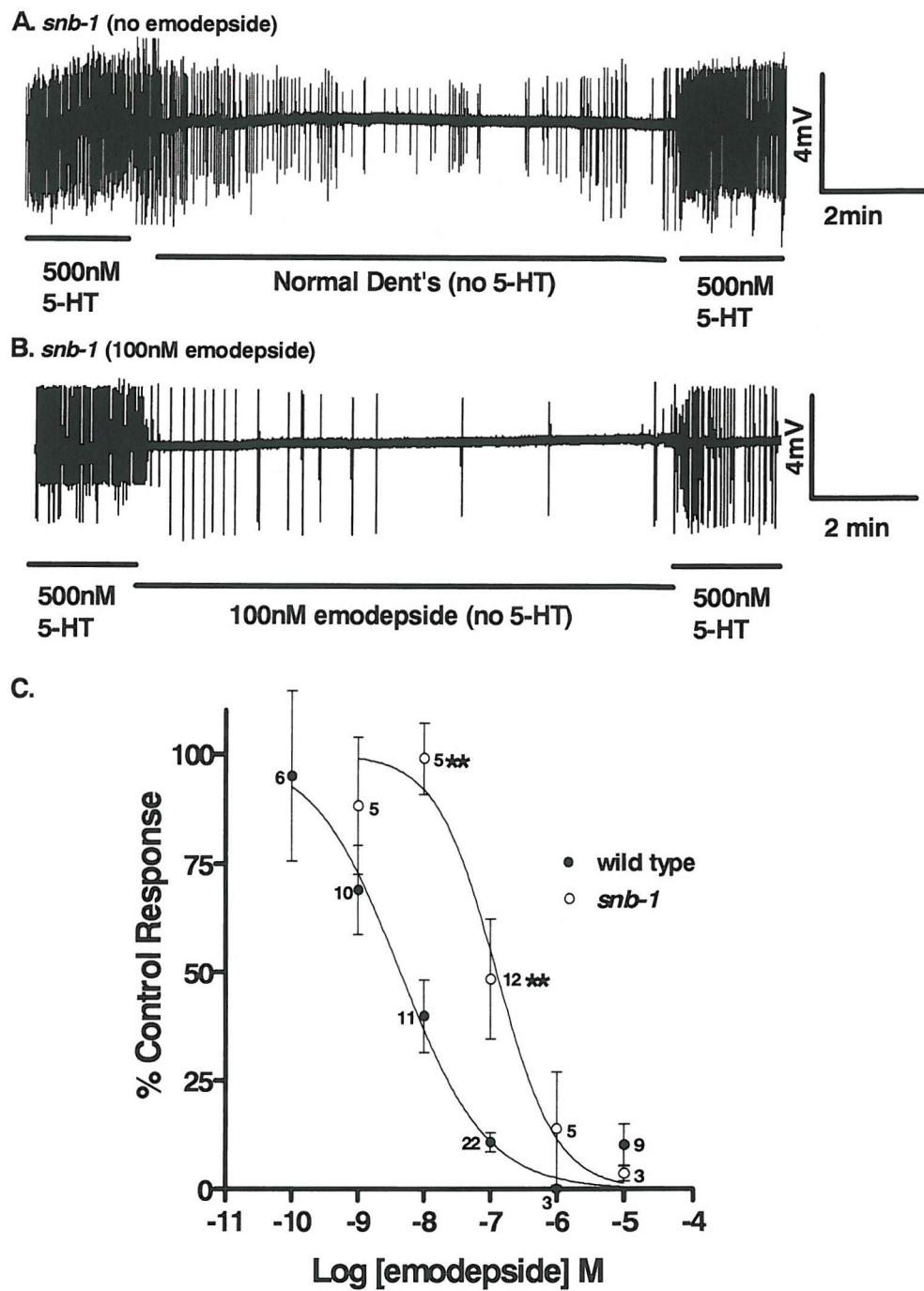


**Fig 5.17 Effect of emodepside on *snb-1* *C. elegans*.** Protocol was as described in Fig 5.4. **A.** a typical result from a control experiment in which the pharynx continues to pump throughout the entire time-course of the experiment. **B.** The effect of 100nM emodepside on pharyngeal pumping in *snb-1* *C. elegans*. Note following emodepside addition the muscle still responds to a second application of 5-HT. This is compared to wild type *C. elegans* (p.113 Fig 5.4) where, following 100nM emodepside application, there is a near complete inhibition of pharyngeal pumping. **C.** Concentration response curve for the effect of varying concentrations of emodepside on pharyngeal pumping rates in *snb-1* *C. elegans*. % control response is the rate of pumping in 5-HT following emodepside application compared to the initial pumping rate in 5-HT. Each point is the mean  $\pm$  S.E.Mean of (n) determinations \*\*  $P < 0.01$ , 10nM emodepside, n=5, 100nM emodepside, n=12. The activity of emodepside was confirmed with parallel wild type controls in conjunction with these experiments.

## 5.17 Effect of emodepside on pharyngeal pumping in *unc-13* *C. elegans*.

UNC-13 primes synaptic vesicles for fusion by promoting the open configuration of syntaxin (Richmond *et al.*, 2001), a protein localized primarily on the pre-synaptic plasma membrane (Bennett, 1992 305 /id). *Unc-13* loss of function mutants show uncoordinated phenotypes with varying degrees of paralysis. The cloned sequence of *unc-13* *C. elegans* shows three regions termed left (L), the middle (M) and the right (R)(Kohn *et al.*, 2000). Alternative splicing of these regions results in two important variants; L-R is located at pre-synaptic densities, whereas M-R is located diffusely along axons. Mutations in the UNC-13 gene cause varying degrees of paralysis and uncoordinated movement; with severity dependent on the mutation point within the *unc-13* gene. Here two loss of function alleles; *e1091* which has a mutation in the L region (therefore affecting the L-R splice variants), and the more severe *s69* allele which has a mutation in the R-region (which affects both the L-R and M-R splice variants).

Both *unc-13 e1091* and *s69* mutants pump poorly in the presence of 500nM 5-HT, so 1 $\mu$ M 5-HT was used. *unc-13 (e1091)* mutants were 78 fold less sensitive to emodepside than wild type controls ( $IC_{50}$ = 203nM, 95% confidence limits, 28 to 1454nM, compared to 4nM, 95% confidence limits, 1.7 to 9.8, Fig 5.18). Significance was observed for 100nM ( $P<0.05$ , n=15) and 10nM ( $P<0.05$ , n=5) emodepside. *unc-13* allele (*s69*) mutants were 206 fold less sensitive to emodepside than wild type controls ( $IC_{50}$ = 360nM, 95% confidence limits 68 to 1905nM) compared to  $IC_{50}$ = 4nM, 95% confidence limits, 1.7 to 9.8nM, Fig 5.18). Significance was observed for 1 $\mu$ M ( $P<0.05$ , n=4), 100nM ( $P<0.05$ , n=7) and 10nM ( $P<0.05$ , n=5) emodepside.

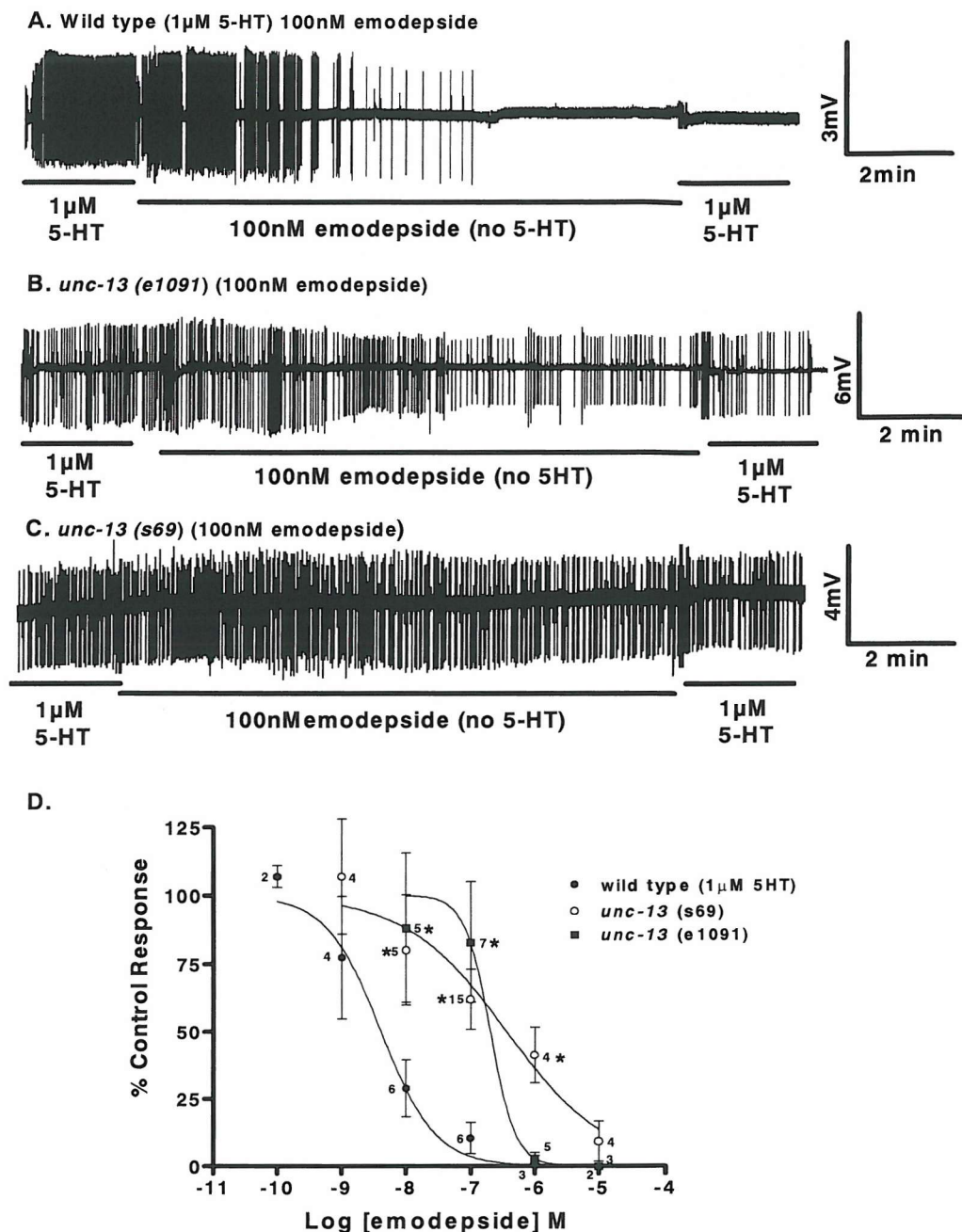


**Fig 5.18. Effect of emodepside on *unc-13* *C. elegans* pharyngeal pumping.** Protocol was as described in Fig 5.4 A. The effect of 100nM emodepside on pharyngeal pumping (1 $\mu$ M 5-HT) in wild type *C. elegans*. Note the disappearance of the pumps during the period of emodepside application and the failure of the muscle to respond to the second application of 5-HT. B. The effect of 100nM emodepside on pharyngeal pumping in *unc-13* (e1091) *C. elegans*. Note following emodepside addition the continued pumping in the presence of 5-HT. C. The effect of 100nM emodepside on pharyngeal pumping in *unc-13* (s69) *C. elegans*. Note following emodepside addition the continued pumping in the presence of 5-HT. D. Concentration response curve for the effect of varying concentrations of emodepside on pharyngeal pumping rates in *unc-13* (e1091, s69) *C. elegans*. % control response is the rate of pumping in 5-HT following emodepside application compared to the initial pumping rate in 5-HT. Each point is the mean  $\pm$  S.E.M. of (n) determinations \*  $P < 0.05$ , 10nM emodepside, n=5 (s69 and e1091), 100nM emodepside n=7 (e1091) and n=15 (s69), 1 $\mu$ M emodepside, n=4 (s69). The activity of emodepside was confirmed with parallel wild type controls in conjunction with these experiments.

## 5.18 Effect of emodepside on pharyngeal pumping in *unc-10* *C. elegans*.

*unc-10* *C. elegans* are deficient in the RAB3 interacting protein (RIM). RIM is localised to the pre-synaptic active zone. RIM has been shown to interact with other proteins important in vesicle release like RAB-3 and *unc-13* (Koushika *et al.*, 2001). RIM may therefore regulate steps involved in vesicle exocytosis, specifically docking of synaptic vesicles, or priming of synaptic vesicles for rapid release. Emodepside caused a similar decrease in pumping rates on *unc-10* *C. elegans* ( $IC_{50}$  2.3nM 95% confidence limits, 1 to 5.5) as wild type ( $IC_{50}$  4.4nM 95% confidence limits, 1.5 to 10, Fig 5.19). No points in the graph were significantly different between wild type and *unc-10* *C. elegans*.

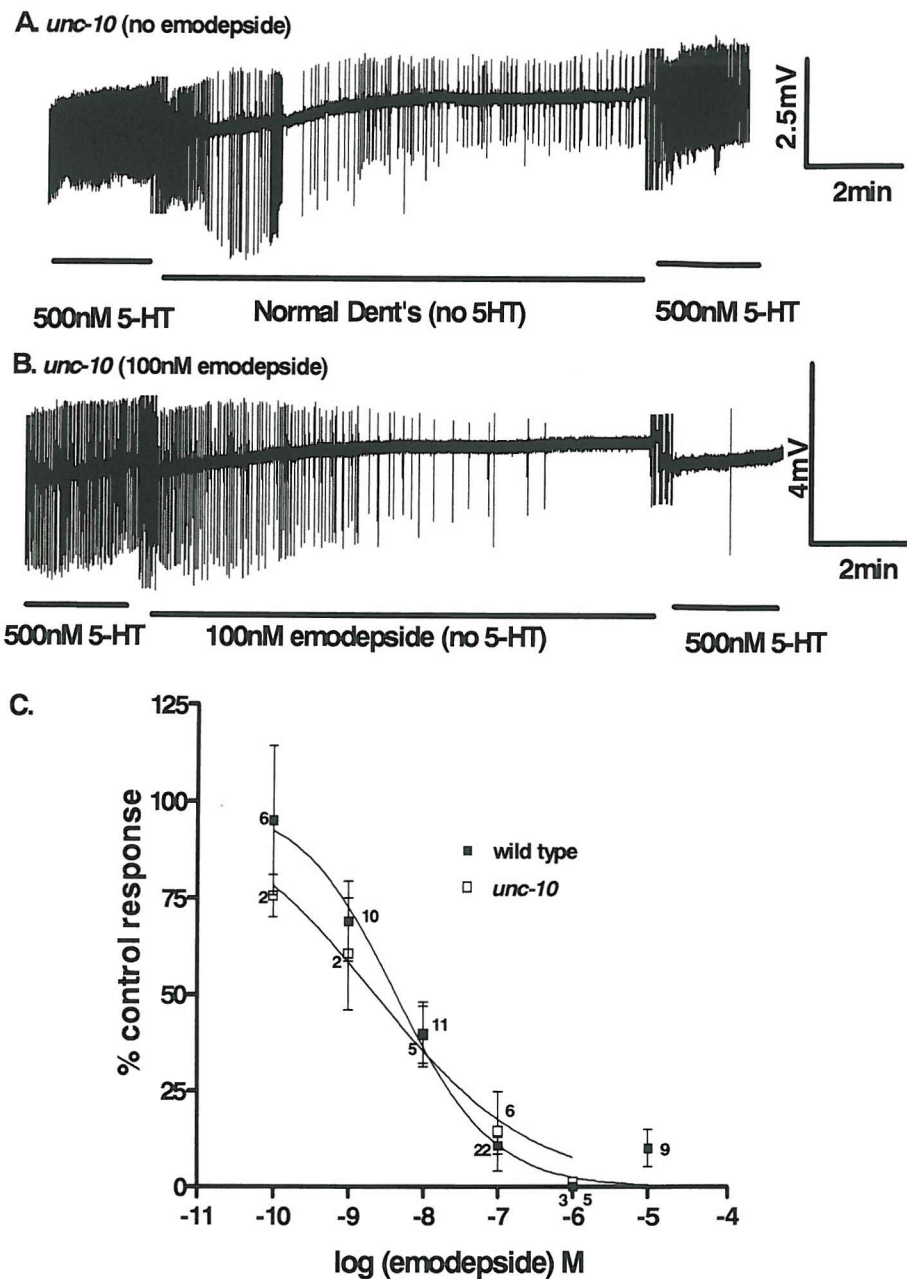


**Fig 5.19 Effect of emodepside on *unc-10* *C. elegans* pharyngeal pumping.** Protocol was as described in Fig 5.4 A. a typical result from a control experiment in which the pharynx continues to pump throughout the entire time-course of the experiment. B. The effect of 100nM emodepside on pharyngeal pumping. Note the disappearance of the pumps during the period of emodepside application and the failure of the muscle to respond to the second application of 5-HT.C. Concentration response curve for the effect of varying concentrations of emodepside on pharyngeal pumping rates of *unc-10* *C. elegans*. % control response is the rate of pumping in 5-HT following emodepside application compared to the initial pumping rate in 5-HT. Each point is the mean  $\pm$  S.E. Mean of (n) determinations

## **5.19 Investigating the signalling Pathway through which emodepside acts.**

### **5.19.1 Effect of emodepside on pharyngeal pumping in *egl-30* ( $G\alpha_q$ ) *C. elegans*.**

Latrophilin has been shown to couple to  $G\alpha_q$  (Rahman *et al.*, 1999). In *C. elegans* the *egl-30* gene codes for  $G\alpha_q$ . Application of 100nM emodepside caused a decrease in pharyngeal pumping in wild type *C. elegans* of  $84 \pm 6\%$  (n=10). In *egl-30* mutant *C. elegans* 100nM application of emodepside caused a significant  $43 \pm 9.8\%$  ( $P<0.01, n=5$ ) decrease in pharyngeal pumping. 1 $\mu$ M application of emodepside to wild type *C. elegans* caused a  $96 \pm 1\%$  (n=12) reduction in pharyngeal pumping, compared to only a  $60 \pm 13\%$  ( $P<0.01, n=5$ ) in *egl-30* mutants. At the highest emodepside concentration (10 $\mu$ M), application of emodepside to *egl-30* *C. elegans* caused a  $94 \pm 3\%$  (n=8) decrease in pharyngeal pumping rates similar to  $92 \pm 4\%$  in the wild type control (Fig 5.20).

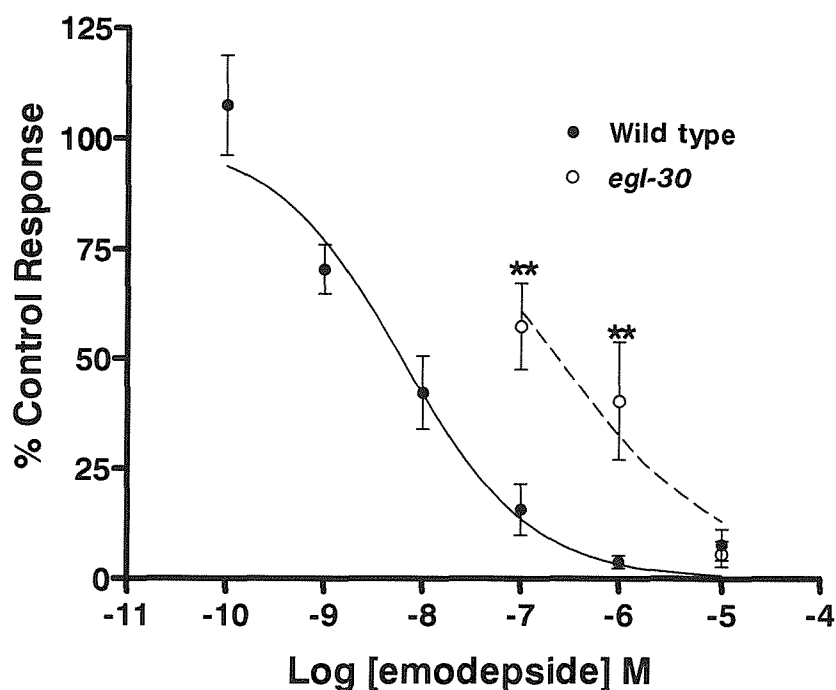


**Fig 5.20.** The effect of emodepside on *egl-30* (Gαq) *C. elegans* pharyngeal pumping (counting assay). The protocol was as described in Fig 5.2. The concentration response curve for the effect of varying concentrations of emodepside on pharyngeal pumping rates on *egl-30* *C. elegans*. % control response is the rate of pumping in 5-HT following emodepside application compared to the initial pumping rate in 5-HT. Each point is the mean  $\pm$  S.E.M. of 10 determinations. \*\*  $P < 0.01$ . The activity of emodepside was confirmed with parallel wild type controls in conjunction with these experiments.

### **5.19.2 Effect of emodepside on pharyngeal pumping in *egl-30* ( $G\alpha_q$ ) gain of function *C. elegans*.**

A gain of function (gf) allele (*tg26*) exists for *egl-30* in *C. elegans* (Doi & Iwasaki, 2002). *egl-30* (gf) were 20 fold more sensitive to emodepside compared to wild type control ( $IC_{50}= 0.2\text{nM}$ , 95% confidence limits, 0.05 to 0.9nM, Fig 5.21, compared to,  $IC_{50}=4.1\text{nM}$ , 95% confidence limits, 1.2 to 14.7nM, Fig 5.21). Significance was observed for 10nM ( $P<0.05$ ,  $n=5$ ) and 1nM ( $P<0.05$ ,  $n=4$ ) emodepside. As *egl-30* (gf) are hypersensitive to emodepside, example traces for 10nM emodepside are shown in Fig 5.21

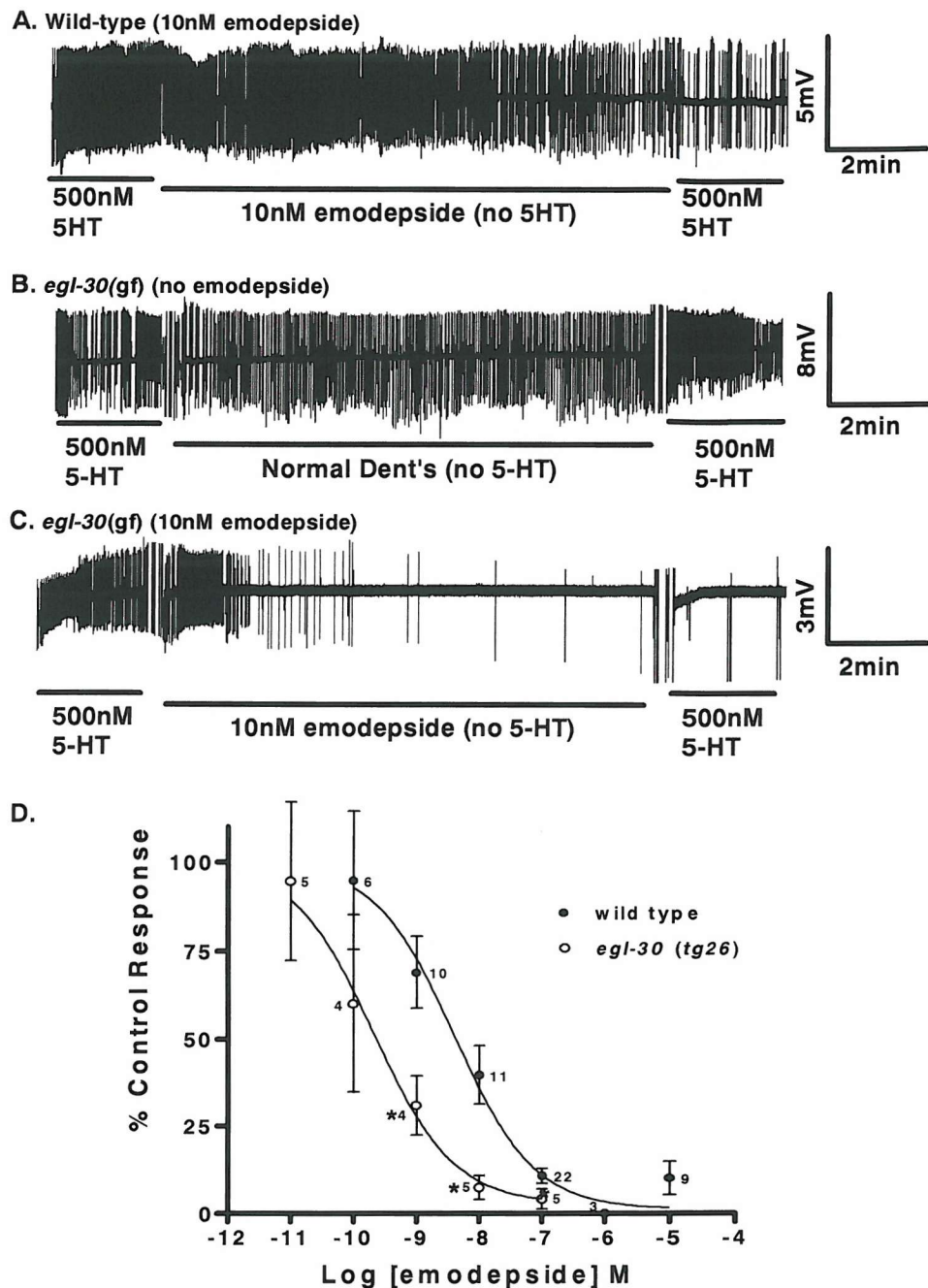


**Fig 5.21. Effect of emodepside on *egl-30* gain of function *C. elegans* pharyngeal pumping.** Protocol was as described in Fig 5.4. Trace examples for 10nM emodepside are shown here. **A.** The effect of 10nM emodepside on pharyngeal pumping in wild type *C. elegans*. Note the decrease in the number of pumps during the period of emodepside application and a reduced muscle respond to the second application of 5-HT. **B.** A typical result from an *egl-30* (gf) control experiment in which the pharynx continues to pump throughout the entire time-course of the experiment. **C.** The effect of 10nM emodepside on pharyngeal pumping in *egl-30* (gf) *C. elegans*. Note the disappearance of the pumps during the period of emodepside application and the failure of the muscle to respond to the second application of 5-HT. **D.** Concentration response curve for the effect of varying concentrations of emodepside on pharyngeal pumping rates in *egl-30* (gf) *C. elegans*. % control response is the rate of pumping in 5-HT following emodepside application compared to the initial pumping rate in 5-HT. Each point is the mean  $\pm$  S.E.M. of (n) determinations \*  $P < 0.05$ , 1nM emodepside, n=4 and 10nM emodepside, n=5.

### 5.19.3 Effect of emodepside on pharyngeal pumping in *goa-1* ( $G\alpha_o$ ) *C. elegans*.

Previous studies on the neuromuscular junction of *C. elegans* have shown that  $G\alpha_q$  (*egl-30*) and  $G\alpha_o$  (*goa-1*) have reciprocal effects on ACh release, with the former stimulating release through activation of phospholipase-C  $\beta$  (PLC- $\beta$ ) and production of diacylglycerol (DAG) (Taylor & Exton, 1991; Lee *et al.*, 1992), with the latter inhibiting release through activation of a DAG kinase (Nurrish *et al.*, 1999). The possibility of whether  $G\alpha_o$  loss of function mutant would also have altered sensitivity to emodepside was therefore tested. *goa-1* mutants were 10 fold more sensitive to emodepside compared to wild type control ( $IC_{50} = 0.4\text{nM}$ , 95% confidence limits, 0.1 to  $1.4\text{nM}$ , compared to,  $IC_{50} = 4.1\text{nM}$ , 95% confidence limits, 1.2 to  $14.7\text{nM}$ , Fig 5.22). Significance was observed at  $100\text{nM}$  ( $P < 0.05$ ) and  $10\text{nM}$  ( $P < 0.05$ ) emodepside concentrations. As *goa-1* are hypersensitive to emodepside example traces for  $10\text{nM}$  emodepside are shown in Fig 5.22

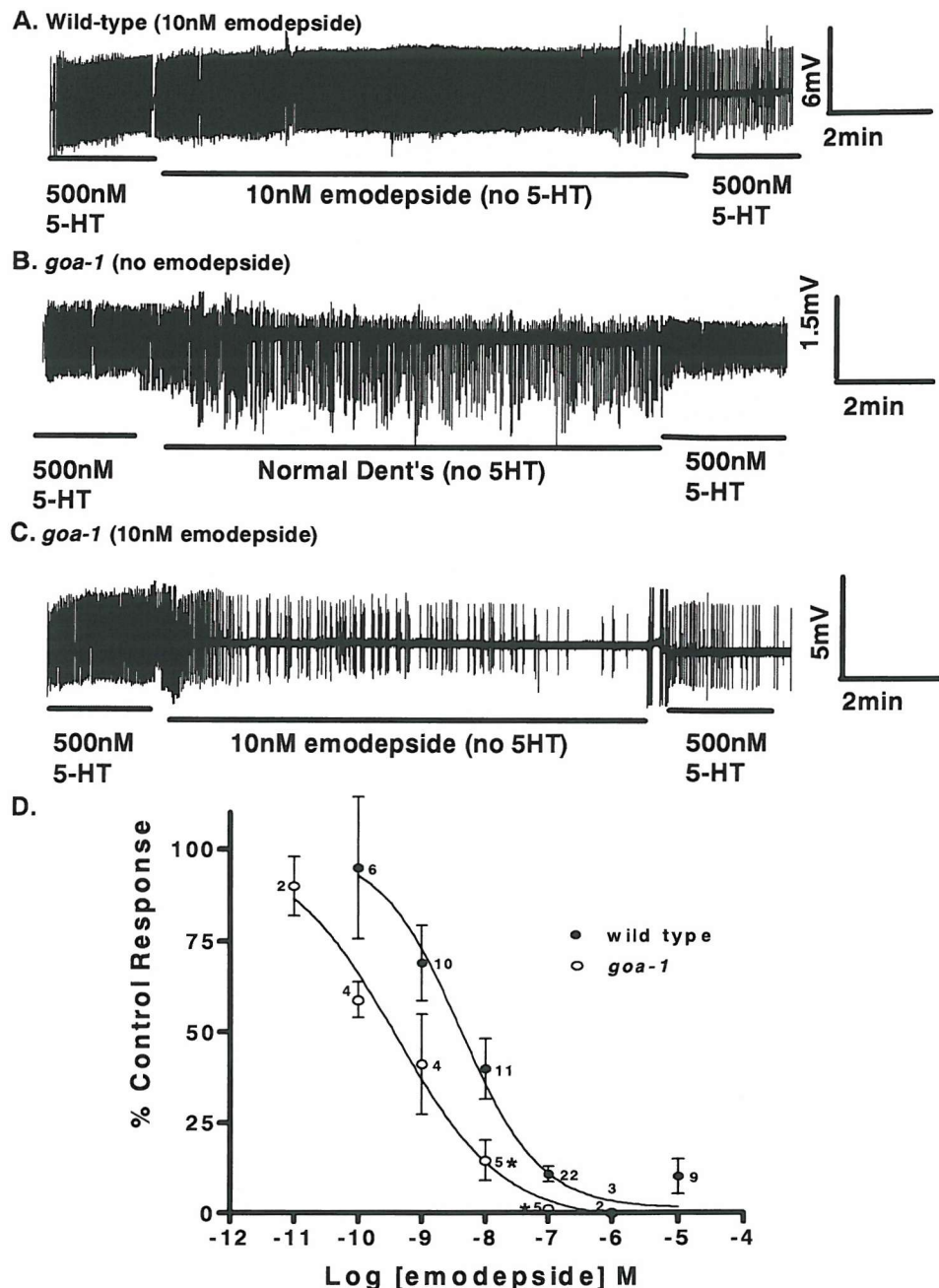


**Fig5.22 Effect of emodepside on *goa-1* *C. elegans* pharyngeal pumping.** Protocol was as described in Fig 5.4. Trace examples for 10nM emodepside are shown here A. The effect of 10nM emodepside on pharyngeal pumping in wild type *C. elegans*. Note the decrease in the number of pumps during the period of emodepside application and a reduced muscle respond to the second application of 5-HT. B. a typical result from an *goa-1* control experiment in which the pharynx continues to pump throughout the entire time-course of the experiment. C. The effect of 10nM emodepside on pharyngeal pumping in *goa-1* *C. elegans*. Note the reduction in pumping during the period of emodepside application and the reduced response of the muscle to the second application of 5-HT D. Concentration response curve for the effect of varying concentrations of emodepside on pharyngeal pumping rates in *goa-1* *C. elegans*. % control response is the rate of pumping in 5-HT following emodepside application compared to the initial pumping rate in 5-HT. Each point is the mean  $\pm$  S.E.M. of (n) determinations \*  $P<0.05$ ,  $n=5$ . The activity of emodepside was confirmed with parallel wild type controls in conjunction with these experiments.

#### **5.19.4 Effect of emodepside on pharyngeal pumping in *egl-8* (phospholipase-C $\beta$ ) *C. elegans*.**

$\text{G}\alpha_q$  has been shown to stimulate phospholipase C $\beta$  activity (Taylor & Exton, 1991; Lee *et al.*, 1992) encoded in *C. elegans* by *egl-8* (Miller *et al.*, 1999; Lackner *et al.*, 1999). To determine if *egl-8* mutations affect the efficacy of emodepside, alleles that most strongly reduce EGL-8 function were assayed. Such alleles are those which disrupt the highly conserved catalytic Y domain, namely *egl-8* (*md1971*) and *egl-8* (*n488*), the former being a more severe mutation (Miller *et al.*, 1999). *egl-8* (*md1971*) mutants were 19 fold less sensitive to emodepside than wild type control ( $\text{IC}_{50} = 79\text{nM}$ , 95% confidence limits, 32 to 192nM compared to  $\text{IC}_{50} = 4.1\text{nM}$ , 95% confidence limits, 1.2 to 14.7nM, Fig 5.23C). Significance was observed for 100nM ( $P < 0.05$ ,  $n = 11$ ) and 10nM emodepside ( $P < 0.001$ ,  $n = 6$ ). *egl-8* (*n488*) mutants were 14 fold less sensitive to emodepside compared to wild type control ( $\text{IC}_{50} = 59\text{nM}$ , 95% confidence limits, 23 to 147nM, compared to,  $\text{IC}_{50} = 4.1\text{nM}$ , 95% confidence limits, 1.5 to 11nM, Fig 5.23F). Significance was observed for 100nM ( $P < 0.001$ ,  $n = 12$ ) and 10nM ( $P < 0.05$ ,  $n = 9$ ) emodepside.

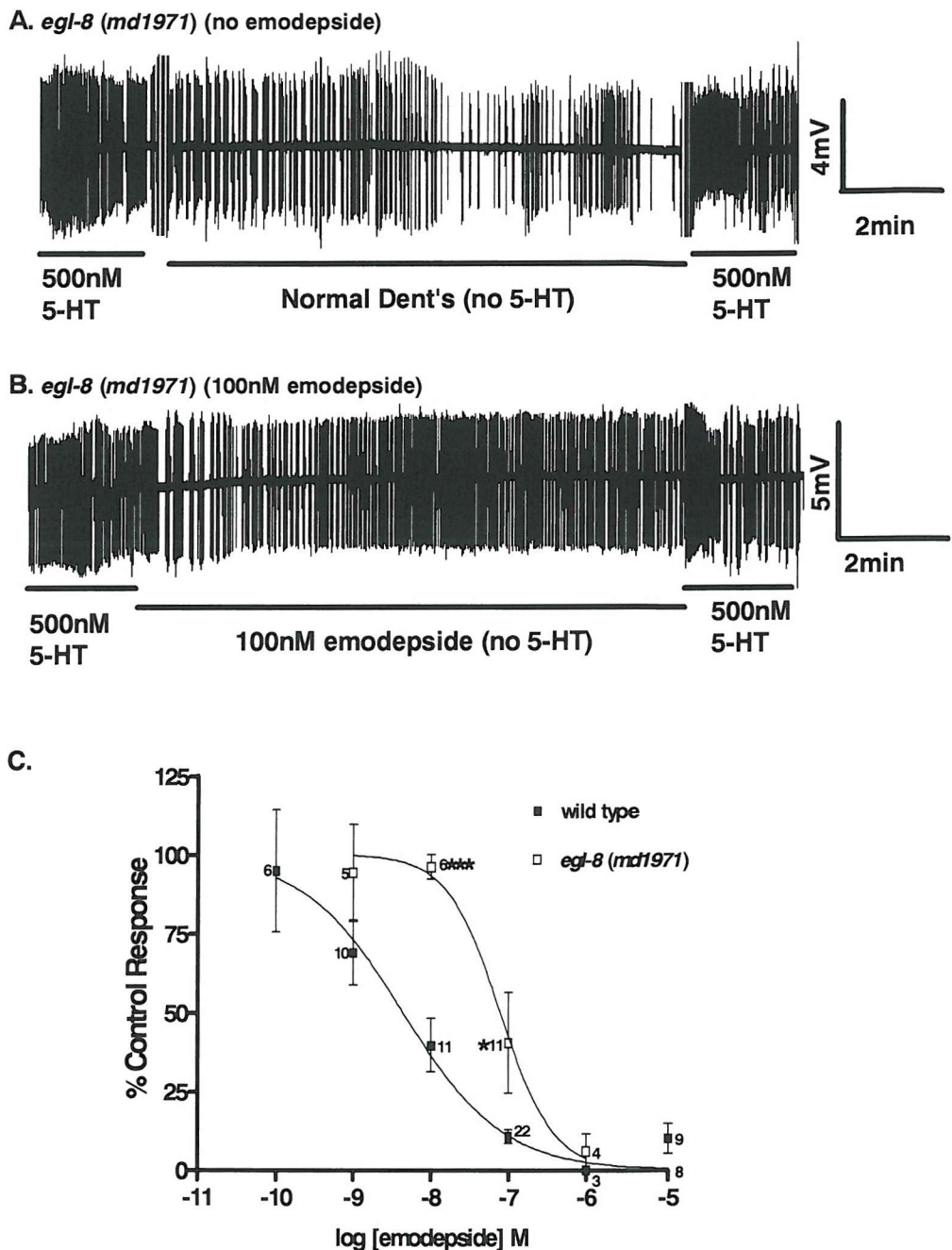
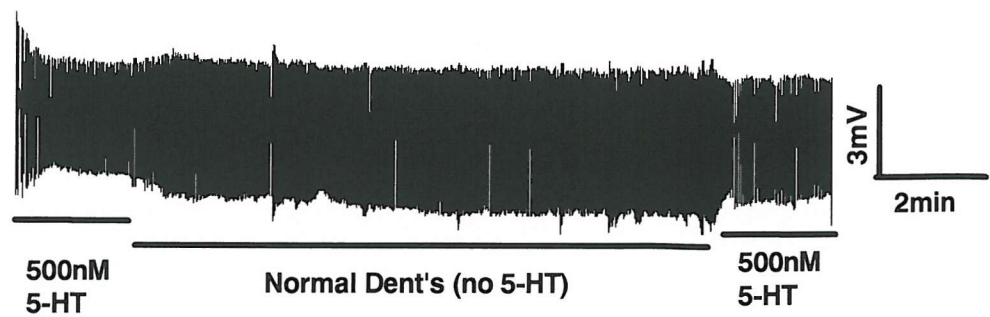
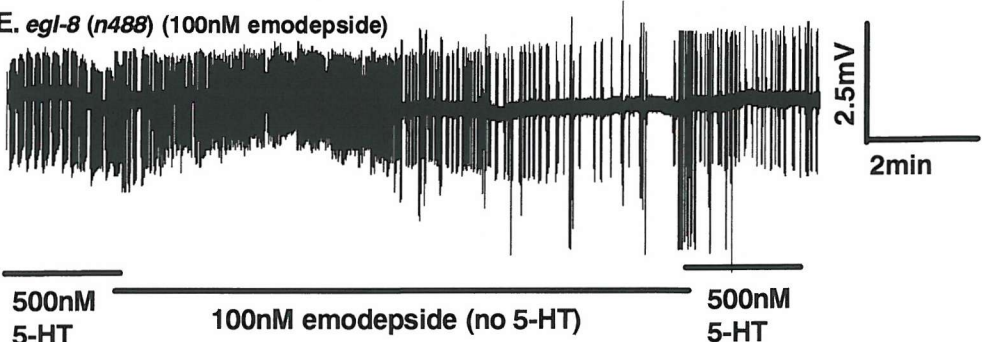


**Fig 5.23 Effect of emodepside on *egl-8 (md1971)* *C. elegans* pharyngeal pumping.** Protocol was as described in Fig 5.4. **A.** A typical result from a control experiment in which the pharynx continues to pump throughout the entire time-course of the experiment. **B.** The effect of 100nM emodepside on pharyngeal pumping in *egl-8 (md1971)**C. elegans*. Note following emodepside addition continued pumping in the presence of 5-HT. This is compared to wild type *C. elegans* (p.113 Fig 5.4) where, following 100nM emodepside application, there is a near complete inhibition of pharyngeal pumping. **C.** Concentration response curve for the effect of varying concentrations of emodepside on pharyngeal pumping rates in *egl-8 (md1971)**C. elegans*. % control response is the rate of pumping in 5-HT following emodepside application compared to the initial pumping rate in 5-HT. Each point is the mean  $\pm$  S.E.Mean of (n) determinations \*P<0.05, n=6 \*\*\* P<0.001, n=11. The activity of emodepside was confirmed with parallel wild type controls in conjunction with these experiments.

D. *egl-8* (n488) (no emodepside)



E. *egl-8* (n488) (100nM emodepside)



F.

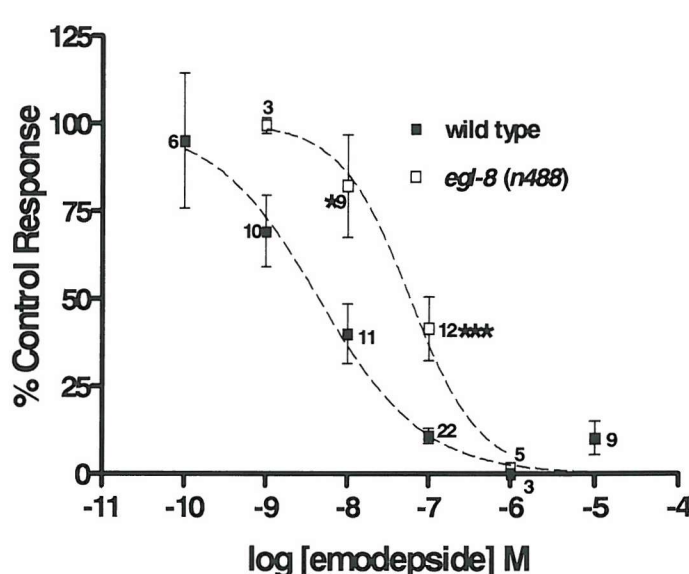


**Fig 5.23(cont) Effect of emodepside on *egl-8* (n488) *C. elegans* pharyngeal pumping.** Protocol was as described in Fig 5.4. **D.** a typical result from a control experiment in which the pharynx continues to pump throughout the entire time-course of the experiment. **E.** The effect of 100nM emodepside on pharyngeal pumping in *egl-8* (n488) *C. elegans*. Note following emodepside addition the continued pumping in the presence of 5-HT. This is compared to wild type *C. elegans* (p.113 Fig 5.4) where, following 100nM emodepside application, there is a near complete inhibition of pharyngeal pumping. **F.** Concentration response curve for the effect of varying concentrations of emodepside on pharyngeal pumping rates in *egl-8* (n488) *C. elegans*. % control response is the rate of pumping in 5-HT following emodepside application compared to the initial pumping rate in 5-HT. Each point is the mean  $\pm$  S.E.Mean of (n) determinations \*  $P<0.05$ ,  $n=9$ . \*\*\*  $P<0.001$ ,  $n=12$ . The activity of emodepside was confirmed with parallel wild type controls in conjunction with these experiments.

## **5.20 Emodepside and neurotransmitter release.**

A number of neurotransmitters and neuromodulators are known to affect nematode body wall and pharyngeal muscle (Walker *et al.*, 2000) To elucidate which neurotransmitters or neuromodulators may be released by emodepside, *C. elegans* mutants to these neurotransmitters / neuromodulators were tested for emodepside resistance. In cases where relevant mutants were not available RNAi techniques were used to knock-down gene expression.

### **5.20.1 Effect of emodepside on pharyngeal pumping in *eat-2* *C. elegans*.**

*eat-2* *C. elegans* mutants are deficient in a non-alpha nicotinic acetylcholine receptor subunit, in the MC neuron. *eat-2* *C. elegans* mutants pump poorly in the presence of 500nM 5-HT, so 1 $\mu$ M 5-HT was used. Application of 100nM emodepside to wild type *C. elegans* caused a reduction in pharyngeal pumping of 89 $\pm$ 7%, (n=5). Application of 100nM emodepside to *eat-2* *C. elegans* mutants caused a similar reduction in pharyngeal pumping of 90 $\pm$ 10%,(n=5)(Fig 5.24).

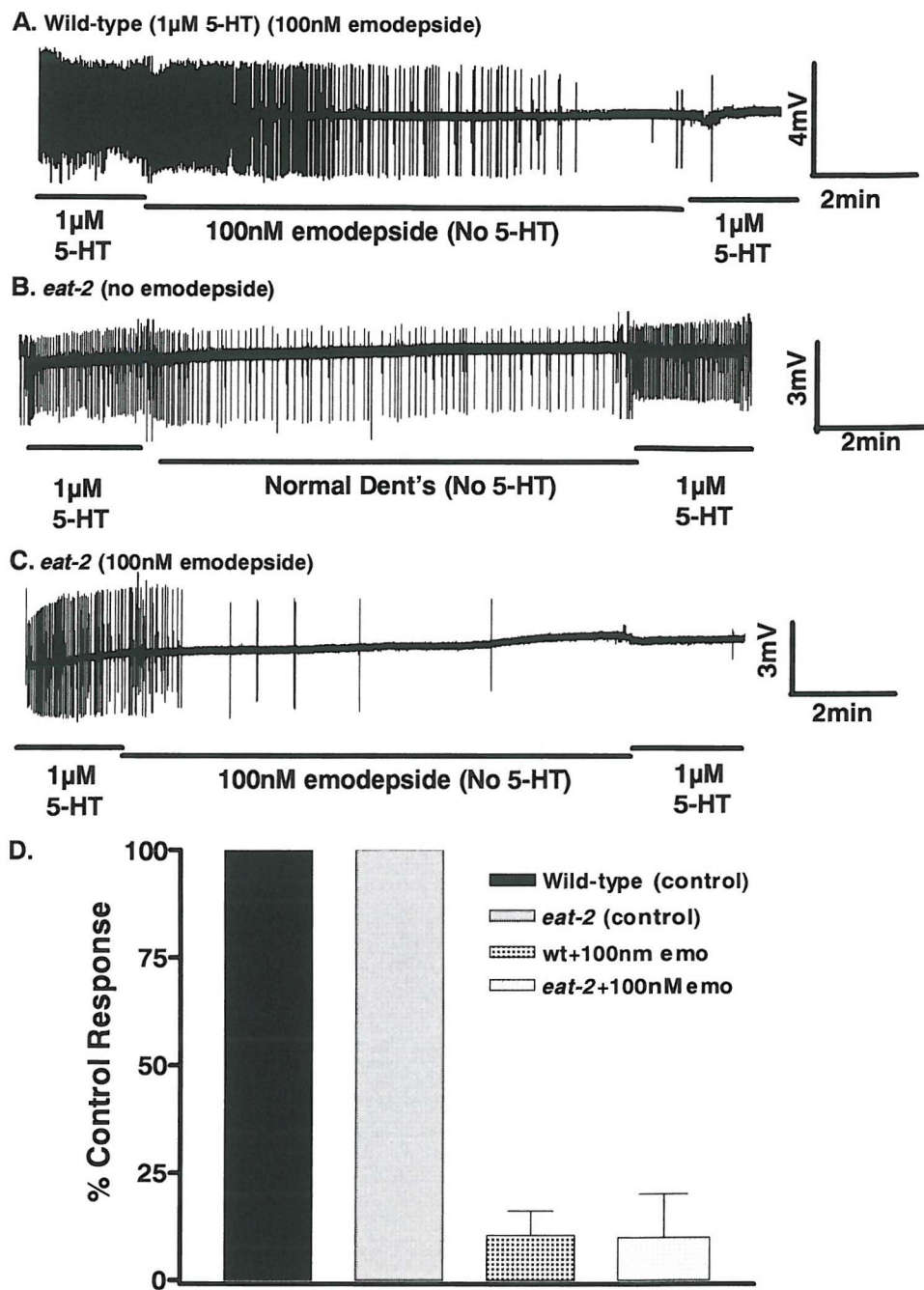


**Fig 5.24 Effect of emodepside on *eat-2* *C. elegans* pharyngeal pumping.** Protocol was as described in Fig 5.4 A. The effect of 100nM emodepside on pharyngeal pumping of wild type *C. elegans* (in 1 $\mu$ M 5-HT). Note the disappearance of the pumps during the period of emodepside application and the failure of the muscle to respond to the second application of 5-HT. B. A typical result from a control experiment in which the pharynx of *eat-2* *C. elegans* continues to pump throughout the entire time-course of the experiment. C. The effect of 100nM emodepside on pharyngeal pumping in *eat-2* *C. elegans*. Note the disappearance of the pumps during the period of emodepside application and the failure of the muscle to respond to the second application of 5-HT. D. Histogram showing the effect of 100nM emodepside on pharyngeal pumping rates in wild type (black bars) and *eat-2* (*C. elegans*). % control response is the rate of pumping in 5-HT following emodepside application compared to the initial pumping rate in 5-HT. Each point is the mean  $\pm$  S.E.M. of 6 (wild type) and 5 (*eat-2*) determinations.

### 5.20.2 Effect of emodepside on pharyngeal pumping in *avr-15* *C. elegans*.

*avr-15* *C. elegans* mutants lack the GluCl- $\alpha$ 2 subunit of the glutamate gated chloride channel important in the action of ivermectin, an anthelmintic that potently inhibits pharyngeal pumping in *C. elegans* (Avery & Horvitz, 1990). The effect of emodepside on these *avr-15* mutants was therefore investigated to see whether emodepside acts through the glutamate-gated chloride channel. Emodepside (100nM) caused an  $85\% \pm 4$ , n=16, inhibition of pharyngeal pumping in *avr-15* *C. elegans*, similar to wild type ( $83\% \pm 4$ , n=10) (Fig 5.25).

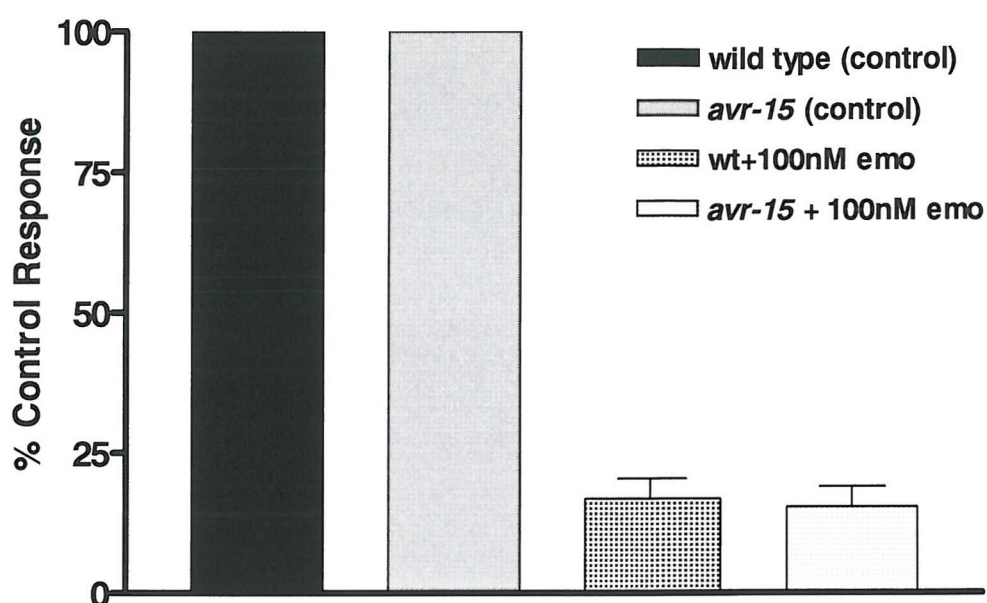


Fig 5.25 The effect of 100nM emodepside on *avr-15* *C. elegans* pharyngeal pumping (counting assay). Emodepside inhibited pharyngeal pumping in *avr-15* *C. elegans* similar to wild type. Protocol as described in Fig 5.2. Histogram showing the effect of 100nM emodepside on pharyngeal pumping rates in wild type (black bars) and *avr-15* (grey bars) *C. elegans*. % control response is the rate of pumping in 5-HT following emodepside application compared to the initial pumping rate in 5-HT. Each point is the mean  $\pm$  S.E.Mean of 16(wild type) and 10(*avr-15*) determinations

### **5.20.3 The effect of emodepside on peptide release in *C. elegans*.**

In chapter 3, it was demonstrated that emodepside mimicked the action of the FMRFamide peptide PF2 when applied to *A. suum* DMS. The effect of emodepside on peptide release was therefore investigated in the *C. elegans* system.

#### **5.20.3.1 Effect of emodepside on pharyngeal pumping of *unc-31* *C. elegans*.**

The calcium activated protein for secretion (CAPS) is essential for neuronal exocytosis of large dense core vesicles in mammals (Berwin *et al.*, 1998) and *C. elegans* (Miller *et al.*, 1996) In *C. elegans* the *unc-31* gene codes for the CAPS protein.

*unc-31* *C. elegans* have a constitutively pumping pharynx so no 5-HT was used. A 5 fold reduction in emodepside sensitivity was observed in *unc-31* ( $IC_{50}=12\text{nM}$ , 95% confidence limits 0.4 to 397nM, Fig 5.26) *C. elegans* compared to wild type ( $IC_{50}=2.2\text{nM}$ , 95% confidence limits 0.4 to 12nM). Significance was observed for 10nM ( $P<0.05$ ,  $n=5$ ) emodepside

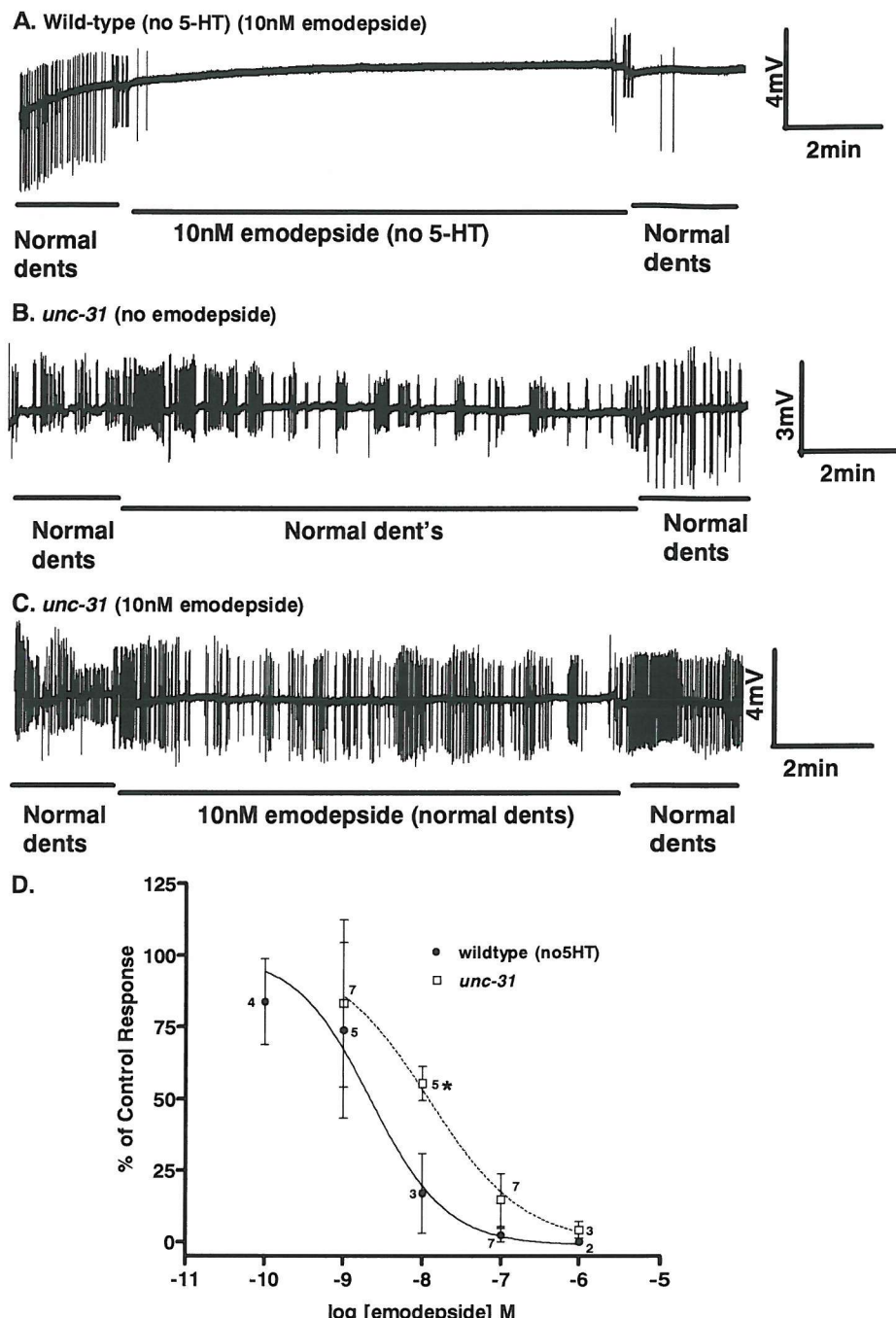
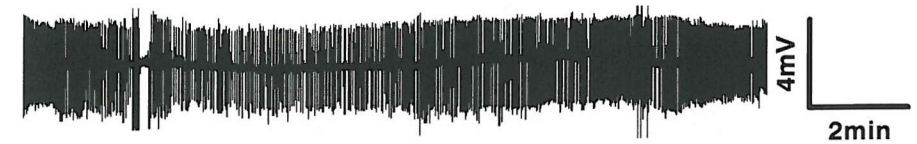


**Fig 5.26 Effect of emodepside on *unc-31* *C. elegans* pharyngeal pumping.** Protocol was as described in Fig 5.4 A. The effect of 10nM emodepside on pharyngeal pumping (no 5-HT) in wild type *C. elegans*. Note the disappearance of the pumps during the period of emodepside application and the failure of the muscle to respond following a subsequent wash in normal Dent's. B. a typical result from an *unc-31* control experiment in which the pharynx continues to pump throughout the entire time-course of the experiment C. The effect of 10nM emodepside on pharyngeal pumping in *unc-31* *C. elegans*. Note following emodepside addition pumping was still observed. D. Concentration response curve for the effect of varying concentrations of emodepside on pharyngeal pumping rates in *unc-31* *C. elegans*. % control response is the pumping rate following emodepside application compared to the initial resting pumping rate. Each point is the mean  $\pm$  S.E.Mean of (n) determinations \*  $P<0.05$ ,  $n=5$ . The activity of emodepside was confirmed with parallel wild type controls in conjunction with these experiments.

### 5.20.3.2 Investigating a role for *flp-13* in emodepside action.

FLP-13 causes inhibition of *C. elegans* pharyngeal pumping (Rogers *et al.*, 2001). FLP-13 is therefore a possible candidate for release following emodepside-induced stimulation. No mutant is available for *flp-13* therefore RNAi (feeding) was performed on the *flp-13* gene. RNAi of *flp-13* (induced) *C. elegans* (*rrf3*) were 5 fold less sensitive to emodepside ( $IC_{50}=18\text{nM}$ , 95% confidence limits, 2.8nM to 114nM, Fig 5.27, compared to uninduced control  $IC_{50}=3.6\text{nM}$ , 95% confidence limits 1.6nM to 8nM, Fig 5.27). Significance was observed for 10nM ( $P<0.05$ ,  $n=7$ ) emodepside addition. The example trace shown in Fig 5.27 is for 10nM emodepside.

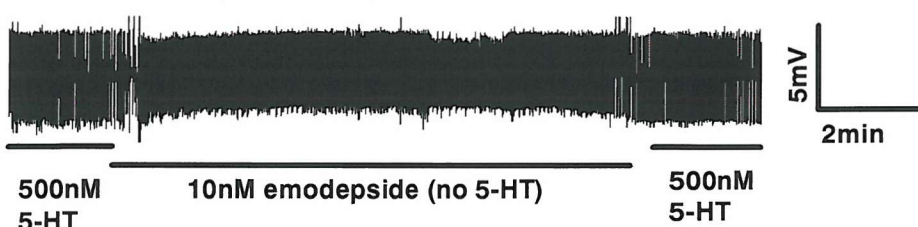
**A. Uninduced *flp-13* (no emodepside)**



**B. Uninduced *flp-13* (10nM emodepside)**



**C. Induced *flp-13* (10nM emodepside)**



**D.**

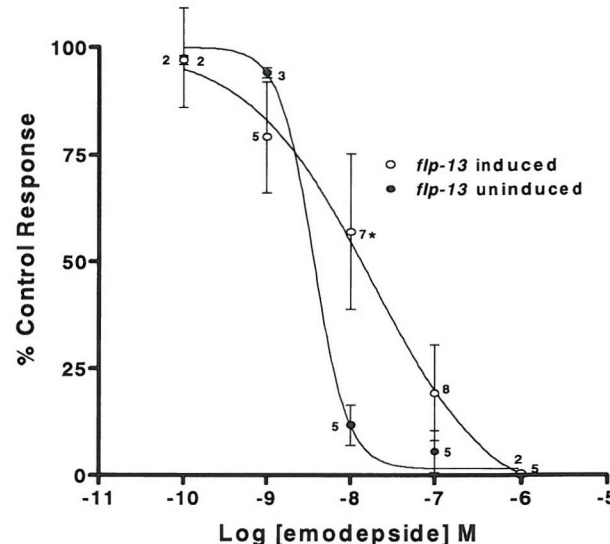


**Fig 5.27 Effect of emodepside on RNAi uninduced (in the absence of IPTG) and induced (+ IPTG) inhibition of *flp-13* in *rrf-3* *C. elegans* pharyngeal pumping.** A. a typical result from an uninduced *flp-13* control experiment in which the pharynx continues to pump throughout the entire time-course of the experiment. B. The effect of 10nM emodepside on pharyngeal pumping in uninduced *flp-13* *rrf-3* *C. elegans*. Note the reduction in pumps during the period of emodepside application and reduced response of the muscle to the second application of 5-HT. C. The effect of 10nM emodepside on pharyngeal pumping in induced *flp-13* *rrf-3* *C. elegans*. Note the pharynx continues to pump throughout the entire time-course of the experiment. **D.** Concentration response curve for the effect of varying concentrations of emodepside on pharyngeal pumping rates in *flp-13* RNAi *C. elegans*. % control response is the pumping rate following emodepside application compared to the initial resting pumping rate. Each point is the mean  $\pm$  S.E.M. of (n) determinations \*  $P < 0.05$ ,  $n=7$ .

### **5.20.3.3 Investigating a role for *flp-1* in emodepside action.**

The *C. elegans* *flp-1* gene codes for 6 peptide sequences, one of which is identical to PF2(Nelson *et al.*, 1998b). *Flp-1*-deletion phenotypes in *C. elegans* included hyperactivity (Nelson *et al.*, 1998b; Waggoner *et al.*, 2000) indicating that *flp-1* peptides may be inhibitory and negatively regulate locomotion. A comparison of the action of three *flp-1* peptides and emodepside, and the effect of emodepside on *C. elegans* exposed to RNAi for the *flp-1* gene were therefore investigated on the *C. elegans* pharynx.

### **5.20.3.4 The effect of a simultaneous application of a SADPNFLRF amide, SDPNFLRFamide and AGSDPNFLRFamide (100nM) to *C. elegans* pharyngeal pumping.**

A simultaneous application of three predicted peptides (100nM) from the *flp-1* gene, (SADPNFLRFamide, SDEPNFLRFamide<sup>2</sup> and AGSDPNFLRFamide) caused a  $50 \pm 2\%$  ( $P < 0.05$ ,  $n=4$ , Fig 5.28) decrease in pharyngeal pumping.

<sup>2</sup> Subsequent analysis of this peptide revealed a SDENFLRFamide sequence

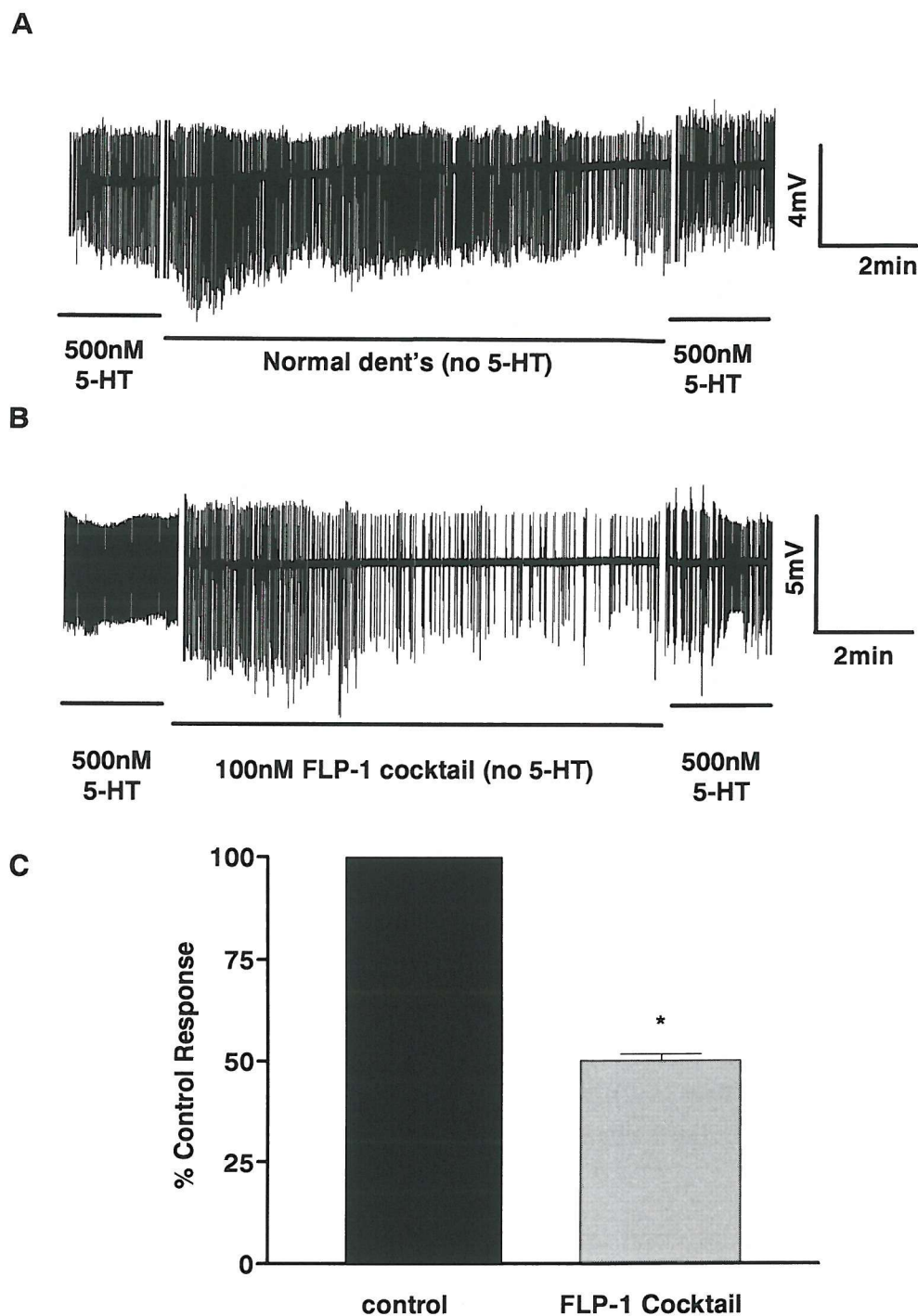
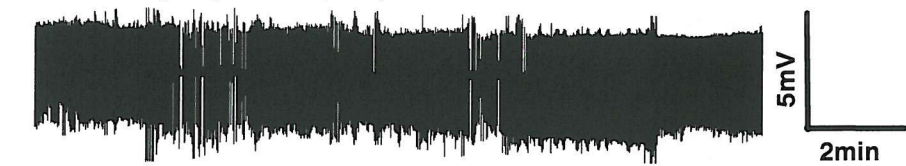


**Fig 5.28 Effect of the application of a cocktail of 3 predicted *flp-1* peptides (SADPNFLRF amide, SDPNFLRFamide and AGSDPNFLRFamide) on wild type *C. elegans* pharyngeal pumping.** Protocol was as described in Fig 5.4 A. a typical result from a control experiment in which the pharynx continues to pump throughout the entire time-course of the experiment. B. The effect of 100nM application of the three *flp-1* peptides on pharyngeal pumping in wild type *C. elegans*. Note the reduction of the pumps during the period of peptide application and a reduced response of the muscle to the second application of 5-HT. C. Histogram showing the effect of 100nM *flp-1* cocktail on pharyngeal pumping rates in wild type *C. elegans*. % control response is the rate of pumping in 5-HT following emodepside application compared to the initial pumping rate in 5-HT. Each point is the mean  $\pm$  S.E.Mean of 4 determinations \*  $P < 0.05$

### **5.20.3.5 Effect of emodepside on pharyngeal pumping in *C. elegans* fed on bacteria expressing dsRNA against the *flp-1* gene.**

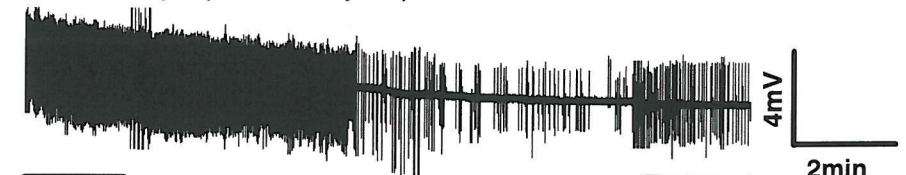
RNAi of *flp-1* (induced) *C. elegans* (*rrf-3*) were 3.5 fold less sensitive to emodepside ( $IC_{50}=26\text{nM}$ , 95% confidence limits, 1pM to 7 $\mu\text{M}$ , Fig 5.29, compared to uninduced control  $IC_{50}=7.6\text{nM}$ , 95% confidence limits 7pM to 71nM, Fig 5.29). Significance was observed for 1nM ( $P<0.05$ ,  $n=4$ ) emodepside addition. RNAi of *flp-1* (induced) *C. elegans* (*rrf-3*) were 9 fold less sensitive to emodepside, compared to non-RNAi *rrf-3* (*rrf-3*  $IC_{50}=2.9\text{nM}$ , 95% confidence limits 1.8 to 4.5nM). The example trace shown in Fig 5.29 is for 10nM emodepside.

**A. Uninduced *flp-1* (no emodepside)**



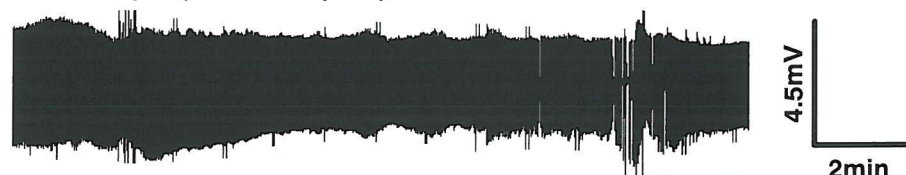
500nM 5-HT      Normal Dent's (no 5-HT)      500nM 5-HT

**B. Uninduced *flp-1* (10nM emodepside)**



500nM 5-HT      10nM emodepside (no 5-HT)      500nM 5-HT

**C. Induced *flp-1* (10nM emodepside)**



500nM 5-HT      10nM emodepside (no 5-HT)      500nM 5-HT

**D.**

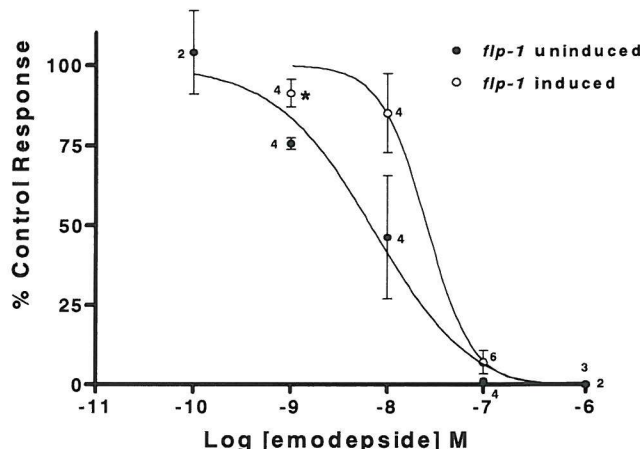


**Fig 5.29 Effect of emodepside on RNAi uninduced (in the absence of IPTG) and induced (+ IPTG) inhibition of *flp-1* in *rrf-3* *C. elegans* pharyngeal pumping. A. a typical result from an uninduced *flp-1* control experiment in which the pharynx continues to pump throughout the entire time-course of the experiment. B. The effect of 10nM emodepside on pharyngeal pumping in uninduced *flp-1 rrf-3* *C. elegans*. Note the inhibition of pumps during the period of emodepside application and reduced response of the muscle to the second application of 5-HT. C. The effect of 10nM emodepside on pharyngeal pumping in induced *flp-1 rrf-3* *C. elegans*. Note the pharynx continues to pump throughout the entire time-course of the experiment. \*P<0.05 D. Concentration response curve for the effect of varying concentrations of emodepside on pharyngeal pumping rates in *flp-1* RNAi *C. elegans*. % control response is the pumping rate following emodepside application compared to the initial resting pumping rate. Each point is the mean  $\pm$  S.E.M of (n) determinations \* P<0.05, n=4.**

## 5.21 Discussion.

Emodepside caused a paralysis of *C. elegans* over a twenty four hour period which is consistent with the findings of the relaxation of *A. suum* muscle (chapter 3), as well as paralysis of a number of different nematodes (Samson-Himmelstjerna *et al.*, 2000; Terada, 1992). Although, emodepside was 1000 fold more potent on *C. elegans* compared to *A. suum* muscle. A 10 minute application of emodepside to exposed *C. elegans* pharynxes also potently inhibited pharyngeal pumping, with an IC<sub>50</sub> of 4nM. Ivermectin, a commercially used anthelmintic, has been shown to potently inhibit pharyngeal pumping in *H. contortus*, with an EC<sub>50</sub> of between 1 and 10pM (Geary *et al.*, 1993) and *C. elegans*, with an EC<sub>50</sub> of between 2.7 and 5 nM (Avery & Horvitz, 1990; Pemberton *et al.*, 2001), similar to emodepside. Ivermectin acts through a glutamate-gated chloride channel (Cully *et al.*, 1994; Vassilatis *et al.*, 1997). *avr-15* mutant *C. elegans*, confer resistance to ivermectin as they continue to pump in the presence of the drug (Dent *et al.*, 1997). If emodepside is acting through a similar mechanism to ivermectin then emodepside should not inhibit pharyngeal pumping in *avr-15* *C. elegans*. However the data shown here indicates that emodepside is not acting through the glutamate-gated chloride channel, as pharyngeal pumping is still inhibited in the *avr-15* *C. elegans*, following emodepside application.

Emodepside must, therefore, be acting through a novel site. Emodepside interacts with a latrophilin-like G-protein coupled receptor in the parasitic nematode *H. contortus*, HC110-R (Saeger *et al.*, 2001). There are two candidate genes encoding latrophilin-like receptors in *C. elegans*, *lat-1* and *lat-2*. To determine whether emodepside requires either of these for its biological effect, RNAi was utilized to reduce the expression of both of these receptors. RNAi for *lat-1* resulted in a number of behavioural abnormalities consistent with a neuronal function (uncoordinated movement and prolonged pump duration) and further, led to a reduction in sensitivity to emodepside. Interestingly, RNAi of *lat-2* resulted in one observable behavioural abnormality, the resting pumping rate without stimulation in these animals was lower, and produced only a slightly reduced sensitivity to emodepside suggesting, that *lat-1* and *lat-2* have differential roles in the animal. Simultaneous RNAi for both *lat-1* and *lat-2* was less marked than for *lat-1* RNAi.

This is consistent with the findings of Kameth *et al* (2000) who previously demonstrated that simultaneous RNAi for two genes greatly reduced the strength of phenotype produced when RNAi is performed for just the single gene.

In other systems, synaptically expressed latrophilin- like (Matsushita *et al.*, 1999) receptors appear important in facilitating vesicular release and neurotransmission. In *Drosophila* the G-protein coupled receptor Methuselah (Mth), related to latrophilin, appears important in pre-synaptic regulation of neurotransmission. Decreasing Mth function results in a 50% decrease in evoked transmitter release (Song *et al.*, 2002). Latrophilin is also one of the receptors implicated in the action of  $\alpha$ LTX (Davletov *et al.*, 1996; Krasnoperov *et al.*, 1996) and appears to be the main receptor required for receptor mediated action of  $\alpha$ LTX (Volynski *et al.*, 2003).  $\alpha$ LTX isolated from the venom of the black widow spider causes massive vesicular release (Henkel & Sankaranarayanan, 1999; Sudhof, 2001). Studies on the parasitic nematode *A. suum* in chapter 3 have shown that the action of emodepside is predominantly pre-synaptic. This raises the question of whether emodepside exerts anthelmintic activity *via* a pre-synaptic mechanism causing vesicle-mediated transmitter release similar to the effect of  $\alpha$ LTX. Evidence for stimulation of vesicle release by emodepside was provided by imaging of synapses using the fluorescent dye FM4-64. Intracellular uptake of FM4-64 results in fluorescence of synaptic boutons. Neuronal uptake of the dye was confirmed by co-localisation with a pan neuronal GFP strain of *C. elegans* (Altun-Gultekin *et al.*, 2001). When the labelled vesicles fuse with the synaptic membrane, FM4-64 fluorescence decreases. This was utilized to see whether emodepside is stimulating vesicle release. A rapid and selective loss of fluorescence was observed following application of emodepside, indicating vesicle exocytosis in the presence of emodepside.

What signalling pathway is latrophilin acting through to stimulate vesicle release?. Latrophilin acts through a  $G\alpha_q$ , PLC $\beta$  mediated pathway (Rahman *et al.*, 1999). Using a *C. elegans* mutant strain *egl-30*, which has defects in the  $\alpha$  subunit of  $G\alpha_q$ , the effects of emodepside on pharyngeal pumping and locomotion in these mutants was examined. A significant reduction in the sensitivity to emodepside in the pharyngeal pumping assay was observed. Further evidence for a  $G\alpha_q$ -mediated pathway in emodepside action came from analyses of gain of function mutants for

$G\alpha_q$  which were hypersensitive to emodepside.

$G\alpha_q$  subunit couples to the signalling molecule PLC- $\beta$  which is a key modulator of pathways that regulate vesicle release in *C. elegans* (Miller *et al.*, 1999; Lackner *et al.*, 1999). Both  $G\alpha_q$  and PLC- $\beta$  are co-expressed in ventral cord motorneurones and many pharyngeal neurones in *C. elegans* (Lackner *et al.*, 1999) from where the FM4-64 imaging was taken. To further track the mechanism of action of emodepside the *C. elegans* mutant strains *egl-8 (md1971)* and *egl-8(n488)* were utilised. These two alleles have disruptions to the catalytic Y domain of the gene which encodes PLC $\beta$  (Lackner *et al.*, 1999). A significantly reduced sensitivity to emodepside in terms of the inhibition of pharyngeal pumping was seen. *egl-8(md1971)*, a strong loss of function allele (Miller *et al.*, 1999) exhibited the greatest resistance to the inhibitory effects of emodepside in the pharyngeal pumping assay.

PLC- $\beta$  hydrolyses PIP2 to generate inositol 1,4,5-trisphosphate (IP<sub>3</sub>) and DAG, a process which is negatively regulated through the action of  $G\alpha_o$  on DAGkinase (Miller *et al.*, 1999; Lackner *et al.*, 1999); Nurrish 1999). *goa-1* mutants with a loss of function of the  $G\alpha_o$  subunit are characterized by hyperactivity resulting from increased synaptic activity (Mendel *et al.*, 1995). Application of emodepside to these mutants resulted in an increased sensitivity to emodepside, providing further evidence that the emodepside mechanism involves  $G\alpha_q$  and PLC $\beta$  stimulation of pre-synaptic vesicular neurotransmitter release. Block of IP3 signalling in mammalian systems leads to a decrease in  $\alpha$ LT $\alpha$  receptor mediated activation of vesicle release (Capogna *et al.*, 2003). However, in *C. elegans*, stimulation of pharyngeal pumping by 5-HT is not affected by an IP3-receptor sponge that decreases IP3 levels in the pharynx (Walker *et al.*, 2002). DAG generation may therefore be the functional molecule following PIP2 hydrolysis in regulating synaptic activity in the pharynx, rather than IP3.

(M)UNC-13 is the major pre-synaptic DAG receptor in hippocampal neurons (Rhee *et al.*, 2002). In response to DAG, UNC-13 is recruited to synaptic membranes, where it increases the size of the readily releasable pool in hippocampal neurons and chromaffin cells (Gillis *et al.*, 1996; Stevens & Sullivan, 1998). Furthermore,

UNC-13-dependent vesicular release through DAG signalling is evident in *C. elegans*, via a pathway involving cholinergic and serotonergic control of motorneurons (Lackner *et al.*, 1999; Miller *et al.*, 1999; Nurrish *et al.*, 1999).

The cloned sequence of *C. elegans* UNC-13 has C1 and C2 binding domains which bind DAG, phorbol esters, calcium and phospholipids. Alternative splicing of *unc-13* (Kohn *et al.*, 2000) results in two variants; L-R which is located at pre-synaptic densities and M-R which is located diffusely along axons. Mutations in the *unc-13* gene cause varying degrees of paralysis and uncoordinated movement, with severity dependent on the mutation point within the *unc-13* gene. In this study two loss of function alleles were looked at; *e1091* which has a mutation in the L region (therefore effecting the L-R isoform) and the more severe *s69* allele which has a mutation in the R-region (which effects both the L-R and M-R isoforms). Both *unc-13* alleles resulted in a pronounced reduction in emodepside efficacy (more than any other mutation). Notably, *s69* was the most emodepside resistant allele. These data, together with the imaging assays for exocytosis, suggest that emodepside exerts its action by facilitating neurotransmitter release.

Activation of UNC-13 leads to facilitation of vesicle release by promoting the open configuration of syntaxin (Richmond *et al.*, 2001). The consequence of this is an increase in the number of vesicles in the releasable pool (Augustin *et al.*, 1999; Ashery *et al.*, 2000). This pool is then ready to engage the SNARE proteins synaptobrevin, syntaxin and SNAP-25 (Sollner *et al.*, 1993). The reduced sensitivity of synaptobrevin mutants to emodepside suggests that emodepside facilitation of vesicle release is upstream of SNARE complex formation. In *C. elegans* facilitation of vesicular release by  $G\alpha_q$ ,  $PLC\beta$  and UNC-13, has been observed, as has a similar signalling pathway regulating DUNC-13 synaptic expression in *Drosophila* (Aravamudan & Broadie, 2003). Interestingly evidence for a receptor mediated presynaptic facilitation of vesicle release, by an as yet unidentified presynaptic receptor, through  $G\alpha_q$  and UNC-13 by the novel protein AEX-1, has also been reported (Doi & Iwasaki, 2002). RIM is involved in regulating priming of synaptic vesicles, it would therefore be expected that the *unc-10* (RIM) deficient *C. elegans* would have a reduced sensitivity to emodepside, however, they responded similar to wild type. A possible explanation for this is that the *unc-10* *C. elegans* do not have a

severe mutation that will inhibit emodepside action. *unc-10* *C. elegans* were demonstrated to have normal levels of docked vesicles and their calcium sensitivity to vesicle release was unchanged (Koushika *et al.*, 2001). *unc-10* also did not show the phenotypic behaviours associated with reduced synaptic transmission (such as prolonged pump duration and slow movement).

If emodepside is stimulating vesicle release, then what transmitters are being released to have such a potent effect on the *C. elegans* pharynx? Bath-applied glutamate inhibits pharyngeal pumping in wild type *C. elegans* (Pemberton *et al.*, 2001). This effect is reduced in *avr-15* *C. elegans*. Application of emodepside to *avr-15* *C. elegans* inhibited pharyngeal pumping similar to wild type. The same effect was also observed in *eat-2* mutants which do not respond to ACh. This suggest that neither ACh nor glutamate are solely involved in emodepside action.

In Chapter 3 it was observed that emodepside mimics the effects of the FMRF-amide peptides PF1 and PF2. In *C. elegans* there are 23 genes that code for at least 63 FMRF-amide like peptides (Li *et al.*, 1999; Nelson *et al.*, 1998a). These peptides have been shown to cause a number of effects on nematode muscle (Walker *et al.*, 2000). Neuropeptides are released from large dense core vesicles (Burgoyne & Morgan, 2003). This release requires the calcium-activated protein for secretion (CAPS) (Berwin *et al.*, 1998). In *C. elegans* this is coded for by the *unc-31* gene. *unc-31* *C. elegans* are deficient in this CAPS protein. Interestingly this causes an abnormally high resting pharyngeal pumping rate, suggesting neuropeptides in the pharynx have a largely inhibitory role. Following application of emodepside to *unc-31* *C. elegans* a reduced sensitivity to emodepside was observed, suggesting a role for inhibitory peptides in emodepside action. Both the *flp-1* and *fip-13* genes have been shown to code for peptides that are inhibitory on the pharynx (Rogers *et al.*, 2001). This was confirmed as a cocktail of 3 products of the *fip-1* gene caused a 50% reduction in *C. elegans* pharyngeal pumping. RNAi was therefore performed on both the *fip-1* and *fip-13* gene to investigate a role for these peptides in emodepside action. A resistance to emodepside was observed for both genes, suggesting a role for these peptides in emodepside action.

Emodepside's novel mechanism of action appears pre-synaptic, involving the

receptor latrophilin. Stimulation of the latrophilin receptor activates  $G_q$ , G-protein. This may then activate PLC $\beta$  causing an increase in levels of DAG. DAG then binds UNC-13 which activates syntaxin (Richmond *et al.*, 2001). This allows binding and activation of the SNARE complexes that bring vesicles and pre-synaptic membranes into close position to drive membrane fusion (Weber *et al.*, 1998). A bias towards release of inhibitory peptides may then occur.

## **CHAPTER 6**

### **Discussion**

Resistance to existing anthelmintics requires the search for novel compounds which target unique sites. The cyclooctadepsipeptides appear a promising new group of anthelmintics. One member of this class of compound PF1022A and its bis-para-morphonyl-derivative, semi-synthetic derivative emodepside has potent broad spectrum anthelmintic activity on numerous nematode species (Samson-Himmelstjerna *et al.*, 2000; Harder & Samson-Himmelstjerna, 2001). Previously, little was known about how these compounds exert their anthelmintic action.

The basis of this study was therefore to investigate and provide insight into the mode of action of the emodepside. Two nematode species were used, the intestinal parasite of the pig *A. suum* and the free-living non-parasitic model genetic organism *C. elegans*. The fast onset of paralysis of PF1022A and emodepside suggested that these compounds are neuropharmacologically active. Two nerve muscle preparations, the body wall muscle system and the pharyngeal muscle system were used to investigate this hypothesis. Initial application of emodepside to both these preparations demonstrated an inhibitory action on muscle activity. In *C. elegans* movement (body bends) and pharyngeal pumping was potently inhibited. In order to control for the possibility that this action of emodepside simply derives from pore-forming capability PF1022-001, a structural isomer of emodepside with no anthelmintic activity (Geßner *et al.*, 1996) was tested on the pharynx. This had no inhibitory action at concentrations up to 10 $\mu$ M. On *A. suum* muscle emodepside caused a relaxation of basal muscle tension and a relaxation of body wall muscle pre-contracted with both ACh and the neuropeptide AF1. Emodepside exerts its anthelmintic activity by relaxing muscle resulting in paralysis and an inhibition of nematode feeding.

Many existing anthelmintics exert their action by paralysis of muscle, such as mimicking the excitatory transmitter ACh (Harrow & Gration, 1985), or the inhibitory transmitter GABA (Martin, 1982). The question therefore arose could emodepside be acting at similar target sites? Emodepside inhibited the ACh induced contraction of *A. suum* dorsal muscle suggesting emodepside could act by directly blocking the action of ACh. However,

previous work by (Martin *et al.*, 1996) demonstrated that PF1022A did not antagonise the action of the nicotinic agonist levamisole. Also, in this study the magnitude of the depolarisation and change in input conductance elicited by ACh was not effected by emodepside. Emodepside also inhibited pharyngeal pumping of *eat-2* *C. elegans* (deficient in a  $\beta$ -subunit of the nAChR receptor) similar to wild type. Taken together, emodepside appears not to block the ACh-receptor or sodium channel directly, thus inhibition of ACh induced contraction appears to be as an indirect result of the paralysis effect emodepside has on nematode muscle i.e. physiological antagonism.

The role for GABA in emodepside action has been previously described (section 1.11.2). However evidence from this study suggests emodepside mechanism of action differs from that of GABA. Emodepside caused only a slight, irreversible, long lasting hyperpolarisation of *A. suum* muscle with no change in input conductance. The relaxation of *A. suum* muscle by GABA is also faster than that of emodepside, and in the presence of zero chloride ions, GABA causes a contraction of *A. suum* muscle whereas emodepside causes a relaxation (Willson *et al.*, 2003), indicating that GABA is not involved in emodepside action. Future experiments on *ext-1* (which encodes for the excitatory GABA-gated cation channel, (Beg *et al* 2003)) and *unc-49* mutants, (which codes for the main inhibitory GABA receptor at the neuromuscular junction (Richmond *et al* 1999)) will be required to completely eliminate a GABA component in emodepside action.

The anthelmintic ivermectin inhibits pharyngeal pumping and locomotion of *C. elegans* at concentrations that are similar to emodepside (Avery & Horvitz, 1990; Pemberton *et al.*, 2001). The mechanism for this requires a class of receptor the glutamate-gated chloride channel, unique to the invertebrate phyla (Dent *et al.*, 1997; Pemberton *et al.*, 2001). The question whether emodepside is acting at the same site as ivermectin was therefore addressed. This study demonstrated that *avr-15* *C. elegans* which have a mutation in the  $\alpha 2$  subunit of the Glu-Cl-R and are resistant to ivermectin, show no resistance to emodepside. PF1022A has also been demonstrated to

have resistance breaking properties against ivermectin resistant *H. contortus* in sheep (Samson-Himmelstjerna *et al.*, 2000; Harder *et al.*, 2003; Sangster & Gill, 1999). Taken together this suggests ivermectin and emodepside mechanism of action differ.

Many neuropeptides have been isolated from nematode species which have been shown to have potent effects on nematode muscle (Walker *et al.*, 2000). They both inhibit and excite pharyngeal and body wall muscle. Of interest in the context of this study are the neuropeptides PF1 and PF2. Emodepside appears to have similar effects on *A. suum* and *C. elegans* as these two peptides. The *C. elegans* *flp-1* gene encodes for six neuropeptides two of which are identical to PF1 and PF2. FLP-1 neuropeptides inhibit pharyngeal pumping in *C. elegans* (Rogers *et al.*, 2001) and shown in this study by the inhibition caused by the addition of a cocktail of three of the *flp-1* predicted peptides to the *C. elegans* pharynx. Mutations in the *flp-1* gene in *C. elegans* also results in hyperactivity suggesting these peptides play an inhibitory role in *C. elegans* (Nelson *et al.*, 1998; Waggoner *et al.*, 2000). On *A. suum* muscle PF2 inhibits ACh induced contraction, and causes a slight long lasting hyperpolarisation of *A. suum* muscle similar to emodepside. PF2 action on *A. suum* muscle was demonstrated to be potassium dependent (Franks, 1996) which is interesting as emodepside action is also dependent on potassium ions. PF2 was also shown to relax *A. suum* muscle pre-contracted with ACh at a rate similar to emodepside. Taken together, emodepside therefore appears to mimic the action of PF1/PF2 like peptides. A major difference, however, between the actions of emodepside and PF2 was observed on the *A. suum* denervated muscle preparation. PF2 caused inhibition of ACh-induced contraction, whereas emodepside failed to inhibit ACh-induced contraction of the denervated muscle strip. This suggests that emodepside is acting pre-synaptically and therefore not acting directly on a post-synaptic PF2-like receptor. A direct effect of emodepside on the muscle cannot completely be ruled out as a slight relaxation of the muscle was observed in the denervated preparation. Emodepside's main target site appears pre-synaptic and may stimulate release of PF2-like inhibitory peptides. Selective vesicle release of neuropeptides is a surprising mechanism of action for anthelmintics.

The lack of molecular and genetic experimental techniques for *A. suum* limited the extent to which this intriguing mechanism could be studied further in this organism. *C. elegans* however are more suited for these types of experiments. To understand emodepsides' pre-synaptic mechanism further it was important to identify the receptor through which emodepside acts. In the course of this study a potential receptor was identified from the parasitic nematode *H. contortus*. The receptor HC110R was shown to have similar homology to a mammalian like latrophilin receptor. Latrophilin is a seven transmembrane G-protein coupled receptor described in section 1.15.2 HC110R closest mammalian homologue Latrophilin-1 (Saeger *et al.*, 2001) is expressed predominantly pre-synaptically in mammalian brain (Krasnoperov *et al.*, 1997). Low levels however are expressed post-synaptically through-out tissue (Sugita *et al.*, 1998), perhaps explaining a slight post-synaptic emodepside effect on the denervated muscle strip. In *C. elegans* two latrophilin-like receptors exist. Antibodies raised to HC110R has demonstrated a strong expression of *lat-1* in the pharynx of *C. elegans* (Harder *et al.*, 2003) although whether this receptor is expressed both pre and post-synaptically is still unclear. RNAi for one of these genes, *lat-1* resulted in phenotypes typical of a defect in neuronal function, longer pump duration and uncoordinated movement. A significant resistance to emodepside was also observed following RNAi for *lat-1*, and only a slight but not significant resistance was observed following RNAi for *lat-2*. Emodepside action therefore preferentially acts through the *lat-1* receptor in *C. elegans* to inhibit pharyngeal pumping.

Latrophilin was initially identified as a receptor for the black widow spider venom  $\alpha$ LTX.  $\alpha$ LTX action may therefore provide insight into emodepsides mechanism of action.  $\alpha$ LTX causes a massive synaptic vesicle release. The proteins involved in synaptic vesicle release docking, priming and fusion of synaptic vesicles are highly conserved. In *C. elegans*, mutations in these proteins result in phenotypes associated with defects in neurotransmission. Two *C. elegans* mutants with defects in synaptobrevin (which binds syntaxin and SNAP-25 to form the SNARE complex (Weber *et al.*, 1998) which is essential for vesicle release and UNC-13 (which promotes the open form of syntaxin allowing binding to synaptobrevin and SNAP-25

(Richmond *et al.*, 2001) were therefore used to confirm a pre-synaptic requirement for emodepside action. A strong resistance to emodepside was observed in these mutants. The requirement for calcium ions in emodepside induced hyperpolarisation of *A. suum* muscle may also suggests a synaptic component to emodepside action. Stimulation of vesicle release by emodepside was further confirmed using the endocytotic marker FM4-64 which labels active synapses. Emodepside application resulted in a loss of fluorescence of this endocytotic marker from *C. elegans* nerve terminals indicative of increased vesicle release. Taken together these data confirm that the synaptic machinery is essential for emodepside induced stimulation of vesicle release.

If emodepside is acting through the latrophilin receptor then understanding what signalling pathway that is being activated to achieve this not only provides information on the control of synaptic vesicle release, but will also provide insights into novel target sites for anthelmintic compounds. Results from this study suggest that emodepside requires the G-protein  $G\alpha_q$ . Both *C. elegans* mutants with a loss of function of  $G\alpha_q$  were resistant to emodepside whereas a gain of function strain were hypersensitive to emodepside. This confirms the observation that latrophilin binds  $G\alpha_q$  (Rahman *et al.*, 1999).  $G\alpha_q$  subunit couples to PLC- $\beta$  which is a key modulator of pathways that regulate vesicle release in *C. elegans* (Miller *et al.*, 1999; Lackner *et al.*, 1999). PLC $\beta$  is also required in emodepside action as PLC $\beta$  mutants are resistant to emodepside. PLC $\beta$  hydrolyses PIP2 to DAG. In *C. elegans*,  $G_o\alpha$  negatively regulates the levels of DAG by activating DAGkinase, thus *goa-1* mutants are predicted to have increased levels of DAG. Interestingly *goa-1* were shown to be hypersensitive to emodepside suggesting that the second messenger DAG is important in mediating the action of emodepside.

UNC-13 is the major DAG receptor in hippocampal neurones (Rhee *et al.*, 2002), and appears essential in emodepside action. DAG recruits UNC-13 to the pre-synaptic membrane increasing the number of vesicles primed at the pre-synaptic membrane (Gillis *et al.*, 1996; Stevens & Sullivan, 1998). In *C.*

*elegans* UNC-13 dependent vesicular release through DAG signalling is evident via a pathway involving cholinergic and serotonergic control of motorneurones (Lackner *et al.*, 1999; Miller *et al.*, 1999; Nurrish *et al.*, 1999), and is involved in the action of the retrograde signal AEX-1 (Doi & Iwasaki, 2002). In *Drosophila* a similar signalling pathway regulating DUNC-13 synaptic expression has been observed (Aravamudan & Broadie, 2003). This signalling pathway therefore appears important in regulating synaptic transmission in nematodes.

$\alpha$ LTX stimulates release of a number of vesicles containing different neurotransmitters and neuromodulators. The question that was addressed was whether emodepside is stimulating release of a number of different neurotransmitters or more specific certain neurotransmitters. From this study ACh and GABA do not appear to be required for emodepside action. Glutamate release is not solely being stimulated as *avr-15* are not resistant to emodepside. On *A. suum* muscle emodepside appears to mimic the action of the neuropeptide PF2. RNAi of the *flp-1* gene (which codes for an identical PF2 peptide in *C. elegans*) caused a resistance to emodepside. *C. elegans* with a mutation in CAPS, a protein required for dense core vesicle release (in which neuropeptides are packaged) were demonstrated to be resistance to emodepside. RNAi for the *flp-13* which codes for neuropeptides that have an inhibitory action on the pharynx (Rogers *et al.*, 2001) were also resistant to emodepside. This data perhaps indicates neuropeptides are preferentially released by emodepside. This specificity of emodepside to selectively release inhibitory peptides is a surprising mechanism for anthelmintics. The FM4-64 imaging data however suggests that emodepside appears to be stimulating release from a number of different neurones in the pharynx. Therefore whether emodepside solely stimulates release of peptides, or a number of different transmitters but which is biased towards peptide release, cannot be resolved yet and requires further investigation. Determining the expression pattern of latrophilin in the different types of *C. elegans* neurones will provide insight into the possible potential neurotransmitters which emodepside could be releasing.

An interesting finding in this study was the difference in potency of emodepside action on *A. suum* and *C. elegans*. Emodepside was a 1000 times more potent on the *C. elegans* pharynx than it was on *A. suum* dorsal muscle. The type of muscle cells investigated in each organism (pharyngeal and body wall) have different properties. This may therefore explain the different sensitivity in both organisms to emodepside. Future experiments on the effect of emodepside on *A. suum* pharyngeal muscle would provide a greater insight into the potency of this compound on this parasitic species. Isolation and sequencing of a latrophilin-like receptor, expression levels and patterns in *A. suum* may also provide insights into explaining the differences in potency of emodepside on *A. suum* and *C. elegans* muscle.

In conclusion the data presented here suggests the novel anthelmintic emodepside causes paralysis of nematode muscle through activation of a latrophilin-like receptor. Presumably selective toxicity of emodepside is achieved by its activation of latrophilin receptors that are specific to parasitic nematodes in preference to the mammalian host. PF1022A was demonstrated not to cross the blood brain barrier, and in mammalian system latrophilin-1 is primarily expressed in the brain, further adding to emodepside's selective toxicity. Latrophilin activation through  $G\alpha_q$ ,  $PLC\beta$  and crucially  $UNC-13$ , results in a preferential release of vesicles containing inhibitory peptides. (Fig 6.1).

If emodepside acts to stimulate release of inhibitory neuropeptides then future work such as a chemical mutagenesis screen, could be employed to identify emodepside resistant mutants, and thus provide insights into novel components within the signalling pathway described in figure 6.1. This generic signalling pathway has been described in many experimental organisms to modulate vesicle release of a number of different neurotransmitters (Lackner *et al.*, 1999; Miller *et al.*, 1999; Nurrish *et al.*, 1999 ; Aravamudan & Broadie, 2003). Of interest for future studies would be to discover where in this common pathway is the breakpoint that distinguishes between the release of inhibitory peptides compared with other neurotransmitters. Also, a mutagenesis screen would identify the molecular components that underlie this selective release. Initial insights into

components controlling peptide specific release have been identified in this study. The fact that *unc-10* (RIM) mutants are not resistant to emodepside is intriguing, as RIM has previously been demonstrated to be a component involved in vesicle exocytosis in *C. elegans*. (Koushika *et al.*, 2001). Other related RIM isoforms or related proteins such as NIM may therefore be important in the control of the release of inhibitory neuropeptides. The different isoforms of UNC-13 (MR and LR) may also play a role in this preferential release of inhibitory peptides. In this study the *C. elegans* mutant that effects both LR and MR *unc-13* isoforms (*s69*) exhibited the highest resistance to emodepside. In mammalian systems RIM1 $\alpha$  does not bind to MUNC-13-2 (Schoch *et al* 2002), which is homologues to the MR form of *unc-13* (Brose *et al* 2000) therefore recruitment of this MR form could provide selectivity for inhibitory peptide release. Future work could also determine whether emodepside stimulated release of inhibitory peptides engages the IP<sub>3</sub> signalling cascade.

In summary, emodepside's mechanism of action not only opens up insights into the receptor mediated modulation of transmission via nerve terminal signalling cascades, it also provides a novel target for the treatment of parasitic diseases. The ability of emodepside to stimulate vesicle release is unique among existing anthelmintics.

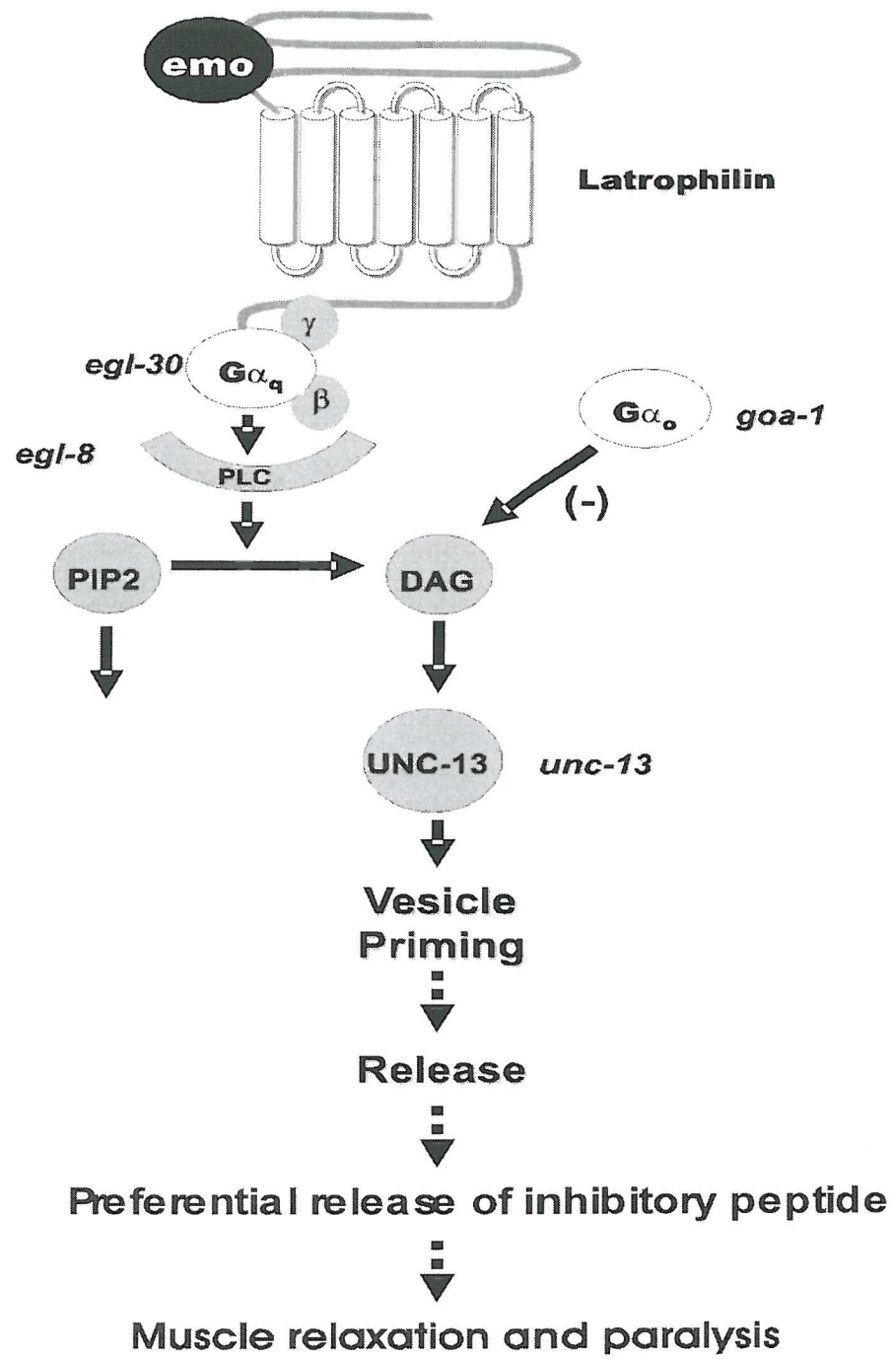


Fig 6.1. Proposed mechanism of action for the novel anthelmintic emodepside (see text for details).

## **CHAPTER 7**

### **References**

Albertson, D. G. & Thomson, J. N. (1976). The pharynx of *Caenorhabditis elegans*. *Philos.Trans.R.Soc.Lond B Biol.Sci.* **275**, 299-325.

Alfonso, A., Grundahl, K., McManus, J. R., & Rand, J. B. (1994). Cloning and characterization of the choline acetyltransferase structural gene (cha-1) from *C. elegans*. *J Neurosci.* **14**, 2290-2300.

Altun-Gultekin, Z., Andachi, Y., Tsalik, E. L., Pilgrim, D., Kohara, Y., & Hobert, O. (2001). A regulatory cascade of three homeobox genes, ceh-10, ttx-3 and ceh-23, controls cell fate specification of a defined interneuron class in *C. elegans*. *Development* **128**, 1951-1969.

Aravamudan, B. & Broadie, K. (2003). Synaptic *Drosophila* UNC-13 is regulated by antagonistic G-protein pathways via a proteasome-dependent degradation mechanism. *J Neurobiol.* **54**, 417-438.

Aravamudan, B., Fergestad, T., Davis, W. S., Rodesch, C. K., & Broadie, K. (1999). *Drosophila* UNC-13 is essential for synaptic transmission. *Nat.Neurosci.* **2**, 965-971.

Aronin, N. & DiFiglia, M. (1992). The subcellular localization of the G-protein Gi alpha in the basal ganglia reveals its potential role in both signal transduction and vesicle trafficking. *J Neurosci.* **12**, 3435-3444.

Ashery, U., Varoqueaux, F., Voets, T., Betz, A., Thakur, P., Koch, H., Neher, E., Brose, N., & Rettig, J. (2000). Munc13-1 acts as a priming factor for large dense-core vesicles in bovine chromaffin cells. *EMBO J* **19**, 3586-3596.

Ashton, A. C., Volynski, K. E., Lelianova, V. G., Orlova, E. V., Van Renterghem, C., Canepari, M., Seagar, M., & Ushkaryov, Y. A. (2001). alpha-Latrotoxin, acting via two Ca<sup>2+</sup>-dependent pathways, triggers exocytosis of two pools of synaptic vesicles. *J Biol.Chem.* **276**, 44695-44703.

Augustin, I., Rosenmund, C., Sudhof, T. C., & Brose, N. (1999). Munc13-1 is essential for fusion competence of glutamatergic synaptic vesicles. *Nature* **400**, 457-461.

Avery, L. (1993). Motor neuron M3 controls pharyngeal muscle relaxation timing in *Caenorhabditis elegans*. *J Exp.Biol.* **175**, 283-297.

Avery, L. & Horvitz, H. R. (1987). A cell that dies during wild-type *C. elegans* development can function as a neuron in a ced-3 mutant. *Cell* **51**, 1071-1078.

Avery, L. & Horvitz, H. R. (1989). Pharyngeal pumping continues after laser killing of the pharyngeal nervous system of *C. elegans*. *Neuron* **3**, 473-485.

Avery, L. & Horvitz, H. R. (1990). Effects of starvation and neuroactive drugs on feeding in *Caenorhabditis elegans*. *J Exp.Zool.* **253**, 263-270.

Avery, L., Raizen, D., & Lockery, S. (1995). Electrophysiological methods. *Methods Cell Biol.* **48**, 251-269.

Baldwin, E. & Moyle, V. (1949). A contribution to the physiology and pharmacology of *Ascaris lumbricoides* from the pig. *Br.J Pharmacol.* **4**, 145-152.

Ballivet, M., Alliod, C., Bertrand, S., & Bertrand, D. (1996). Nicotinic acetylcholine receptors in the nematode *Caenorhabditis elegans*. *J Mol.Biol.* **258**, 261-269.

Barnett, D. W., Liu, J., & Misler, S. (1996). Single-cell measurements of quantal secretion induced by alpha-latrotoxin from rat adrenal chromaffin cells: dependence on extracellular Ca<sup>2+</sup>. *Pflugers Arch.* **432**, 1039-1046.

Baylis, H. A., Matsuda, K., Squire, M. D., Fleming, J. T., Harvey, R. J., Darlison, M. G., Barnard, E. A., & Sattelle, D. B. (1997). ACR-3, a *Caenorhabditis elegans* nicotinic acetylcholine receptor subunit. Molecular cloning and functional expression. *Receptor Channels* **5**, 149-158.

Beg, A.A, Jorgensen,E.M, (2003) EXP-1 is an excitatory GABA-gated cation channel. *Nat Neurosci*, **6**, 1145-1152.

Berwin, B., Floor, E., & Martin, T. F. (1998). CAPS (mammalian UNC-31) protein localizes to membranes involved in dense-core vesicle exocytosis. *Neuron* **21**, 137-145.

Betz, A., Telemanakis, I., Hofmann, K., & Brose, N. (1996). Mammalian Unc-13 homologues as possible regulators of neurotransmitter release. *Biochem.Soc.Trans.* **24**, 661-666.

Betz, W. J., Mao, F., & Bewick, G. S. (1992). Activity-dependent fluorescent staining and destaining of living vertebrate motor nerve terminals. *J Neurosci.* **12**, 363-375.

Blumenthal, T. & Thomas, J. (1988). Cis and trans mRNA splicing in *C. elegans*. *Trends Genet.* **4**, 305-308.

Brading, A. F. & Caldwell, P. C. (1971). The resting membrane potential of the somatic muscle cells of *Ascaris lumbricoides*. *J Physiol* **217**, 605-624.

Brenner, S. (1974). The genetics of *Caenorhabditis elegans*. *Genetics* **77**, 71-94.

Brose, N., Hofmann, K., Hata, Y., & Sudhof, T. C. (1995). Mammalian homologues of *Caenorhabditis elegans unc-13* gene define novel family of C2-domain proteins. *J Biol. Chem.* **270**, 25273-25280.

Brose, N., Rosenmund, C., Rettig, J. (2000). Regulation of transmitter release by *unc-13* and its homologus. *Curr. Opin. Neuro. Biol* **10** 303-311.

Brownlee, D., Holden-Dye, L., & Walker, R. (2000). The range and biological activity of FMRFamide-related peptides and classical neurotransmitters in nematodes. *Adv. Parasitol.* **45**, 109-180.

Brownlee, D. J., Fairweather, I., Johnston, C. F., Smart, D., Shaw, C., & Halton, D. W. (1993). Immunocytochemical demonstration of neuropeptides in the central nervous system of the roundworm, *Ascaris suum* (Nematoda: Ascaridia). *Parasitology* **106**, 305-316.

Brownlee, D. J., Holden-Dye, L., & Walker, R. J. (1997). Actions of the anthelmintic ivermectin on the pharyngeal muscle of the parasitic nematode, *Ascaris suum*. *Parasitology* **115**, 553-561.

Burgoyne, R. D. & Morgan, A. (2003). Secretory granule exocytosis. *Physiol Rev.* **83**, 581-632.

Burns, D. J. & Bell, R. M. (1991). Protein kinase C contains two phorbol ester binding domains. *J Biol. Chem.* **266**, 18330-18338.

Butz, S., Okamoto, M., & Sudhof, T. C. (1998). A tripartite protein complex with the potential to couple synaptic vesicle exocytosis to cell adhesion in brain. *Cell* **94**, 773-782.

Capogna, M., Gahwiler, B. H., & Thompson, S. M. (1996). Calcium-independent actions of alpha-latrotoxin on spontaneous and evoked synaptic transmission in the hippocampus. *J Neurophysiol.* **76**, 3149-3158.

Capogna, M., Volynski, K. E., Emptage, N. J., & Ushkaryov, Y. A. (2003). The alpha-latrotoxin mutant LTXN4C enhances spontaneous and evoked transmitter release in CA3 pyramidal neurons. *J Neurosci.* **23**, 4044-4053.

Cappe de Baillon, P. (1911). Etude sur les fibres musculaires d'*Ascaris*. I. Fibres pariétales. *Cellule* **27**, 165-211.

Changeux, J. P. & Edelstein, S. J. (1998). Allosteric receptors after 30 years. *Neuron* **21**, 959-980.

Chen, W., Terada, M., & Cheng, J. T. (1996). Characterization of subtypes of gamma-aminobutyric acid receptors in an *Ascaris* muscle preparation by binding assay and binding of PF1022A, a new anthelmintic, on the receptors. *Parasitol.Res.* **82**, 97-101.

Cochilla, A. J., Angleson, J. K., & Betz, W. J. (1999). Monitoring secretory membrane with FM1-43 fluorescence. *Annu.Rev.Neurosci.* **22**, 1-10.

Colquhoun, L., Holden-Dye, L., & Walker, R. J. (1991). The pharmacology of cholinoreceptors on the somatic muscle cells of the parasitic nematode *Ascaris suum*. *J.Exp.Biol.* **158**, 509-530.

Conder, G. A., Johnson, S. S., Nowakowski, D. S., Blake, T. E., Dutton, F. E., Nelson, S. J., Thomas, E. M., Davis, J. P., & Thompson, D. P. (1995). Anthelmintic profile of the cyclodepsipeptide PF1022A in in vitro and in vivo models. *J.Antibiot.(Tokyo)* **48**, 820-823.

Cully, D. F., Vassilatis, D. K., Liu, K. K., Paress, P. S., Van der Ploeg, L. H., Schaeffer, J. M., & Arena, J. P. (1994). Cloning of an avermectin-sensitive glutamate-gated chloride channel from *Caenorhabditis elegans*. *Nature* **371**, 707-711.

Danilevich, V. N., Luk'ianov, S. A., & Grishin, E. V. (1999). [Cloning and structure of gene encoded alpha-latrocrustoxin from the Black widow spider venom]. *Bioorg.Khim.* **25**, 537-547.

Davey, K. G. (1966). Neurosecretion and molting in some parasitic nematodes. *Am.Zool.* **6**, 243-249.

Davletov, B. A., Krasnoperov, V., Hata, Y., Petrenko, A. G., & Sudhof, T. C. (1995). High affinity binding of alpha-latrotoxin to recombinant neurexin I alpha. *J Biol.Chem.* **270**, 23903-23905.

Davletov, B. A., Meunier, F. A., Ashton, A. C., Matsushita, H., Hirst, W. D., Lelianova, V. G., Wilkin, G. P., Dolly, J. O., & Ushkaryov, Y. A. (1998). Vesicle exocytosis stimulated by alpha-latrotoxin is mediated by latrophilin and requires both external and stored Ca<sup>2+</sup>. *EMBO J.* **17**, 3909-3920.

Davletov, B. A., Shamotienko, O. G., Lelianova, V. G., Grishin, E. V., & Ushkaryov, Y. A. (1996). Isolation and biochemical characterization of a Ca<sup>2+</sup>-independent alpha-latrotoxin-binding protein. *J.Biol.Chem.* **271**, 23239-23245.

De Bell, J. T., Del Castillo, J., & Sanchez, V. (1963). Electrophysiology of the somatic muscle cells of *Ascaris lumbricoides*. *J. Cell. Comp. Phys.* **62**, 159-177.

Del Castillo, J., De Mello, W. C., & Morales, T. (1964). Influence of some ions on the membrane potential of *Ascaris* muscle. *Journal of General Physiology* **48**, 129-140.

Del Castillo, J., Morales, T., & Sanchez, V. (1963). Action of piperazine on the neuromuscular system of *Ascaris lumbricoides*. *Nature* **200**, 706-707.

Dent, J. A., Davis, M. W., & Avery, L. (1997). *avr-15* encodes a chloride channel subunit that mediates inhibitory glutamatergic neurotransmission and ivermectin sensitivity in *Caenorhabditis elegans*. *EMBO J.* **16**, 5867-5879.

Dent, J. A., Smith, M. M., Vassilatis, D. K., & Avery, L. (2000). The genetics of ivermectin resistance in *Caenorhabditis elegans*. *Proc.Natl.Acad.Sci.U.S.A* **97**, 2674-2679.

Dixon, D. M., Valkanov, M., & Martin, R. J. (1993). A patch-clamp study of the ionic selectivity of the large conductance, Ca-activated chloride channel in muscle vesicles prepared from *Ascaris suum*. *J.Membr.Biol.* **131**, 143-149.

Doi, M. & Iwasaki, K. (2002). Regulation of retrograde signaling at neuromuscular junctions by the novel C2 domain protein AEX-1. *Neuron* **33**, 249-259.

Doncaster, C. C. (1962). Nematode feeding mechanism. Observations on *Rhabditis* and *Pelodera*. *Nematologica* **8**, 313-320.

Dulubova, I. E., Krasnoperov, V. G., Khvotchev, M. V., Pluzhnikov, K. A., Volkova, T. M., Grishin, E. V., Vais, H., Bell, D. R., & Usherwood, P. N. (1996). Cloning and structure of delta-latroinsectotoxin, a novel insect-specific member of the latrotoxin family: functional expression requires C-terminal truncation. *J Biol. Chem.* **271**, 7535-7543.

Elchebly, M., Wagner, J., Kennedy, T. E., Lanctot, C., Michaliszyn, E., Itie, A., Drouin, J., & Tremblay, M. L. (1999). Neuroendocrine dysplasia in mice lacking protein tyrosine phosphatase sigma. *Nat. Genet.* **21**, 330-333.

Filipov, A. K., Kobrinsky, E. M., Tsurupa, G. P., Pashkov, V. N., & Grishin, E. (1990). Expression of Receptor for a-latrotoxin in *Xenopus* oocytes after injection of mRNA from rat brain. *Neuroscience* **39**, 809-814.

Finklestein, A., Rubin, L. L., & Tzeng, M. C. (1976). Black widow Spider venom: Effect of Purified toxin lipid bilyaer membranes. *Science* **193**, 1009-1011.

Fleming, J. T., Squire, M. D., Barnes, T. M., Tornoe, C., Matsuda, K., Ahnn, J., Fire, A., Sulston, J. E., Barnard, E. A., Sattelle, D. B., & Lewis, J. A. (1997). *Caenorhabditis elegans* levamisole resistance genes *lev-1*, *unc-29*, and *unc-38* encode functional nicotinic acetylcholine receptor subunits. *J Neurosci.* **17**, 5843-5857.

Fon, E. A. & Edwards, R. H. (2001). Molecular mechanisms of neurotransmitter release. *Muscle Nerve* **24**, 581-601.

Francis, M. M., Mellem, J. E., & Maricq, A. V. (2003). Bridging the gap between genes and behavior: recent advances in the electrophysiological analysis of neural function in *Caenorhabditis elegans*. *Trends Neurosci.* **26**, 90-99.

Franks, C. J. Studies on the action of the nematode FMRFamide-like neuropeptide PF1. 1996. PhD Thesis, University of Southampton.

Franks, C. J., Holden-Dye, L., Williams, R. G., Pang, F. Y., & Walker, R. J. (1994). A nematode FMRFamide-like peptide, SDPNFLRFamide (PF1), relaxes the dorsal muscle strip preparation of *Ascaris suum*. *Parasitology* **108**, 229-236.

Geary, T. G., Price, D. A., Bowman, J. W., Winterrowd, C. A., Mackenzie, C. D., Garrison, R. D., Williams, J. F., & Friedman, A. R. (1992). Two FMRFamide-like peptides from the free-living nematode *Panagrellus redivivus*. *Peptides* **13**, 209-214.

Geary, T. G., Sims, S. M., Thomas, E. M., Vanover, L., Davis, J. P., Winterrowd, C. A., Klein, R. D., Ho, N. F., & Thompson, D. P. (1993). *Haemonchus contortus*: ivermectin-induced paralysis of the pharynx. *Exp. Parasitol.* **77**, 88-96.

Geppert, M., Goda, Y., Hammer, R. E., Li, C., Rosahl, T. W., Stevens, C. F., & Sudhof, T. C. (1994). Synaptotagmin I: a major Ca<sup>2+</sup> sensor for transmitter release at a central synapse. *Cell* **79**, 717-727.

Geppert, M., Khvotchev, M., Krasnoperov, V., Goda, Y., Missler, M., Hammer, R. E., Ichtchenko, K., Petrenko, A. G., & Sudhof, T. C. (1998). Neurexin I alpha is a major alpha-latrotoxin receptor that cooperates in alpha-latrotoxin action. *J. Biol. Chem.* **273**, 1705-1710.

Geßner, G., Meder, S., Rink, T., Boheim, G., Harder, A., Jeschke, P., Scherkenbeck, J., & Londershausen, M. (1996). Ionophore and Anthelmintic Activity of PF1022A, a Cyclooctadepsipeptide, are not related. *Pesticide Science* **48**, 399-407.

Gillis, K. D., Mossner, R., & Neher, E. (1996). Protein kinase C enhances exocytosis from chromaffin cells by increasing the size of the readily releasable pool of secretory granules. *Neuron* **16**, 1209-1220.

Goldschmidt, R. Das nervensystem von *Ascaris lumbricoides* und megalocephala. *Zeitchrift fur Wissenschaftliche Zoologie* **90**, 73-136. 1908.

Goodman, M. B., Hall, D. H., Avery, L., & Lockery, S. R. (1998). Active currents regulate sensitivity and dynamic range in *C. elegans* neurons. *Neuron* **20**, 763-772.

Gorio, A., Rubin, L. L., & Mauro, A. (1978). Double mode of action of black widow spider venom on frog neuromuscular junction. *J Neurocytol.* **7**, 193-202.

Grishin, E. V. (1998). Black widow spider toxins: the present and the future. *Toxicon* **36**, 1693-1701.

Gross, R. E., Bagchi, S., Lu, X., & Rubin, C. S. (1990). Cloning, characterization, and expression of the gene for the catalytic subunit of cAMP-dependent protein kinase in *Caenorhabditis elegans*. Identification of highly conserved and unique isoforms generated by alternative splicing. *J Biol. Chem.* **265**, 6896-6907.

Harder, A. & Samson-Himmelstjerna, G. (2001). Activity of the cyclic depsipeptide emodepside (BAY 44-4400) against larval and adult stages of nematodes in rodents and the influence on worm survival. *Parasitol Res.* **87**, 924-928.

Harder, A. & Samson-Himmelstjerna, G. (2002). Cyclooctadepsipeptides--a new class of anthelmintically active compounds. *Parasitol Res.* **88**, 481-488.

Harder, A., Schmitt-Wrede, H. P., Krucken, J., Marinovski, P., Wunderlich, F., Willson, J., Amliwala, K., Holden-Dye, L., & Walker, R. (2003). Cyclooctadepsipeptides-an anthelmintically active class of compounds exhibiting a novel mode of action. *Int.J Antimicrob Agents* **22**, 318-331.

Harris, J. E. & Crofton, H. D. (1957). Structure and function in the nematodes. Internal pressure and cuticular structure in *Ascaris*. *Journal of Experimental Biology* **34**, 116-130.

Harrow, I. D. & Gration, K. A. F. (1985). Mode of Action of the anthelmintis morantel, pyrantel and levamisole on the muscle cell membrane of the nematode *Ascaris suum*. *Pesticide Science* **16**, 672.

Hata, Y., Butz, S., & Sudhof, T. C. (1996). CASK: a novel dlg/PSD95 homolog with an N-terminal calmodulin-dependent protein kinase domain identified by interaction with neurexins. *J Neurosci.* **16**, 2488-2494.

Henkel, A. W. & Sankaranarayanan, S. (1999). Mechanisms of alpha-latrotoxin action. *Cell Tissue Res.* **296**, 229-233.

Hobson, A. D., Stephenson, W., & Eden, A. (1952). Studies on the physiology of *Ascaris lumbricoides*. I. The relation of total osmotic pressure, conductivity and chloride content of the body fluid to that of the external environment. *Journal of Experimental Biology* **29**, 1-21.

Holden-Dye, L., Brownlee, D. J., & Walker, R. J. (1997). The effects of the peptide KPNFIRFamide (PF4) on the somatic muscle cells of the parasitic nematode *Ascaris suum*. *Br.J.Pharmacol.* **120**, 379-386.

Holden-Dye, L., Franks, C. J., Williams, R. G., & Walker, R. J. (1995). The effect of the nematode peptides SDPNFLRFamide (PF1) and SADPNFLRFamide (PF2) on synaptic transmission in the parasitic nematode *Ascaris suum*. *Parasitology* **110**, 449-455.

Holden-Dye, L., Krogsgaard-Larsen, P., Nielsen, L., & Walker, R. J. (1989). GABA receptors on the somatic muscle cells of the parasitic nematode, *Ascaris suum*: stereoselectivity indicates similarity to a GABAA-type agonist recognition site. *Br.J.Pharmacol.* **98**, 841-850.

Hurlbut, W. P., Chieregatti, E., Valtorta, F., & Haimann, C. (1994). Alpha-latrotoxin channels in neuroblastoma cells. *J.Membr.Biol.* **138**, 91-102.

Ichchenko, K., Bittner, M. A., Krasnoperov, V., Little, A. R., Chepurny, O., Holz, R. W., & Petrenko, A. G. (1999). A novel ubiquitously expressed alpha-latrotoxin receptor is a member of the CIRL family of G-protein-coupled receptors. *J.Biol.Chem.* **274**, 5491-5498.

Ichchenko, K., Hata, Y., Nguyen, T., Ullrich, B., Missler, M., Moomaw, C., & Sudhof, T. C. (1995). Neuroligin 1: a splice site-specific ligand for beta-neurexins. *Cell* **81**, 435-443.

Johnson, C. D. & Stretton, A. O. (1985). Localization of choline acetyltransferase within identified motoneurons of the nematode *Ascaris*. *J.Neurosci.* **5**, 1984-1992.

Johnson, C. D. & Stretton, A. O. (1987). GABA-immunoreactivity in inhibitory motor neurons of the nematode *Ascaris*. *J.Neurosci.* **7**, 223-235.

Kaibuchi, K., Fukumoto, Y., Oku, N., Takai, Y., Arai, K., & Muramatsu, M. (1989). Molecular genetic analysis of the regulatory and catalytic domains of protein kinase C. *J Biol.Chem.* **264**, 13489-13496.

Kamath, R. S., Fraser, A. G., Martinez-Campos, M., Zipperlen, P., & Ahringer, J. (2000). Effectiveness of specific RNA-mediated interference through ingested double-stranded RNA in *Caenorhabditis elegans*. *Genome Biology* Vol 2 No 1, 1-9

Kamath, R. S., Fraser, A. G., Dong, Y., Poulin, G., Durbin, R., Gotta, M., Kanapin, A., Le Bot, N., Moreno, S., Sohrmann, M., Welchman, D. P., Zipperlen, P., & Ahringer, J. (2003). Systematic functional analysis of the *Caenorhabditis elegans* genome using RNAi. *Nature* **421**, 231-237.

Kass, I. S., Stretton, A. O., & Wang, C. C. (1984). The effects of avermectin and drugs related to acetylcholine and 4- aminobutyric acid on neurotransmission in *Ascaris suum*. *Mol.Biochem.Parasitol.* **13**, 213-225.

Kass, I. S., Wang, C. C., Walrond, J. P., & Stretton, A. O. (1980). Avermectin B1a, a paralyzing anthelmintic that affects interneurons and inhibitory motoneurons in *Ascaris*. *Proc.Natl.Acad.Sci.U.S.A* **77**, 6211-6215.

Khvotchev, M. & Sudhof, T. C. (2000). alpha-latrotoxin triggers transmitter release via direct insertion into the presynaptic plasma membrane. *EMBO J* **19**, 3250-3262.

Kiyatkin, N., Dulubova, I., & Grishin, E. (1993). Cloning and structural analysis of alpha-latroinsectotoxin cDNA. Abundance of ankyrin-like repeats. *Eur.J Biochem.* **213**, 121-127.

Kohn, R. E., Duerr, J. S., McManus, J. R., Duke, A., Rakow, T. L., Maruyama, H., Moulder, G., Maruyama, I. N., Barstead, R. J., & Rand, J. B. (2000). Expression of multiple UNC-13 proteins in the *Caenorhabditis elegans* nervous system. *Mol.Biol.Cell* **11**, 3441-3452.

Koushika, S. P., Richmond, J. E., Hadwiger, G., Weimer, R. M., Jorgensen, E. M., & Nonet, M. L. (2001). A post-docking role for active zone protein Rim. *Nat.Neurosci.* **4**, 997-1005.

Krasnoperov, V., Bittner, M. A., Mo, W., Buryanovsky, L., Neubert, T. A., Holz, R. W., Ichtchenko, K., & Petrenko, A. G. (2002a). Protein-tyrosine phosphatase-sigma is a novel member of the functional family of alpha-latrotoxin receptors. *J Biol.Chem.* **277**, 35887-35895.

Krasnoperov, V., Lu, Y., Buryanovsky, L., Neubert, T. A., Ichtchenko, K., & Petrenko, A. G. (2002b). Post-translational proteolytic processing of the calcium-independent receptor of alpha-latrotoxin (CIRL), a natural chimera of the cell adhesion protein and the G protein-coupled receptor. Role of the G protein-coupled receptor proteolysis site (GPS) motif. *J Biol.Chem.* **277**, 46518-46526.

Krasnoperov, V. G., Beavis, R., Chepurny, O. G., Little, A. R., Plotnikov, A. N., & Petrenko, A. G. (1996). The calcium-independent receptor of alpha-latrotoxin is not a neurexin. *Biochem.Biophys.Res.Commun.* **227**, 868-875.

Krasnoperov, V. G., Bittner, M. A., Beavis, R., Kuang, Y., Salnikow, K. V., Chepurny, O. G., Little, A. R., Plotnikov, A. N., Wu, D., Holz, R. W., & Petrenko, A. G. (1997). alpha-Latrotoxin stimulates exocytosis by the interaction with a neuronal G-protein-coupled receptor. *Neuron* **18**, 925-937.

Krueger, N. X., Van Vactor, D., Wan, H. I., Gelbart, W. M., Goodman, C. S., & Saito, H. (1996). The transmembrane tyrosine phosphatase DLAR controls motor axon guidance in *Drosophila*. *Cell* **84**, 611-622.

Kubiak, T. M., Larsen, M. J., Davis, J. P., Zantello, M. R., & Bowman, J. W. (2003). AF2 interaction with *Ascaris suum* body wall muscle membranes involves G-protein activation. *Biochem.Biophys.Res.Commun.* **301**, 456-459.

Lackner, M. R., Nurrish, S. J., & Kaplan, J. M. (1999). Facilitation of synaptic transmission by EGL-30 Gqalpha and EGL-8 PLCbeta: DAG binding to UNC-13 is required to stimulate acetylcholine release. *Neuron* **24**, 335-346.

Lee, C. H., Park, D., Wu, D., Rhee, S. G., & Simon, M. I. (1992). Members of the Gq alpha subunit gene family activate phospholipase C beta isozymes. *J Biol.Chem.* **267**, 16044-16047.

Lelianova, V. G., Davletov, B. A., Sterling, A., Rahman, M. A., Grishin, E. V., Totty, N. F., & Ushkaryov, Y. A. (1997). Alpha-latrotoxin receptor, latrophilin, is a novel member of the secretin family of G protein-coupled receptors. *J.Biol.Chem.* **272**, 21504-21508.

Lewis, J. A., Wu, C. H., Berg, H., & Levine, J. H. (1980a). The genetics of levamisole resistance in the nematode *Caenorhabditis elegans*. *Genetics* **95**, 905-928.

Lewis, J. A., Wu, C. H., Levine, J. H., & Berg, H. (1980b). Levamisole-resistant mutants of the nematode *Caenorhabditis elegans* appear to lack pharmacological acetylcholine receptors. *Neuroscience* **5**, 967-989.

Li, C. & Chalfie, M. FMRFamide-like immunoreactivity in *C.elegans*. Society for Neuroscience Abstracts 12, 246. 1986.

Li, C., Kim, K., & Nelson, L. S. (1999a). FMRFamide-related neuropeptide gene family in *Caenorhabditis elegans*. *Brain Res.* **848**, 26-34.

Li, C., Nelson, L. S., Kim, K., Nathoo, A., & Hart, A. C. (1999b). Neuropeptide gene families in the nematode *Caenorhabditis elegans*. *Ann.N.Y.Acad.Sci.* **897**, 239-252.

Li, L. & Chin, L. S. (2003). The molecular machinery of synaptic vesicle exocytosis. *Cell Mol.Life Sci.* **60**, 942-960.

Liu, J. & Misler, S. (1998a). alpha-Latrotoxin alters spontaneous and depolarization-evoked quantal release from rat adrenal chromaffin cells: evidence for multiple modes of action. *J Neurosci.* **18**, 6113-6125.

Liu, J. & Misler, S. (1998b). alpha-Latrotoxin-induced quantal release of catecholamines from rat adrenal chromaffin cells. *Brain Res.* **799**, 55-63.

Martin, R. J. (1982). Electrophysiological effects of piperazine and diethylcarbamazine on *Ascaris suum* somatic muscle. *Br.J Pharmacol.* **77**, 255-265.

Martin, R. J. (1997). Modes of action of anthelmintic drugs. *Vet.J.* **154**, 11-34.

Martin, R. J., Harder, A., Londershausen, M., & Jeschke, P. (1996). Anthelmintic Actions of the Cyclic Depsipeptide PF1022A and its Electrophysiological Effects on Muscle Cells of *Ascaris suum*. *Pesticide Science* **48**, 343-349.

Martin, R. J., Pennington, A. J., Duittoz, A. H., Robertson, S., & Kusel, J. R. (1991). The physiology and pharmacology of neuromuscular transmission in the nematode parasite, *Ascaris suum*. *Parasitology* **102 Suppl**, S41-S58.

Martin, R. J., Robertson, A. P., & Bjorn, H. (1997). Target sites of anthelmintics. *Parasitology* **114 Suppl**, S111-S124.

Martin, T. F. (2002). Prime movers of synaptic vesicle exocytosis. *Neuron* **34**, 9-12.

Maruyama, I. N. & Brenner, S. (1991). A phorbol ester/diacylglycerol-binding protein encoded by the unc-13 gene of *Caenorhabditis elegans*. *Proc.Natl.Acad.Sci.U.S.A* **88**, 5729-5733.

Matsushita, H., Lelianova, V. G., & Ushkaryov, Y. A. (1999). The latrophilin family: multiply spliced G protein-coupled receptors with differential tissue distribution. *FEBS Lett.* **443**, 348-352.

Maule, A. G., Bowman, J. W., Thompson, D. P., Marks, N. J., Friedman, A. R., & Geary, T. G. (1996). FMRFamide-related peptides (FaRPs) in nematodes: occurrence and neuromuscular physiology. *Parasitology* **113 Suppl**, S119-S135.

Maule, A. G., Shaw, C., Bowman, J. W., Halton, D. W., Thompson, D. P., Geary, T. G., & Thim, L. (1994). KSAYMRFamide: a novel FMRFamide-related heptapeptide from the free-living nematode, *Panagrellus redivivus*, which is myoactive in the parasitic nematode, *Ascaris suum*. *Biochem.Biophys.Res.Commun.* **200**, 973-980.

Mejia, M. E., Fernandez Igartua, B. M., Schmidt, E. E., & Cabaret, J. (2003). Multispecies and multiple anthelmintic resistance on cattle nematodes in a farm in Argentina: the beginning of high resistance? *Vet.Res.* **34**, 461-467.

Mendel, J. E., Korswagen, H. C., Liu, K. S., Hajdu-Cronin, Y. M., Simon, M. I., Plasterk, R. H., & Sternberg, P. W. (1995). Participation of the protein Go in multiple aspects of behavior in *C. elegans*. *Science* **267**, 1652-1655.

Miller, K. G., Alfonso, A., Nguyen, M., Crowell, J. A., Johnson, C. D., & Rand, J. B. (1996). A genetic selection for *Caenorhabditis elegans* synaptic transmission mutants. *Proc.Natl.Acad.Sci.U.S.A* **93**, 12593-12598.

Miller, K. G., Emerson, M. D., & Rand, J. B. (1999). Galpha and diacylglycerol kinase negatively regulate the Gqalpha pathway in *C. elegans*. *Neuron* **24**, 323-333.

Missler, M. & Sudhof, T. C. (1998). Neurexins: three genes and 1001 products. *Trends Genet.* **14**, 20-26.

Missler, M., Zhang, W., Rohlmann, A., Kattenstroth, G., Hammer, R. E., Gottmann, K., & Sudhof, T. C. (2003). Alpha-neurexins couple Ca<sup>2+</sup> channels to synaptic vesicle exocytosis. *Nature* **424**, 939-948.

Mongan, N. P., Baylis, H. A., Adcock, C., Smith, G. R., Sansom, M. S., & Sattelle, D. B. (1998). An extensive and diverse gene family of nicotinic acetylcholine receptor alpha subunits in *Caenorhabditis elegans*. *Receptors.Channels* **6**, 213-228.

Mongan, N. P., Jones, A. K., Smith, G. R., Sansom, M. S., & Sattelle, D. B. (2002). Novel alpha7-like nicotinic acetylcholine receptor subunits in the nematode *Caenorhabditis elegans*. *Protein Sci.* **11**, 1162-1171.

Nathoo, A. N., Moeller, R. A., Westlund, B. A., & Hart, A. C. (2001). Identification of neuropeptide-like protein gene families in *Caenorhabditis elegans* and other species. *Proc.Natl.Acad.Sci.U.S.A* **98**, 14000-14005.

Nelson, L. S., Kim, K., Memmott, J. E., & Li, C. (1998a). FMRFamide-related gene family in the nematode, *Caenorhabditis elegans*. *Brain Res.Mol.Brain Res.* **58**, 103-111.

Nelson, L. S., Rosoff, M. L., & Li, C. (1998b). Disruption of a neuropeptide gene, *fpl-1*, causes multiple behavioral defects in *Caenorhabditis elegans*. *Science* **281**, 1686-1690.

Nicolay, F., Harder, A., Samson-Himmelstjerna, G., & Mehlhorn, H. (2000). Synergistic action of a cyclic depsipeptide and piperazine on nematodes. *Parasitol.Res.* **86**, 982-992.

Nonet, M. L., Grundahl, K., Meyer, B. J., & Rand, J. B. (1993). Synaptic function is impaired but not eliminated in *C. elegans* mutants lacking synaptotagmin. *Cell* **73**, 1291-1305.

Nonet, M. L., Saifee, O., Zhao, H., Rand, J. B., & Wei, L. (1998). Synaptic transmission deficits in *Caenorhabditis elegans* synaptobrevin mutants. *J Neurosci.* **18**, 70-80.

Nurrish, S., Segalat, L., & Kaplan, J. M. (1999). Serotonin inhibition of synaptic transmission: Galphao decreases the abundance of UNC-13 at release sites. *Neuron* **24**, 231-242.

Nurrish, S. J. (2002). An overview of *C. elegans* trafficking mutants. *Traffic* **3**, 2-10.

Orlova, E. V., Rahman, M. A., Gowen, B., Volynski, K. E., Ashton, A. C., Manser, C., van Heel, M., & Ushkaryov, Y. A. (2000). Structure of alpha-latrotoxin oligomers reveals that divalent cation-dependent tetramers form membrane pores. *Nat.Struct.Biol.* **7**, 48-53.

Pang, F. Y., Mason, J., Holden-Dye, L., Franks, C. J., Williams, R. G., & Walker, R. J. (1995). The effects of the nematode peptide, KHEYLRFamide (AF2), on the somatic musculature of the parasitic nematode *Ascaris suum*. *Parasitology* **110**, 353-362.

Parri, H. R., Holden-Dye, L., & Walker, R. J. (1991). Studies on the ionic selectivity of the GABA-operated chloride channel on the somatic muscle bag cells of the parasitic nematode *Ascaris suum*. *Exp. Physiol.* **76**, 597-606.

Pemberton, D. J., Franks, C. J., Walker, R. J., & Holden-Dye, L. (2001). Characterization of glutamate-gated chloride channels in the pharynx of wild-type and mutant *Caenorhabditis elegans* delineates the role of the subunit GluCl-alpha2 in the function of the native receptor. *Mol. Pharmacol.* **59**, 1037-1043.

Pennisi, E. (1998). Worming secrets from the *C. elegans* genome. *Science* **282**, 1972-1974.

Petrenko, A. G., Kovalenko, V. A., Shamotienko, O. G., Surkova, I. N., Tarasyuk, T. A., Ushkaryov, Y., & Grishin, E. V. (1990). Isolation and properties of the alpha-latrotoxin receptor. *EMBO J.* **9**, 2023-2027.

Petrenko, A. G., Perin, M. S., Davletov, B. A., Ushkaryov, Y. A., Geppert, M., & Sudhof, T. C. (1991). Binding of synaptotagmin to the alpha-latrotoxin receptor implicates both in synaptic vesicle exocytosis. *Nature* **353**, 65-68.

Rahman, M. A., Ashton, A. C., Meunier, F. A., Davletov, B. A., Dolly, J. O., & Ushkaryov, Y. A. (1999). Norepinephrine exocytosis stimulated by alpha-latrotoxin requires both external and stored Ca<sup>2+</sup> and is mediated by latrophilin, G proteins and phospholipase C. *Philos. Trans. R. Soc. Lond. B Biol. Sci.* **354**, 379-386.

Raizen, D. M. & Avery, L. (1994). Electrical activity and behavior in the pharynx of *Caenorhabditis elegans*. *Neuron* **12**, 483-495.

Raizen, D. M., Lee, R. Y., & Avery, L. (1995). Interacting genes required for pharyngeal excitation by motor neuron MC in *Caenorhabditis elegans*. *Genetics* **141**, 1365-1382.

Rhee, J. S., Betz, A., Pyott, S., Reim, K., Varoqueaux, F., Augustin, I., Hesse, D., Sudhof, T. C., Takahashi, M., Rosenmund, C., & Brose, N. (2002). Beta phorbol ester- and diacylglycerol-induced augmentation of transmitter release is mediated by Munc13s and not by PKCs. *Cell* **108**, 121-133.

Richmond, J. E., Davis, W. S., & Jorgensen, E. M. (1999). UNC-13 is required for synaptic vesicle fusion in *C. elegans*. *Nat.Neurosci.* **2**, 959-964.

Richmond, J. E. & Jorgensen, E. M. (1999). One GABA and two acetylcholine receptors function at the *C. elegans* neuromuscular junction. *Nat.Neurosci.* **2**, 791-797.

Richmond, J. E., Weimer, R. M., & Jorgensen, E. M. (2001). An open form of syntaxin bypasses the requirement for UNC-13 in vesicle priming. *Nature* **412**, 338-341.

Rogers, C. M., Franks, C. J., Walker, R. J., Burke, J. F., & Holden-Dye, L. (2001). Regulation of the pharynx of *Caenorhabditis elegans* by 5-HT, octopamine, and FMRFamide-like neuropeptides. *J.Neurobiol.* **49**, 235-244.

Rogers, W. P. (1968). Neurosecretory granules in the infective stage of *Haemonchus contortus*. *Parasitology* **58**, 657-662.

Rosenbluth, J. (1965a). Ultrastructural organization of obliquely striated muscle fibers in *Ascaris lumbricoides*. *J Cell Biol.* **25**, 495-515.

Rosenbluth, J. (1965b). Ultrastructure of somatic muscle cells in *Ascaris lumbricoides*. II. Intermuscular junctions, neuromuscular junctions, and glycogen stores. *J Cell Biol.* **26**, 579-591.

Rosenmund, C. & Stevens, C. F. (1996). Definition of the readily releasable pool of vesicles at hippocampal synapses. *Neuron* **16**, 1197-1207.

Saeger, B., Schmitt-Wrede, H. P., Dehnhardt, M., Benten, W. P., Krucken, J., Harder, A., Samson-Himmelstjerna, G., Wiegand, H., & Wunderlich, F. (2001). Latrophilin-like receptor from the parasitic nematode *Haemonchus contortus* as target for the anthelmintic depsipeptide PF1022A. *FASEB J.* **15**, 1332-1334.

Saibil, H. R. (2000). The black widow's versatile venom. *Nat.Struct.Biol.* **7**, 3-4.

Sambrook, J., Fritsch, E. F., & Maniatis, T. Molecular Cloning A laboratory Manual. 1989. Cold Spring Harbor Laboratory Press.

Samson-Himmelstjerna, G., Harder, A., Schnieder, T., Kalbe, J., & Mencke, N. (2000). In vivo activities of the new anthelmintic depsipeptide PF 1022A. *Parasitol.Res.* **86**, 194-199.

Sangster, N. (1996). Pharmacology of anthelmintic resistance. *Parasitology* **113 Suppl**, S201-S216.

Sangster, N. C., Davis, C. W., & Collins, G. H. (1991). Effects of cholinergic drugs on longitudinal contraction in levamisole-susceptible and -resistant *Haemonchus contortus*. *Int.J.Parasitol.* **21**, 689-695.

Sangster, N. C. & Gill, J. (1999). Pharmacology of anthelmintic resistance. *Parasitol.Today* **15**, 141-146.

Sargent, P. B. (1993). The diversity of neuronal nicotinic acetylcholine receptors. *Annu.Rev.Neurosci.* **16**, 403-443.

Sasaki, T., Takagi, M., Yaguchi, T., Miyadoh, S., Okada, T., & Koyama, M. (1992). A new anthelmintic cyclodepsipeptide, PF1022A. *J.Antibiot.(Tokyo)* **45**, 692-697.

Saz, H. J. & Weil, A. (1962). A pathway of formation of a-methyl valerate by *Ascaris lumbricoides*. *Journal of Biological Chemistry* **237**, 2053-2056.

Scheiffele, P., Fan, J., Choih, J., Fetter, R., & Serafini, T. (2000). Neuroligin expressed in nonneuronal cells triggers presynaptic development in contacting axons. *Cell* **101**, 657-669.

Scheller, R. H. (1995). Membrane trafficking in the presynaptic nerve terminal. *Neuron* **14**, 893-897.

Schoch, S., Castillo, P. E., Jo, T., Mukherjee, K., Geppert, M., Wang, Y. (2002). RIM1alpha forms a protein scaffold for regulating neurotransmitter release at the active zone. *Nature* **415**: 312-326.

Seymour, M. K., Wright, K. A., & Doncaster, C. C. (1983). The action of the anterior feeding apparatus of *Caenorhabditis elegans* (Nematoda:Rhabditida). *J.Zool.Soc.Lond* **201**, 527-539.

Simmer, F., Tijsterman, M., Parrish, S., Koushika, S. P., Nonet, M. L., Fire, A., Ahringer, J., & Plasterk, R. H. (2002). Loss of the putative RNA-directed RNA polymerase RRF-3 makes *C. elegans* hypersensitive to RNAi. *Curr.Biol.* **12**, 1317-1319.

Simmer, F., Moorman, C. Van Der Lindem , A. M., Kuijk, E., Van Den Berghe, P.V.E., Kamath, R.S., Fraser, A. G., Ahringer, J., & Plasterk, R. H. (2003). Genome-wide RNAi of *C. elegans* using the hypersensitive strain reveals novel gene functions. *PLoS Biology*, **1**, 077-084.

Sollner, T., Bennett, M. K., Whiteheart, S. W., Scheller, R. H., & Rothman, J. E. (1993). A protein assembly-disassembly pathway in vitro that may correspond to sequential steps of synaptic vesicle docking, activation, and fusion. *Cell* **75**, 409-418.

Song, W., Ranjan, R., Dawson-Scully, K., Bronk, P., Marin, L., Seroude, L., Lin, Y. J., Nie, Z., Atwood, H. L., Benzer, S., & Zinsmaier, K. E. (2002). Presynaptic regulation of neurotransmission in *Drosophila* by the g protein-coupled receptor methuselah. *Neuron* **36**, 105-119.

Squire, M. D., Tornoe, C., Baylis, H. A., Fleming, J. T., Barnard, E. A., & Sattelle, D. B. (1995). Molecular cloning and functional co-expression of a *Caenorhabditis elegans* nicotinic acetylcholine receptor subunit (acr-2). *Receptors.Channels* **3**, 107-115.

Stevens, C. F. & Sullivan, J. M. (1998). Regulation of the readily releasable vesicle pool by protein kinase C. *Neuron* **21**, 885-893.

Stretton, A. O. (1976). Anatomy and development of the somatic musculature of the nematode *Ascaris*. *J.Exp.Biol.* **64**, 773-788.

Stretton, A. O., Cowden, C., Sithigorngul, P., & Davis, R. E. (1991). Neuropeptides in the nematode *Ascaris suum*. *Parasitology* **102 Suppl**, S107-S116.

Stretton, A. O., Fishpool, R. M., Southgate, E., Donmoyer, J. E., Walrond, J. P., Moses, J. E., & Kass, I. S. (1978). Structure and physiological activity of the motoneurons of the nematode *Ascaris*. *Proc.Natl.Acad.Sci.U.S.A* **75**, 3493-3497.

Stryer, L. *Biochemistry*. 1995. New York. W.H. Freeman and Company.

Sudhof, T. C. (1995). The synaptic vesicle cycle: a cascade of protein-protein interactions. *Nature* **375**, 645-653.

Sudhof, T. C. (2001). alpha-Latrotoxin and its receptors: neurexins and CIRL/latrophilins. *Annu.Rev.Neurosci.* **24**, 933-962.

Sugita, S., Ichtchenko, K., Khvotchev, M., & Sudhof, T. C. (1998). alpha-Latrotoxin receptor CIRL/latrophilin 1 (CL1) defines an unusual family of ubiquitous G-protein-linked receptors. G-protein coupling not required for triggering exocytosis. *J.Biol.Chem.* **273**, 32715-32724.

Sulston, J. E. & Horvitz, H. R. (1977). Post-embryonic cell lineages of the nematode, *Caenorhabditis elegans*. *Dev.Biol.* **56**, 110-156.

Sulston, J. E., Schierenberg, E., White, J. G., & Thomson, J. N. (1983). The embryonic cell lineage of the nematode *Caenorhabditis elegans*. *Dev.Biol.* **100**, 64-119.

Tabara, H., Grishok, A., & Mello, C. C. (1998). RNAi in *C. elegans*: soaking in the genome sequence. *Science* **282**, 430-431.

Taylor, S. J. & Exton, J. H. (1991). Two alpha subunits of the Gq class of G proteins stimulate phosphoinositide phospholipase C-beta 1 activity. *FEBS Lett.* **286**, 214-216.

Terada, M. (1992). Neuropharmacological mechanism of action of PF1022A, an antinematode anthelmintic with a new structure of cyclodepsipeptide, on *Angiostrongylus cantonensis* and isolated frog rectus. *Jpn J Parasitol* **32**, 633-642.

The *C. elegans* Genome Sequencing Consortium. (1998). Genome sequence of the nematode *C. elegans*: a platform for investigating biology. The *C. elegans* Sequencing Consortium. *Science* **282**, 2012-2018.

Timmons, L., Court DL, & Fire, A. (2001). Ingestion of bacterially expressed dsRNAs can produce specific and potent genetic interference in *Caenorhabditis elegans*. *Gene* **263**, 103-112.

Timmons, L. & Fire, A. (1998). Specific interference by ingested dsRNA. *Nature* **395**, 854.

Trim, J. E., Holden-Dye, L., Willson, J., Lockyer, M., & Walker, R. J. (2001). Characterization of 5-HT receptors in the parasitic nematode, *Ascaris suum*. *Parasitology* **122**, 207-217.

Trim, N., Holden-Dye, L., Ruddell, R., & Walker, R. J. (1997). The effects of the peptides AF3 (AVPGVLRFamide) and AF4 (GDVPGVLRFamide) on the somatic muscle of the parasitic nematodes *Ascaris suum* and *Ascaridia galli*. *Parasitology* **115** (Pt 2), 213-222.

Tsang, V. C. & Saz, H. J. (1973). Demonstration and function of 2-methylbutyrate racemase in *Ascaris lumbricoides*. *Comp Biochem. Physiol B* **45**, 617-623.

Umbach, J. A., Grasso, A., & Gundersen, C. B. (1990). Alpha-latrotoxin triggers an increase of ionized calcium in Xenopus oocytes injected with rat brain mRNA. *Brain Res.Mol.Brain Res.* **8**, 31-36.

Unwin, N. (1995). Acetylcholine receptor channel imaged in the open state. *Nature* **373**, 37-43.

Ushkaryov, Y. A., Petrenko, A. G., Geppert, M., & Sudhof, T. C. (1992). Neurexins: synaptic cell surface proteins related to the alpha-latrotoxin receptor and laminin. *Science* **257**, 50-56.

Valkanov, M., Martin, R. J., & Dixon, D. M. (1994). The Ca-activated chloride channel of *Ascaris suum* conducts volatile fatty acids produced by anaerobic respiration: a patch-clamp study. *J Membr.Biol.* **138**, 133-141.

Valkanov, M. A. & Martin, R. J. (1995). A Cl channel in *Ascaris suum* selectivity conducts dicarboxylic anion product of glucose fermentation and suggests a role in removal of waste organic anions. *J Membr.Biol.* **148**, 41-49.

Vassilatis, D. K., Arena, J. P., Plasterk, R. H., Wilkinson, H. A., Schaeffer, J. M., Cully, D. F., & Van der Ploeg, L. H. (1997). Genetic and biochemical evidence for a novel avermectin-sensitive chloride channel in *Caenorhabditis elegans*. Isolation and characterization. *J.Biol.Chem.* **272**, 33167-33174.

Volynski, K. E., Capogna, M., Ashton, A. C., Thomson, D., Orlova, E. V., Manser, C. F., Ribchester, R. R., & Ushkaryov, Y. A. (2003). Mutant alpha-latrotoxin (LTXN4C) does not form pores and causes secretion by receptor stimulation. This action does not require neurexins. *J Biol.Chem.*

Waggoner, L. E., Hardaker, L. A., Golik, S., & Schafer, W. R. (2000). Effect of a neuropeptide gene on behavioral states in *Caenorhabditis elegans* egg-laying. *Genetics* **154**, 1181-1192.

Walker, D. S., Gower, N. J., Ly, S., Bradley, G. L., & Baylis, H. A. (2002). Regulated disruption of inositol 1,4,5-trisphosphate signaling in *Caenorhabditis elegans* reveals new functions in feeding and embryogenesis. *Mol.Biol.Cell* **13**, 1329-1337.

Walker, R. J., Colquhoun, L., & Holden-Dye, L. (1992). Pharmacological profiles of the GABA and acetylcholine receptors from the nematode, *Ascaris suum*. *Acta Biol.Hung.* **43**, 59-68.

Walker, R. J., Franks, C. J., Pemberton, D., Rogers, C., & Holden-Dye, L. (2000). Physiological and pharmacological studies on nematodes. *Acta Biol.Hung.* **51**, 379-394.

Wanke, E., Ferroni, A., Gattanini, P., & Meldolesi, J. (1986). alpha Latrotoxin of the black widow spider venom opens a small, non-closing cation channel. *Biochem.Biophys.Res.Commun.* **134**, 320-325.

Wann, K. T. (1987). The electrophysiology of the somatic muscle cells of *Ascaris suum* and *Ascaridia galli*. *Parasitology* **94**, 555-566.

Weber, T., Zemelman, B. V., McNew, J. A., Westermann, B., Gmachl, M., Parlati, F., Sollner, T. H., & Rothman, J. E. (1998). SNAREpins: minimal machinery for membrane fusion. *Cell* **92**, 759-772.

White, J. G., Southgate, E., Thomas, E. M., & Brenner, S. (1986). The structure of the nervous system of the nematode *C.elegans*. *Philosophical Transactions of the Royal Society of London.Series B, Biological Sciences*, **314**, 1-340.

White, J. G., Southgate, E., Thomson, J. N., & Brenner, S. (1976). The structure of the ventral nerve cord of *Caenorhabditis elegans*. *Philos.Trans.R.Soc.Lond B Biol.Sci.* **275**, 327-348.

White, J. G., Southgate, E., Thomson, J. N., & Brenner, S. (1983). Factors that determine connectivity in the nervous system of *Caenorhabditis elegans*. *Cold Spring Harb.Symp.Quant.Biol.* **48**, 633-640.

Willson, J., Amliwala, K., Harder, A., Holden-Dye, L., & Walker, R. J. (2003). The effect of the anthelmintic emodepside at the neuromuscular junction of the parasitic nematode *Ascaris suum*. *Parasitology* **126**, 79-86.

World Health Organisation (1999). World health report, making a difference. Geneva.

Yokoe, H., Anholt, R. R. (1993). Molecular cloning of olfactomedin an extracellular matrix protein specific to olfactory neuroepithelium *Proc.Natl.Acad.Sci.U.S.A* **90**, 4655-4659.

## **APPENDIX 1**

<i>C. elegans</i> Strain	Allele	Location obtained	Gene Description
<i>avr-15</i>	<i>ad501</i>	Joe Dent	<i>avr-15</i> encodes, via alternative splicing, two glutamate-gated chloride channel $\alpha$ -2 subunit homologs
<i>dpy-20 (NW1229)</i>	<i>evIs111</i>	J. Culotti	Pan-neuronal GFP expression
<i>eat-2 (DA465)</i>	<i>ad465</i>	WGC	<i>eat-2</i> encodes a beta subunit of the nicotinic acetylcholine receptor (nAChR) superfamily
<i>egl-8 (RM2221)</i>	<i>md1971</i>	WGC	encodes a phospholipase C beta homolog
<i>egl-8 (MT1083)</i>	<i>n488</i>	WGC	encodes a phospholipase C beta homolog
<i>egl-30 (DA1096)</i>	<i>ad810</i>	WGC	encodes an ortholog of the heterotrimeric G protein alpha subunit Gq (Gq/G11 class)
<i>egl-30 (gf)( KY26)</i>	<i>tg26</i>	Dr K Iwasaki	encodes an ortholog of the heterotrimeric G protein alpha subunit Gq (Gq/G11 class)
<i>goa-1 (MT2426)</i>	<i>n1134</i>	Lauren Segalat	encodes an alpha subunit of G protein (G alpha o)
<i>rrf-3 (NL2099)</i>	<i>pk1426</i>	WGC	encodes an RNA-directed RNA polymerase. Increased sensitivity to RNAi when compared to Wild type animals.
<i>Snb-1 (NM467)</i>	<i>md248</i>	WGC	encodes synaptobrevin, a synaptic vesicle protein orthologous to human vesicle-associated membrane protein 1 (VAMP1 VAMP2)
<i>unc-10 (CNM1657)</i>	<i>md1117</i>	WGC	encodes for RAB interacting protein (RIM).
<i>unc-13 (BC168)</i>	<i>s69</i>	A. Rose	encodes for the UNC-13 protein required in the synaptic vesicle pathway
<i>unc-13 (CB1091)</i>	<i>e1091</i>	WGC	encodes for the UNC-13 protein required for the synaptic vesicle pathway

<i>unc-31</i>	<i>e169</i>	WGC	Encodes a protein orthologous to human calcium-dependent activator protein for secretion involved in post-docking calcium-regulated dense-core vesicle fusion
Wild Type (Bristol N2)	-	WGC	Isolated from mushroom compost near Bristol, England

WGC Washington Genetics Centre.